Structural Design with Ultra-High Performance Concrete

U.S. Department of Transportation
Federal Highway Administration

FOREWORD

Structural design of bridge components is a well-established field that is built on the fundamentals of engineering mechanics, the behaviors of the engaged materials, and the engineering judgment of the associated experts. Ultra-high performance concrete (UHPC) is a class of concrete with compelling properties that lie outside of those for which existing structural design guidance was developed. The Federal Highway Administration's efforts to advance the state of the practice related to UHPC have recently focused on facilitating the development of formal U.S.-based structural design provisions for this class of materials. The information presented in this document provides background, context, and foundational knowledge to bridge owners, designers, and associated individuals interested in engaging this innovative solution in the design of our Nation's highway bridges.

Jean A. Nehme, Ph.D., P.E.,
Director, Office of Infrastructure
Research and Development

TECHNICAL REPORT DOCUMENTATION PAGE

1. Report No. FHWA-HRT-23-077	2. Government Accession No.	3. Recipient's Catalog No.
4. Title and Subtitle Structural Design with Ultra-High Performance Concrete		5. Report Date October 2023
		6. Performing Organization Code:
7. Author(s) Benjamin A. Graybeal (ORCID: 0000-0002-3694-1369) and Rafic G. Helou (ORCID: 0000-0003-0061-9439)		8. Performing Organization Report No.
9. Performing Organization Name and Address Office of Infrastructure Research and Development Federal Highway Administration 6300 Georgetown Pike McLean, VA 22101-2296		10. Work Unit No.
		11. Contract or Grant No.
12. Sponsoring Agency Name and Address Office of Infrastructure Research and Development Federal Highway Administration 6300 Georgetown Pike McLean, VA 22101-2296		13. Type of Report and Period Covered Final Report; 2017–2023
		14. Sponsoring Agency Code HRDI-40
15. Supplementary Notes		

16. Abstract
Ultra-high performance concrete (UHPC) is a class of concrete that has emerged as a compelling material for use in the design, construction, and preservation of structures. UHPC provides mechanical and durability properties that are enhanced and distinct relative to conventional concrete, thus necessitating the use of design methodologies that facilitate the appropriate use of the material. With recent research and development-based advancements related to UHPC, and with a growing interest from bridge owners in the possibilities presented by this material, the U.S. bridge engineering community has an opportunity to consider and potentially adopt formal structural design guidance for UHPC structural elements. This document aims to support the development of formal UHPC structural design guidance by delivering a potential design framework for the community to consider. The report also provides two examples that will assist readers in better understanding key concepts included in the design framework.

17. Key Words UHPC, structural design, material models, flexure, shear, design examples, analysis, pretensioned girder, fiber reinforced concrete	18. Distribution Statement No restrictions. This document is available to the public through the National Technical Information Service, Springfield, VA 22161. https://www.ntis.gov		
19. Security Classif. (of this report) Unclassified	20. Security Classif. (of this page) Unclassified	21. No. of Pages 290	22. Price N/A

Form DOT F 1700.7 (8-72)   Reproduction of completed page authorized.

SI* (MODERN METRIC) CONVERSION FACTORS

APPROXIMATE CONVERSIONS TO SI UNITS

Symbol	When You Know	Multiply By	To Find	Symbol
LENGTH				
in	inches	25.4	millimeters	mm
ft	feet	0.305	meters	m
yd	yards	0.914	meters	m
mi	miles	1.61	kilometers	km
AREA				
in^2	square inches	645.2	square millimeters	mm^2
ft^2	square feet	0.093	square meters	m^2
yd^2	square yard	0.836	square meters	m^2
ac	acres	0.405	hectares	ha
mi^2	square miles	2.59	square kilometers	km^2
VOLUME				
fl oz	fluid ounces	29.57	milliliters	mL
gal	gallons	3.785	liters	L
ft^3	cubic feet	0.028	cubic meters	m^3
yd^3	cubic yards	0.765	cubic meters	m^3
NOTE: volumes greater than 1,000 L shall be shown in m^3				
MASS				
oz	ounces	28.35	grams	g
lb	pounds	0.454	kilograms	kg
T	short tons (2,000 lb)	0.907	megagrams (or "metric ton")	Mg (or "t")
TEMPERATURE (exact degrees)				
°F	Fahrenheit	5 (F-32)/9 or (F-32)/1.8	Celsius	°C
ILLUMINATION				
fc	foot-candles	10.76	lux	lx
fl	foot-Lamberts	3.426	candela/m^2	cd/m^2
FORCE and PRESSURE or STRESS				
lbf	poundforce	4.45	newtons	N
lbf/in^2	poundforce per square inch	6.89	kilopascals	kPa

APPROXIMATE CONVERSIONS FROM SI UNITS

Symbol	When You Know	Multiply By	To Find	Symbol
LENGTH				
mm	millimeters	0.039	inches	in
m	meters	3.28	feet	ft
m	meters	1.09	yards	yd
km	kilometers	0.621	miles	mi
AREA				
mm^2	square millimeters	0.0016	square inches	in^2
m^2	square meters	10.764	square feet	ft^2
m^2	square meters	1.195	square yards	yd^2
ha	hectares	2.47	acres	ac
km^2	square kilometers	0.386	square miles	mi^2
VOLUME				
mL	milliliters	0.034	fluid ounces	fl oz
L	liters	0.264	gallons	gal
m^3	cubic meters	35.314	cubic feet	ft^3
m^3	cubic meters	1.307	cubic yards	yd^3
MASS				
g	grams	0.035	ounces	oz
kg	kilograms	2.202	pounds	lb
Mg (or "t")	megagrams (or "metric ton")	1.103	short tons (2,000 lb)	T
TEMPERATURE (exact degrees)				
°C	Celsius	1.8C+32	Fahrenheit	°F
ILLUMINATION				
lx	lux	0.0929	foot-candles	fc
cd/m^2	candela/m2	0.2919	foot-Lamberts	fl
FORCE and PRESSURE or STRESS				
N	newtons	2.225	poundforce	lbf
kPa	kilopascals	0.145	poundforce per square inch	lbf/in^2

*SI is the symbol for International System of Units. Appropriate rounding should be made to comply with Section 4 of ASTM E380.
(Revised March 2003)

TABLE OF CONTENTS

LIST OF FIGURES

LIST OF TABLES

CHAPTER 1. INTRODUCTION

Ultra-high performance concrete (UHPC) is a class of concrete that has emerged as a compelling material for use in the design, construction, and preservation of structures. It is a versatile material that can be used in primary structural components, field-cast connections between prefabricated components, and repair applications. UHPC provides mechanical and durability properties that are enhanced and distinct relative to conventional concrete, thus necessitating the use of design methodologies that facilitate the appropriate use of the material. Until now, there has not been any formal design guidance in the United States for structural design with UHPC. Recent research and development-based advancements related to UHPC, and a growing interest from bridge owners in the possibilities presented by this material, have provided an opportunity for the bridge engineering community to consider and potentially adopt formal structural design guidance for UHPC structural elements.

OBJECTIVE AND USE

This report is intended for bridge owners, designers, and their supporting professionals who are interested in the design of UHPC structural components as used, or considered for use, in the highway infrastructure. This document aims to support the development of formal UHPC structural design guidance by delivering a potential framework for the bridge engineering community to consider.

REPORT CONTENT

The main body of the report provides an overview of UHPC in the context of structural design. Chapter 2 discusses UHPC as a class of materials, along with its availability and use in the United States. It also provides some background on directly relevant aspects of the Federal Highway Administration's (FHWA) engagement with the topic of UHPC. The proposed framework for UHPC structural design and the associated design examples are also discussed in Chapter 2. Chapter 3 provides concluding remarks.

CHAPTER 2. UHPC STRUCTURAL DESIGN

UHPC is a structural material that exhibits compelling structural behaviors. These behaviors are distinct from those exhibited by other more common materials used in the civil infrastructure, such as conventional concrete or steel. In comparison to conventional concrete, UHPC offers sustained postcracking tensile resistance, along with an increased compressive strength, an increased elastic modulus, and a decreased susceptibility to liquid permeation. To effectively engage the enhanced behaviors of UHPC, structural design guidance must rationally and conservatively provide a framework within which designers can appropriately conceive UHPC structures and proportion UHPC elements. With a look toward the future, UHPC can most likely allow for the design of novel structures whose composition is efficient, whose functionality is improved, and whose lifespan is extended.

UHPC

As with conventional concrete, UHPC is composed of inert and reactive constituents that, when combined with water and chemical admixtures, undergoes a hydration reaction to transform from a semifluid mixture into a competent structural material. UHPC does not have a standard mixture. This class of concrete is defined through prescriptive and performance requirements. UHPC commonly contains a high concentration of steel fiber reinforcement, generally near or greater than 2 percent per volume. UHPC also commonly contains supplementary cementitious materials and graded inert fillers. UHPC rarely contains coarse aggregate.

MATERIAL PROPERTIES

The material properties of UHPC can vary within the ranges of behavior that define UHPC-class materials. Choices made in the selection of constituent materials, the mixing process, and the curing process will affect the fresh and hardened properties of a particular UHPC. Research completed at FHWA's Turner-Fairbank Highway Research Center (TFHRC) during the past two decades has demonstrated some of the material properties that a UHPC might exhibit (Graybeal 2006a; Haber et al. 2018).

AVAILABILITY

UHPC is available in the U.S. marketplace in a variety of forms and from a variety of sources. Researchers have developed and published open-source mix designs that allow interested parties to develop their own local mixes. Commercial precast concrete fabricators have developed mixes that they use within their operations to fabricate finished products composed of UHPC. Finally, commercial material suppliers have developed products that they sell as bagged constituents for use on construction sites or in fabrication facilities. As long as the delivered solution meets the project requirements, the origin of the UHPC mix is generally not relevant.

UHPC USAGE IN BRIDGE CONSTRUCTION

Some of the first uses of UHPC in the civil infrastructure occurred in bridges (Russell and Graybeal 2013). A pedestrian bridge built in Quebec in 1997 that used UHPC preceded other pedestrian bridges in Canada, as well as other countries such as Japan, Germany, and France. A highway

bridge in France built in 2001 using UHPC preceded initial deployments of UHPC in primary structural elements in bridges in France, the United States, and other countries during the 2000s. The first U.S. roadway bridge was constructed in Iowa using UHPC pretensioned girders and has been in service since 2006.

From 2010 through the present, a significant increase has occurred in the number and types of applications for which UHPC is engaged. Applications in Switzerland have largely focused on using UHPC for repair and rehabilitation of deteriorated structures. Usage in South Korea has resulted in construction of some signature bridges. French applications have tended toward optimized solutions that demonstrate the benefits of UHPC. Malaysia has been a leader in adopting this technology, having more than 180 bridges constructed from UHPC prefabricated components (e.g., segmental box girders, pretensioned I-girders) over the past decade. Further international perspectives on the use of UHPC in bridge applications can be found in Graybeal et al. (2020).

In the United States, bridge-related applications of UHPC have expanded over time through a series of phases. Through 2009, UHPC was largely considered an emerging material that was thought to have potential applications in prefabricated components such as pretensioned bridge girders. During the 2010–2017 timeframe, UHPC gained traction as a field-cast grout used in connections between prefabricated bridge components (Graybeal 2014, 2019). From 2018 through the present, UHPC began to be deployed as a material capable of offering an extended lifespan to deteriorated structures through repair and preservation applications.

Between 2006 and 2021, UHPC was used in more than 350 bridge construction applications across the United States. FHWA has been tracking these deployments, and readers can learn more by accessing FHWA's interactive map (FHWA 2021).

FHWA RESEARCH ON MATERIAL TEST METHODS FOR UHPC

FHWA has a long history of UHPC research, conducted at TFHRC, with an eye toward developing innovative solutions that address current challenges in the highway sector. A vertically integrated series of research programs have investigated UHPC from the material scale up through the structural scale. Individual studies have helped build the knowledge base in topics as varied as basic material performance, mechanical property test method development, performance of optimized pretensioned bridge girders, field-cast connections for prefabricated bridge systems, and rehabilitative overlays for deteriorated bridge decks.

The tensile response of UHPC is a defining characteristic of this class of concrete, and early FHWA research was conducted to investigate methodologies that could be used to quantify the behavior (Graybeal 2006a). A bilateral U.S.-French collaborative research project, focused specifically on developing a solution to this challenge, began in 2010. An outgrowth of this research was a test method akin to that used for tensile assessment of metals, wherein a UHPC prism is held in a fixed-end condition and then subjected to a direct tensile load (Graybeal and Baby 2013). The test offers significant advantages in that it is minimally susceptible to reporting unconservative results due to incorrect boundary conditions during testing or incorrect behavioral assumptions during results analysis. This test method has been further exercised and refined in the ensuing years, leading to the recent passage of American Association of State Highway and

Transportation Officials (AASHTO) T 397, *Standard Method of Test for Uniaxial Tensile Response of Ultra-High Performance Concrete* (AASHTO 2022b).

The durability properties of UHPC are also distinctly different from those of conventional concrete. Concrete durability testing is often time-intensive, and many tests were developed in such a way that they cannot differentiate between materials that are more durable than conventional concrete. FHWA researchers addressed the need for a simple test method by investigating AASHTO TP 119, *Standard Method of Test for Electrical Resistivity of a Concrete Cylinder Tested in a Uniaxial Resistance Test* (AASHTO 2022a). This test method was found to deliver results that were indicative of the discontinuous pore structure commonly present in UHPC-class materials, a pore structure that resists ingress of liquids and thus enhances durability (Spragg et al. 2022).

FHWA RESEARCH ON STRUCTURAL BEHAVIOR OF UHPC

From the beginning of FHWA's UHPC research program in 2001, a significant emphasis has been placed on assessing the structural behavior of UHPC components and developing compelling UHPC-based structural solutions. The first project focused on the structural behavior of AASHTO Type II pretensioned girders composed of UHPC and containing no mild steel reinforcement (Graybeal 2006b). Researchers investigated the flexural and shear response of this girder shape and began to recognize the initial indications of the unique tensile response of UHPC-class materials. Further studies in the mid- to late 2000s focused on developing structurally optimized pretensioned girder cross sections that could better utilize the structural behaviors of UHPC (Graybeal 2009a, 2009b).

Recently, a significant portion of FHWA's UHPC research program has focused on the behavior of primary structural components. The program's goal has been to develop foundational knowledge that supports an extension of existing U.S.-based bridge design guidance into the realm of UHPC. One aspect of the program focused on mechanical behaviors of UHPC and behavioral models that could be used in structural design (El-Helou, Haber, and Graybeal 2022). Another aspect of the program focused on the flexural behavior of UHPC beams and associated design concepts (El-Helou and Graybeal 2022a). A third aspect focused on the shear performance and shear behavior modeling of UHPC beams (El-Helou and Graybeal 2022b, 2023). Interface shear behavior was investigated in a different part of the program (Muzenski, Haber, and Graybeal 2022, 2023). Research was also conducted on time-dependent behaviors and prestress loss models (Mohebbi and Graybeal 2022; Mohebbi, Graybeal, and Haber 2022).

CONCEPTUAL DRAFT UHPC STRUCTURAL DESIGN GUIDANCE

UHPC provides mechanical and durability properties that are significantly different from those of conventional concrete, thus necessitating distinct design methodologies that facilitate the appropriate use of the material. These design methodologies must be founded on principles of engineering mechanics, while also recognizing where the behaviors of UHPC differ from those of more common structural materials. Developing a design framework that engages the behaviors of UHPC as viewed through the lens of engineering mechanics should allow for a robust foundation on which formal structural design guidance can be developed.

As interest in the use of UHPC for structural applications has grown, various jurisdictions around the world have developed guidance to assist their communities in appropriately engaging UHPC. The French have been at the forefront with a standard published as a national addition for UHPC design (Association Française de Normalisation 2016) that builds on *Eurocode 2: EN 1992– Design of Concrete Structures* (British Standards Institution 2004). Other notable guidance includes the recommendations in Switzerland (Swiss Institute of Architects and Engineers 2016) and the informative annex to Section 8 of the *Canadian Highway Bridge Design Code* (Canadian Standards Association 2019).

Until now, there has not been any formal design guidance in the United States for structural design with UHPC. However, given the guidance developed elsewhere and given recent research and development-based advancements related to UHPC, the opportunity for developing U.S.-based design guidance that is readily adoptable by the bridge design community appears to have arrived.

The AASHTO Committee on Bridges and Structures subcommittee on concrete structural design, commonly known as T-10, is aware of the opportunities afforded by UHPC and has expressed an interest in UHPC structural design specifications. FHWA staff offered to assist T-10 in taking steps toward the anticipated eventual adoption of an AASHTO guide specification of structural design with UHPC. FHWA focused research efforts to address identified knowledge gaps and develop performance models that facilitate the design of structures. Once sufficient knowledge had been developed through internal research and collected from external sources, FHWA staff began drafting a proposed framework for structural design.

The proposed framework addresses structural considerations that are integral to the design of common structural components, with a focus toward design of reinforced concrete and pretensioned concrete components. Although many of the concepts are certainly relevant, the framework was not developed with a focus toward post-tensioned components or the design of components subjected to seismic demands. The framework parallels the *AASHTO LRFD Bridge Design Specifications*, 9th edition, in particular building on the provisions related to conventional concrete (AASHTO 2020). The format of the framework is similar to guide specifications that AASHTO has previously published in relation to other innovative technologies.

The framework, developed in the format commonly used for AASHTO guide specifications, is presented in Appendix A—Guide Specification for Structural Design with Ultra-High Performance Concrete. Section 1 of Appendix A focuses on structural design guidance, while Section 2 focuses material conformance guidance. Of note, Section 2 allows potential UHPC-class materials to be tested for qualification in advance of use and to be tested for compliance during and after use.

ANALYSIS AND DESIGN EXAMPLES

To assist readers in understanding the potential application of the proposed structural design framework, a pair of design examples has been developed to demonstrate some of the basic concepts embedded in the framework. The first example focuses on using the methods in the design framework to analyze the behavior of a rectangular beam. This example can be found in Appendix B—Analysis of a Rectangular, Mild Steel Reinforced UHPC Beam. The second example demonstrates the design of a slab-on-stringer bridge superstructure using pretensioned girders. This example can be found in Appendix C—Design Example of a Pretensioned UHPC I-Beam Bridge with a Conventional Concrete Deck.

CHAPTER 3. CONCLUDING REMARKS

Continuing advancements in concrete technology have led to the widespread availability of a new class of concrete, UHPC. This material exhibits properties that, when engaged in structural components, can make possible structural solutions that were, until now, not feasible. The creation of formal structural design guidance, based on foundational principles of engineering mechanics and interpreted through the lens of demonstrated UHPC behaviors, is a critical step on the path toward common usage of UHPC in the highway infrastructure. The framework provided here is expected to assist the broader bridge engineering community in achieving this goal.

APPENDIX A. GUIDE SPECIFICATION FOR STRUCTURAL DESIGN WITH ULTRA-HIGH PERFORMANCE CONCRETE

This Appendix is a draft of a potential AASHTO Committee on Bridges and Structures subcommittee T-10 working agenda item. It shall not be relied upon as design guidance or a design standard.

SECTION 1. STRUCTURAL DESIGN WITH ULTRA-HIGH PERFORMANCE CONCRETE

1.1. SCOPE

1.1.1. General

The provisions in Section 1 of this Appendix apply to the design of bridge and ancillary structures constructed of ultra-high performance concrete (UHPC). UHPC shall be a portland cement composite with a discontinuous pore structure and reinforced with steel fiber reinforcement.

The provisions are based on UHPC materials exhibiting a strain-hardening behavior and having the following minimum property values for use in design determined according to Article 1.4 and Section 2 of this Appendix:

- A minimum compressive strength, f'_c, of 17.5 ksi,

- A minimum effective cracking strength, $f_{t,cr}$, of 0.75 ksi,

- A minimum crack localization strength, $f_{t,loc}$, greater than or equal to the effective cracking strength, $f_{t,cr}$,

- A minimum crack localization strain, $\varepsilon_{t,loc}$, of 0.0025, and

- A minimum durability performance as defined in Article 2.6.5 of this Appendix or as specified by the owner.

C1.1.1

UHPC is a class of concrete that has emerged as a compelling material for use in the design, construction, and preservation of structures. It is a versatile material that can be used in primary structural components, field-cast connections between prefabricated components, and repair applications. As with conventional concrete, UHPC is composed of inert and reactive constituents that, when combined with water and chemical admixtures, undergo a hydration reaction to transform from a semifluid mixture into a competent structural material.

UHPC is a strain-hardening fiber reinforced concrete, meaning that this type of concrete can resist tensile loads beyond cracking of the cementitious composite (Graybeal 2015b). Engagement of this tensile response in structural design necessitates a reconsideration of some of the fundamental behavioral assumptions associated with conventional reinforced concrete.

UHPC-class materials have been demonstrated to deliver significantly enhanced durability compared with conventional concretes (Haber et al. 2018). Formulations that meet the performance requirements have been demonstrated to have reduced permeability and thus are more resistant to liquid permeation and associated degradation mechanisms.

There is no standard mixture for UHPC. This class of concrete is defined through prescriptive and performance requirements stated herein. UHPC commonly contains a high concentration of steel fiber reinforcement, generally near or greater than 2 percent per volume. A mix may

include additional, supplementary non-steel fiber reinforcement, but these fibers may not supplant the steel fiber reinforcement. UHPC commonly contains supplementary cementitious materials and graded inert fillers. UHPC rarely contains coarse aggregate.

The recommendations of this Appendix are not intended to supplant proper training or the exercise of judgment by the design professional. They state only the minimum requirements necessary to provide public safety. The owner or the Designer may require the sophistication of the design or the quality of materials and construction, or both, to be higher than the minimum requirements.

The Designer shall be familiar with the provisions of the *AASHTO LRFD Bridge Design Specifications*, 9th edition, hereafter referred to as "AASHTO LRFD BDS," and with the design of conventional reinforced and prestressed concrete structures (AASHTO 2020).

1.1.2. Design Philosophy

C1.1.2

The guidance in this Appendix is based on limit state design principles where structural components shall be proportioned to satisfy the requirements of all appropriate limit states. In many instances, serviceability limits may control the design.

The design professional is referred to AASHTO LRFD BDS (AASHTO 2020) for provisions on limit state design principles, general design and location features, and structural analysis and evaluation.

The serviceability and capacity provisions herein are based on the observed and anticipated performance of example UHPC-class materials when configured for, and subjected to, structural loading. In general, fundamental structural behaviors (e.g., tension, compression, flexure, shear) are treated based

on the intersection of the principles of engineering mechanics and the performance of UHPC. In situations where the performance of UHPC is expected to significantly outperform conventional concrete and there is a lack of specific UHPC test results, AASHTO LRFD BDS (AASHTO 2020) provisions for conventional concrete may have been adopted.

The tensile behavior of UHPC at crack localization is of critical importance. Beyond the crack localization strain, UHPC offers decreasing tensile resistance, causing loads to be shed to available alternate load paths. In general, crack localization within a UHPC structural element results in concentrated deformations (e.g., wide cracking, flexural hinging) that are to be avoided.

Crack localization refers to a point in the tensile stress-strain response of UHPC where the tensile deformation starts to accumulate into a single dominant crack and the tensile resistance starts to continuously decline without substantial recovery. Crack localization occurs when the fiber reinforcement bridging a crack debonds and starts to pull out of the cementitious matrix. In unreinforced members, crack localization coincides with a loss of member capacity. In reinforced members, the loss of the UHPC tensile resistance and the concentrated deformation at a single localized crack within the member cause local redistribution of the applied stresses, potentially straining the tensile reinforcement that bridges the crack beyond its capacity to resist. This reinforcement straining behavior is accentuated by the shorter length over which discrete reinforcements can be developed in UHPC and should be avoided.

The tensile resistance behavior of UHPC depends on the distribution and orientation of the fiber reinforcement in the UHPC. These provisions rely on the use of appropriate construction methods to ensure that the fiber reinforcement is evenly dispersed through the member and that adverse fiber orientation effects have been avoided.

Contract documents should require the use of appropriate construction methods. Disturbance of fiber distribution, as would occur at a cold joint or when fiber flow is restricted from reaching a part of the member, will affect the structural performance of the member.

1.1.3. Loads and Load Combinations

Refer to AASHTO LRFD BDS (AASHTO 2020) for provisions on loads, load combinations, and load factors.

The provisions of AASHTO LRFD BDS (2020) Table 3.5.1-1 shall be supplemented by Article 1.4.2.2 of this Appendix, which defines the unit weight of UHPC.

1.1.4. Limitations

The provisions in Section 1 of Appendix A shall not apply to:

- The non-UHPC portion of composite structural members, and

- The design of earthquake resisting components in Seismic Zones 2, 3, or 4, as defined within AASHTO LRFD BDS (AASHTO 2020).

The provisions in Section 1 of Appendix A do not address the provisions for specific structure components and types discussed in AASHTO LRFD BDS Article 5.12.

The provisions in Section 1 of Appendix A were not developed to address the special considerations and detailing inherent in post-tensioned structures.

C1.1.4

This Appendix does not provide guidance on the design of conventional concrete or structural steel portions of a member partially composed of UHPC. Refer to Section 5.0 and Section 6.0 of AASHTO LRFD BDS for provisions applicable to these structural materials (AASHTO 2020).

Although many of the concepts contained in these provisions may be applicable to the design of earthquake resisting components in Seismic Zones 2, 3, and 4, these provisions were not specifically developed for application in these Seismic Zones.

This provision is not intended to prohibit use of post-tensioning with UHPC or the structure types listed in AASHTO LRFD BDS Article 5.12; however, these items are not specifically addressed in Section 1 of this Appendix, and the guidance provided in AASHTO LRFD Article 5.12 may not necessarily apply to UHPC.

1.2. DEFINITIONS

Anchor—A steel element either cast into UHPC or post-installed into a hardened UHPC member and used to transmit applied loads to the UHPC. Cast-in-place anchors include headed bolts, hooked bolts (J-bolt or L-bolt), and headed studs. Post-installed anchors include expansion anchors, undercut anchors, and adhesive anchors. Steel elements for adhesive anchors include threaded rods, deformed reinforcing bars, or internally threaded steel sleeves with external deformations.

Anchorage—In pretensioning, a device used to anchor the tendon until the UHPC has reached a predetermined strength, and the prestressing force has been transferred to the UHPC. For

reinforcing bars, a length of reinforcement, or a mechanical anchor or hook, or combination thereof at the end of a bar needed to transfer the force carried by the bar into the UHPC.

Anchorage Zone—The portion of the structure in which the prestressing force is transferred from the anchorage device onto the local zone of the UHPC and then distributed more widely into the general zone of the structure.

At Jacking—At the time of tensioning the prestressing tendons.

At Loading—The maturity of the UHPC when loads are applied. Such loads include prestressing forces and permanent loads but generally not live loads.

At Transfer—Immediately after the transfer of prestressing force to the UHPC.

Beam or Bernoulli Region (B-Region)—The regions of UHPC members in which Bernoulli's hypothesis of straight-line strain profiles, linear for bending, and uniform for shear, applies.

Bonded Tendon—A tendon that is bonded to the UHPC.

Bridge—Any structure with an opening not less than 20.0 ft that forms part of a highway or that is located over or under a highway.

Component—Either a discrete element of the bridge or a combination of elements requiring individual design consideration; synonymous to member.

Composite Section—UHPC components, UHPC and conventional concrete components, or UHPC and steel components, interconnected to respond to force effects as a unit.

Crack Localization—The instance at which the tensile deformation starts to accumulate into a single dominant crack and the tensile resistance starts to continuously decline without substantial recovery.

Confinement—A condition where the disintegration of the UHPC under compression is prevented by the development of lateral and/or circumferential forces such as may be provided by appropriate reinforcement, steel or composite tubes, or similar devices.

Creep—The time-dependent deformation of UHPC under permanent load.

Curvature Ductility Ratio—The ratio of sectional curvature at nominal flexural capacity to the sectional curvature when the service stress limit in extreme tension steel is reached.

Debonded Strand—A pretensioned, prestressing strand that is bonded for a portion of its length and intentionally debonded elsewhere through the use of mechanical or chemical means. Also called shielded or blanketed strand.

Deep Component—Components in which the distance from the point of 0.0 shear to the face of the support is less than $2d$, or components in which a load causing more than one-third of the shear at a support is closer than $2d$ from the face of the support.

Deformation—A change in structural geometry due to force effects, including axial displacement, shear displacement, and/or rotations.

Design—The process of proportioning and detailing the components and connections of a bridge.

Design Compressive Strength—The nominal compressive strength of UHPC specified for the work and assumed for design and analysis of new structures.

Design Crack Localization Strain—The nominal crack localization strain of UHPC specified for the work and assumed for design and analysis of new structures.

Design Crack Localization Strength—The nominal crack localization strength of UHPC specified for the work and assumed for design and analysis of new structures.

Design Effective Cracking Strength—The nominal effective cracking strength of UHPC specified for the work and assumed for design and analysis of new structures.

Design Professional—The architect, engineer, architectural firm, or engineering firm responsible for the design of the bridge and issuing contract documents or administering the work under contract documents, or both.

Disturbed or Discontinuity Region (D-Region)—The regions of UHPC members encompassing abrupt changes in geometry or concentrated forces in which strain profiles more complex than straight lines exist.

Ductility—The property of a component or connection that allows inelastic response.

Effective Depth—The depth of a component effective in resisting flexural or shear forces.

Effective Prestress—The stress or force remaining in the prestressing steel after all losses have occurred.

Elastic—A structural material behavior in which the ratio of stress to strain is constant; the material returns to its original unloaded state on load removal.

Element—A part of a component or member consisting of one material.

Equilibrium—A state where the sum of forces and moments about any point in space is 0.0.

Extreme Event Limit States—Limit states relating to events such as earthquakes, ice load, and vehicle and vessel collision, with return periods in excess of the design life of the bridge.

Extreme Tension Steel—The prestressed or nonprestressed reinforcement that is farthest from the extreme compression fiber.

Factored Load—The nominal loads multiplied by the appropriate load factors specified for the load combination under consideration.

Factored Resistance—The nominal resistance multiplied by a resistance factor.

Fiber Reinforcement—Discrete, fine, threadlike steel filament included in the UHPC mix.

Inelastic—Any structural behavior in which the ratio of stress and strain is not constant, and part of the deformation remains after load removal.

Limit State—A condition beyond which the bridge or component ceases to satisfy the provisions for which it was designed.

Load and Resistance Factor Design (LRFD)—A reliability-based design methodology in which force effects caused by factored loads are not permitted to exceed the factored resistance of the components.

Maturity of Concrete—The duration of time between time of loading and the time being considered for creep effects, or duration of time between the end of concrete curing and the time being considered for shrinkage effects.

Member—Same as *Component*.

Model—A mathematical or physical idealization of a material, structure, or component used for analysis.

Monolithic—A portion of an element that was cast through a single, continuous placement of UHPC and contains no cold joints.

Net Tensile Strain—The tensile strain at nominal resistance exclusive of strains due to effective prestress, creep, shrinkage, and temperature.

Nominal Resistance—The resistance of a component or connection to force effects, as indicated by the dimensions specified in the contract documents and by permissible stresses, deformations, or specified strength of materials.

Owner—The person or agency with jurisdiction over the bridge.

Precast Members—UHPC elements cast in a location other than their final position.

Prestressed UHPC—UHPC components in which stresses and deformations are introduced by application of prestressing forces.

Pretensioning—A method of prestressing in which the strands are tensioned before the UHPC is placed.

Reinforced UHPC—Structural UHPC containing prestressing tendons or nonprestressed reinforcement.

Reinforcement—Reinforcing bars, welded wire reinforcement, and/or prestressing steel.

Relaxation—The time-dependent reduction of stress in prestressing tendons.

Resistance Factor—A statistically based multiplier applied to nominal resistance, accounting primarily for variability of material properties, structural dimensions, and workmanship, as well as uncertainty in the prediction of resistance. It is also related to the statistics of the loads through the calibration process.

Sectional Curvature—Ratio of the strain in extreme compression fiber to the distance from the extreme compression fiber to the neutral axis.

Service Limit States—Limit states relating to stress, deformation, and cracking under regular operating conditions.

Slab—A component with a width of at least four times its effective depth.

Spiral—Continuously wound bar or wire in the form of a cylindrical helix.

Strain Hardening—A tensile stress-strain response characterized by increasing tensile resistance after initial cracking of the UHPC.

Strain Offset—The strain value added to a linear fit of the elastic stress-strain response to create a parallel line that intersects the measured stress-strain response of a test specimen after the elastic limit.

Strength Limit States—Limit states relating to strength and stability during the design life.

Stress Range—The algebraic difference between the maximum and minimum stresses due to transient loads.

Structural UHPC—All UHPC used for structural purposes.

Strut-and-Tie Method—A procedure used principally in regions of concentrated forces and geometric discontinuities to determine UHPC member proportions and reinforcement quantities and patterns based on an analytic model consisting of compression struts in the UHPC, tensile ties in the reinforcement, and the geometry of nodes at their points of intersection.

Superstructure—Structural parts of the bridge that provide the horizontal span.

Tendon—A high-strength steel element used to prestress the UHPC.

Transfer—The operation of imparting the force in a pretensioning anchoring device to the UHPC.

Transfer Length—The length over which the pretensioning force is transferred to the UHPC by bond and friction in a pretensioned member.

Transient Loads—Loads and forces that can vary over a short time interval relative to the lifetime of the structure.

Transverse Reinforcement—Reinforcement used to resist shear, torsion, and lateral forces or to confine UHPC in a structural member. The terms "stirrups" and "web reinforcement" are usually

applied to transverse reinforcement in flexural members, and the terms "ties," "cross-ties," "hoops," and "spirals" are applied to transverse reinforcement in compression members.

UHPC Cover—The specified minimum distance between the surface of the reinforcing bars, strands, anchorages, or other embedded items and the surface of the UHPC.

Yield Strength—The specified yield strength of reinforcement.

1.3. NOTATION

A_{cp} = area enclosed by outside perimeter of UHPC cross section (in.^{2})

A_{ct} = area of UHPC on the flexural tension side of the member (in.^{2})

A_{cv} = area of UHPC considered to be engaged in interface shear transfer (in.^{2})

A_g = gross area of the cross section of the member (in.^{2})

A_o = area enclosed by the shear flow path, including any area of holes therein (in.^{2})

A_{ps} = area of prestressing steel (in.^{2}); area of prestressing steel on the flexural tension side of the member (in.^{2}), as shown in AASHTO LRFD BDS Figure 5.7.3.4.2-1 (AASHTO 2020)

A_s = area of nonprestressed tension reinforcement (in.^{2}); area of nonprestressed steel on the flexural tension side of the member at the section under consideration (in.^{2}), as shown in AASHTO LRFD BDS Figure 5.7.3.4.2-1 (AASHTO 2020); total area of reinforcement located within the distance $h/4$ from the end of the beam (in.^{2})

A_t = area of one leg of closed transverse torsion reinforcement in solid members, or total area of transverse torsion reinforcement in the exterior web and flange of hollow members (in.^{2})

A_v = area of transverse reinforcement to resist shear within a distance s (in.^{2})

A_{vf} = area of interface reinforcement crossing the shear plane within the area A_{cv} (in.^{2})

b_e = effective width of the shear flow path taken as the minimum thickness of the exterior webs or flanges comprising the closed box section (in.)

b_v = effective web width taken as the minimum web width within the depth d_v (in.)

b_{vi} = interface width considered to be engaged in shear transfer (in.)

C = total compressive force due to flexure (kip)

C_1 = normal clamping force provided by steel reinforcement (kip)

C_2 = normal clamping force provided by UHPC (kip)

c = depth of neutral axis (in.); cohesion factor (ksi)

c_c = distance from the extreme compression fiber of the member to the neutral axis when the UHPC compression strain limit, ε_{cu}, at extreme compression fiber is reached (in.)

c_L = distance from the extreme compression fiber of the member to the neutral axis when the UHPC tensile strain limit, $\gamma_u\varepsilon_{t,loc}$, at extreme tension fiber is reached (in.)

$c_{s\ell}$ = distance from the extreme compression fiber of the member to the neutral axis when the steel stress in the extreme tension steel is equal to the steel service stress limit, $f_{s\ell}$ (in.)

d_b = nominal strand diameter (in.); nominal diameter of reinforcing bar (in.); nominal diameter of reinforcing bar or wire (in.)

d_e = effective depth taken as the distance, measured perpendicular to the neutral axis, between the extreme compression fiber of the section to the forces in the tensile reinforcement (in.)

d_ℓ = distance from the extreme compression fiber of the member to the centroid of extreme tension steel element (in.)

d_p = distance from extreme compression fiber to the centroid of the of the prestressing tendons (in.)

d_s = distance from extreme compression fiber to the centroid of the nonprestressed tensile reinforcement measured along the centerline of the web (in.)

d_v = effective shear depth taken as the distance, measured perpendicular to the neutral axis, between the resultants of the tensile and compressive forces due to flexure (in.)

E_c = modulus of elasticity of UHPC for use in design (ksi)

E_p = modulus of elasticity of prestressing steel for use in design (ksi)

E_s = modulus of elasticity of the nonprestressed steel reinforcement (ksi); modulus of elasticity of the steel reinforcement crossing the interface plane (ksi)

f_2 = compressive stress in the compression strut (ksi)

f_c = compressive stress in the UHPC section at the extreme compression fiber (ksi)

f'_c = compressive strength of UHPC for use in design (ksi)

f'_{ci} = design UHPC compressive strength at the time of prestressing for pretensioned members and at the time of initial loading for nonprestressed members (ksi)

f_{pc} = unfactored compressive stress in UHPC after prestress losses have occurred, either at the centroid of the cross section resisting transient loads, or at the junction of the web and flange where the centroid lies in the flange (ksi)

f_{pe} = effective stress in prestressing steel after losses (ksi)

f_{po} = a parameter taken as modulus of elasticity of prestressing steel multiplied by the locked-in difference in strain between the prestressing steel and the surrounding UHPC (ksi)

f_{ps} = average stress in prestressing steel at the time for which the nominal resistance of the member is required (ksi)

f_{pu} = specified tensile strength of prestressing steel (ksi)

f_{px} = design stress in pretensioned strand at nominal flexural strength at the section of the member under consideration (ksi)

f_{py} = specified yield strength of prestressing steel (ksi)

f_s	=	stress in the nonprestressed tension reinforcement at nominal flexural resistance (ksi); stress in the interface steel reinforcement at the time of UHPC crack localization in tension (ksi); stress in longitudinal steel (ksi)
$f_{s\ell}$	=	stress limit in steel at service loads after losses (ksi)
$f_{t,cr}$	=	effective cracking strength of UHPC for use in design (ksi)
$f_{t,cri}$	=	design UHPC effective cracking strength at the time of prestressing for pretensioned members and at the time of initial loading for nonprestressed members (ksi)
$f_{t,loc}$	=	crack localization strength of UHPC for use in design (ksi)
$f_{v,\alpha}$	=	uniaxial stress in the transverse steel reinforcement at nominal shear resistance (ksi)
f_y	=	specified minimum yield strength of reinforcement (ksi)
H	=	average annual ambient relative humidity (percent)
h	=	overall dimension of precast member in the direction in which splitting resistance is being evaluated (in.); overall thickness or depth of the member (in.)
K	=	limiting interface shear resistance (ksi)
K_1	=	correction factor for modulus of elasticity to be taken as 1.0, unless determined by a physical test, and as approved by the owner
K_3	=	correction factor for creep to be taken as 1.0, unless determined by physical tests, and as approved by the owner
K_4	=	correction factor for shrinkage to be taken as 1.0, unless determined by physical tests, and as approved by the owner
k_f	=	factor for the effect of UHPC strength
k_{hc}	=	humidity factor for creep
k_{hs}	=	humidity factor for shrinkage
k_ℓ	=	factor for the effect of loading age
k_s	=	factor for the effect of the volume-to-surface ratio of the component
k_{td}	=	time development factor
L_{vi}	=	interface length considered to be engaged in shear transfer (in.)
ℓ_d	=	development length (in.)
ℓ_{dh}	=	development length of deformed bars in tension terminating in a standard hook (in.)
ℓ_{px}	=	distance from free end of pretensioned strand to the section of member under consideration (in.)
ℓ_t	=	transfer length of the prestressing strand (in.)
M	=	nominal flexural moment (kip-in.)
M_c	=	nominal crushing moment (kip-in.)
M_{cr}	=	nominal cracking moment (kip-in.)

M_L	=	nominal crack localization moment (kip-in.)
M_n	=	nominal flexural resistance (kip-in.)
M_r	=	factored flexural resistance (kip-in.)
$M_{s\ell}$	=	nominal flexural moment when the steel stress in the extreme tension steel is equal to the steel service stress limit, $f_{s\ell}$ (kip-in.)
M_u	=	factored moment at the section (kip-in.)
M_y	=	nominal yielding moment (kip-in.)
N_u	=	factored axial force, taken as positive if tensile and negative if compressive (kip)
P_c	=	permanent net compressive force, normal to the shear plane (kip)
P_n	=	nominal resistance of a tension member (kip)
P_r	=	factored axial resistance (kip); factored splitting resistance of pretensioned anchorage zones (kip)
$P_{r,UHPC}$	=	splitting resistance of pretensioned anchorage zones provided by the UHPC (kip)
P_{UHPC}	=	axial compression resistance provided by the UHPC
P_s	=	axial compression resistance provided by the longitudinal steel reinforcement
p_c	=	length of outside perimeter of the UHPC section (in.)
s	=	spacing of transverse reinforcement measured in a direction parallel to the longitudinal reinforcement (in.)
s_{max}	=	maximum spacing of transverse reinforcement (in.)
T_{cr}	=	torsional cracking moment (kip-in.)
T_n	=	nominal torsional resistance (kip-in.)
T_r	=	factored torsional resistance (kip-in.)
T_u	=	applied factored torsional moment (kip-in.)
t	=	maturity of UHPC (day)
t_i	=	age of UHPC at time of load application (day)
V_{eff}	=	effective factored shear resistance (kip)
V_n	=	nominal shear resistance (kip)
V_{ni}	=	nominal interface shear resistance (kip)
V_p	=	component of prestressing force in the direction of the shear force (kip)
V_{ri}	=	factored interface shear resistance (kip)
V_s	=	shear resistance provided by transverse reinforcement (kip)
V_u	=	factored shear force (kip)
V_{UHPC}	=	nominal shear resistance of the UHPC (kip)

v_u	=	shear stress (ksi)
W/CM	=	water/cementitious materials ratio
α	=	angle of inclination of transverse reinforcement to longitudinal axis (degrees)
α_u	=	reduction factor to account for the nonlinearity of the UHPC compressive stress-strain response
γ_{LL}	=	load factor for live load for Service III load combination
γ_u	=	factor to allow for the reduction of UHPC tensile parameter values; it shall not be taken greater than 1.0
ε_2	=	strain in the UHPC diagonal compressive strut (in./in.)
ε_c	=	compressive strain in extreme compression fiber of the UHPC section (in./in.)
ε_{cL}	=	strain in the extreme compression fiber of the UHPC section when the UHPC tensile strain limit, $\gamma_u \varepsilon_{t,loc}$, at extreme tension fiber is reached (in./in.)
ε_{cp}	=	elastic compressive strain limit (in./in.)
$\varepsilon_{cs\ell}$	=	strain in the extreme compression fiber of the UHPC section when the steel stress in the extreme tension steel is equal to the steel service stress limit, $f_{s\ell}$ (in./in.)
ε_{cu}	=	ultimate compressive strain of UHPC for use in design (in./in.)
ε_s	=	net longitudinal tensile strain in the section at the centroid of the tension reinforcement (in./in.)
ε_{sh}	=	UHPC shrinkage strain at a given time (in./in.)
$\varepsilon_{s\ell}$	=	net tensile strain in the extreme tension steel when the steel service stress limit, $f_{s\ell}$, is reached (in./in.)
ε_t	=	net tensile strain in extreme tension fiber of the UHPC section (in./in.)
$\varepsilon_{t,cr}$	=	elastic tensile strain limit of UHPC corresponding to a tensile stress of $\gamma_u f_{t,cr}$ (in./in.)
$\varepsilon_{t,loc}$	=	crack localization strain of UHPC for use in design (in./in.)
ε_v	=	strain along the transverse direction of the member (in./in.)
ε_y	=	strain in the steel reinforcement corresponding to f_y (in./in.)
θ	=	angle of inclination of diagonal compressive stresses (degrees)
λ_{rl}	=	reinforcement location factor
μ	=	curvature ductility ratio; friction factor
μ_ℓ	=	curvature ductility ratio limit
ξ	=	multiplier for transfer length of prestressing strand
$\rho_{v,\alpha}$	=	ratio of area of transverse shear reinforcement to gross UHPC area of a horizontal section
ϕ	=	resistance factor
ϕ_c	=	resistance factor for axial resistance

ϕ_f	=	resistance factor for flexure
ϕ_v	=	resistance factor for shear
ϕ_w	=	hollow column reduction factor, as defined in AASHTO LRFD BDS Article 5.6.4.7.2c (AASHTO 2020)
$\Psi(t, t_i)$	=	creep coefficient at time t for loading applied at t_i
ψ	=	sectional curvature at nominal flexural moment, M (1/in.)
ψ_{cr}	=	sectional curvature at nominal cracking moment, M_{cr} (1/in.)
ψ_L	=	sectional curvature at nominal crack localization moment, M_L (1/in.)
ψ_n	=	sectional curvature at nominal flexural strength, M_n (1/in.)
$\psi_{s\ell}$	=	baseline section curvature at $M_{s\ell}$ (1/in.)
ψ_y	=	sectional curvature at nominal yielding moment, M_y (1/in.)

1.4. MATERIAL PROPERTIES

1.4.1. General

Designs shall be based on the material properties cited herein and on the use of materials that conform to qualification and acceptance testing standards.

The contract documents shall define the grades or properties of all materials to be used.

1.4.2. Ultra-High Performance Concrete

1.4.2.1. General

The material properties and idealized stress-strain behaviors of UHPC for use in design shall be determined according to the methods cited in this Article and in Section 2 of this Appendix.

The minimum acceptable material property values, including their statistical variability, shall be established prior to design and shown in the contract documents.

Typical material property values are given in Addendum A1.

C1.4.2.1

When specifying minimum acceptable material properties for UHPC to be used in design, designers may refer to material qualification results produced in accordance with Section 2 of this Appendix, supplier certification reports, and/or the typical values given in Addendum A1. Utilizing the minimum property values specified in Article 1.1.1 of this Appendix, particularly the minimum value of the crack localization strain, $\varepsilon_{t,loc}$, for products with property values that exceed these thresholds, may result in overly conservative and uneconomical designs.

The typical values given in Addendum A1 are based on the experimental work of El-Helou, Haber, and Graybeal (2022) and Haber et al. (2018), which included 11 UHPC products commercially available in Europe and North America. The studies showed that the mechanical property values of the considered products exceeded the minimum values specified in Article 1.1.1.

1.4.2.2. Unit Weight

In the absence of more precise information, the unit weight of UHPC may be taken equal to 0.155 kcf.

C1.4.2.2

The unit weight of UHPC includes the weight of the fiber reinforcement in the UHPC mix design.

For UHPC components reinforced with prestressed or nonprestressed steel, the unit weight may generally be increased by 0.005 kcf to account for the weight of the reinforcement in dead load calculations. UHPC components may contain different proportions of reinforcement than commonly occur in conventional concrete components, so the increased unit weight to account for the dead load of the reinforcement may need to be more accurately determined.

1.4.2.3. Modulus of Elasticity

The modulus of elasticity of UHPC, E_c, is used to describe the elastic behavior in tension and compression.

The modulus of elasticity, E_c, may be determined by physical tests in accordance with ASTM C1856/C1856M (ASTM 2017a).

In the absence of measured data, the modulus of elasticity, E_c, shall be taken as:

$$E_c = 2,500\, K_1 f_c'^{0.33} \tag{1.4.2.3-1}$$

where:

f_c' = compressive strength of UHPC for use in design (ksi)

C1.4.2.3

ASTM C1856/C1856M provides procedures for producing and testing UHPC specimens for the purpose of determining the properties of the material (ASTM 2017a). The test method to determine the modulus of elasticity is based on ASTM C469/C469M (ASTM 2022g), with exceptions listed in Section 8.3 of ASTM C1856/C1856M (ASTM 2017a).

Eq. 1.4.2.3-1 with $K_1 = 1.0$ is similar to Eq. C5.4.2.4-1 for normal weight concrete specified in AASHTO LRFD BDS (AASHTO 2020) and is verified to be applicable for UHPC-class materials with a typical unit weight of approximately 0.155 kcf based on the experimental work of El-Helou, Haber, and Graybeal (2022).

K_1 = correction factor for modulus of elasticity to be taken as 1.0 unless determined by physical test, and as approved by the owner

The factor K_1 is included to allow the calculated modulus to be adjusted for different types of UHPC. Unless a value has been determined by physical tests, K_1 should be taken as 1.0. Use of a measured K_1 factor permits a more accurate prediction of modulus of elasticity and, thus, will increase the accuracy of associated design calculations.

1.4.2.4. Compression Behavior

1.4.2.4.1. Compressive Strength

The compressive strength of the UHPC, f'_c, for use in design shall be based on test cylinders produced, tested, and evaluated in accordance with ASTM C1856/C1856M (ASTM 2017a).

For each component, the compressive strength for use in design, f'_c, shall be shown in the contract documents.

C1.4.2.4.1

The testing procedure of the compressive strength of UHPC is based on ASTM C39/C39M (ASTM 2020d), with exceptions listed in Section 8.1 of ASTM C1856/C1856M (ASTM 2017a).

1.4.2.4.2. Ultimate Compressive Strain

The ultimate compressive strain for use in design, ε_{cu}, shall be taken as equal to or less than the strain corresponding to the compressive strength, f'_c, and may be determined by physical tests in accordance with ASTM C1856/C1856M (ASTM 2017a).

Unless determined by physical tests, the ultimate compressive strain of UHPC, ε_{cu}, shall be taken as the greater of the elastic compressive strain limit, ε_{cp}, or 0.0035. The elastic compressive strain limit shall be taken as:

$$\varepsilon_{cp} = \frac{\alpha_u f'_c}{E_c}$$ (1.4.2.4.2-1)

where:
  α_u = reduction factor to account for the nonlinearity of the compressive stress-strain response; it shall not be greater than 0.85

C1.4.2.4.2

The experimental value of the ultimate compressive strain, ε_{cu}, may be recorded when testing for the modulus of elasticity in accordance with ASTM C1856/C1856M (ASTM 2017a).

The recommendation for ε_{cu}, and α_u are based on the experimental work of El-Helou, Haber, and Graybeal (2022), which included 11 UHPC products commercially available in Europe and North America.

The value of ε_{cu} = 0.0035, applicable in the absence of physical tests, is selected to be lower than the average value of ε_{cu} for the tested products.

The value of α_u coincides with the stress value at which the initial elastic compressive stress-strain response of the tested products deviated not more than 10 percent from linearity.

1.4.2.4.3. Compression Design Model

The idealized uniaxial stress-strain model of UHPC under compression loading shall be defined by modulus of elasticity, E_c, compressive strength, f'_c, and ultimate compressive strain, ε_{cu}, as shown in Figure 1.4.2.4.3-1.
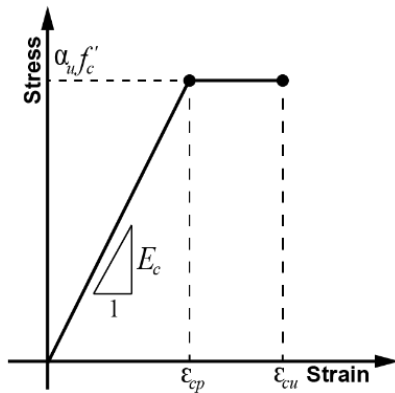
Source: FHWA.

Figure 1.4.2.4.3-1—Idealized compressive stress-strain model for UHPC.

1.4.2.5. Tension Behavior

1.4.2.5.1. Effective Cracking Strength

The effective cracking strength for use in design, $f_{t,cr}$, is the stress at the onset of the formation of the first crack under uniaxial loading. It shall be determined based on direct tension testing produced, tested, and evaluated in accordance with AASHTO T 397 (AASHTO 2022b).

For each component, the minimum effective cracking strength for use in design shall be shown in the contract documents.

C1.4.2.4.2

The idealized stress-strain model of UHPC under compression loading is based on the work of El-Helou, Haber, and Graybeal (2022). The model mimics the experimental stress-strain response of UHPC in the elastic range and until the response deviates more than 10 percent from linearity at a stress equal to $\alpha_u f'_c$ occurring at a strain ε_{cp}. Beyond this point, the model sustains the reduced compressive resistance until the strain at the material's compressive strength is reached, ε_{cu}. The compression design model allows the full compressive strain capacity through peak compressive stress resistance to be used in design.

C1.4.2.5.1

AASHTO T 397 is titled *Standard Method of Test for Uniaxial Tensile Response of Ultra-High Performance Concrete* (AASHTO 2022b). In this method, the effective cracking strength, $f_{t,cr}$, is determined as the stress corresponding to the intersection of a 0.02 percent strain offset to the initial elastic portion of the captured stress-strain response and the portion of the stress-strain response in the inelastic region. As demonstrated by the research of El-Helou, Haber, and Graybeal (2022) and Haber et al. (2018), the effective cracking strength value may not exactly coincide with the true value of the first cracking stress, as it is generally slightly higher than the elastic stress limit. The value of the effective cracking strength, $f_{t,cr}$, generally coincides with the formation of the first discrete crack over the

29

full cross section of a prismatic specimen tested in accordance with AASHTO T 397.

1.4.2.5.2. Crack Localization Strength

The crack localization strength for use in design, $f_{t,loc}$, is the first tensile stress value at which the tensile stress continuously decreases with increasing strain or permanently drops below the value of the effective cracking strength, whichever occurs first. It shall be determined based on direct tension testing produced, tested, and evaluated in accordance with AASHTO T 397 (AASHTO 2022b).

If the value of the crack localization strength, $f_{t,loc}$, is less than $1.20f_{t,cr}$ (i.e., $f_{t,loc} < 1.20f_{t,cr}$), it shall be taken as equal to the effective cracking strength, $f_{t,cr}$, defined in Article 1.4.2.5.1 of this Appendix (i.e., $f_{t,loc} = f_{t,cr}$).

For each component, the minimum crack localization strength for use in design shall be shown in the contract documents.

1.4.2.5.3. Crack Localization Strain

The crack localization strain for use in design, $\varepsilon_{t,loc}$, is the strain corresponding to the crack localization strength, $f_{t,loc}$. It shall be determined based on direct tension testing produced, tested, and evaluated in accordance with AASHTO T 397 (AASHTO 2022b).

For each component, the minimum crack localization strain for use in design shall be shown in the contract documents.

C1.4.2.5.2

The localization of cracks corresponds to the end of the multicracking phase of the tensile behavior. During the multicracking phase, the tensile resistance remains approximately equal to the effective cracking strength or continuously increases with increasing strain. The localization of cracks marks the beginning of the softening phase, in which the tensile resistance decreases with increasing strain. In the softening phase, the tensile deformation generally accumulates into a single crack prompted by the pullout of the crack bridging fiber reinforcement.

C1.4.2.5.3

See commentary on crack localization strength in Article 1.4.2.5.2 of this Appendix.

30

1.4.2.5.4. Tension Design Models

The idealized uniaxial stress-strain model of UHPC under tension loading shall be defined by the modulus of elasticity, E_c; the effective cracking strength, $f_{t,cr}$; the crack localization strength, $f_{t,loc}$; and the crack localization strain, $\varepsilon_{t,loc}$.

The models include a factor, γ_u, applied to the values of $f_{t,cr}$, $f_{t,loc}$, and $\varepsilon_{t,loc}$ to allow for the reduction of tensile response parameter values. The value of γ_u shall not be taken greater than 1.0.

For UHPC materials with $f_{t,loc} < 1.20f_{t,cr}$, the idealized stress-strain model shall be taken as shown in Figure 1.4.2.5.4-1 with $f_{t,loc}$ taken equal to $f_{t,cr}$.
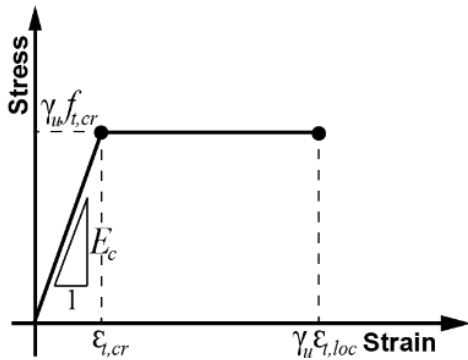
Source: FHWA.

Figure 1.4.2.5.4-1—Idealized tensile stress-strain model for UHPC.

For UHPC materials with $f_{t,loc} \geq 1.20f_{t,cr}$, the idealized stress-strain model shall be taken as shown in either Figure 1.4.2.5.4-1 or Figure 1.4.2.5.4-2.

C1.4.2.5.4

The idealized stress-strain model of UHPC subjected to tensile loading is based on the work of El-Helou, Haber, and Graybeal (2022).

Two types of tensile stress-strain responses are idealized for use in design.

The first type, shown in the stress-strain model of Figure 1.4.2.5.4-1, describes materials exhibiting a stress plateau where the postcracking strength remains equal to or greater than the effective cracking strength, $f_{t,cr}$, until crack localization occurs at $\varepsilon_{t,loc}$. This behavior corresponds to response Type H-2 as classified in AASHTO T 397 and generally describes the behavior of UHPC materials reinforced with fiber proportions of 2 percent by volume or less (AASHTO 2022b).

The second type, shown in the stress-strain model of Figure 1.4.2.5.4-2, corresponds to materials where the postcracking strength continuously increases with increasing strain until crack localization occurs at a peak stress $f_{t,loc}$ equal to or greater than $1.20f_{t,cr}$ and at a strain $\varepsilon_{t,loc}$. This behavior corresponds to response Type H-1 as classified in AASHTO T 397 and generally describes the behavior of UHPC materials reinforced with fiber proportions greater than 3 percent by volume (AASHTO 2022b).

The postcrack localization capacity of the UHPC (i.e., the softening phase where the strain is greater than the crack localization strain) is not accounted for in the design models since strains in excess of the localization strain are not permitted by the provisions in this Appendix and the response is a function of crack opening, which is not consistent with a strain-based design approach.

The factor γ_u accounts for the cases in which the values of the tensile properties of the UHPC placed in the structural components are
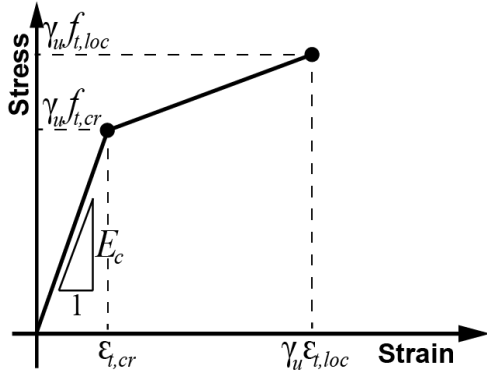
Source: FHWA.

Figure 1.4.2.5.4-2—Idealized tensile stress-strain model for UHPC with $f_{t,loc} \geq 1.20f_{t,cr}$.

in which:

$$\varepsilon_{t,cr} = \frac{\gamma_u f_{t,cr}}{E_c} \qquad (1.4.2.5.4\text{-}1)$$

where:

$\varepsilon_{t,cr}$ = elastic tensile strain limit corresponding to a tensile stress of $\gamma_u f_{t,cr}$

1.4.2.6. Poisson's Ratio

Poisson's ratio of UHPC may be determined by physical tests in accordance with ASTM C1856/C1856M (ASTM 2017a).

Unless determined by physical tests, Poisson's ratio of UHPC may be assumed as 0.15.

1.4.2.7. Coefficient of Thermal Expansion

The coefficient of thermal expansion should be determined by the laboratory tests on the specific product to be used.

In the absence of more precise data, the thermal coefficient of expansion of UHPC-class materials may be taken as $7.0 \times 10^{-6}/°F$.

C1.4.2.6

The testing procedure for Poisson's ratio of UHPC is in accordance with ASTM C469/C469M (ASTM 2022g), with exceptions listed in Section 8.3 of ASTM C1856/C1856M (ASTM 2017a).

The proposed value of Poisson's ratio is based on the experimental work of El-Helou, Haber, and Graybeal (2022) and Haber et al. (2018).

C1.4.2.7

The coefficient of thermal expansion should be determined from laboratory tests in accordance with AASHTO T 336 (AASHTO 2019) for hydraulic cement concrete and with the following modification: specimens should be sealed before testing by applying an epoxy layer to their exterior surfaces, with the exception of the bearing points of the supports and the

expected to be lower than their respective qualified values determined according to Section 2 of this Appendix. Casting processes should be considered by the Designer to ensure that the member is constructed without producing undesirable fiber distributions or orientations that impair the tensile behavior of as-cast UHPC. Different values of γ_u may be assigned to each of the tensile parameters. These values may be informed from prototype testing of structural components and/or from extracted tension specimens tested in accordance with AASHTO T 397 (AASHTO 2022b).

displacement transducer (Graybeal 2006a). Sealing the specimens reduces the effects of water saturation, given the low permeability of UHPC.

The proposed value of the coefficient of thermal expansion is based on the experimental work of Mohebbi, Graybeal, and Haber (2022).

1.4.2.8. Creep and Shrinkage

1.4.2.8.1. General

In lieu of alternate models for creep and shrinkage strains in UHPC developed based on laboratory test data for the specific UHPC-class material under consideration, the values of creep and shrinkage specified in Articles 1.4.2.8.2 and 1.4.2.8.3 of this Appendix shall be used.

The designer shall consider the variability in estimates of creep and shrinkage.

C1.4.2.8.1

Creep and shrinkage of UHPC are variable properties that depend on many factors, some of which may not be known at the time of design.

The methods for determining creep and shrinkage specified in Articles 1.4.2.8.2 and 1.4.2.8.3 of this Appendix are based on the experimental work of Mohebbi, Graybeal, and Haber (2022) and Mohebbi and Graybeal (2022). The development of these methods parallel the concepts of the creep and shrinkage methods specified in AASHTO LRFD BDS Articles 5.4.2.3.2 and 5.4.2.3.3 (AASHTO 2020) and recalibrate the different empirical factor equations based on experimental data of eight UHPC products available in Europe and North America.

Predictive relationships for creep and shrinkage behavior of UHPC provide an estimate of the actual material behavior. An approach that considers higher and lower estimates for these behaviors should be engaged when designing and constructing members sensitive to these effects.

1.4.2.8.2. Creep

Unless verified by physical tests and as approved by the owner, the provisions in this Article shall apply for compressive strengths at the time of prestressing for pretensioned members and at the time of initial loading for nonprestressed members, f'_{ci}, equal to or

C1.4.2.8.2

The provisions in this Article are based on experimental data of Mohebbi, Graybeal, and Haber (2022) in which the creep specimens were loaded at compressive strengths equal to or greater than 14.0 ksi. The creep coefficient for components loaded at compressive strength values less than 14.0 ksi is expected to be

greater than 14.0 ksi.

The creep coefficient may be taken as:

$$\Psi(t, t_i) = 1.2 k_s\, k_{hc}\, k_f\, k_{td}\, k_\ell\, K_3 \qquad \text{(1.4.2.8.2-1)}$$

in which:

$$k_s = 1.0 \qquad \text{(1.4.2.8.2-2)}$$

$$k_{hc} = 1.12 - 0.0024H \qquad \text{(1.4.2.8.2-3)}$$

$$k_f = \frac{18}{1.5 f'_{ci} - 3} \qquad \text{(1.4.2.8.2-4)}$$

$$k_{td} = \frac{t}{\left(\dfrac{300}{f'_{ci} + 30}\right) + 0.8 t^{0.98}} \qquad \text{(1.4.2.8.2-5)}$$

where:

$\Psi(t, t_i) =$ creep coefficient at time t for loading applied at t_i

k_s = factor for the effect of the volume-to-surface ratio of the component

k_{hc} = humidity factor for creep

k_f = factor for the effect of UHPC strength

k_{td} = time development factor

k_ℓ = factor for the effect of loading age determined according to Eqs. 1.4.2.8.2-6 and 1.4.2.8.2-7

K_3 = correction factor for creep to be taken as 1.0 unless determined by physical test, and as approved by the owner

higher than determined by the methods in this Article, particularly when subjected to high compressive stresses.

The creep coefficient is applied to the compressive strain caused by permanent loads to obtain the strain due to creep.

Creep is influenced by the same factors as shrinkage, and by the magnitude and duration of stress, the maturity of the UHPC at the time of loading, and temperature.

The factor for the volume-to-surface ratio, k_s, is taken as 1.0 because UHPC has a dense microstructure and a disconnected pore structure that significantly reduces the rate of moisture exchange with the outside environment (Mohebbi and Graybeal 2022).

The factor K_3 is included to allow calculated creep coefficient values to be adjusted for a specific UHPC product. It is assumed to be 1.0, except for situations where specific knowledge is available. The K_3 factor may be determined from physical tests on creep performed according to ASTM C1856/C1856M and with a sustained compressive stress equal to 65 percent of the compressive strength at the time of loading. The testing procedure for the compression creep of UHPC is in accordance with ASTM C512/C512M (ASTM 2015c), with exceptions listed in Section 8.4 of ASTM C1856/C1856M (ASTM 2017a).

In cases where the correction factor for modulus of elasticity K_1 is different than 1.0 and physical tests on creep are not available, K_3 may be taken as equal to $1/K_1$. This adjustment accounts for the potential impact of the modulus of elasticity on the ultimate creep coefficient.

H = average annual ambient relative humidity (percent). In the absence of better information, H may be taken from AASHTO LRFD BDS Figure 5.4.2.3.3-1 (AASHTO 2020)

f'_{ci} = design UHPC compressive strength at the time of pre-stressing for pretensioned members and at the time of initial loading for nonprestressed members (ksi)

t = maturity of UHPC (day)

t_i = age of UHPC at time of load application (day)

The factor for the effect of loading age, k_ℓ, shall be determined as follows:

If $t_i < 7.0$ days, then $k_\ell = 1.0$ (1.4.2.8.2-6)

If $t_i \geq 7.0$ days, then $k_\ell = (t_i - 6)^{-0.15} \geq 0.5$

(1.4.2.8.2-7)

1.4.2.8.3. Shrinkage

The strain due to shrinkage, ε_{sh}, at time, t, may be taken as:

$$\varepsilon_{sh} = 0.6 \times 10^{-3}\, k_s\, k_{hs}\, k_f\, k_{td}\, K_4 \qquad (1.4.2.8.3\text{-}1)$$

in which:

$$k_{hs} = 1.5 - 0.01H \qquad (1.4.2.8.3\text{-}2)$$

where:

k_{hs} = humidity factor for shrinkage

K_4 = correction factor for shrinkage to be taken as 1.0 unless determined by physical test, and as approved by the owner

C1.4.2.8.3

Shrinkage of UHPC is caused by both drying effects and autogenous behaviors associated with hydration and other chemical reactions occurring during curing. Autogenous shrinkage in UHPC is proportionally much larger than that occurring in conventional concrete and predominantly takes place during the early strength development of the material. This effect is in contract to conventional concrete, where most of the shrinkage is related to drying effects and occurs later in the curing process. Additional information on shrinkage in UHPC can be found in Haber et al. 2018.

The constraining effects of reinforcement and composite actions with other elements of the structure tend to reduce the dimensional changes in some components.

The factor K_4 is included to allow calculated shrinkage strain values to be adjusted for a specific UHPC product. It is assumed to be 1.0, except for situations where specific knowledge is available. The K_4 factor may be determined from physical tests on shrinkage performed according to ASTM C1856/C1856M. The testing procedure for the shrinkage strain of UHPC is in accordance with ASTM C157/C157M (ASTM 2017e), with exceptions listed in Section 8.5 of ASTM C1856/C1856M (ASTM 2017a).

1.4.3. Reinforcing Steel

The provisions of AASHTO LRFD BDS Article 5.4.3 (AASHTO 2020) shall apply.

C1.4.3

The total elongation under load for reinforcing steel conforming to the requirements of AASHTO LRFD BDS Article 5.4.3 (AASHTO 2020) are defined within the referenced documents. The value is contingent on the type of steel, the grade of steel, and the size of the reinforcing bar.

1.4.4. Prestressing Steel

The provisions of AASHTO LRFD BDS Article 5.4.4 (AASHTO 2020) shall apply.

When 0.62-in.- or 0.7-in.-diameter strands are used, the provisions for 0.6-in.-diameter strands in AASHTO LRFD BDS Article 5.4.4 (AASHTO 2020) shall apply.

The total elongation under load for prestressing strands and bars conforming to the material standards specified in AASHTO LRFD BDS Article 5.4.4.1 (AASHTO 2020) shall not be less than 0.035 and 0.04, respectively.

1.5. LIMIT STATES AND DESIGN METHODOLOGIES

1.5.1. General

The provisions of AASHTO LRFD BDS Articles 5.5.1.1, 5.5.1.2.1, and 5.5.1.2.2 (AASHTO 2020) shall apply; reference to Articles 5.6 and 5.7 (AASHTO 2020) shall be replaced by Articles 1.6 and 1.7 of this Appendix, respectively. Design practices for D-Regions shall be in accordance with Article 1.8.

1.5.2. Service Limit State

C1.5.2

Actions to be considered at the service limit state shall be cracking, deformations, stresses, and strains. The following provisions shall apply:

- The cracking strength shall be taken as $\gamma_u f_{t,cr}$ as specified in Articles 1.4.2.5.1 and 1.4.2.5.4 of this Appendix.
- Deformations shall be in accordance with Article 1.6.3.5 of this Appendix.

For prestressed components:

- The section properties for service limit state may be based on uncracked sections when the extreme fiber tensile stress due to Service III load combination specified in AASHTO LRFD BDS Table 3.4.1-1 (AASHTO 2020) does not exceed $\gamma_u f_{t,cr}$.

- The stress limits for prestressing steel and stresses at the service limit state after losses shall be in accordance with Articles 1.9.2.2 and 1.9.2.3 of this Appendix, respectively.

For nonprestressed components with or without reinforcement:

- Service stress limit shall be investigated using the Service Limit State Combination I specified in AASHTO LRFD BDS Table 3.4.1-1 (AASHTO 2020).

- The section properties for service limit state investigations shall be based on cracked sections when the extreme tensile stress exceeds $\gamma_u f_{t,cr}$.

- The strain in the UHPC at extreme tension fiber shall not exceed the lesser of $0.25\gamma_u \varepsilon_{t,loc}$ or 0.001, where $\varepsilon_{t,loc}$ is the crack localization strain specified in Article 1.4.2.5.3 of this Appendix.

  The upper limit of 0.001 on the service strain for nonprestressed UHPC is adopted from the Swiss recommendation SIA 2052 *UHPFRC: Materials, Design, and Application* (Swiss Institute of Architects and Engineers 2016).

- The compressive stress at extreme compression fiber shall not exceed $0.45f'_c$ due to permanent loads and $0.60\phi_w f'_c$ due to permanent and transient loads, as well as during shipping and handling. The reduction factor, ϕ_w, shall be taken equal to 1.0 when the web and flange slenderness ratio, calculated according to AASHTO LRFD BDS Article 5.6.4.7.1 (AASHTO 2020), is not greater than 15. When either the web or flange slenderness ratio is greater than 15, the reduction factor, ϕ_w, shall be calculated according to AASHTO LRFD BDS Article 5.6.4.7.2 (AASHTO 2020).

  The compressive strength limits for non-prestressed UHPC at the service limit state are similar to the limits on prestressed elements as specified in AASHTO LRFD BDS Article 5.9.2.3.2a (AASHTO 2020).

- The principal tensile stresses in webs of components shall not exceed $\gamma_u f_{t,cr}$ when the superstructure element is subjected to loadings of Service I load combination. The principal tensile stresses shall be determined using the combination of axial and shear stress which produces the greatest principal tensile stress, and the shear stresses shall be determined using vertical shear and concurrent torsion.

  The principal tensile stress check addresses limit web cracking at a service limit state. Shear flow may be determined by analytical methods and/or finite element analysis. The provisions of Article 1.9.2.3.3 of this Appendix may apply.

- The stress limit for steel reinforcement in nonprestressed components shall be taken as $0.80f_y$, where f_y is the steel yielding stress.

1.5.3. Fatigue Limit State

The fatigue limit state shall be evaluated as follows:

- The tensile stress in UHPC due to the Service I load combinations shall not exceed $0.95\gamma_u f_{t,cr}$.

C1.5.3

Due to lack of sufficient experimental data on fatigue of cracked UHPC, members subjected to cyclic stresses from live loads must be designed to be uncracked. Members that have been subjected to tensile stresses exceeding the cracking strength (e.g., members subjected to loads approaching the Strength I limit state) may be susceptible to fatigue damage from subsequent cyclic loadings.

The Service I load combination is used for the Fatigue Limit State in UHPC in order to reduce the likelihood that cracked UHPC will be subjected to cyclic loads. This requirement often controls the design of nonprestressed components; per Article 1.5.2 of this Appendix, prestressed components are designed to be uncracked at service.

This tensile stress limit of $0.95\gamma_u f_{t,cr}$ applies to the tensile stress in members in all directions, including the longitudinal, transverse, and principal directions.

The specified fatigue tensile stress limit is adopted from the French Standard for fatigue considerations of UHPC components (NF P18-710, Association Française de Normalisation 2016).

- Discrete steel elements embedded in UHPC shall be checked for fatigue in accordance with AASHTO LRFD BDS Eq. 5.5.3.1-1 and Articles 5.5.3.2, 5.5.3.3, and 5.5.3.4 (AASHTO 2020).

Due to the lack of sufficient experimental data on fatigue of UHPC, these provisions require all discrete steel elements to be checked to ensure their stress ranges, in the uncracked section, remain less than the fatigue threshold. While these provisions require that sections designed for fatigue remain uncracked, checking discrete

steel elements is required since the compressive and tensile strengths of UHPC are greater than that of conventional concrete and certain design scenarios may elevate the stress ranges in discrete steel elements more than if they were embedded in the same design of conventional concrete.

- For prestressed components, the compressive stress due to the Fatigue I load combination and one-half the sum of the unfactored effective prestress and permanent loads shall not exceed $0.40f'_c$ after losses.

The compressive stress limit for prestressed UHPC is adopted from AASHTO LRFD BDS Article 5.5.3.1 (AASHTO 2020).

- For nonprestressed components, the compressive stress due to the Fatigue I load combination and one-half of the unfactored permanent loads shall not exceed $0.40f'_c$.

The compressive stress limit for nonprestressed UHPC is adopted from AASHTO LRFD BDS Article 5.5.3.1 (AASHTO 2020).

1.5.4. Strength Limit State

1.5.4.1. General

The strength limit state issues to be considered shall be those of strength, ductility, and stability.

Factored resistance shall be the product of nominal resistance as determined in accordance with the applicable provisions of Articles 1.6, 1.7, 1.9, and 1.10 of this Appendix, unless another limit state is specifically identified, and the resistance factor as specified in Article 1.5.4.2 of this Appendix.

1.5.4.2. Resistance Factors

The provisions of this Article are applicable to prestressed and nonprestressed UHPC sections.

Resistance factor ϕ shall be taken as:

C1.5.4.2

The resistance factors for flexural capacity are based on sectional ductility considerations. A curvature ductility ratio, μ, is defined as the ratio of the sectional curvature at the nominal moment resistance over a baseline sectional curvature as specified in Article 1.6.3.2.3 of this Appendix. The background for these provisions is given in El-Helou and Graybeal (2022a).

40

- For flexural capacity of sections with curvature ductility ratio, μ, greater than the curvature ductility ratio limit, μ_ℓ .... 0.90.

- For flexural capacity of sections with curvature ductility ratio, μ, less than 1.0 .... 0.75.

- For flexural capacity of sections with no tensile reinforcement......... 0.75.

- For compression members ..... 0.75.

- For tension members and members subjected to combined tension and flexure .... 0.75.

- For shear and torsion in reinforced and unreinforced sections .... 0.90.

- For bearing on UHPC .... 0.70.

- For resistance during pile driving .... 1.00.

For sections in which the curvature ductility ratio, μ, is between the curvature ductility ratio limit, μ_ℓ, and 1.0, the value of ϕ associated with the curvature ductility ratio may be obtained by a linear interpolation from 0.75 to 0.90.

This variation of ϕ may be computed for prestressed and nonprestressed members such that:

$$0.75 \leq \phi = 0.75 + \frac{0.15(\mu - 1.0)}{(\mu_\ell - 1.0)} \leq 0.90$$

(1.5.4.2-1)

Sections are assumed to be ductile and assigned a ϕ factor of 0.90 if their curvature ductility ratio, μ, is equal to or greater than the curvature ductility ratio limit, μ_ℓ.

Sections with μ less than or equal to 1.0 are less ductile and are assigned a ϕ factor of 0.75, akin to the ϕ factor for compression-controlled sections specified in AASHTO LRFD BDS Article 5.5.4.2 for conventional concrete (AASHTO 2020).

Sections with μ between 1.0 and μ_ℓ are classified as transitional and assigned a linearly varying ϕ factor in the transition zone between the two extreme values of μ, as shown in Figure C1.5.4.2-1.
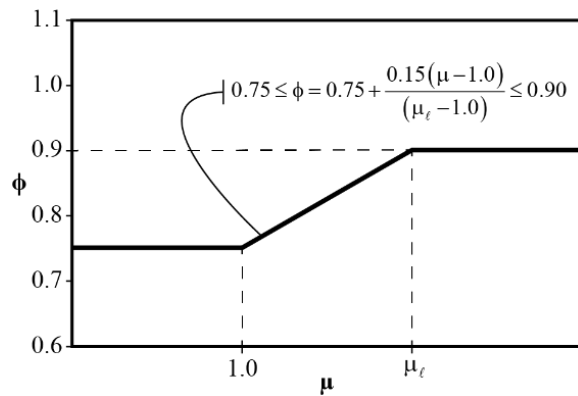
Source: FHWA.

Figure C1.5.4.2-1—Variation of the flexural resistance factor, ϕ, with the curvature ductility ratio, μ, for UHPC sections reinforced with prestressed steel, nonprestressed steel, or both.

The resistance factor ϕ for shear capacity is assigned a value of 0.90, in line with AASHTO LRFD BDS Article 5.5.4.2 provisions for shear in reinforced concrete sections (AASHTO 2020).

Where combinations of different grades of reinforcement, or of prestressed and nonprestressed reinforcement, are used in design, the lowest resistance factor calculated for each grade or type of reinforcement shall be used.

The value of the yield stress of different types or grades of reinforcement will result in different values of the baseline sectional curvature, $\psi_{s\ell}$, as specified in Article 1.6.3.2.3 of this Appendix, which, consequently, leads to different values of μ_ℓ and ϕ. The lowest value of ϕ should be used to calculate the flexural resistance of the member.

1.5.4.3. Stability

The provisions of AASHTO LRFD BDS Article 5.5.4.3 (AASHTO 2020) shall apply.

1.5.5. Extreme Event Limit State

The provisions of AASHTO LRFD BDS Article 5.5.5 (AASHTO 2020) shall apply.

1.6. DESIGN FOR FLEXURAL AND AXIAL FORCE EFFECTS—B REGIONS

1.6.1. Assumptions for Service and Fatigue Limit States

The provisions of AASHTO LRFD BDS Article 5.6.1 shall apply with the following amendments:

- Reference to the provisions of AASHTO LRFD BDS Article 5.6.6 (AASHTO 2020) shall not apply.

- Reference to AASHTO LRFD BDS Article 5.4.2.3.2 (AASHTO 2020) shall be replaced by Article 1.4.2.8.2 of this Appendix.

Nonprestressed UHPC not subject to fatigue loads resists tension when the tensile strain does not exceed the lesser of $0.25\gamma_u\varepsilon_{t,loc}$ or 0.001. The tensile strains shall be determined from a strain compatibility approach, utilizing a representative steel stress-strain curve and the tensile design models of Article 1.4.2.5.4 of this Appendix.

Nonprestressed and prestressed UHPC subject to fatigue loads resists tension at sections that are uncracked when the extreme tension stress does not exceed $0.95\gamma_u f_{t,cr}$.

1.6.2. Assumptions for Strength and Extreme Event Limit States

Factored resistance of UHPC components shall be based on the conditions of equilibrium and strain compatibility as specified in Article 1.6.3 of this Appendix, the resistance factors as specified in Article 1.5.4.2 of this Appendix, and the following assumptions:

- In components with bonded reinforcement or prestressing, or in the bonded length of debonded strands, strain is directly proportional to the distance from the neutral axis, except for deep components that shall satisfy the requirements for disturbed regions.

- If the UHPC is unconfined, the maximum usable strain at extreme UHPC compression fiber is not greater than the ultimate compression strain, ε_{cu}, as specified in Article 1.4.2.4.2 of this Appendix.

- If the UHPC is confined, a maximum usable strain exceeding ε_{cu} in the confined core may be utilized if verified by physical test. Calculation of the factored resistance shall consider that the UHPC cover may be lost at strains compatible with those in the confined core.

- The UHPC compressive stress-strain distribution is assumed to follow the uniaxial compression design model specified in Article 1.4.2.4.3 of this Appendix.

- In components with prestressed and nonprestressed reinforcement, the

maximum usable strain at extreme UHPC tensile fiber is not greater than $\gamma_u \varepsilon_{t,loc}$.

- In components with no tensile reinforcement, the maximum usable strain in extreme UHPC tensile fiber is not greater than $0.5\gamma_u \varepsilon_{t,loc}$.

Components with no tensile reinforcement have lesser ability to share tensile loads between the UHPC and the reinforcement, thus necessitating extra restrictions on the tensile strain capacity.

- The UHPC tensile stress-strain distribution is assumed to follow the uniaxial tensile design models specified in Article 1.4.2.5.4 of this Appendix.

- The strain in the reinforcement is not greater than the minimum total elongation strain determined according to Article 1.4.3 of this Appendix for reinforcing steel and Article 1.4.4 of this Appendix for prestressing steel.

- The stress in the reinforcement is based on a stress–strain curve representative of the steel or on an approved mathematical representation, including development of reinforcement and prestressing elements and transfer of pretensioning.

- Except as specified in Article 1.6.3.3 of this Appendix, the calculated stress in nonprestressed reinforcement shall not be taken as greater than the specified minimum yield strength.

Unless specifically permitted by provisions in this Appendix, the strain hardening strength of nonprestressed reinforcement may not be used in design.

- The development of reinforcement and prestressing elements and transfer of pretensioning are considered.

- The curvature ductility ratio limit, μ_ℓ, defined in Article 1.5.4.2 of this Appendix, shall be greater than or equal to 3.0.

- The use of compression reinforcement in conjunction with additional tension reinforcement is permitted to increase the strength of flexural members.

Additional limitations on the maximum usable extreme UHPC compressive strain in hollow rectangular compression members shall be investigated as specified in Article 1.6.4 of this Appendix.

1.6.3. Flexural Members

The following methods shall be used for UHPC sections with bonded reinforcement.

1.6.3.1. Strain Compatibility Approach

The strain compatibility approach shall be used to determine the nominal moment resistance, M_n, the sectional curvature at nominal moment resistance, ψ_n, and the sectional curvature when the stress in the extreme tension steel is equal to the steel service stress, $\psi_{s\ell}$, as specified in Article 1.6.3.2 of this Appendix.

The stress and corresponding strain in any given layer of the UHPC, prestressing steel, and/or nonprestressed reinforcement shall be taken from representative stress-strain models as specified in Articles 1.4.2.4.3, 1.4.2.5.4, and 1.6.2 of this Appendix. The conditions of force equilibrium in the section shall be satisfied, and the nominal flexural strength shall be calculated directly from the stresses resulting from this analysis.

C1.6.3

The proposed framework for flexural members is derived from El-Helou and Graybeal (2022a) and validated for prestressed and non-prestressed UHPC beams performed by El-Helou and Graybeal (2022a), Chen et al. (2018), Yoo, Banthia, and Yoon (2017), Qiu et al. (2020), Yoo and Yoon (2015), and Graybeal (2006b, 2009a).

C1.6.3.1

The idealized moment-curvature (M-ψ) response for a nonprestressed flexural member utilizing the full tensile strain capacity of UHPC is shown in Figure C1.6.3.1-1. The M-ψ response can be idealized with the key points identified in Figure C1.6.3.1-1. The first point in the behavior (M_{cr}-ψ_{cr}) is the nominal moment and curvature at the initiation of the first flexural crack. At this point, the strain at extreme UHPC tensile fiber, ε_t, is equal to the cracking strain $\varepsilon_{t,cr}$. The second point ($M_{s\ell}$-$\psi_{s\ell}$) is an intermediate point defining the nominal moment and curvature when the stress in the extreme tensile steel layer is equal to steel service stress limit, $f_{s\ell}$. This point defines the baseline sectional curvature for calculation of the section ductility ratio as specified in Article 1.6.3.2.3 of this Appendix. The third point in the moment-curvature response (M_y-ψ_y) coincides with the yielding of the extreme tension steel layer. The yielding moment occurs prior to the localization of cracks, as depicted in Figure C1.6.3.1-1 when the UHPC crack

45

localization strain is greater than the yielding strain of flexural steel reinforcement ($\gamma_u \varepsilon_{t,loc} > \varepsilon_y$). The fourth point in the behavior corresponds to the nominal moment resistance and curvature at localization of cracks (M_L-ψ_L) occurring when the strain at extreme UHPC tensile fiber, ε_t, is equal to $\gamma_u \varepsilon_{t,loc}$, as shown in Figure C1.6.3.2.2-1. Note that the case demonstrated in the figure shows the UHPC tensile strain limit larger than the yielding strain of the flexural steel reinforcement ($\gamma_u \varepsilon_{t,loc} > \varepsilon_y$); this may not always be the case.
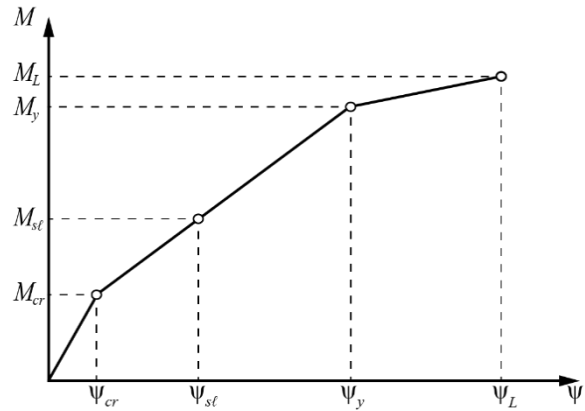
Source: FHWA.

Figure C1.6.3.1-1—Moment-curvature response of UHPC sections reinforced with nonprestressed steel failing at localization of cracks ($\varepsilon_t = \gamma_u \varepsilon_{t,loc}$) and with $\gamma_u \varepsilon_{t,loc} > \varepsilon_y$.

1.6.3.2. Flexural Resistance

1.6.3.2.1. Factored Flexural Resistance

The factored flexural resistance, M_r, shall be taken as:

$$M_r = \phi M_n \qquad (1.6.3.2.1-1)$$

where:

M_n = nominal flexural resistance (kip-in.)

ϕ = resistance factor as specified in Article 1.5.4.2 of this Appendix

1.6.3.2.2. Nominal Flexural Resistance

The nominal flexural resistance shall be obtained from a strain compatibility analysis according to Article 1.6.3.1 of this Appendix and shall be taken as the moment corresponding to the lesser of the sectional curvature values calculated when:

- The compressive strain at the extreme compression fiber of the UHPC section is equal to the compression strain limit, ε_{cu},

- The net tensile strain at extreme tension fiber of the UHPC section is equal to the UHPC tensile strain limit, $\gamma_u \varepsilon_{t,loc}$, and,

- The strain in the extreme tension steel is equal to the minimum total elongation strain of reinforcing steel.

C1.6.3.2.2

The nominal flexural resistance is based on strain compatibility and equilibrium computations at key points in the behavior corresponding to the attainment of the strain limits of the UHPC in tension or compression. Limit states pertaining to other materials used in a composite section, such as the crushing limit of a conventional concrete deck acting compositely with a UHPC beam, should also be considered when relevant. The nominal flexural resistance should always be taken at the smallest sectional curvature value corresponding to all relevant limit states.

For sections fully utilizing the postcracking capacity of UHPC, the nominal flexural resistance is taken when the strain in the UHPC at extreme tension fiber, ε_t, is equal to the UHPC tensile strain limit, $\gamma_u \varepsilon_{t,loc}$, as shown in Figure C1.6.3.2.2-1 (i.e., $M_n = M_L$). In this failure mode, the UHPC stresses in compression remain elastic if the strain at extreme compression fiber, ε_c, is less than ε_{cp}, as shown in part (a) of Figure C1.6.3.2.2-1, or become plastic if $\varepsilon_{cp} < \varepsilon_c < \varepsilon_{cu}$, as shown in part (b) of Figure C1.6.3.2.2-1.

The flexural behavior after crack localization ($\varepsilon_t > \gamma_u \varepsilon_{t,loc}$) is not considered for use in design because of the formation of a localized crack on the tension side of the beam, the loss of UHPC fiber bridging capacity, and the hinging of the beam about the section with the localized crack. The large crack opening at the section with the localized crack strains the tensile reinforcement over a short distance, increasing the risk of reinforcement rupture.

For flexural members with significant axial compressive stress or high levels of longitudinal steel reinforcement, the nominal flexural resistance may occur at the crushing of UHPC ($M_n = M_c$). In this failure mode, the strain in the UHPC at the extreme compression layer, ε_c, is equal to the ultimate compressive strain, ε_{cu},

while the strain in the extreme tensile fiber, ε_t, is less than the UHPC tensile strain limit, $\gamma_u\varepsilon_{t,loc}$, as shown in Figure C1.6.3.2.2-1.

Figure C1.6.3.2.2-1 and Figure C1.6.3.2.2-2 depict the tensile stresses of a UHPC material by adopting the idealized stress-strain model of Figure 1.4.2.5.4-1. When $f_{t,loc} > 1.20f_{t,cr}$, the idealized stress-strain model of Figure 1.4.2.5.4-2 may be used instead.
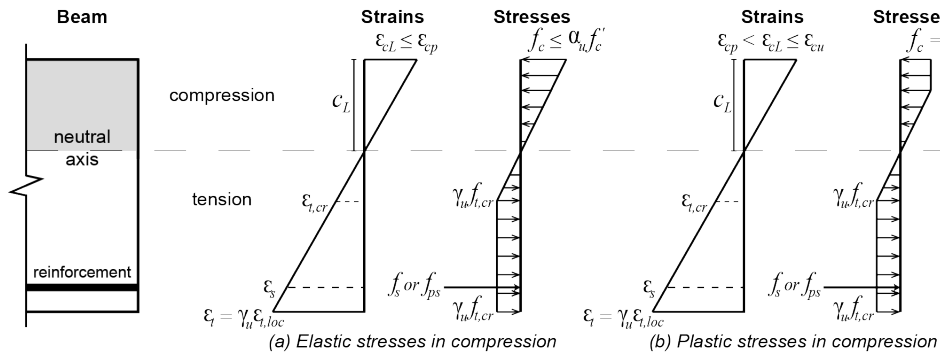
Source: FHWA.
Note: See notation list in Article 1.3 of this Appendix for variable definitions.

Figure C1.6.3.2.2-1—Stress and strain conditions for UHPC sections in flexure at the onset of crack localization, shown for UHPC material exhibiting the tensile stress-strain behavior of Figure 1.4.2.5.4-1.
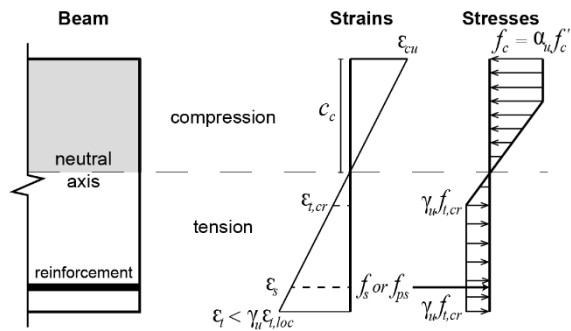
Source: FHWA.
Note: See notation list in Article 1.3 of this Appendix for variable definitions.

Figure C1.6.3.2.2-2—Stress and strain conditions for UHPC sections in flexure at UHPC crushing, shown for UHPC material exhibiting the tensile stress-strain behavior of Figure 1.4.2.5.4-1.

48

1.6.3.2.3. Curvature Ductility Ratio

The curvature ductility ratio, μ, defined as the ratio of the sectional curvature at the nominal moment resistance over the baseline sectional curvature, shall be calculated at nominal flexural strength such as:

$$\mu = \frac{\psi_n}{\psi_{s\ell}}$$
(1.6.3.2.3-1)

in which:

$$\psi_{s\ell} = \frac{\varepsilon_{cs\ell}}{c_{s\ell}}$$
(1.6.3.2.3-2)

where:

ψ_n = sectional curvature of the UHPC section at nominal flexural strength, as specified in Article 1.6.3.2.2 of this Appendix (1/in.)

$\psi_{s\ell}$ = sectional curvature of the UHPC section when the steel stress in the extreme tension steel is equal to the steel service stress limit, $f_{s\ell}$ (1/in.)

$c_{s\ell}$ = distance from the extreme compression fiber of the UHPC section to the neutral axis when the steel stress in the extreme tension steel is equal to the steel service stress limit, $f_{s\ell}$ (in.)

$\varepsilon_{cs\ell}$ = strain in the extreme compression fiber of the UHPC section when the steel stress in the extreme tension steel is equal to the steel service stress limit, $f_{s\ell}$ (in./in.)

$f_{s\ell}$ = stress limit in steel at service loads, as defined in Article 1.5.2 of this Appendix (ksi)

For sections controlled by the UHPC tensile strain limit, $\gamma_u \varepsilon_{t,loc}$, at extreme tension fiber, the sectional curvature at nominal flexural strength, ψ_n, shall be taken as:

$$\psi_n = \frac{\varepsilon_{cL}}{c_L}$$
(1.6.3.2.3-3)

C1.6.3.2.3

The flexural resistance is based on sectional curvature ductility considerations to ensure that large deformations occur before failure of the member. The approach is based on calculating a curvature ductility ratio, μ, defined as the ratio of the sectional curvature at the nominal moment resistance, ψ_n, over the baseline sectional curvature, $\psi_{s\ell}$. The baseline sectional curvature is computed when the stress in the extreme tension steel is equal to 80 percent of the yielding stress of the reinforcement, as shown in Figure C1.6.3.2.3-1. For prestressed members, this limit coincides with the stress limit for prestressing steel at service limit state, as specified in AASHTO LRFD BDS Article 5.9.2.2 (AASHTO 2020). The UHPC compression stresses depicted in Figure C1.6.3.2.3-1 are assumed to remain elastic.
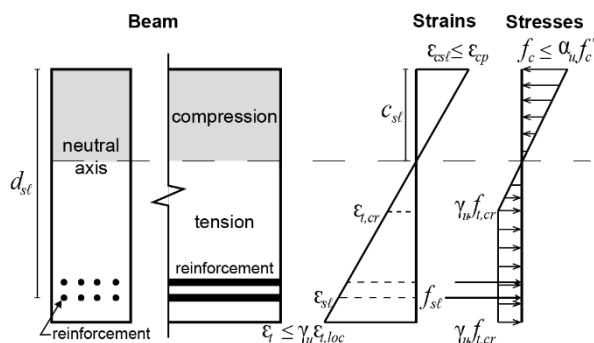
Source: FHWA.

Note: See notation list in Article 1.3 of this Appendix for variable definitions.

Figure C1.6.3.2.3-1—Stress and strain conditions for UHPC sections when the stress in the extreme tension steel is equal to $f_{s\ell}$, shown for UHPC material exhibiting the tensile stress-strain behavior of Figure 1.4.2.5.4-1.

Sections with curvature ductility ratios, μ, greater than the ductility ratio limit, $\mu_\ell = 3.0$, are considered ductile and assumed to provide sufficient member deformation before crack

For sections controlled by the UHPC compression strain limit, ε_{cu}, at extreme compression fiber, the sectional curvature at nominal flexural strength, ψ_n, shall be taken as:

$$\psi_n = \frac{\varepsilon_{cu}}{c_c} \qquad (1.6.3.2.3\text{-}4)$$

where:

ε_{cL} = strain in the extreme compression fiber of the UHPC section when the UHPC tensile strain limit, $\gamma_u \varepsilon_{t,loc}$, at extreme tension fiber is reached (in./in.)

c_L = distance from the extreme compression fiber of the UHPC section to the neutral axis when the UHPC tensile strain limit, $\gamma_u \varepsilon_{t,loc}$, at extreme tension fiber is reached (in.)

c_c = distance from the extreme compression fiber of the UHPC section to the neutral axis when the UHPC compression strain limit, ε_{cu}, at extreme compression fiber is reached (in.)

1.6.3.3. Minimum Reinforcement

The provisions of AASHTO LRFD BDS Article 5.6.3.3 shall apply with the following amendments:

- The modulus of rupture of concrete in AASHTO LRFD BDS Eq. 5.6.3.3-1 (AASHTO 2020) shall be replaced with the UHPC effective cracking strength, $f_{t,cr}$, as specified in Article 1.4.2.5.1 of this Appendix.

- Reference to AASHTO LRFD BDS Article 5.4.2.6 (AASHTO 2020) shall not apply.

- The provisions of AASHTO LRFD BDS Article 5.10.6 (AASHTO 2020) need not apply.

localization. When members have curvature ductility less than μ_ℓ, a reduced resistance factor, ϕ, is imposed in recognition of the nonductile behavior, as specified in Article 1.5.4.2 of this Appendix.

For composite sections made with UHPC beams and UHPC or conventional concrete decks:

- $\psi_{s\ell}$ should be calculated for the UHPC beam when the steel service stress limit, $f_{s\ell}$, is first reached in the extreme tension steel of either the UHPC beam or composite section, and

- ψ_n should be computed for the UHPC beam at the governing limit state at nominal flexural strength pertaining to all materials used in the composite section.

The factor γ_u is conservatively not applied to the effective cracking stress, $f_{t,cr}$.

1.6.3.4. Moment Redistribution

Unless refined analysis is performed and as approved by the owner, redistribution of moments is not permitted.

1.6.3.5. Deformations

The provisions of AASHTO LRFD BDS Article 5.6.3.5 shall apply with the following amendments:

- Reference to AASHTO LRFD BDS Articles 5.4.2.2, 5.4.2.3, and 5.4.2.4 (AASHTO 2020) shall be replaced by Articles 1.4.2.7, 1.4.2.8, and 1.4.2.3 of this Appendix, respectively.

- The modulus of rupture of concrete in AASHTO LRFD BDS Eq. 5.6.3.5.2-2 (AASHTO 2020) shall be replaced with $\gamma_u f_{t,cr}$, as specified in Article 1.4.2.5.1 of this Appendix.

- Reference to AASHTO LRFD BDS Article 5.4.2.6 (AASHTO 2020) shall not apply.

C1.6.3.4

Any analysis for moment redistribution should consider the UHPC strain capacity.

C1.6.3.5

Calculated camber values should be treated as estimates. The effects of camber variation, roadway profile, and roadway cross slope can affect key geometric parameters such as haunch height, among others. These can affect the design of the beams due to the variation of the dead loads and can also affect the detailing of items such as bearing size, beam seat elevations, and the roadway profile.

The following are the major causes of camber variation:

- UHPC modulus of elasticity variation based on the mix design, curing, and storage.

- Prestress loss variation.

- UHPC strength and stiffness variation at the time of prestress application.

These variables, which are part of the normal component fabrication process, are not known to the designer during design stage when camber estimates are calculated. Tolerances on camber predictions should be considered. Camber predictions should be revisited once initial UHPC member fabrication commences.

1.6.4. Compression Members

Except for the limit on design compressive strengths, the provisions of AASHTO LRFD BDS Articles 5.6.4.1 through 5.6.4.6 and Article 5.6.4.7.1 shall apply, in which references to AASHTO LRFD BDS Articles 5.5.4.2 and 5.10.4 (AASHTO 2020) shall be replaced with Articles 1.5.4.2 and 1.10.4 of this Appendix.

1.6.5. Bearing

The provisions of AASHTO LRFD BDS Article 5.6.5 (AASHTO 2020) shall apply.

1.6.6. Tension Members

1.6.6.1. Resistance to Tension

Members in which the factored loads induce tensile stresses throughout the cross section shall be regarded as tension members.

The factored resistance to uniform tension shall be taken as:

$$P_r = \phi P_n \qquad (1.6.6.1\text{-}1)$$

where:

P_n = nominal resistance of a tension member determined according to Eq. 1.6.6.1-2 (kip)

ϕ = resistance factor specified in Article 1.5.4.2 of this Appendix

The nominal resistance of a tension member shall be taken as:

$$P_n = P_{UHPC} + P_s \qquad (1.6.6.1\text{-}2)$$

in which:

$$P_{UHPC} = 0.60\gamma_u f_{t,cr} A_g \qquad (1.6.6.1\text{-}3)$$

$$P_s = 0.50 E_s\, \gamma_u\, \varepsilon_{t,loc}\, A_s + A_{ps}\, [f_{pe} + 0.50 E_s\, \gamma_u\, \varepsilon_{t,loc}] \qquad (1.6.6.1\text{-}4)$$

where:

A_g = gross area of the cross section of the member (in.^{2})

E_s = modulus of elasticity of the nonprestressed steel reinforcement (ksi)

A_s = total area of longitudinal nonprestressed reinforcement (in.^{2})

A_{ps} = area of prestressing steel (in.^{2})

C1.6.6.1

The design approach for tension members applies reduction factors to the UHPC and steel mechanical properties because more research is needed to investigate the behavior of UHPC in tension members.

The nominal resistance of a tension member described in Eqs. 1.6.6.1-1 through 1.6.6.1-4 reduces the effective cracking strength, $f_{t,cr}$, to $0.60\gamma_u f_{t,cr}$ and ignores the increased postcracking resistance for materials exhibiting the bilinear behavior shown in Figure 1.4.2.5.4-2. The maximum usable tensile strain of UHPC is also reduced to $0.50\gamma_u\varepsilon_{t,loc}$. The stress in nonprestressed reinforcement is limited to $0.80f_y$, and the stress in prestressed reinforcement is limited to $0.80f_{py}$.

f_{pe} = effective stress in prestressing steel after losses (ksi)

In use of Eqs. 1.6.6.1-1 through 1.6.6.1-4, the following should be considered:

- The sum of f_{pe} and $0.50E_s\gamma_u\varepsilon_{t,loc}$ shall not be taken as greater than 80 percent of the yield strength of the prestressing steel, $0.80f_{py}$.

- The term $0.50E_s\gamma_u\varepsilon_{t,loc}$ shall not be taken as greater than 80 percent of the yield strength of the nonprestressed longitudinal steel, $0.80f_y$.

- The nominal resistance of the steel contribution, P_s, shall exceed $0.80P_n$.

- The provisions of AASHTO LRFD BDS Article 5.10.8.4.4 (AASHTO 2020) shall apply.

1.6.6.2. Resistance to Combined Tension and Flexure

Members subjected to eccentric tension loading, which induces both tensile and compressive stresses in the cross section, shall be proportioned in accordance with the provisions of Article 1.6.3 of this Appendix with the following amendments:

- The values of the effective cracking strength, $f_{t,cr}$, and localization strength, $f_{t,loc}$, specified in Articles 1.4.2.5.1 and 1.4.2.5.2 of this Appendix, shall be taken as $0.60\gamma_u f_{t,cr}$ and $0.60\gamma_u f_{t,loc}$, respectively.

- The crack localization strain, $\varepsilon_{t,loc}$, specified in Article 1.4.2.5.3 of this Appendix shall be taken as $0.50\varepsilon_{t,loc}$.

- The yield stress of tension reinforce-ment shall be taken as $0.80f_{py}$ for prestressed reinforcement and $0.80f_y$ for nonprestressed reinforcement.

- The ultimate strength, f_{pu}, of pre-stressing strands shall be taken as $0.80f_{pu}$.

1.7. DESIGN FOR SHEAR AND TORSION—B-REGIONS

1.7.1. Design Procedures

The provisions of AASHTO LRFD BDS Articles 5.7.1.1 through 5.7.1.4 (AASHTO 2020) shall apply with the following amendments:

- References to AASHTO LRFD BDS Articles 5.7.2, 5.7.3, and 5.7.4 (AASHTO 2020) shall be replaced by Articles 1.7.2, 1.7.3, and 1.7.4 of this Appendix.

- References to AASHTO LRFD BDS Articles 5.8.2 and 5.8.4 (AASHTO 2020) shall be replaced by Article 1.8 of this Appendix.

- The provisions of Articles 5.12.5.3.8 and 5.12.8.6 (AASHTO 2020) shall not apply.

1.7.2. General Requirements

1.7.2.1. General   *C1.7.2.1*

The provisions of AASHTO LRFD BDS Article 5.7.2.1 (AASHTO 2020) shall apply with the following amendments:

- References to AASHTO LRFD BDS Articles 5.9.2.3.3 (AASHTO 2020) shall be replaced by Articles 1.5.2 and 1.9.2.3.3 of this Appendix.

- The upper limit on the compressive strength of concrete for use in design shall not apply.

- References to AASHTO LRFD BDS Articles 5.5.4.2, 5.7.3, 5.7.3.3, and 5.7.3.6 (AASHTO 2020) shall be replaced by Articles 1.5.4.2, 1.7.3, 1.7.3.3, and 1.7.3.6 of this Appendix, respectively.

- Torsional moment redistribution is not permitted.

- AASHTO LRFD BDS Eqs. 5.7.2.1-3 through 5.7.2.1-6 (AASHTO 2020) shall be replaced with Eqs. 1.7.2.1-1 through 1.7.2.1-4 of this Appendix, respectively.

Torsional effects shall be investigated where:

$$T_u > 0.10\phi T_{cr} \qquad (1.7.2.1\text{-}1)$$

The indicated fraction of the factored pure torsional cracking moment (i.e., $0.10\phi T_{cr}$) is expected to cause a very small reduction in the shear capacity or flexural capacity and, hence, can be neglected. In the absence of sufficient data on torsional resistance of UHPC, the indicated fraction of Eq. 1.7.2.1-1 is chosen to be 2.5 times smaller than the fraction specified in AASHTO LRFD BDS Eq. 5.7.2.1-3 (AASHTO 2020). This smaller fraction offsets the increased tensile resistance of UHPC compared to conventional concrete, resulting in a comparatively similar requirement for torsional transverse reinforcement. This reduction is necessary to reserve a portion of the tensile resistance to resist shear loads in members subjected to combined shear and torsion.

For solid shapes:

$$T_{cr} = \gamma_u f_{t,cr} \, K \, \frac{A_{cp}^{\,2}}{p_c} \qquad (1.7.2.1\text{-}2)$$

For hollow shapes:

$$T_{cr} = \gamma_u f_{t,cr} \, K (2A_o \, b_e) \qquad (1.7.2.1\text{-}3)$$

Eqs. 1.7.2.1-1 through 1.7.2.1-4 were developed by replacing the tensile resistance term of conventional concrete in AASHTO LRFD BDS Eqs. 5.7.2.1-4 through 5.7.2.1-6 (AASHTO 2020) with $\gamma_u f_{t,cr}$ and taking the concrete density factor equal to 1.0.

55

in which:

$$K = \sqrt{1+\frac{f_{pc}}{f_{t,cr}}} \leq 2.0 \qquad (1.7.2.1\text{-}4)$$

where:

T_u = applied factored torsional moment (kip-in.)

ϕ = resistance factor specified in Article 1.5.4.2 of this Appendix

T_{cr} = torsional cracking moment (kip-in.)

K = limiting interface shear resistance

A_{cp} = area enclosed by the outside perimeter of the UHPC cross section (in.^{2})

p_c = length of the outside perimeter of the UHPC section (in.)

A_o = area enclosed by the shear flow path, including any area of holes therein (in.^{2})

b_e = effective width of the shear flow path taken as the minimum thickness of the exterior webs or flanges comprising the closed box section (in.); b_e shall be adjusted to account for the presence of ducts, voids, or openings

f_{pc} = unfactored compressive stress in UHPC after prestress losses have occurred, either at the centroid of the cross section resisting transient loads, or at the junction of the web and flange where the centroid lies in the flange (ksi)

b_e defined in the preceding list shall not exceed A_{cp}/p_c, unless a more refined analysis is utilized to determine a larger value.

The effects of any openings or ducts in members shall be considered. K shall not be taken as greater than 1.0 for any section where the stress in the extreme tension fiber, calculated on the basis of gross section properties, due to factored load and effective prestress force after losses, exceeds $\gamma_u f_{t,cr}$ in tension.

The factor, γ_u, is conservatively not applied to the effective cracking strength, $f_{t,cr}$, in Eq. 1.7.2.1-4.

When calculating K for a section subject to factored axial force, N_u, f_{pc} shall be replaced with $f_{pc} - N_u/A_g$. N_u shall be taken as a positive value when the axial force is tensile and as a negative value when it is compressive.

1.7.2.2. Transfer and Development Length

The provisions of Article 1.9.4.3 of this Appendix shall be considered for longitudinal reinforcement resisting tension caused by shear.

1.7.2.3. Regions Requiring Transverse Reinforcement

Transverse reinforcement shall be provided where:

$$V_u > \phi(V_{UHPC} + V_p) \qquad (1.7.2.3\text{-}1)$$

or where consideration of torsion is required by Eq. 1.7.2.1-1.

where:

V_u	=	factored shear force (kip)
ϕ	=	resistance factor specified in Article 1.5.4.2 of this Appendix
V_{UHPC}	=	nominal shear resistance of the UHPC as determined in Article 1.7.3.3 of this Appendix (kip)
V_p	=	component of prestressing force in the direction of the shear force; positive if resisting the applied shear

1.7.2.4. Types of Transverse Reinforcement

The provisions of AASHTO LRFD BDS Article 5.7.2.4 (AASHTO 2020) shall apply with the following amendments:

- Transverse reinforcement to resist shear may consist of anchored individual bars.

C1.7.2.3

Full-scale shear tests on UHPC girders without transverse steel reinforcement showed significant postcracking ductility (El-Helou and Graybeal 2022b). This postcracking perfor-mance is attributed to the presence of fibers that compensate for the lost resistance of the UHPC matrix at cracks and result in the occurrence of multiple parallel diagonal cracks before shear failure. For this reason, transverse steel reinforcement to resist shear is not required when the shear demand load does not exceed the sum of shear capacity of UHPC and the component of prestressing force in the direction of the shear force.

- Transverse reinforcement to resist shear may not consist of bent longitudinal bars in nonprestressed members.

- The referenced provisions of AASHTO LRFD BDS Article 5.10.8.2.6d (AASHTO 2020) shall be amended by the provisions of Article 1.10.8.2.6 of this Appendix.

1.7.2.5. Minimum Transverse Reinforcement

Transverse shear reinforcement need not be provided where not required, as specified in Article 1.7.2.3 of this Appendix.

1.7.2.6. Maximum Spacing of Transverse Reinforcement

The spacing of the transverse reinforcement shall not exceed the maximum permitted spacing, s_{max}, determined as:

$$s_{max} = 0.25 d_v \cot \theta \leq 24.0 \text{ in.} \qquad (1.7.2.6\text{-}1)$$

where:

d_v = effective shear depth, as defined in Article 1.7.2.8 of this Appendix (in.)

θ = angle of inclination of diagonal compressive stresses, as determined in Article 1.7.3.4 of this Appendix (degrees)

1.7.2.7. Design and Detailing Requirements

The provisions of AASHTO LRFD BDS Article 5.7.2.7 (AASHTO 2020) shall apply in which the referenced provisions of Article 5.10.8.2.6 shall be amended by the provisions of Article 1.10.8.2.6 of this Appendix.

1.7.2.8. Shear Stress on UHPC

The shear stress on the concrete shall be determined as:

$$v_u = \frac{|V_u - \phi V_p|}{\phi b_v d_v}$$ (1.7.2.8-1)

where:

ϕ = resistance factor for shear as specified in Article 1.5.4.2 of this Appendix

b_v = effective web width taken as the minimum web width, measured parallel to the neutral axis, between the resultants of the tensile and compressive forces due to flexure, or for circular sections, the diameter of the section, modified for the presence of ducts where applicable (in.)

d_v = effective shear depth taken as the distance, measured perpendicular to the neutral axis, between the resultants of the tensile and compressive forces due to flexure; it need not be taken to be less than the greater of $0.9d_e$ or $0.72h$ (in.)

h = overall depth of the component (in.)

in which:

$$d_e = \frac{A_{ps}f_{ps}d_p + A_s f_s d_s}{A_{ps}f_{ps} + A_s f_s}$$ (1.7.2.8-2)

where:

d_e = effective depth taken as the distance, measured perpendicular to the neutral axis, between the extreme compression fiber of the section to the resultant of the forces in the tensile reinforcement (in.)

f_{ps} = average stress in the prestressing steel at the time for which nominal flexural resistance of the member is required (in.)

C1.7.2.8

Refer to AASHTO LRFD BDS Article C5.7.2.8 (AASHTO 2020) for commentary with the following amendments:

- AASHTO LRFD BDS Eq. C5.7.2.8-1 (AASHTO 2020) does not apply; the distance between the resultants of the tensile and compressive forces due to flexure, d_v, can be determined utilizing the strain compatibility approach described in Article 1.6.3.1 of this Appendix. Alternatively, it can be taken as the greater of $0.9d_e$ or $0.72h$. For circular sections, d_v can be taken as $0.9d_e$, where d_e is calculated according to AASHTO LRFD BDS Eq. C5.7.2.8-2 (AASHTO 2020).
- AASHTO LRFD BDS Figure C5.7.2.8-1 (AASHTO 2020) does not apply. For sections made with UHPC, refer to Figure C1.7.2.8-1.
- AASHTO LRFD BDS Figure C5.7.2.8-2 (AASHTO 2020) does not apply. For circular sections made with UHPC, refer to Figure C1.7.2.8-2.

f_s = average stress in the nonprestressed tension reinforcement at the time for which nominal flexural resistance of the member is required (in.); it shall not be taken a value greater than f_y

d_p = distance from extreme compression fiber to the centroid of prestressing tendons (in.)

d_s = distance from extreme compression fiber to the centroid of nonprestressed tensile reinforcement measured along the centerline of the web (in.)
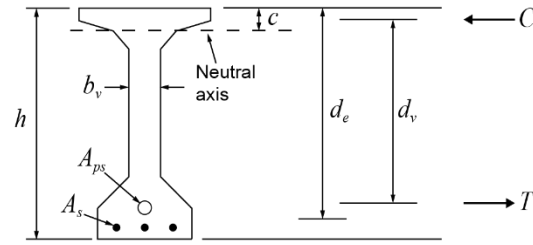
Source: FHWA.

Figure C1.7.2.8-1—Illustration of the terms b_v, d_v, and d_e for UHPC sections.
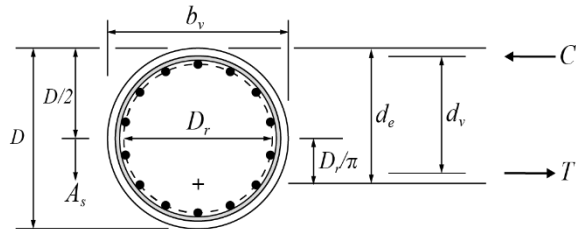
Source: FHWA.

Figure C1.7.2.8-2—Illustration of the terms b_v, d_v, and d_e for circular UHPC sections.

Note that, due to the additional resistance provided by the UHPC on the flexural tensile side of the section, the location of the resultant tensile force may not coincide with the centroid of the tensile steel reinforcement, as shown in Figure C1.7.2.8-1 and Figure C1.7.2.8-2. This UHPC resistance generally raises the centroid of the flexural tensile force towards the center of the section.

In composite sections made with UHPC beams and conventional concrete decks, the effective shear depth, d_v, shall not exceed the distance, measured perpendicular to the neutral axis, between the resultant of the forces in the tensile reinforcement and the extreme UHPC fiber on the flexural compression side. In cases where tensile reinforcement is not provided on the flexural tensile side of the UHPC beam, the effective shear depth, d_v, shall not exceed the depth of the UHPC beam.

In composite UHPC beams with conventional concrete decks, the limit on the effective shear depth, d_v, governs when the distance, measured perpendicular to neutral axis, between the resultant of the forces in the tensile reinforcement in the UHPC beam and the extreme UHPC fiber on the flexural compression side is less than the greater of $0.9d_e$ and $0.72h$, as shown in Figure C1.7.2.8-3.
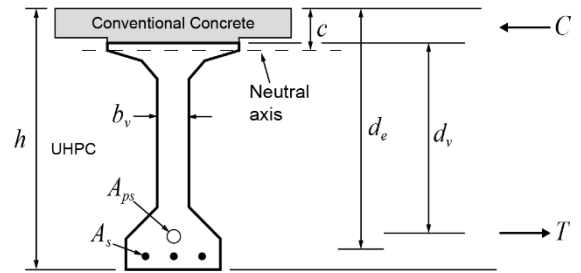
Source: FHWA.

Figure C1.7.2.8-3—Illustration of the terms b_v, d_v, and d_e for composite sections with UHPC beams and conventional concrete decks showing the maximum allowable d_v in composite sections.

In cases where steel reinforcement is not provided on the tension side of the UHPC beam (e.g., simply supported beams made continuous for live loads through a UHPC or conventional concrete deck and subjected to bending moments causing tensile stresses in the deck), the limit on the effective shear depth, d_v, governs when the height of the UHPC beam is less than $0.72h$, as shown in Figure C1.7.2.8-3.

1.7.3. Sectional Design Model

1.7.3.1. General

The provisions of AASHTO LRFD BDS Article 5.7.3.1 (AASHTO 2020) shall apply with the following amendments:

- Reference to AASHTO LRFD BDS Article 5.7.1 (AASHTO 2020) shall be replaced by Article 1.7.1 of this Appendix.

- The upper limit on the compressive strength of concrete for use in design shall not apply.

1.7.3.2. Sections Near Supports

The provisions of AASHTO LRFD BDS Article 5.7.3.2 (AASHTO 2020) shall apply, in which references to Articles 5.7.1.2, 5.7.2.8, 5.8.2, and 5.9.4.4 shall be replaced by

Articles 1.7.1, 1.7.2.8, 1.8, and 1.9.4.4 of this Appendix, respectively.

If the shear stress at the design section calculated in accordance with Article 1.7.2.8 of this Appendix exceeds $0.18f'_c$ and the beam-type element is not built integrally with the support, its end region shall be designed according to the provisions of Article 1.8 of this Appendix.

1.7.3.3. Nominal Shear Resistance

The nominal shear resistance, V_n, shall be determined as the lesser of both of the following:

$$V_n = V_{UHPC} + V_s + V_p \qquad (1.7.3.3-1)$$

$$V_n = 0.25f'_c\, b_v\, d_v + V_p \qquad (1.7.3.3-2)$$

in which:

$$V_{UHPC} = \gamma_u f_{t,loc}\, b_v\, d_v \cot\theta \qquad (1.7.3.3-3)$$

$$V_s = \frac{A_v f_{v,\alpha} d_v\,(\cot\theta + \cot\alpha)\sin\alpha}{s} \qquad (1.7.3.3-4)$$

where:

- b_v = effective web width taken as the minimum web width within the depth d_v, as specified in AASHTO LRFD BDS Article 5.7.2.8 (AASHTO 2020) (in.)
- V_s = shear resistance provided by transverse reinforcement (kip)
- d_v = effective shear depth, as specified in Article 1.7.2.8 (in.)
- $f_{v,\alpha}$ = uniaxial stress in the transverse steel reinforcement at nominal shear resistance, as determined in Article 1.7.3.4 of this Appendix (ksi); it shall not be greater than the specified minimum yield strength of transverse steel reinforcement
- A_v = area of transverse reinforcement to resist shear within a distance s (in.²)
- α = angle of inclination of transverse

C1.7.3.3

The shear design framework in Article 1.7.3.3 of this Appendix was derived from El-Helou and Graybeal (2023). It is based on the principles of the Modified Compression Field Theory (MCFT), originally developed for conventional concrete by Vecchio and Collins (1986), but integrates modifications to the material constitutive models that apply to UHPC behavior. The method is validated by experiments on prestressed and nonprestressed UHPC beams performed by El-Helou and Graybeal (2022b) and Baby, Marchand, and Toutlemonde (2014).

The shear failure in UHPC members is generally prompted by a localized and dominant crack forming from an existing crack or a coalescence of closely spaced cracks. The localization of the critical crack occurs when the bridging fibers start to pull out and the crack propagates through the depth of the web, which can occur before the yielding of the transverse reinforcement or crushing of the compressed UHPC in the member.

The upper limit on V_n given by Eq. 1.7.3.3-2 is intended to capture the failure mode in which the UHPC in the web of the beam crushes prior to, or at the development of, the critical crack. It is in line with the limit on V_n specified in AASHTO LRFD BDS Article 5.7.3.3 (AASHTO 2020). For a more detailed analysis, the crushing limit in a cracked UHPC member subjected to shear forces can be checked by

reinforcement to longitudinal axis (degrees)

s = spacing of transverse reinforcement measured in a direction parallel to the longitudinal reinforcement (in.)

ensuring that the stress in the compression strut, f_2, is less than half of the compression strength, $f_2 \leq 0.5f'_c$. f_2 can be computed by multiplying the compression principal strain, ε_2, calculated according to Eq. 1.7.3.4.1-2 by the UHPC modulus of elasticity: $f_2 = 0.5E_c\varepsilon_2$. The reduction on the modulus of elasticity (i.e., $0.5E_c$) and compressive strength (i.e., $0.5f'_c$) accounts for the potential weakening of UHPC in compression when subjected to a tensile strain field in the orthogonal direction.

Where $\alpha = 90$ degrees, Eq. 1.7.3.3-4 reduces to:

$$V_s = \frac{A_v f_{v,\alpha} d_v \cot\ \theta}{s}$$
(C1.7.3.3-1)

1.7.3.4. Procedures for Determining Shear Resistance Parameters θ and $f_{v,\alpha}$

C1.7.3.4

Design for shear shall utilize either of the two methods identified herein for the determination of the angle of inclination of diagonal compressive stresses, θ, and the stress in the transverse shear reinforcement, $f_{v,\alpha}$, at nominal shear resistance, provided that all requirements for usage of the chosen method are satisfied.

Two complementary approaches are given for evaluating the shear resistance of a UHPC member, with or without transverse shear reinforcement. The first approach, specified in Article 1.7.3.4.1 of this Appendix, involves a direct evaluation of the resistance parameters θ and $f_{v,\alpha}$ at shear failure. The second approach, specified in Article 1.7.3.4.2 of this Appendix, is a simplified and conservative approach where the shear resistance parameters are evaluated using tabularized values presented in Addendum A2.

1.7.3.4.1. General Approach

C1.7.3.4.1

The parameters θ and $f_{v,\alpha}$ shall be determined by iteratively solving Eqs. 1.7.3.4.1-1 through 1.7.3.4.1-4:

$$\gamma_u \varepsilon_{t,loc} = \frac{\varepsilon_s}{2}(1 + \cot^2\theta) + \frac{2f_{t,loc}}{E_c}\cot^4\theta$$

$$+ \frac{2\rho_{v,\alpha}f_{v,\alpha}}{E_c}\cot^2\theta\,(1 + \cot^2\theta) \quad (1.7.3.4.1-1)$$

The general design approach of Article 1.7.3.4.1 of this Appendix was derived from the comprehensive behavioral model of El-Helou and Graybeal (2023) for the response of a diagonally cracked UHPC membrane element subject to in-plane shear and normal stresses. The behavioral model is founded on the equilibrium and strain compatibility equations while incorporating the material models and shear failure modes particular to UHPC.

$$\varepsilon_2 = -\frac{2f_{t,loc}}{E_c}\cot^2\theta - \frac{2\rho_{v,\alpha}f_{v,\alpha}}{E_c}(1+\cot^2\theta)$$

$$(1.7.3.4.1\text{-}2)$$

$$\varepsilon_v = \gamma_u\varepsilon_{t,loc} - 0.5\varepsilon_s + \varepsilon_2 \qquad (1.7.3.4.1\text{-}3)$$

$$f_{v,\alpha} = \frac{E_s\varepsilon_v}{\sin\alpha} \leq f_y \qquad (1.7.3.4.1\text{-}4)$$

in which:

$$\rho_{v,\alpha} = \frac{A_v}{b_v s}\left(1+\frac{\cot\alpha}{\cot\theta}\right)\sin\alpha \qquad (1.7.3.4.1\text{-}5)$$

In Eqs. 1.7.3.4.1-1 through 1.7.3.4.1-4, ε_s is the net longitudinal tensile strain in the section at the centroid of the tension reinforcement, as shown in AASHTO LRFD BDS Figure 5.7.3.4.2-1 (AASHTO 2020). In lieu of more involved procedures, ε_s may be determined by Eq. 1.7.3.4.1-6:

$$\varepsilon_s = \frac{\dfrac{|M_u|}{d_v}+0.5N_u+|V_u-V_p|-A_{ps}f_{po}-\gamma_u f_{t,loc}A_{ct}}{E_sA_s+E_pA_{ps}}$$

$$(1.7.3.4.1\text{-}6)$$

If the value of ε_s calculated from Eq. 1.7.3.4.1-6 is negative or is positive and less than $\varepsilon_{t,cr}$, it should be taken as $\varepsilon_{t,cr}$, or the value should be recalculated according to Eq. 1.7.3.4.1-7:

$$\varepsilon_s = \frac{\dfrac{|M_u|}{d_v}+0.5N_u+|V_u-V_p|-A_{ps}f_{po}}{E_sA_s+E_pA_{ps}+E_cA_{ct}}$$

$$(1.7.3.4.1\text{-}7)$$

where:

ε_2 = strain in the UHPC diagonal compressive strut (in./in.)

ε_v = strain along the transverse direction of the member (in./in.)

The shear stresses of a UHPC member are not uniform over the depth of the beam, as shown in AASHTO LRFD BDS Figure C5.7.3.4.2-1 (AASHTO 2020). Similar to the shear resistance procedure implemented in AASHTO LRFD BDS Article 5.7.3.4.2 (AASHTO 2020), the procedure given herein assumes that the UHPC shear stresses are uniformly distributed over an area b_v wide and d_v deep, that the direction of principal compressive stresses, defined by angle θ, remains constant over d_v, and that the shear strength of the section can be determined by considering the biaxial stress conditions at just one location in the web, as shown in AASHTO LRFD BDS Figure C5.7.3.4.2-2 (AASHTO 2020). The axial stress at that location is assumed to be equal to half the value of ε_s, calculated using Eqs. 1.7.3.4.1-6 and 1.7.3.4.1-7.

To account for the fact that compressed UHPC subjected to tensile strain fields in the orthogonal direction is softer than uniaxially compressed UHPC, the modulus of elasticity in Eqs. 1.7.3.4.1-1 and 1.7.3.4.1-2 is taken as half the value of E_c specified in Article 1.4.2.3 of this Appendix.

The shear design procedure described in Eqs. 1.7.3.4.1-1 through 1.7.3.4.1-4 calculates the resistance parameters θ and $f_{v,\alpha}$ when the principal tensile strain in the web of the beam is equal to the tensile strain limit, $\gamma_u\varepsilon_{t,loc}$. The formulation accounts for the effect of the modulus of elasticity, E_c, the strain in the longitudinal steel reinforcement, ε_s, the crack localization strength of UHPC, $f_{t,loc}$, and the ratio of shear reinforcement, $\rho_{v,\alpha}$, on the inclination angle of the compressive stresses, θ, and the stress in the steel bars at shear failure, $f_{v,\alpha}$.

The solution of Eq. 1.7.3.4.1-1 for θ and $f_{v,\alpha}$ can be iteratively solved for a given reinforcement ratio, $\rho_{v,\alpha}$, by calculating θ based on an assumed value of $f_{v,\alpha}$. Eqs. 1.7.3.4.1-2 through 1.7.3.4.1-4 are then evaluated using θ and $f_{v,\alpha}$.

$|M_u|$ = absolute value of the factored moment at the section, not taken less than $|V_u - V_p|d_v$ (kip-in.)

N_u = factored axial force, taken as positive if tensile and negative if compressive (kip)

V_u = factored shear force (kip)

E_p = modulus of elasticity of prestressing steel (ksi)

A_{ps} = area of prestressing steel on the flexural tension side of the member (in.^{2}), as shown in AASHTO LRFD BDS Figure 5.7.3.4.2-1 (AASHTO 2020)

f_{po} = a parameter taken as modulus of elasticity of prestressing steel multiplied by the locked-in difference in strain between the prestressing steel and the surrounding UHPC (ksi). For the usual levels of prestressing, a value of 0.7 f_{pu} will be appropriate for both pretensioned and post-tensioned members

A_{ct} = area of UHPC on the flexural tension side of the member (in.^{2}) as shown in AASHTO LRFD BDS Figure 5.7.3.4.2-1 (AASHTO 2020)

A_s = area of nonprestressed steel on the flexural tension side of the member at the section under consideration (in.^{2}), as shown in AASHTO LRFD BDS Figure 5.7.3.4.2-1 (AASHTO 2020)

Where consideration of torsion is required by the provisions of Article 1.7.2.1 of this Appendix, the following provisions shall apply:

The value of $f_{v,\alpha}$ calculated according to Eq. 1.7.3.4.1-4 must be checked against the assumed value $f_{v,\alpha}$, and the analysis is repeated until the assumed and calculated values of $f_{v,\alpha}$ converge. If the calculated value of $f_{v,\alpha}$ is greater than f_y, it must be taken as equal to f_y, as specified in Eq. 1.7.3.4.1-4, before the convergence check between the assumed and calculated values of $f_{v,\alpha}$ is performed. A possible starting value for $f_{v,\alpha}$ can be set equal to the minimum yield strength of the transverse steel, f_y. The design value of $f_{v,\alpha}$ can be lower than f_y, especially for UHPC beams with high ratios of transverse steel reinforcement, $\rho_{v,\alpha}$, and/or low values of crack localization strain capacity, $\varepsilon_{t,loc}$.

The factor, γ_u, is conservatively omitted from the tensile stress parameters in Eqs. 1.7.3.4.1-1 and 1.7.3.4.1-2. Using higher values of the crack localization strength, $f_{t,loc}$, in these equations would increase the value of θ, resulting in conservative predictions of the shear strength.

For sections without transverse steel reinforcement ($\rho_{v,\alpha}$ = 0), Eqs. 1.7.3.4.1-1 and 1.7.3.4.1-2 reduce to:

$$\gamma_u \varepsilon_{t,loc} = \frac{\varepsilon_s}{2}(1+\cot^2\theta) + \frac{2f_{t,loc}}{E_c}\cot^4\theta \qquad \text{(C1.7.3.4.1-1)}$$

$$\varepsilon_2 = -\frac{2f_{t,loc}}{E_c}\cot^2\theta \qquad \text{(C1.7.3.4.1-2)}$$

For sections with transverse steel reinforcement perpendicular to the longitudinal axis (α = 90 degrees), Eqs. 1.7.3.4.1-4 and 1.7.3.4.1-5 reduce to:

$$f_{v,\alpha} = E_s\,\varepsilon_v \leq f_y \qquad \text{(C1.7.3.4.1-3)}$$

$$\rho_{v,\alpha} = \frac{A_v}{b_v s} \qquad \text{(C1.7.3.4.1-4)}$$

- V_u in Eqs. 1.7.3.4.1-6 and 1.7.3.4.1-7 shall be replaced by the effective factored shear resistance, V_{eff}, as determined in AASHTO LRFD BDS Eqs. 5.7.3.4.2-5 and 5.7.3.4.2-6 (AASHTO 2020).

- A_v in Eq. 1.7.3.4.1-5 shall be replaced by A_v plus the total area of transverse torsion reinforcement in the web or webs of members.

The value of $\rho_{v,\alpha}$ calculated in accordance with Eq. 1.7.3.4.1-5 is modified to account for the total area of transverse reinforcement provided to resist both shear and torsion, because the values of θ and $f_{v,\alpha}$ depend on $\rho_{v,\alpha}$.

Within the transfer length, f_{po} shall be increased linearly from zero at the location where the bond between the strands and UHPC commences to its full value at the end of the transfer length.

In the use of Eqs. 1.7.3.4.1-1 through 1.7.3.4.1-7, the following shall be considered:

- $|M_u|$ should not be taken as less than $|V_u - V_p| \, d_v$.

- In calculating A_s and A_{ps}, the area of bars or tendons terminated less than their development length from the section under consideration should be reduced in proportion to their lack of full development.

- For sections closer than d_v to the face of the support, the value of ε_s calculated at d_v from the face of the support may be used in evaluating θ and $f_{v,\alpha}$, unless there is a concentrated load within d_v from the support, in which case ε_s should be calculated at the face of the support. The limit on d_v in composite sections in accordance with Article 1.7.3.2 of this Appendix shall apply.

The longitudinal strain, ε_s, is determined following the same procedure described in AASHTO LRFD BDS Article 5.7.3.4.2 and illustrated in AASHTO LRFD BDS Figure C5.7.3.4.2-3 (AASHTO 2020) but with accounting for the UHPC contribution to tensile flexural stresses in the longitudinal direction: $\gamma_u f_{t,cr} A_{ct}$. Note that Eq. 1.7.3.4.1-6 conservatively ignores the increase in the postcracking strength for materials showing a tensile stress-strain behavior idealized in Figure 1.4.2.5.4-2. The value of ε_s must be equal to or less than the UHPC tensile strain limit, $\gamma_u \varepsilon_{t,loc}$, to prevent localization of UHPC around the longitudinal tensile reinforcement at critical shear sections. The localization of UHPC in the extreme tensile fiber of the section is considered a flexural failure mode, as specified in Article 1.6.3.2.2 of this Appendix.

For pretensioned members, f_{po} can be taken as the stress in the strands when the UHPC is cast around them, i.e., approximately equal to the jacking stress, as specified in AASHTO LRFD BDS Article 5.7.3.4.2 (AASHTO 2020).

66

- In evaluating Eqs. 1.7.3.4.1-6 and 1.7.3.4.1-7, the limit on d_v in composite sections made of UHPC beams and conventional concrete decks need not apply.

- The area of UHPC on the flexural tension side of the member, A_{ct}, is shown in AASHTO LRFD BDS Figure 5.7.3.4.2-1 (in.^{2}) (AASHTO 2020). The flexural tension side of the member shall be taken as the half-depth containing the flexural tension zone.

- If the axial tension is large enough to crack the flexural compression face of the section, the value calculated from Eqs. 1.7.3.4.1-6 and 1.7.3.4.1-7 should be doubled.

- Eq. 1.7.3.4.1-6 is not applicable when the value of ε_s is greater than the lesser of the yield strain of nonprestressed reinforcement or 0.0025. In these instances, the value of ε_s shall be determined from a detailed analysis.

- The value of ε_s must be equal to or less than the UHPC tensile strain limit, $\gamma_u\varepsilon_{t,loc}$, for the applicability of Eqs. 1.7.3.4.1-1 through 1.7.3.4.1-4.

Eq. 1.7.3.4.1-6 assumes a linear elastic behavior of the longitudinal reinforcement and is not applicable when the steel strain is greater than the yield strain of prestressed or nonprestressed reinforcement. For prestressed reinforcement, the strain in the strands is assumed to be less than the yield strain when ε_s is less than or equal to 0.0025.

1.7.3.4.2. Simplified Approach

For members made of UHPC with $E_c \geq$ 6,500 ksi, $f_{t,loc} \leq$ 1.80 ksi, and without transverse steel reinforcement (i.e., $\rho_{v,\alpha} =$ 0 percent), the values of θ may be determined from Table A2.2-1 of Addendum A2 at a specific value of $\gamma_u\varepsilon_{t,loc}$ and ε_s.

For members made of UHPC with $E_c \geq$ 6,500 ksi, $f_{t,loc} \leq$ 1.80 ksi, and reinforced with transverse steel with $f_y \leq$ 75.0 ksi, $\rho_{v,\alpha} \leq$ 3.0 percent, and α = 90 degrees, the values of θ and $f_{v,\alpha}$ may be determined from the appropriate tables of Addendum A2 (i.e., Table A2.3-1

C1.7.3.4.2

The simplified approach was developed to provide an alternative conservative procedure for the determination of the resistance parameters θ and f_v at a known value of ε_s and as a function of the material parameters that have the most significant effect on the shear capacity.

Considering the shear Eqs. 1.7.3.4.1-1 through 1.7.3.4.1-4, a parametric study on the effects of the UHPC and transverse steel reinforcement parameters revealed that the parameter with the highest overall effect on the shear capacity is

through Table A2.3-6) based on the value of $\rho_{v,\alpha}$ and at a specific value of $\gamma_u\varepsilon_{t,loc}$ and ε_s.

For members with inclined steel reinforcement ($\alpha \neq 90$ degrees), the general method of Article 1.7.3.4.1 of this Appendix should be used.

In lieu of more involved procedures, the value of ε_s may be determined by Eq. 1.7.3.4.1-6 or Eq. 1.7.3.4.1-7, as specified in Article 1.7.3.4.1 of this Appendix.

The value of $f_{v,\alpha}$ used in Eq. 1.7.3.3-4 shall be determined as the lesser of the value obtained from the tables of Addendum A2 and the specified minimum yield strength of the transverse steel, f_y.

The provisions of Addendum A2 shall apply when utilizing the simplified approach for determining parameters θ and $f_{v,\alpha}$.

the crack localization strain of UHPC, $\varepsilon_{t,loc}$, followed by the ratio of transverse steel reinforcement, $\rho_{v,\alpha}$. An increase in the values of the crack localization strength, $f_{t,loc}$, or a decrease in the values of the modulus of elasticity, E_c, would increase θ, but this variation is much less significant than variations in $\varepsilon_{t,loc}$, $\rho_{v,\alpha}$, or ε_s. Therefore, the design tables of Addendum A2 were developed with fixed values of $E_c = 6,500$ ksi and $f_{t,loc} = 1.80$ ksi and can be conservatively used for any UHPC material with higher values of E_c and lower values of $f_{t,loc}$ than the ones used to develop the design tables. Because increases in the values of $\rho_{v,\alpha}$ would increase θ, the tables pertaining to a specific value of $\rho_{v,\alpha}$ can be conservatively used for members with values of $\rho_{v,\alpha}$ lower than the one used to produce the design table.

The design tables of Addendum A2 are developed assuming a linearly elastic behavior of transverse steel stress, $f_{v,\alpha}$, up to a minimum yield strength, f_y, of 75 ksi. Because the value of θ decreases with decreased values of $f_{v,\alpha}$, the design tables of Addendum A2 will lead to conservative estimates of θ for UHPC members reinforced with transverse steel and having a minimum yield strength, f_y, equal to or less than 75 ksi.

1.7.3.5. Longitudinal Reinforcement

C1.7.3.5

Except as specified herein, at each section, the tensile capacity of the longitudinal reinforcement on the flexural tension side of the member shall be proportioned to satisfy:

$$A_{ps}f_{ps}+A_sE_s\gamma_u\varepsilon_{t,loc}+A_{ct}\gamma_uf_{t,cr} \geq$$

$$\frac{|M_u|}{d_v\phi_f} + 0.5\frac{N_u}{\phi_c} + \left(\left|\frac{V_u}{\phi_v} - V_p\right| - 0.5V_s\right)\cot\theta$$

$$(1.7.3.5-1)$$

In determining the axial force that the longitudinal reinforcement is expected to resist, Eqs. 1.7.3.5-1 and 1.7.3.5-2 follow the same procedure described in AASHTO LRFD BDS Article 5.7.3.5 (AASHTO 2020) but with accounting for the UHPC contribution to tensile flexural stresses in the longitudinal direction: $A_{ct}\gamma_uf_{t,cr}$. Note that the increase in the postcracking strength for materials showing a tensile stress-strain behavior idealized in Figure 1.4.2.5.4-2 is conservatively ignored.

where:

ϕ_f, ϕ_v, ϕ_c = resistance factors taken from Article 1.5.4.2 of this Appendix as appropriate for moment, shear, and axial resistance, respectively

V_s = shear resistance provided by transverse reinforcement at the section under investigation as given by Eq. 1.7.3.3-4, except V_s shall not be taken as greater than V_u/ϕ_v in Eqs. 1.7.3.5-1 and 1.7.3.5-2 (kip)

θ = angle of inclination of diagonal compressive stresses used in determining the nominal shear resistance of the section under investigation as determined by Article 1.7.3.4 of this Appendix (degrees)

Eq. 1.7.3.5-1 shall be evaluated where simply supported girders are made continuous for live loads and where longitudinal reinforcement is discontinuous.

At the inside edge of the bearing area of simple end supports to the section of critical shear, the longitudinal reinforcement on the flexural tension side of the member shall satisfy:

$$A_{ps}f_{ps} + A_sE_s\gamma_u\varepsilon_{t,loc} + 0.6\,A_{ct}\gamma_u f_{t,cr} \geq$$

$$\left(\frac{V_u}{\phi_v} - 0.5V_s - V_p\right)\cot\theta \qquad (1.7.3.5\text{-}2)$$

Eqs. 1.7.3.5-1 and 1.7.3.5-2 shall be taken to apply to sections not subjected to torsion in which the term $E_s\gamma_u\varepsilon_{t,loc}$ shall not exceed f_y. Any lack of full development shall be accounted for.

In evaluating Eqs. 1.7.3.5-1 and 1.7.3.5-2, the limit on d_v in composite sections made of UHPC beams and conventional concrete decks need not apply.

The 0.6 factor applied to A_{ct} is intended to conservatively account for the tension resistance of the UHPC in determining the required longitudinal reinforcement near the critical shear section. This approach is similar to that taken for tension members in Article 1.6.6.1 of this Appendix.

For pretensioned sections, including those with debonded strands, the tensile force in the prestressed reinforcement (i.e., $A_{ps}f_{ps}$) shall exceed the tensile forces of the nonprestressed reinforcement (i.e., $A_sE_s\gamma_u\varepsilon_{t,loc} \leq A_sf_y$) at all sections. Development of straight and bent-up strands as well as overhangs, if present, shall be considered for determining the value of $A_{ps}f_{ps}$ and $A_sE_s\gamma_u\varepsilon_{t,loc} \leq A_sf_y$.

Except as may be required by Article 1.7.3.6.3 of this Appendix, where the reaction force or the load at the maximum moment location introduces direct compression into the flexural compression face of the member, the area of longitudinal reinforcement on the flexural tension side of the member need not exceed the area required to resist the maximum moment acting alone.

Longitudinal or transverse reinforcing steel, or a combination thereof, with specified minimum yield strengths up to 100 ksi, may be used in elements and connections specified in AASHTO LRFD BDS Article 5.4.3.3 (AASHTO 2020).

1.7.3.6. Sections Subjected to Combined Shear and Torsion

1.7.3.6.1. Transverse Reinforcement

The provisions of AASHTO LRFD BDS Article 5.7.3.6.1 (AASHTO 2020) shall apply in which references to Articles 5.7.2.1, 5.7.3.3, and 5.7.3.6.2 shall be replaced by Articles 1.7.2.1, 1.7.3.3, and 1.7.3.6.2 of this Appendix, respectively.

1.7.3.6.2. Torsional Resistance

The nominal torsional resistance shall be taken as:

$$T_n = \frac{2A_o A_t f_{v,\alpha} \cot \theta}{s}$$

(1.7.3.6.2-1)

C1.7.3.6.2

In the absence of sufficient data on combined torsional and shear resistance of UHPC, resistance to torsion is assumed to be solely provided by additional transverse steel reinforcement proportioned to satisfy $T_n \geq T_u$. The specified torsional resistance equation (i.e.,

where:

A_o = area enclosed by the shear flow path, including any area of holes therein (in.^{2})

A_t = area of one leg of the closed transverse torsion reinforcement in solid members, or total area of the transverse torsion reinforcement in the exterior web and flange of hollow members (in.^{2})

θ = angle of inclination of diagonal compressive stresses, as determined in accordance with the provisions of Article 1.7.3.4 of this Appendix (degrees)

$f_{v,\alpha}$ = stress in the transverse steel reinforcement at nominal shear resistance as determined in Article 1.7.3.4 of this Appendix (ksi)

s = spacing of transverse reinforcement measured in a direction parallel to the longitudinal reinforcement (in.)

For composite sections made with UHPC beams and conventional concrete decks where tensile reinforcement is not provided on the tension side of the UHPC beam, ε_s in Equations 1.7.3.4.1-1 through 1.7.3.4.1-4 is the net longitudinal tensile strain in the extreme tension layer of the UHPC beam. The value of ε_s shall account for the effects of bending moment and the applied shear and axial forces.

Eq. 1.7.3.6.2-1) is adopted from AASHTO LRFD BDS Eq. 5.7.3.6.2-1 (AASHTO 2020) with the following amendments:

- The shear strength factor is taken as equal to 1.0 because this Appendix does not provide guidance on post-tensioned UHPC elements. However, the effect of voids and/or openings in the section must be considered.

- The yield strength term, f_y, is replaced by the stress in the transverse reinforcement, $f_{v,\alpha}$, determined according to the provisions of Article 1.7.3.4 of this Appendix, because the stress in the steel at nominal resistance might be lower than the yield stress of reinforcement.

The nominal resistance for shear (Eqs. 1.7.3.3-3 and 1.7.3.3-4) and torsion (Eq. 1.7.3.6.2-1) should be calculated from the same set of values for θ and $f_{v,\alpha}$, determined in accordance with Article 1.7.3.4 of this Appendix. In calculating $\rho_{v,\alpha}$, A_v in Eq. 1.7.3.4.1-5 should be replaced by A_v plus the total area of additional transverse reinforcement provided to resist torsion. This modification accounts for the effect of the increase in transverse reinforcement on values for θ and $f_{v,\alpha}$.

In cases where composite sections made with UHPC beams and conventional concrete decks have no steel tensile reinforcement on the tension side of the UHPC beam (e.g., simply supported beams made continuous for live loads through a conventional concrete deck and subjected to bending moments causing tensile stresses in the deck), in lieu of more involved procedures, ε_s may be calculated by subtracting the strain in the UHPC beam at the interface between the beam and deck at the time of deck placement from the value obtained from Equation 1.7.3.4.1-6 with $A_{ps} = 0$ and $f_{t,loc} = 0$. In this computation, the strain in the UHPC beam at the interface between the beam and deck must be taken as a negative value when in

compression and a positive value when in tension.

1.7.3.6.3. Longitudinal Reinforcement

The provisions of Article 1.7.3.5 of this Appendix shall be replaced with the provisions of AASHTO LRFD BDS Article 5.7.3.6.3 (AASHTO 2020) with the following amendments:

- Reference to AASHTO LRFD BDS Article 5.7.3.5 (AASHTO 2020) shall be replaced by Article 1.7.3.5 of this Appendix.

- The expression $A_{ps}f_{ps} + A_sE_s\gamma_u\varepsilon_{t,loc} + A_{ct}\gamma_uf_{t,loc}$ shall replace the left-hand side of AASHTO LRFD BDS Eq. 5.7.3.6.3-1 (i.e., $A_{ps}f_{ps} + A_sf_y$) (AASHTO 2020) in which the term $E_s\gamma_u\varepsilon_{t,loc}$ shall not exceed f_y.

1.7.4. Interface Shear Transfer–Shear Friction

1.7.4.1. General

The provisions of Article 5.7.4.1 of the AASHTO LRFD BDS (AASHTO 2020) shall apply.

C1.7.4.1

The commentary of Article 5.7.4.1 of the AASHTO LRFD BDS shall apply to UHPC; however, an additional source of resistance to shear displacement along the interface plane shall be provided by UHPC tensile forces crossing the plane of the interface (for UHPC cast monolithically).

1.7.4.2. Minimum Area of Interface Shear Reinforcement

For monolithic UHPC, interface shear reinforcement need not be provided if the clamping force provided by the fiber reinforcement exceeds the following limit:

$$\gamma_uf_{t,loc}A_{cv} > 0.05A_{cv} \qquad (1.7.4.2\text{-}1)$$

For monolithic UHPC, the fiber reinforcement should provide a clamping force that exceeds the requirement of AASHTO LRFD BDS Eq. 5.7.4.2-1 (AASHTO 2020).

where:

A_{cv} = area of UHPC considered to be engaged in interface shear transfer (in.^{2})

$f_{t,loc}$ = the crack localization strength of the UHPC in tension specified in Article 1.4.2.5.4 of this Appendix (ksi); it shall not be taken greater than 1.75 ksi

For all other cases, the provisions of Article 5.7.4.2 of the AASHTO LRFD BDS (AASHTO 2020) shall apply with the following amendments:

- Reference to Eq. 5.7.4.3-3 shall be replaced by Eq. 1.7.4.3-4.

- The minimum reinforcement provisions of Article 5.7.4.2 of the AASHTO LRFD BDS (AASHTO 2020) shall not be waived for any non-monolithic interfaces.

1.7.4.3. Interface Shear Resistance

The factored interface shear resistance, V_{ri}, shall be determined in accordance with AASHTO LRFD BDS Eq. 5.7.4.3-1 (AASHTO 2020), and the design shall satisfy AASHTO LRFD BDS Eq. 5.7.4.3-2 (AASHTO 2020).

The nominal shear resistance of the interface plane for UHPC placed monolithically shall be taken as:

$$V_{ni} = cA_{cv} + \mu(C_1 + C_2 + P_c) \qquad (1.7.4.3\text{-}1)$$

in which:

$$C_1 = A_{vf}f_s \qquad (1.7.4.3\text{-}2)$$

$$C_2 = A_{cv}\gamma_u f_{t,loc} \qquad (1.7.4.3\text{-}3)$$

The value $f_{t.loc}$ is limited to 1.75 ksi due to the lack of available data greater than this value in the literature.

Article 5.7.4.2 of AASHTO LRFD BDS (AASHTO 2020) waives the minimum reinforcement requirements for conventional concrete girder/slab interfaces when the factored interface shear stress is less than 0.210 ksi and when the minimum transverse shear reinforcement required in the web are extended across the interface and adequately anchored in the slab. Given that UHPC girders do not necessarily contain transverse reinforcement in the web, the aforementioned provision is not applicable.

C1.7.4.3

The specified nominal shear resistance of the interface plane for UHPC is based on the work of Muzenski, Haber, and Graybeal (2022, 2023). It is founded on the same concepts of the shear-friction model for conventional concrete specified in AASHTO LRFD BDS Eq. 5.7.4.3-3 (AASHTO 2020) but integrates modifications that account for the behaviors specific to UHPC. In particular, in addition to the traditional clamping force (i.e., $A_{vf}f_s + P_c$), the model incorporates an additional clamping force (i.e., $A_{cv}\gamma_u f_{t,loc}$) provided by the tensile resistance of UHPC.

where:

C_1 = normal clamping force provided by steel reinforcement (kip)

A_{vf} = area of interface reinforcement crossing the shear plane within the area A_{cv} (in.^{2})

f_s = stress in the interface steel reinforcement at the time of UHPC crack localization (ksi): $f_s = E_s \gamma_u \varepsilon_{t,loc} \leq f_y$

C_2 = normal clamping force provided by UHPC placed monolithically (kip)

Research conducted by Muzenski, Haber, and Graybeal (2022, 2023) on monolithically placed UHPC interfaces indicated that the interface steel reinforcing bars may not yield before or concurrent with shear failure at the interface plane; thus, the yield stress of the reinforcement is not an appropriate value to use for the clamping force provided by the steel reinforcement, C_1. When the UHPC localizes in tension, it is assumed to no longer provide clamping force (i.e., $C_2 = 0$). In scenarios where the crack localization strain of UHPC is less than the yield strain of the interface steel reinforcement, a portion of the clamping force will be lost before the interface steel yields. Therefore, the value f_s shall be determined by considering the stress in the steel reinforcing bars at the time of UHPC crack localization, assuming compatibility (i.e., $f_s = E_s \gamma_u \varepsilon_{t,loc} \leq f_y$). This consideration for f_s allows for contributions to the clamping force from reinforcement with yield stresses higher than 60 ksi.

The nominal shear resistance of the interface plane for all other cases shall be taken as:

$$V_{ni} = c A_{cv} + \mu(A_{vf} f_y + P_c) \qquad (1.7.4.3-4)$$

The nominal shear resistance, V_{ni}, used in the design shall not exceed the following:

$$V_{ni} \leq K A_{cv} \qquad (1.7.4.3-5)$$

in which:

$$A_{cv} = b_{vi} L_{vi} \qquad (1.7.4.3-6)$$

The limiting interface shear resistance established by Eq. 1.7.4.3-5 is necessitated by the lack of available experimental data beyond the limiting K values provided in Article 1.7.4.4 of this Appendix.

where:

f_y = specified minimum yield strength of reinforcement (ksi); it shall not be taken greater than 60 ksi for cases where UHPC is placed non-monolithically

b_{vi} = interface width considered to be engaged in shear transfer (in.)

L_{vi} = interface length considered to be

engaged in shear transfer (in.)

c = cohesion factor as specified in Article 1.7.4.4 of this Appendix (ksi)

μ = friction factor specified in Article 1.7.4.4 of this Appendix

P_c = permanent net compressive force, normal to the shear plane; if force is tensile, $P_c = 0.0$ (kip)

K = limiting interface shear resistance specified in Article 1.7.4.4 of this Appendix (ksi)

1.7.4.4. Cohesion and Friction Factors

C1.7.4.4

The following values shall be taken for cohesion, c, and friction, μ:

For UHPC placed monolithically:

- c = 1.40 ksi
- μ = 1.00
- K = 4.50 ksi

The values presented for monolithically cast UHPC provide a lower bound based on the experimental data of Muzenski, Haber, and Graybeal (2022, 2023) and Crane (2010). In these tests, the interface steel reinforcement ratios varied between 0 percent and 2.76 percent, and the nominal interface reinforcement yield stresses varied between 40 ksi and 120 ksi.

For UHPC placed against a clean UHPC surface, free of laitance, with surface either intentionally roughened to an amplitude of 0.25 in. or cast to have 0.25-in. amplitude roughness:

- c = 0.075 ksi
- μ = 1.0
- K = 1.8 ksi

For UHPC placed against a clean UHPC surface, free of laitance, but not intentionally roughened to an amplitude of 0.25 in. or cast to have 0.25-in. amplitude roughness:

- c = 0.075 ksi
- μ = 0.6
- K = 0.8 ksi

For UHPC placed against a clean conventional

Interfaces consisting of a substrate material and a secondarily cast material are defined based on the materials and the interface surface type. Behavior of these interfaces is informed by the experimental data presented in Muzenski, Haber, and Graybeal (2023). Where limited experimental data are available, provisions relevant to normal-weight concrete, as provided in AASHTO LRFD BDS Article 5.7.4.4 (AASHTO 2020), are adopted. For situations where UHPC or conventional concrete is cast against a UHPC substrate, the cohesion factor is taken as equal to 0.075 ksi. This value is consistent with the cohesion factor of concrete placed against a clean concrete surface, free of laitance, but not intentionally roughened in AASHTO LRFD BDS Article 5.7.4.4 (AASHTO 2020). UHPC tends to replicate the formwork surface finish, thus creating a smooth

concrete substrate surface, free of laitance, with surface intentionally roughened to an amplitude of 0.25 in.:

- c = 0.24 ksi
- μ = 1.0
- K = 1.8 ksi

For UHPC placed against a clean conventional concrete substrate surface, free of laitance, but not intentionally roughened:

- c = 0.075 ksi
- μ = 0.6
- K = 0.8 ksi

For conventional concrete placed against a clean UHPC substrate surface, free of laitance, with surface intentionally roughened to an amplitude of 0.25 in. or cast to have 0.25-in. amplitude roughness:

- c = 0.075 ksi
- μ = 1.0
- K = 1.8 ksi

For conventional concrete placed against a clean UHPC substrate surface, free of laitance, but not intentionally roughened to an amplitude of 0.25 in. or cast to have 0.25-in. amplitude roughness:

- c = 0.075 ksi
- μ = 0.6
- K = 0.8 ksi

For UHPC anchored to as-rolled structural steel by headed studs or by reinforcing bars, where all steel in contact with UHPC is clean and free of paint:

- c = 0.025 ksi
- μ = 0.7
- K = 0.8 ksi

finish on the microlevel, regardless of the macrotexture present in the formwork.

For situations where UHPC is cast against a clean concrete surface, free of laitance, with a surface intentionally roughened to an amplitude of 0.25 in., the cohesion factor is taken as equal to 0.24 ksi, and the friction coefficient is taken as equal to 1.0. These values are consistent with the values for this situation in AASHTO LRFD BDS Article 5.7.4.4 (AASHTO 2020).

For situations where UHPC is cast against a clean concrete surface, free of laitance, that is not intentionally roughened, the cohesion factor is taken as equal to 0.075 ksi, and the friction coefficient is taken as equal to 0.6. These values are consistent with the values for this situation in AASHTO LRFD BDS Article 5.7.4.4 (AASHTO 2020).

For situations where UHPC is cast against, and anchored to, as-rolled structural steel, the provisions associated with conventional concrete from AASHTO LRFD BDS Article 5.7.4.4 are adopted (AASHTO 2020).

The relevant parameters for UHPC anchored to as-rolled structural steel are adopted from AASHTO LRFD BDS Article 5.7.4.4 (AASHTO 2020) for the same case with conventional concrete.

1.7.4.5. Computation of the Factored Interface Shear Force for Girder/Slab Bridges

The provisions of AASHTO LRFD BDS Article 5.7.4.5 (AASHTO 2020) shall apply.

1.7.4.6. Interface Shear in Box Girder Bridges

The provisions of AASHTO LRFD BDS Article 5.7.4.6 (AASHTO 2020) shall apply.

1.8. DESIGN OF D-REGIONS

Refined analysis, strut-and-tie, and elastic stress analysis methods may be used to determine the internal force effects in disturbed regions, such as those near supports, and the points of application of concentrated loads at strength and extreme limit states. The design method shall be approved by the owner and shown in the contract documents.

The analysis method shall consider the internal strains in the UHPC and reinforcement at strength and extreme limit states, shall use the material properties of Article 1.4 of this Appendix, and shall consider the potential presence of unfavorable fiber distributions in the member. The tensile strain in the UHPC at any location or orientation shall not be permitted to exceed $\gamma_u \varepsilon_{t,loc}$.

The calculated resistance of a member should be justified by performance testing of a prototype.

C1.8

The guidance provided herein relates to structural design with UHPC in B-Regions. More research is needed to explore the applicability of the D-Regions provisions of AASHTO LRFD BDS Article 5.5.1.2.3 (AASHTO 2020) to UHPC.

1.9. PRESTRESSING

1.9.1. General Design Consideration

1.9.1.1. General

The provisions of AASHTO LRFD BDS Article 5.9.1.1 (AASHTO 2020) shall apply, in which references to Articles 5.4, 5.5, 5.6, 5.7, and 5.9.2.3 shall be replaced by Articles 1.4, 1.5, 1.6, 1.7, and 1.9.2.3 of this Appendix, respectively.

The load factor for live load for Service III load combination, γ_{LL} in AASHTO LRFD BDS Table 3.4.1-4 (AASHTO 2020) shall not be less than 1.0.

1.9.1.2. Design UHPC Strengths

The design strengths, f'_c, $f_{t,cr}$, $f_{t,loc}$, f'_{ci}, and the effective cracking strength at the time of prestressing for pretensioned members and at initial loading for nonprestressed members, $f_{t,cri}$, shall be identified in the contract documents for each component. Stress limits relating to design strengths shall be as specified in Article 1.9.2.3 of this Appendix.

UHPC strength at transfer shall be adequate for the requirements of the anchorages or for transfer through bond as well as for camber or deflection requirements.

Unless approved by the owner, the value of f'_{ci} shall not be less than 14.0 ksi.

Unless determined by physical tests and as approved by the owner, the value of $f_{t,cri}$ shall not be taken as greater than $0.75f_{t,cr}$ when f'_{ci} is less than or equal to $0.90f'_c$.

C1.9.1.1

The applicability of the provisions of AASHTO LRFD BDS Article 5.9.3.3 (AASHTO 2020) for UHPC materials has not been investigated.

The Service III live load factor, γ_{LL}, is keyed to the prestress loss method in AASHTO LRFD BDS Table 3.4.1-4 (AASHTO 2020). In this Appendix, the refined estimates of time-dependent losses are in accordance with AASHTO LRFD BDS Article 5.9.3.4 (AASHTO 2020), as amended by Article 1.9.3 of this Appendix; thus, the γ_{LL} should be taken as equal to 1.0.

C1.9.1.2

Uniaxial compression and tension tests performed by El-Helou, Haber, and Graybeal (2022) showed a clear correlation between the compressive and tensile strength gains in which the effective cracking strength was found to increase with increasing compressive strength. The upper limit on $f_{t,cri}$ is prescribed to prevent cracking at transfer when uniaxial tension tests to determine $f_{t,cri}$ are not performed. It is based on experimental data in which f'_{ci} was greater than 14.0 ksi.

For commentary on a lower limit of f'_{ci}, refer to Article C1.4.2.8.2 of this Appendix.

1.9.1.3. Section Properties

The provisions of AASHTO LRFD BDS Article 5.9.1.3 (AASHTO 2020) shall apply.

1.9.1.4. Crack Control

The provisions of AASHTO LRFD BDS Article 5.9.1.4 (AASHTO 2020) shall apply, in which reference to Articles 5.5 and 5.6 shall be replaced by Articles 1.5 and 1.6 of this Appendix, respectively.

1.9.1.5. Buckling

The provisions of AASHTO LRFD BDS Article 5.9.1.5 (AASHTO 2020) shall apply.

1.9.2. Stress Limitations

1.9.2.1. Stresses Due to Imposed Deformation

The provisions of AASHTO LRFD BDS Article 5.9.2.1 (AASHTO 2020) shall apply, in which reference to Article 5.4.2.3.2 shall be replaced by Article 1.4.2.8.2 of this Appendix.

1.9.2.2. Stress Limitations for Prestressing Steel

The provisions of AASHTO LRFD BDS Article 5.9.2.2 (AASHTO 2020) and Article 1.4.4 of this Appendix shall apply.

1.9.2.3. Stress Limits for UHPC

1.9.2.3.1. For Temporary Stresses

1.9.2.3.1.a. Compressive Stresses

The provisions for compressive stress limits of AASHTO LRFD BDS Article 5.9.2.3.1a (AASHTO 2020) shall apply for UHPC.

1.9.2.3.1.b. Tensile Stresses

The tensile stress limit for prestressed UHPC components shall be $\gamma_u f_{t,cri}$ (ksi) in accordance with Articles 1.4.2.5 and 1.9.1.2 of this Appendix.

1.9.2.3.2. For Stresses at Service Limit State

1.9.2.3.2.a. Compressive Stresses

Except for the limit on the compressive strengths, the provisions for compressive stress limits of AASHTO LRFD BDS Article 5.9.2.3.2a (AASHTO 2020) shall apply for UHPC.

1.9.2.3.2.b. Tensile Stresses

Other than the provisions for tensile stress limits of AASHTO LRFD BDS Table 5.9.2.3.2b-1, the provisions of AASHTO LRFD BDS Article 5.9.2.3.2b (AASHTO 2020) shall apply for UHPC.

The tensile stress limit for prestressed UHPC at service limit state shall be $\gamma_u f_{t,cr}$ (ksi) in accordance with Article 1.4.2.5 of this Appendix.

1.9.2.3.3. Principal Tensile Stresses in Webs

The provisions of AASHTO LRFD BDS Article 5.9.2.3.3 (AASHTO 2020) shall apply with the following amendments:

- References to Articles 5.7.2 and 5.7.2.1 (AASHTO 2020) shall be replaced by Articles 1.7.2 and 1.7.2.1 of this Appendix, respectively.

- The upper limit on principal tensile stresses in webs shall be replaced by $\gamma_u f_{t,cr}$, in accordance with Article 1.4.2.5 of this Appendix.

1.9.3. Prestress Losses

The provisions of AASHTO LRFD BDS Article 5.9.3 (AASHTO 2020) shall apply with the following amendments:

- The limit on compressive strength of AASHTO LRFD BDS Article 5.9.3.1 (AASHTO 2020) shall not apply.

- The provisions of AASTHO LRFD BDS Article 5.9.3.3 (AASHTO 2020) shall not apply.

- References to AASHTO LRFD BDS Eqs. 5.4.2.3.2-1 and 5.4.2.3.3-1 (AASHTO 2020) shall be replaced by Eqs. 1.4.2.8.2-1 and 1.4.2.8.3-1 of this Appendix, respectively.

1.9.4. Details for Pretensioning

1.9.4.1. Minimum Spacing of Pretensioning Strand

The provisions of AASHTO LRFD BDS Article 5.9.4.1 (AASHTO 2020) shall apply for UHPC components.

When 0.62-in.- or 0.7-in.-diameter strands are used, the provisions for 0.6-in. diameter strands in AASHTO LRFD BDS Article 5.9.4.1 (AASHTO 2020) shall apply.

In addition to the limits specified in AASHTO LRFD BDS Article 5.9.4.1 (AASHTO 2020), the minimum spacing between pretensioning strands or between groups of bundled strands shall not be less than the greater of a clear distance taken as 1.50 times the length of the longest type of fiber reinforcement in the UHPC or 0.75 in.

C1.9.3

The applicability of the prestress loss method for conventional concrete in AASHTO LRFD BDS Article 5.9.3 (AASHTO 2020) for UHPC is verified by the work of Mohebbi and Graybeal (2022).

The applicability of the provisions of AASHTO LRFD BDS Article 5.9.3.3 (AASHTO 2020) for UHPC materials has not been investigated.

C1.9.4.1

The use of 0.7-in.-diameter strands in UHPC structural components has been investigated in the research of El-Helou and Graybeal (2022a, 2022b).

This provision stipulates a geometry that allows for sufficient passing of fibers through constricted spaces during casting. Restrictions to flow can result in undesirable fiber distribution effects within a member.

1.9.4.2. Maximum Spacing of Pretensioning Strand in Slabs

The provisions of AASHTO LRFD BDS Article 5.9.4.2 (AASHTO 2020) shall apply.

1.9.4.3. Development of Pretensioning Strand

1.9.4.3.1. General

In determining the resistance of pretensioned UHPC components in their end zones, the gradual buildup of the strand force in the transfer and development lengths shall be taken into account.

The stress in the prestressing steel may be assumed to vary linearly from 0.0 at the point where bonding commences to the effective stress after losses, f_{pe}, at the end of the transfer length.

Between the end of the transfer length and the development length, the strand stress may be assumed to increase linearly, reaching the stress at nominal resistance, f_{ps}, at the development length.

The transfer length, ℓ_t, shall be taken as:

$$\ell_t = \xi\, 24 d_b \qquad (1.9.4.3.1\text{-}1)$$

where:

ξ = 0.75 when a shorter transfer length value results in more severe stress states within the section

ξ = 1.0 when a longer transfer length value results in more severe stress states within the section

d_b = nominal strand diameter (in.)

C1.9.4.3.1

Between the end of the transfer length and development length, the strand stress grows from the effective stress in the prestressing steel after losses to the stress in the strand at nominal resistance of the member.

Eq. 1.9.4.3.1-1 is based on the results of experimental studies investigating the transfer length of pretensioning strands in UHPC (John et al. 2011; Bertram and Hegger 2012; Mohebbi, El-Helou, and Graybeal 2019).

The transfer length factor, ξ, is typically taken as:

- 0.75 when determining the stresses and/or strains at service and fatigue limit states in accordance with Articles 1.5.2 and 1.9.2.3 of this Appendix.

- 1.0 when determining the stresses and/or strains at strength and extreme event limit states in accordance with Articles 1.6 and 1.7 of this Appendix.

The development length shall be taken as specified in Article 1.9.4.3.2 of this Appendix.

The effects of debonding shall be considered as specified in Article 1.9.4.3.3 of this Appendix.

1.9.4.3.2. Bonded Strands

Pretensioning strand shall be bonded beyond the section required to develop f_{ps} for a development length, ℓ_d, in inches, where ℓ_d shall satisfy:

$$\ell_d \geq \ell_t + 0.30\,(f_{ps} - f_{pe})\,d_b \qquad (1.9.4.3.2\text{-}1)$$

where:

f_{ps} = average stress in prestressing steel at the time for which the nominal resistance of the member is required (ksi)

f_{pe} = effective stress in the prestressing steel after losses (ksi)

The variation of design stress in the pretensioned strand from the free end of the strand may be calculated as follows:

- From the point where bonding commences to the end of transfer length:

$$f_{px} = \frac{f_{pe}\,\ell_{px}}{\xi 24 d_b} \qquad (1.9.4.3.2\text{-}2)$$

- From the end of the transfer length and to the end of the development of the strand:

$$f_{px} \leq f_{pe} + \frac{\ell_{px} - \xi 24 d_b}{0.30 d_b} \qquad (1.9.4.3.2\text{-}3)$$

where:

f_{px} = design stress in the pretensioned strand at nominal flexural strength at a section of the member under consideration (ksi)

C1.9.4.3.2

Eq. 1.9.4.3.2-1 is based on the results of experimental studies that captured information on the development length of pretensioning strands in UHPC (John et al. 2011; Lubbers 2003; Graybeal 2006; Graybeal 2015a). The development length is the sum of the transfer length and a term related to the flexural bond length, expressed as a function of the strand diameter, similar to that originally proposed by Hanson and Kaar (1959).

The correlation between steel stress and the distance over which the strand is bonded to the UHPC can be idealized by the relationship shown in Figure C1.9.4.3.2-1. This idealized variation of strand stress may be used for analyzing sections within the transfer and development length at the end of pretensioned members.
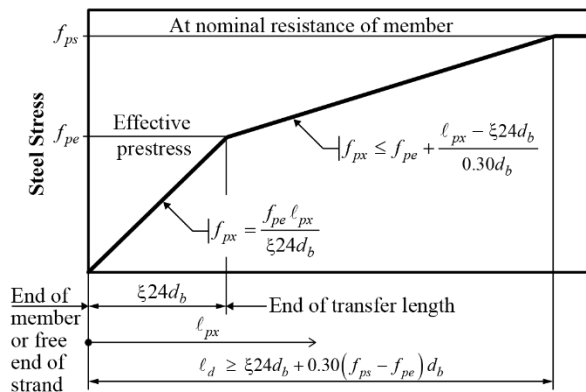
Source: FHWA.

Figure C1.9.4.3.2-1—Idealized relationship between steel stress and distance from the free end of the strand.

ℓ_{px} = distance from the free end of the pretensioned strand to the section of member under consideration (in.)

1.9.4.3.3. Debonded Strands

The provisions of AASHTO LRFD BDS Article 5.9.4.3.3 (AASHTO 2020) shall apply with the following amendments:

- In restriction C, $60d_b$ shall be replaced by ℓ_t in accordance with Article 1.9.4.3.1 of this Appendix with $\xi = 1.00$.

- Restriction F shall not apply.

- In Restriction H, the reference to guidance in AASHTO LRFD BDS Article 5.12.3.3 (AASHTO 2020) shall not apply.

The applicability of the provisions of AASHTO LRFD BDS Article 5.12.3.3 (AASHTO 2020) has not been investigated for UHPC.

1.9.4.4. Pretensioned Anchorage Zones

1.9.4.4.1. Splitting Resistance

Unless amended herein, the provisions of AASHTO LRFD BDS Article 5.9.4.4 (AASHTO 2020) shall apply for pretensioned anchorage zones of UHPC members.

The factored splitting resistance of pretensioned anchorage zones provided by the reinforcement in the ends of pretensioned conventional concrete beams may be replaced by:

$$P_r = f_s A_s + P_{r,UHPC} \qquad (1.9.4.4\text{-}1)$$

in which:

$$P_{r,UHPC} = 0.25\gamma_u f_{t,cri} b_v h \qquad (1.9.4.4\text{-}2)$$

where:

f_s = stress in steel not to exceed 20.0 ksi

The tensile resistance of UHPC (i.e., $\gamma_u f_{t,cri}$) provides a resistance to splitting forces (i.e., $P_{r,UHPC}$) in anchorage zones of pretensioned UHPC beams. In calculating $P_{r,UHPC}$ according to Eq. 1.9.4.4-2, it is assumed that the UHPC tensile resistance $\gamma_u f_{t,cri}$ acts uniformly over an area bound by a distance of $h/4$ from the end of the member and a width b_v, where h is the overall height of the member and b_v is the effective web width taken as the minimum web width within the depth d_v.

A_s = total area of reinforcement located within the distance $h/4$ from the end of the beam (in.²)

$P_{r,UHPC}$ = splitting resistance of pretensioned anchorage zones provided by UHPC (kip)

$f_{t,cri}$ = design UHPC effective cracking strength at the time of pre-stressing determined according to Article 1.9.1.2 of this Appendix (ksi)

b_v = effective web width taken as the minimum web width within the depth d_v (in.)

h = overall dimension of precast member in the direction in which splitting resistance is being evaluated (in.)

1.9.4.4.2. Confinement Reinforcement

The provisions of AASHTO LRFD BDS Article 5.9.4.4.2 (AASHTO 2020) shall apply.

1.9.4.5. Temporary Strands

The provisions of AASHTO LRFD BDS Article 5.9.4.5 (AASHTO 2020) shall apply, in which reference to Article 5.9.4.3.3 shall be replaced by Article 1.9.4.3.3 of this Appendix.

1.10. REINFORCEMENT

Unless verified by physical tests and as approved by the owner, the provisions of this Article shall apply for reinforcement embedded in UHPC.

1.10.1. UHPC Cover

The provisions of AASHTO LRFD BDS Article 5.10.1 (AASHTO 2020) shall apply in which the modification factor for *W/CM* ratio

C1.10.1

The cover for UHPC is intended to offer sufficient durability by limiting crack widths in service such that the durability of the structure remains minimally affected. The minimum

shall be taken as equal to or greater than 0.6 (AASHTO 2020).

cover is based on the results of an analysis of section curvature of UHPC members containing main reinforcing steel at the service stress limit for common reinforcing steel bars. The analysis followed the methodology in Frosch (2001) for crack width estimations. To establish limit states, a crack width of 0.004 in. was considered as having a negligible effect on the transport properties of UHPC, while the maximum serviceable crack width was considered to be 0.016 in. These crack widths likely exceed the UHPC tensile strain service limits defined in Article 1.5.2 of this Appendix. The spacing of cracks was considered using the experimentally observed relationship between extreme fiber tensile strain and crack spacing from Graybeal (2006), which is consistent with a weakest link model distribution of cracking in a UHPC member subjected to flexure, in accordance with the Weibull statistical theory for strength.

The design professional should use engineering judgment when applying these provisions to components that are not expected to crack under service loads and to bridge preservation applications, wherein the expected service life of the repair must be considered alongside that of the structure.

The minimum cover shall not be less than the greater of 1.5 times the length of the longest type of fiber reinforcement included in the UHPC or 0.75 in., unless adequate fiber distribution can be otherwise demonstrated for a specific application.

Restrictions to the flow of UHPC during casting can result in undesirable fiber distribution effects. This provision stipulates a geometry that allows for sufficient passing of fibers through constricted spaces. There may be specific applications where this provision could be relaxed, but adequate fiber distribution would need to be demonstrated.

For each component, the maximum fiber length associated with the minimum cover specified in design shall be shown in the contract documents.

1.10.2. Hooks and Bends

The provisions of AASHTO LRFD BDS Article 5.10.2 (AASHTO 2020) shall apply in which reference to Article 5.10.8.2.4 shall be replaced by Article 1.10.8.2.4 of this Appendix.

1.10.3. Spacing of Reinforcement

C1.10.3

The provisions of AASHTO LRFD BDS Article 5.10.3 (AASHTO 2020) shall apply with the following amendments:

- The clear distance between parallel bars specified in AASHTO LRFD BDS Articles 5.10.3.1.1 and 5.10.3.1.2 (AASHTO 2020) shall not be less than the greater of 1.5 times the length of the longest type of fiber reinforcement included in the UHPC or 0.75 in.

This provision stipulates a geometry that allows for sufficient passing of fibers through constricted spaces during casting. Restrictions to flow can result in undesirable fiber distribution effects within a member.

- The clear distance between reinforcement and an interface shall not be less than the greater of 1.5 times the length of the longest type of fiber reinforcement included in the UHPC or 0.75 in., unless adequate fiber distribution can be otherwise demonstrated for a specific application.

- References to AASHTO LRFD BDS Articles 5.10.4, 5.10.5, and 5.10.6 (AASHTO 2020) shall be replaced by Articles 1.10.4, 1.10.5, and 1.10.6, respectively, of this Appendix.

For each component, the maximum fiber length associated with the minimum spacing of reinforcement specified in design shall be shown in the contract documents.

1.10.4. Transverse Reinforcement for Compression Members

C1.10.5

The provisions of AASHTO LRFD BDS Article 5.10.4 (AASHTO 2020) shall apply with the following amendments:

- References to AASHTO LRFD BDS Articles 5.10.8 (AASHTO 2020) shall be replaced by Article 1.10.8 of this Appendix.

- The clear spacing between the bars of spiral reinforcement specified in AASHTO LRFD BDS Article 5.10.4.2 (AASHTO 2020) shall not be less than the greater of 1.5 times the length of the longest type of fiber reinforcement included in the UHPC or 0.75 in. The minimum fiber length associated with this requirement shall be shown on contract documents.

- The maximum limit on the design compressive strength specified in AASHTO LRFD BDS Article 5.10.4.3 (AASHTO 2020) shall not apply.

This provision stipulates a geometry that allows for sufficient passing of fibers through constricted spaces during casting. Restrictions to flow can result in undesirable fiber distribution effects within a member.

1.10.5. Transverse Reinforcement for Flexural Member

The provisions of AASHTO LRFD BDS Article 5.10.5 (AASHTO 2020) shall apply in which reference to Article 5.10.4 shall be replaced by Article 1.10.4 of this Appendix.

1.10.6. Shrinkage and Temperature Reinforcement

C1.10.6

Reinforcement for shrinkage and temperature stresses need not be provided.

Fibers included in UHPC serve the function of shrinkage and temperature reinforcement due to their ability to sustain tensile loads beyond cracking of the cementitious composite.

1.10.7. Reinforcement for Hollow Rectangular Compression Members

The provisions of AASHTO LRFD BDS Article 5.10.7 (AASHTO 2020) shall apply.

1.10.8. Development and Splices of Reinforcement

1.10.8.1. General

The provisions of Article 1.10.8.2.1 and 1.10.8.2.4 of this Appendix, and the provisions for lap splices in tension in AASHTO LRFD BDS Article 5.10.8.4.3a (AASHTO 2020), as

amended by Article 1.10.8.4 of this Appendix, are valid for No. 11 bars or smaller, subject to the limitations as specified in each of these articles (AASHTO 2020).

The provisions of AASHTO LRFD BDS Articles 5.10.8.1.1 and 5.10.8.1.2 (AASHTO 2020) shall apply in which the reference for Article 5.10.8.2 shall be replaced by Article 1.10.8.2 of this Appendix.

1.10.8.2. Development Length of Reinforcement

Development lengths shall be calculated using the specified minimum yield strength of the reinforcement. Use of nonprestressed reinforcement with a specified minimum yield strength up to 100 ksi may be permitted for elements and connections specified in AASHTO LRFD BDS Article 5.4.3.3 (AASHTO 2020) and subject to the provisions and limitations specified in each of the following articles.

1.10.8.2.1. Deformed Bars and Deformed Wire in Tension

For No. 8 bars and smaller embedded in UHPC, having a minimum f'_{ci} of 14.0 ksi and a minimum cover of two times the diameter of the bar, i.e., $2d_b$, the development length, ℓ_d, may be taken as:

- $10d_b$ for bars with yield strength less than or equal to 75 ksi.

- $12d_b$ for bars with yield strength greater than 75 ksi and less than or equal to 100 ksi.

For all other cases, the provisions of AASHTO LRFD BDS Article 5.10.8.2.1 (AASHTO 2020) shall apply with the following amendments:

C1.10.8.2.1

FHWA published guidance on reinforcing bar development length within a document on the design of field-cast UHPC connections (*Design and Construction of Field-Cast UHPC Connections*, FHWA-HRT-19-011) (Graybeal 2019). This guidance is based on testing of UHPC-class materials that meet the baseline requirements for UHPC stated herein. The guidance addresses a subset of deformed bar sizes and covers.

- The maximum limit on the design compressive strength shall not apply.

- References to AASHTO LRFD BDS Articles 5.7.2.5 and 5.10.8.2.6 (AASHTO 2020) shall be replaced by Articles 1.7.2.5 and 1.10.8.2.6 of this Appendix, respectively.

- The referenced provisions of AASHTO LRFD BDS Article 5.10.4.3 (AASHTO 2020) shall be amended by the provisions of Article 1.10.4 of this Appendix.

- The concrete density modification factor shall be taken equal to 1.0.

- The UHPC compressive strength, f'_c, in AASHTO LRFD BDS Eq. 5.10.8.2.1a-2 (AASHTO 2020) shall not be taken as a value greater than 15.0 ksi.

- The reinforcement location factor, λ_{rl}, in AASHTO LRFD BDS Eq. 5.10.8.2.1a-2 (AASHTO 2020) may be taken equal to 1.0.

1.10.8.2.2. Deformed Bars in Compression

The provisions of AASHTO LRFD BDS Article 5.10.8.2.2 (AASHTO 2020), except for Eq. 5.10.8.2.2a-2, shall apply.

1.10.8.2.3. Bundled Bars

The provisions of AASHTO LRFD BDS Article 5.10.8.2.3 shall apply, in which the referenced provisions of Articles 5.10.8.2.1b and 5.10.8.2.1c shall be amended by the provisions of Article 1.10.8.2.1 of this Appendix.

1.10.8.2.4. Standard Hooks in Tension

For standard hooks, made of No. 8 deformed bars and smaller and embedded in UHPC

C1.10.8.2.4

FHWA published guidance on reinforcing bar development length within a document on the

having a minimum f'_{ci} of 14.0 ksi and a minimum cover of $2d_b$, the modified development length, ℓ_{dh}, may be taken as the greater of the following:

- $8d_b$.
- 6.0 in.

For all other cases, the provisions of AASHTO LRFD BDS Article 5.10.8.2.4 shall apply with the following amendments:

- The maximum limit on the design compressive strength shall not apply.

- The referenced provisions of AASHTO LRFD BDS Article 5.10.2.1 (AASHTO 2020) shall be amended by the provisions of Article 1.10.2 of this Appendix.

- The referenced provisions of AASHTO LRFD BDS Article 5.10.4.3 (AASHTO 2020) shall be amended by the provisions of Article 1.10.4 of this Appendix.

- The concrete density modification factor shall be taken as equal to 1.0.

- The UHPC compressive strength, f'_c, in AASHTO LRFD BDS Eq. 5.10.8.2.4a-2 (AASHTO 2020) shall not be taken as a value greater than 15.0 ksi.

1.10.8.2.5. Welded Wire Reinforcement

The provisions of AASHTO LRFD BDS Article 5.10.8.2.5 (AASHTO 2020) shall apply with the following amendments:

design of field-cast UHPC connections (*Design and Construction of Field-Cast UHPC Connections*, FHWA-HRT-19-011) (Graybeal 2019). This guidance is based on testing of UHPC-class materials that meet the baseline requirements for UHPC stated herein. The guidance addresses a subset of deformed bar sizes and covers. The provisions in Article 1.10.8.2.1 of this Appendix are combined here with the detailing requirements for standard hooks in tension.

- Reference to AASHTO LRFD BDS Article 5.10.8.2.6 (AASHTO 2020) shall be replaced by Article 1.10.8.2.6 of this Appendix.

- The referenced provisions of AASHTO LRFD BDS Articles 5.10.8.2.1a and 5.10.8.2.1c (AASHTO 2020) shall be amended by the provisions of Article 1.10.8.2.1 of this Appendix.

- The maximum limit on the design compressive strength shall not apply.

- The UHPC compressive strength, f'_c, in AASHTO LRFD BDS Eqs. 5.10.8.2.5-2, 5.10.8.2.5-3, and 5.10.8.2.5-4 (AASHTO 2020) shall not be taken as a value greater than 15.0 ksi.

- The concrete density modification factor shall be taken as equal to 1.0.

1.10.8.2.6. Shear Reinforcement

The provisions of AASHTO LRFD BDS Article 5.10.8.2.6 (AASHTO 2020) shall apply with the following amendments:

- Shear reinforcement consisting of single bars shall be placed equidistantly to the surfaces of members.

- Bent longitudinal bars shall not act as transverse reinforcement.

- The maximum limit on the design compressive strength shall not apply.

- The UHPC compressive strength, f'_c, in AASHTO LRFD BDS Eq. 5.10.8.2.6b-1 (AASHTO 2020) shall not be taken as a value greater than 15.0 ksi.

- The concrete density modification factor shall be taken as equal to 1.0.

1.10.8.3. Development by Mechanical Anchorages

The provisions of AASHTO LRFD BDS Article 5.10.8.3 (AASHTO 2020) shall apply.

1.10.8.4. Splices of Bar Reinforcement

The provisions of AASHTO LRFD BDS Article 5.10.8.4 (AASHTO 2020) shall apply with the following amendments:

- Reference to AASHTO LRFD BDS Articles 5.7.2.5 and 5.10.8.2.3 (AASHTO 2020) shall be replaced by Articles 1.7.2.5 and 1.10.8.2.3 of this Appendix, respectively.

- The referenced provisions of Articles 5.10.4.3 and 5.10.8.2.1a shall be amended by the provisions of Articles 1.10.4 and 1.10.8.2.1 of this Appendix, respectively.

- The maximum limit on the design compressive strength shall not apply.

- No. 8 bars and smaller embedded in UHPC, having a minimum f'_{ci} of 14.0 ksi and a minimum cover of $2d_b$, and spliced by noncontact lap splices in flexural members may be spaced farther apart transversely at three-fourths the required lap splice but not greater than 6.0 in.

- Lap splices in tension of No. 8 bars and smaller embedded in UHPC, having a minimum f'_{ci} of 14.0 ksi and at a minimum cover of $2d_b$, may be classified as Class A splice for the purposes of AASHTO LRFD BDS Article 5.10.8.4.3a (AASHTO 2020).

C1.10.8.4

FHWA published guidance on splices of bar reinforcement within a document on the design of field-cast UHPC connections (*Design and Construction of Field-Cast UHPC Connections*, FHWA-HRT-19-011) (Graybeal 2019). This guidance is based on testing of UHPC-class materials that meet the baseline requirements for UHPC stated herein. The guidance addresses a subset of deformed bar sizes and covers.

1.10.8.5. Splices of Welded Wire Reinforcement

The provisions of AASHTO LRFD BDS Article 5.10.8.5 (AASHTO 2020) shall apply in which the referenced provisions of Article 5.10.8.4.3a and Eq. 5.10.8.2.5-1 shall be amended by the provisions of Articles 1.10.8.4 and 1.10.8.2.5 of this Appendix, respectively.

SECTION 2. MATERIAL CONFORMANCE GUIDANCE FOR ULTRA-HIGH PERFORMANCE CONCRETE

2.1. SCOPE

2.1.1. General

The provisions in Section 2 of this Appendix relate to material constituents, material qualification, and material acceptance for UHPC.

C2.1.1

The guidance in Section 2 of this Appendix applies to UHPC materials intended for use in structural design following Section 1 of this Appendix.

The material behavior of UHPC is directly related to the mixture ingredients, mixture proportions, mixing procedures, curing regimes, and casting methods. Section 2 of this Appendix delineates the requirements for material constituents of UHPC and provides guidance on the qualification and acceptance testing for a UHPC mixture.

The provisions of Section 2 of this Appendix provide owners, designers, constructors, and material suppliers with a process through which to determine the qualified design values of individual material properties for a particular UHPC mixture. These qualified values are expected to be instrumental in an owner's determination of the specified values that are defined within project procurement documents. At the project execution phase, these specified values are then used to determine the required values that are engaged during acceptance testing to ensure material compliance.

2.1.2. Limitations

The provisions of Section 2 of Appendix A do not address the fabrication of components. Materials manufactured, qualified, and accepted according to Section 2 of this Appendix may express different properties resulting from the means and method of fabrication.

C2.1.1

Fabrication processes may affect the fresh and hardened properties of the UHPC mixture. Some mixing and placing methodologies may result in undesirable entrapment of air within the placed UHPC, as well as undesirable distribution and orientation of fiber reinforcement.

2.2. DEFINITIONS

Acceptance Testing—Testing performed during the construction of structural components to determine compliance of the material properties of the supplied UHPC with the requirements of the project specifications or contract documents.

Design Value—Value of a material property used in structural design.

Qualification Testing—Testing performed before construction of structural components to determine the expected material properties of a UHPC mixture.

Qualified Design Value—Maximum value of a material property that can be used in structural design.

Required Value—Minimum average value of a material property required to be obtained from acceptance testing.

Specified Value—Average value of a material property stipulated in the project specifications or contract documents, which may be greater than the value used in design.

Test Result—The material property value obtained from a standard test conducted on an individual specimen for qualification or acceptance of a UHPC mixture.

2.3. NOTATION

$A_{u,i}$ =   cross-sectional area of test specimen i, measured with an accuracy of less than 1 percent (m^2)

E_c =   modulus of elasticity for use in design (ksi)

$E_{c,i}$ =   modulus of elasticity test result of specimen i (ksi)

$\bar{E}_{cQ}$ =   average value of the modulus of elasticity test results for a mixture obtained from qualification testing (ksi)

f'_c =   compressive strength of UHPC for use in design (ksi)

$f'_{c,i}$ =   compression-strength test result of specimen i (ksi)

f'_{cQ} =   qualified design value of the compressive strength (ksi)

$\bar{f}'_{cQ}$ =   average value of the compressive strength test results for a UHPC mixture obtained from qualification testing (ksi)

f'_{cR} =   required average value of the compressive strength obtained from acceptance testing (ksi)

$f_{t,cr}$ =   effective cracking strength of UHPC for use in design (ksi)

$f_{t,crQ}$ =   qualified design value of the effective cracking strength (ksi)

$\bar{f}_{t,crQ}$ =   average value of the effective cracking strength test results for a mixture obtained from qualification testing (ksi)

$f_{t,crR}$ = required average value of the effective cracking strength obtained from acceptance testing (ksi)

$f_{t,cr,i}$ = effective cracking strength value obtained from tension-test specimen i (ksi)

$f_{t,loc}$ = crack localization strength of UHPC for use in design (ksi)

$f_{t,loc,i}$ = crack localization strength value obtained from tension-test specimen i (ksi)

$f_{t,locQ}$ = qualified design value of the crack localization strength (ksi)

$\overline{f}_{t,locQ}$ = average value of the crack localization strength test results for a UHPC mixture obtained from qualification testing (ksi)

$f_{t,locR}$ = required average value of the crack localization strength obtained from acceptance testing (ksi)

k_{cQ} = modification factor for the total number of compression strength test results, n_{cQ}, considered in calculating the sample standard deviation determined from Table 2.6.4.2-1 of this Appendix

k_{fQ} = modification factor for the total number of flexural test results, n_{fQ}, considered in calculating the sample standard deviation determined from Table 2.6.4.2-1 of this Appendix

k_i = individual specimen geometry factor of test specimen i (m)

k_{tQ} = modification factor for the total number of tension test results, n_{tQ}, considered in calculating the sample standard deviation determined from Table 2.6.4.2-1 of this Appendix

$k_{\rho Q}$ = modification factor for the total number of uniaxial resistivity test results, $n_{\rho Q}$, considered in calculating the sample standard deviation determined from Table 2.6.4.2-1 of this Appendix

$L_{u,i}$ = length of test specimen i, measured with an accuracy less than 1 percent (m)

n_{cQ} = total number of compression strength test results obtained from qualification testing

n_{EQ} = total number of modulus of elasticity test results obtained from qualification testing

n_{fQ} = total number of flexural test results obtained from qualification testing

n_{tQ} = total number of tensile test results exhibiting tension responses of Types H-1 or H-2 (AASHTO T 397) obtained from qualification testing

$n_{\rho Q}$ = total number of uniaxial resistivity test results obtained from qualification testing

P_{pQ} = qualified value of the load P_p for a UHPC mixture obtained from qualification testing (ksi)

$P_{p,i}$ = peak load obtained from the flexural prism test results of specimen i (kip)

$\overline{P}_{pQ}$ = average value of the peak load obtained from qualification testing (ksi)

P_δ = load measured during flexural prism test at δ (kip)

$P_{\delta,i}$ = individual load measured at each increment value of net midspan displacement, δ, obtained from the flexural prism test results of specimen i (kip)

$P_{\delta Q}$ =   qualified value of the load P_δ for the mixture obtained from qualification testing (kip)

$\overline{P}_{\delta Q}$ =   average value of P_δ for a UHPC mixture obtained from qualification testing (kip)

R_i =   electrical resistance obtained from uniaxial resistivity-test specimen i (Ω)

s_{cQ} =   sample standard deviation of the compressive strength test results for a UHPC mixture obtained from qualification testing (ksi)

s_{EQ} =   sample standard deviation of the modulus of elasticity test results for a UHPC mixture obtained from qualification testing (ksi)

s_{pQ} =   sample standard deviation of $\overline{P}_{pQ}$ for a UHPC mixture obtained from qualification testing (ksi)

$s_{t,crQ}$ =   sample standard deviation of the effective crack localization strength test results for a UHPC mixture obtained from qualification testing (ksi)

$s_{t,locQ}$ =   sample standard deviation of the crack localization strength test results for a UHPC mixture obtained from qualification testing (ksi)

$s_{\delta Q}$ =   sample standard deviation of $\overline{P}_{\delta Q}$ for a UHPC mixture obtained from qualification testing (ksi)

$s_{\varepsilon t,locQ}$ =   sample standard deviation of the crack localization strain test results for a UHPC mixture obtained from qualification testing (in./in.)

$\delta_{p,i}$ =   net midspan deflection recorded at peak load, $P_{p,i}$, from the flexural prism test result of specimen i (in.)

$\overline{\delta}_{pQ}$ =   average value of the net midspan deflection at peak load, $\delta_{p,i}$, obtained from qualification testing (ksi)

$s_{\rho Q}$ =   sample standard deviation of the uniaxial resistivity test results for a UHPC mixture obtained from qualification testing (Ω)

$\varepsilon_{t,loc}$ =   crack localization strain of UHPC for use in design (in./in.)

$\varepsilon_{t,loc,i}$ =   crack localization strain value obtained from tension-test specimen i (in./in.)

$\varepsilon_{t,locQ}$ =   qualified design value of the crack localization strain (in./in.)

$\overline{\varepsilon}_{t,locQ}$ =   average value of the crack localization strain test results for a UHPC mixture obtained from qualification testing (in./in.)

$\varepsilon_{t,locR}$ =   required average value of the crack localization strain from acceptance testing (in./in.)

ρ_i =   uniaxial electrical resistivity test result obtained from uniaxial resistivity test specimen i ($\Omega \cdot$m)

ρ_Q =   qualified value of uniaxial resistivity for a UHPC mixture obtained from qualification testing ($\Omega \cdot$m)

$\overline{\rho}_Q$ =   average value of uniaxial resistivity for a UHPC mixture obtained from qualification testing ($\Omega \cdot$m)

2.4. REFERENCED STANDARDS, TEST METHODS, AND REPORTS

AASHTO M 201-21, *Standard Specification for Mixing Rooms, Moist Cabinets, Moist Rooms, and Water Storage Tanks Used in the Testing of Hydraulic Cements and Concretes* (AASHTO 2021).

AASHTO T 397-22, *Standard Method of Test for Uniaxial Tensile Response of Ultra-High Performance Concrete* (AASHTO 2022b).

AASHTO TP 119-22, *Standard Method of Test for Electrical Resistivity of a Concrete Cylinder Tested in a Uniaxial Resistance Test* (AASHTO 2022a).

ACI 214R-11, *Guide to Evaluation of Strength Test Results of Concrete* (ACI Committee 214 2011).

ACI 301-20, *Specifications for Concrete Construction* (ACI Committee 301 2020).

API Specification 10A, *Cements and Materials for Well Cementing* (American Petroleum Institute 2022).

ASTM A820/A820M-22, *Standard Specification for Steel Fibers for Fiber-Reinforced Concrete* (ASTM 2022e).

ASTM C31/C31M-12, *Standard Practice for Making and Curing Concrete Test Specimens in the Field* (ASTM 2012).

ASTM C33/C33M-18, *Standard Specification for Concrete Aggregates* (ASTM 2018b).

ASTM C39/C39M-20, *Standard Test Method for Compressive Strength of Cylindrical Concrete Specimens* (ASTM 2020d).

ASTM C138/C138M-17a, *Standard Test Method for Density (Unit Weight), Yield, and Air Content (Gravimetric) of Concrete* (ASTM 2017d).

ASTM C144-18, *Standard Specification for Aggregate for Masonry Mortar* (ASTM 2018a).

ASTM C150/C150M-22, *Standard Specification for Portland Cement* (ASTM 2022c).

ASTM C157/C157M-17, *Standard Test Method for Length Change of Hardened Hydraulic-Cement Mortar and Concrete* (ASTM 2017e).

ASTM C192/C192M-19, *Standard Practice for Making and Curing Concrete Test Specimens in the Laboratory* (ASTM 2019a).

ASTM C494/C494M-19, *Standard Specification for Chemical Admixtures for Concrete* (ASTM 2019b).

ASTM C469/C469M-22, *Standard Test Method for Static Modulus of Elasticity and Poisson's Ratio of Concrete in Compression* (ASTM 2022g).

ASTM C595/C595M-21, *Standard Specification for Blended Hydraulic Cements* (ASTM 2021).

ASTM C618-22, *Standard Specification for Coal Ash and Raw or Calcined Pozzolan for Use in Concrete* (ASTM 2022a).

ASTM C989/C989M-22, *Standard Specification for Slag Cement for Use in Concrete and Mortars* (ASTM 2022d).

ASTM C1064/C1064M-17, *Standard Practice for Temperature of Freshly Mixed Hydraulic-Cement Concrete* (ASTM 2017b).

ASTM C1240-20, *Standard Specification for Silica Fume Used in Cementitious Mixtures* (ASTM 2020c).

ASTM C1437-20, *Standard Test Method for Flow of Hydraulic Cement Mortar* (ASTM 2020e).

ASTM C1556-22, *Standard Test Method for Determining the Apparent Chloride Diffusion Coefficient of Cementitious Mixtures by Bulk Diffusion* (ASTM 2022f).

ASTM C1602/C1602M-22, *Standard Specification for Mixing Water Used in the Production of Hydraulic Cement Concrete* (ASTM 2022b).

ASTM C1609/C1609M-19a, *Standard Test Method for Flexural Performance of Fiber-Reinforced Concrete (Using Beam With Third-Point Loading)* (ASTM 2019c).

ASTM C1666/C1666M-08, *Standard Specification for Alkali Resistant (AR) Glass Fiber for GFRC and Fiber-Reinforced Concrete and Cement* (ASTM 2008).

ASTM C1712-20, *Standard Test Method for Rapid Assessment of Static Segregation Resistance of Self-Consolidating Concrete Using Penetration Test* (ASTM 2020g).

ASTM C1758/C1758M-15, *Standard Practice for Fabricating Test Specimens with Self-Consolidating Concrete* (ASTM 2015b).

ASTM C1797-17, *Standard Specification for Ground Calcium Carbonate and Aggregate Mineral Fillers for use in Hydraulic Cement Concrete* (ASTM 2017c).

ASTM C1812/C1812M-15, *Standard Practice for Design of Journal Bearing Supports to be Used in Fiber Reinforced Concrete Beam Tests* (ASTM 2015a).

ASTM C1856/C1856-17, *Standard Practice for Fabricating and Testing Specimens of Ultra-High Performance Concrete* (ASTM 2017a).

ASTM D7357-07, *Standard Specification for Cellulose Fibers for Fiber-Reinforced Concrete* (ASTM 2007).

ASTM D7508/D7508M-20, *Standard Specification for Polyolefin Chopped Strands for Use in Concrete* (ASTM 2020b).

PCI TR-9-22, *Guidelines for the Use of Ultra High Performance Concrete (UHPC) in Precast and Prestressed Concrete* (PCI Concrete Materials Technology Committee 2022).

2.5. MATERIAL CONSTITUENTS

Each constituent material used in the manufacture of the UHPC shall be of a consistent type or mill source.

The constituent materials included in a UHPC mixture shall be reported to the owner.

2.5.1. Granular Constituents

2.5.1.1. Hydraulic Cement

The UHPC shall contain hydraulic cement. The hydraulic cement shall be compliant with the requirements of ASTM C150 (ASTM 2022c), ASTM C595 (ASTM 2021), or API Specification 10A (American Petroleum Institute 2022).

2.5.1.2. Fine Aggregates

The fine aggregates shall be compliant with ASTM C33 (ASTM 2018b) or ASTM C144 (ASTM 2018a), except that the grading requirements need not apply.

Constituent materials that are potentially susceptible to alkali-aggregate reactions shall not be used.

2.5.1.3. Supplementary Cementitious Materials, Mineral Fillers, and Other Granular Constituents

2.5.1.3.1. Silica Fume

If included as a constituent material, silica fume shall be compliant with ASTM C1240 (ASTM 2020c).

2.5.1.3.2. Fly Ash

If included as a constituent material, fly ash shall be compliant with ASTM C618 (ASTM 2022a).

2.5.1.3.3. Slag Cement

If included as a constituent material, slag cement shall be compliant with ASTM C989 (ASTM 2022d).

2.5.1.3.4. Ground Calcium Carbonate

If included as a constituent material, ground calcium carbonate shall be compliant with ASTM C1797 (ASTM 2017c).

2.5.1.3.5. Other Natural Pozzolan

If included as a constituent material, other natural pozzolans shall be compliant with ASTM C618 (ASTM 2022a).

2.5.1.3.6. Other Granular Constituents

The suitability of all other granular constituents included in the UHPC mixture shall be demonstrated and approved by the owner.

2.5.2. Liquid and Frozen Water

Liquid and frozen water shall be compliant with ASTM C1602 (ASTM 2022b).

2.5.3. Chemical Admixtures

Chemical admixtures shall be compliant with ASTM C494 (ASTM 2019b).

Chemical admixtures shall not contain calcium chloride. Chemical admixtures shall not contain more than 0.15 percent chloride ions by weight of admixture.

For UHPC mixtures containing more than one chemical admixture, the chemical admixtures

shall be certified by the manufacturer to be compatible.

2.5.4. Fiber Reinforcement

2.5.4.1. Steel Fiber Reinforcement

The UHPC mixture shall contain steel fiber reinforcement as primary fiber reinforcement.

Steel fiber reinforcement shall be compliant with ASTM A820 (ASTM 2022e).

The following properties of each steel fiber reinforcement type shall be reported to the owner:

- Chemical composition
- Tensile yield and ultimate strength
- Length
- Cross-sectional geometry
- Deformations and/or end anchorages
- Coating (if applicable)

The volumetric proportion of steel fiber reinforcement in the UHPC mixture design shall be reported to the owner.

2.5.4.2. Non-steel Fiber Reinforcement

Non-steel fiber reinforcement may be included in a UHPC mixture but shall not be the primary fiber reinforcement.

For each type of non-steel fiber reinforcement included in the mixture, the following properties shall be reported to the owner:

- Chemical composition
- Tensile strength
- Length
- Cross-sectional geometry
- Deformations and/or end anchorages
- Coating (if applicable)

C2.5.4.1

Various compositions of steel, including grades of stainless steel, are allowable.

C2.5.4.2

Non-steel fiber reinforcements may be included to enhance certain performance characteristics of a UHPC mixture, such as to increase fire resistance. When non-steel fiber reinforcements are included in a UHPC mixture, unfavorable effects should be considered. Among other considerations, non-steel fiber reinforcements may segregate relative to the steel fibers due to their different density, may exhibit creep behaviors under sustained load, may degrade more rapidly under certain environmental conditions, and may result in wider cracks that increase permeability.

The volumetric proportion of each type of other fiber reinforcement in the UHPC mixture shall be reported to the owner.

If included in the UHPC mixture, alkali resistant glass fibers shall be compliant with ASTM C1666 (ASTM 2008).

If included in the UHPC mixture, polyolefin fibers shall be compliant with ASTM D7508 (ASTM 2020b).

If included in the UHPC mixture, cellulose fibers shall be compliant with ASTM D7357 (ASTM 2007).

2.6. MATERIAL QUALIFICATION

2.6.1. General

Material qualification testing shall be conducted in accordance with Table 2.6.1-1 and prior to the selection of a UHPC mixture for use in the fabrication of structural components.

Material qualification results pertain to the specific UHPC mixture that was mixed, cured, and tested. Modifications to the constituent materials, mixture design, or curing process necessitate requalification of the UHPC product.

C2.6.1

Qualification testing is performed to determine the suitability of a particular UHPC mixture for use in structures designed according to the provisions of Section 1 of this Appendix.

Material qualification should be based on field-test specimens that represent materials, mixture proportions, batching procedures, and climatic conditions similar to those expected during the fabrication of UHPC elements.

Table 2.6.1-1. Material qualification testing methods and objective.

Property	Article	Objective	Requirement
Flow	2.6.3.2	Qualification	Yes
Fiber segregation	2.6.3.3	Qualification	Yes
Unit weight	2.6.3.4	Information	Yes
Compressive strength	2.6.4.2	Qualification	Yes
Tensile response	2.6.4.3	Qualification	Yes
Durability	2.6.5	Qualification	Yes
Modulus of elasticity	2.6.4.4	Information	Optional
Flexural response	2.6.6	Correlation to acceptance testing	Optional

2.6.2. Qualification Frequency

A complete set of material qualification testing shall be completed at an interval not to exceed 3 years.

2.6.3. Plastic Properties

2.6.3.1. General

The plastic property values of a particular UHPC mixture shall be established according to the methods cited herein and shown in the contract documents.

2.6.3.2. Flow

The flow shall be measured and reported for each batch from which specimens for qualification testing are cast. Flow shall be measured in accordance with ASTM C1856/1856M (ASTM 2017a), which provides direction on the use of ASTM C1437 (ASTM 2020e) when testing UHPC.

Flow shall be measured not more than 10 minutes before the time of specimen casting.

C2.6.3.2

Flow spread values typically range from 8 to 10 in. Lesser values may indicate a stiffer mixture that is difficult to place. Greater values may indicate a fluid mixture that could be more susceptible to fiber segregation.

2.6.3.3. Fiber Segregation

Susceptibility to fiber segregation shall be measured and reported for each batch from which specimens for tensile response qualification testing are cast.

The test shall be completed according to ASTM C1712 (ASTM 2020g) with the following modifications:

- Use of inverted slump mold is not required.

- Minimum mold dimensions are a cylinder with a 4-in. diameter and an 8-in. height.

C2.6.3.3

A 4-in. diameter by 8-in. tall cylinder may be used as the test specimen mold.

Static fiber segregation resistance shall be classified according to the criteria defined in Table X1.1 of ASTM C1712. To qualify as having acceptable fiber segregation resistance, the tested material must perform in the "resistant" category.

Both the penetration depth and the static segregation resistance classification shall be reported.

The elapsed time between the conclusion of mixing and the final reading, defined in ASTM C1712 Section 8.8.2, shall not exceed 10 minutes. The elapsed time shall be reported.

2.6.3.4. Unit Weight

Unit weight shall be measured and recorded according to ASTM C138-17a (ASTM 2017d) with the following modifications:

- The sample container shall be filled in a single, continuous pour as described in ASTM C1758 Section 7.4 (ASTM 2015b).

- The sample shall be consolidated by tapping the outside of the sample container 30 times with a rubber mallet. The sample shall not be rodded or internally vibrated.

2.6.4. Hardened Properties

2.6.4.1. General

The hardened property values of a particular UHPC mixture and their statistical variability shall be established according to the methods cited herein and shown in the contract documents.

C2.6.4.1

Given that the material behaviors of different UHPC mixtures are not unique, qualification testing establishes the maximum property values that can be used in design with a particular UHPC mixture, henceforth referred to as "qualified" values.

The qualified property values are obtained as a function of variability of the test results and the

106

proportion of test results allowed to fall below the qualified property values, such as:

- No more than the 1 percent of the average of three consecutive property test results fall below the qualified value, and

- No more than 1 percent of individual property test results fall below the qualified value by more than 10 percent.

The statistical formulations in this Article assume a normal distribution of the test results of each hardened property and are based on the concepts engaged in the American Concrete Institute *Specification for Concrete Construction* (ACI Committee 301 2020), *Guide to Evaluation of Strength Test Results of Concrete* (ACI Committee 214 2011), and *Building Code Requirements for Structural Concrete* (ACI Committee 318 2019).

The determination of the hardened property values from statistical procedures other than those cited in this Article shall be approved by the owner.

When the test results of a particular property show evidence of skewness or kurtosis, the data may not be normally distributed (ACI Committee 214 2011). The distribution is said to be skewed when the data are not symmetrical about the mean but concentrated to the right or left. Kurtosis is said to exist when the distribution curve is either too peaked or too flat. Simplified equations to calculate the relative skewness and kurtosis for a particular data set can be found in Cook (1989).

Test specimens used for qualification testing shall be fabricated according to ASTM C31 (ASTM 2012) or ASTM C192 (ASTM 2019a), as modified by ASTM C1856 (ASTM 2017a), AASHTO T 397 (AASHTO 2022b), and accompanying articles in this Appendix.

The casting method of the test specimens shall follow the procedures described in the standard of each property test.

The curing of all specimens used for qualification shall follow a defined regime and shall be reported to the owner. The curing regime shall not be more favorable than that anticipated for structural elements.

The curing regime during qualification should represent the curing regime expected during fabrication. Additional qualification testing should be required when field climatic conditions are appreciably different than the climatic conditions during qualification.

The testing of the hardened properties shall be conducted at 28 days or as approved by the owner.

The qualification testing should be performed when the material has reached a mature age where minimum changes of properties are expected to change with time, commonly assumed at 28 days. Other maturity ages may be assumed for components expected to receive loads at times appreciably different than 28 days after placement.

2.6.4.2. Compressive Strength

C2.6.4.2

The qualified design value of the compressive strength of a UHPC mixture, $\bar{f}'_{cQ}$, shall be determined from the results of a minimum of 15 cylinders produced, tested, and evaluated in accordance with ASTM C1856/C1856M (ASTM 2017a).

A minimum of 30 compression test results are recommended to capture the variation (i.e., mean and sample standard deviation) in the compressive strength results of a particular UHPC mixture.

A test result shall not be discarded, except that if any cylinder shows evidence of improper sampling, molding, or testing, said cylinder shall be discarded, and the strength shall be determined from the remaining cylinders.

Qualification testing is performed to capture the variation between the test results due to mixing, sampling, fabrication, curing, or testing. The test result of any specimen should not be discarded unless improper sampling, molding, or testing is evident.

Specimens shall be sampled from at least three separate batches. A minimum of two but not more than half of the tested cylinders shall be obtained from a single batch.

Qualification testing is intended to capture the variation within a batch as well as between different batches of a UHPC mixture.

The average and sample standard deviation of the compression strength, $\bar{f}'_{cQ}$ and s_{cQ}, respectively, shall be calculated based on the total number of tested specimens as follows:

$$\bar{f}'_{cQ} = \frac{1}{n_{cQ}} \sum_{i=1}^{n_{cQ}} f'_{c,i} \qquad (2.6.4.2\text{-}1)$$

$$s_{cQ} = \sqrt{\frac{\sum_{i=1}^{n_{cQ}} \left(f'_{c,i} - \bar{f}'_{cQ}\right)^2}{n_{cQ} - 1}} \qquad (2.6.4.2\text{-}2)$$

where:

n_{cQ} = total number of compression strength test results obtained from qualification testing.

Assuming that the strength results follow a normal distribution and that the number of tests performed during qualification is large enough to provide sufficient data for statistical analysis, the probability density function for the compressive strength, shown in Figure C2.6.4.2-1, is mathematically defined by two statistical parameters: the population mean and the standard deviation, taken as $\bar{f}'_{cQ}$ and s_{cQ}, respectively.

$f'_{c,i}$ = compression-strength test result of specimen i (ksi).
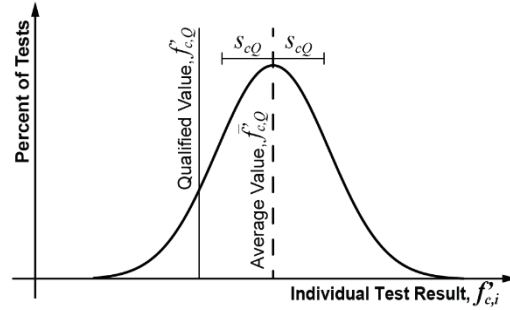
Source: FHWA.

Figure C2.6.4.2-1—Normal frequency curve for compressive strength with an a mean $\bar{f}'_{cQ}$ and standard deviation s_{cQ}.

The qualified design value of the compression strength, f'_{cQ}, shall be determined as the lesser of the following:

$$f'_{cQ} = \bar{f}'_{cQ} - 1.34\, k_{cQ}\, s_{cQ} \qquad (2.6.4.2\text{-}3)$$

$$f'_{cQ} = 1.11\, \bar{f}'_{cQ} - 2.59\, k_{cQ}\, s_{cQ} \qquad (2.6.4.2\text{-}4)$$

where:

k_{cQ} = modification factor for the total number of compression strength test results, n_{cQ}, considered in calculating the sample standard deviation determined from Table 2.6.4.2-1 of this Appendix

Table 2.6.4.2-1. k-factor for increasing the sample standard deviation based on total number of tests considered.

Total Number of Tests Considered	k-Factor for Increasing the Sample Standard Deviation
15	1.16
20	1.08
25	1.03
30 or more	1.00

Note: Linear interpolation for the intermediate number of tests is acceptable.

The qualified design value of the compressive strength, f'_{cQ}, shown in Figure C2.6.4.2-1, is computed following Eqs. 2.6.4.2-3 and 2.6.4.2-4 to satisfy the two criteria defined in Article C2.6.4.1 of this Appendix.

Eqs. 2.6.4.2-3 and 2.6.4.2-4 are derived from the equations of Table 4.2.3.3(a)1 of ACI SPEC-301 (ACI Committee 301 2020), originally developed for conventional concrete with compressive strength greater than 5,000 psi, to obtain the qualified design value of UHPC mixture, f'_{cQ}, as a function of the average value, $\bar{f}'_{cQ}$, and the sample standard deviation, s_{cQ}. In *Specification for Concrete Construction* (ACI Committee 301 2020), $\bar{f}'_{cQ}$ and f'_{cQ} are akin to the required average and the design value of the compressive strength, respectively, when data are available to establish the sample standard deviation.

Confidence in the statistical estimations is a function of the number of test results used to establish the statistical parameters. When fewer than 30 test results are considered, the standard deviation, s_{cQ}, should be multiplied by a modification factor, k_{cQ}, obtained from Table 2.6.4.2-1, to account for the uncertainty in the calculated standard deviation *Specification for Concrete Construction* (ACI Committee 301 2020).

2.6.4.3. Tensile Response

The qualified design values of the effective cracking strength, $f_{t,crQ}$, the design crack localization stress, $f_{t,locQ}$, and the design crack localization strain, $\varepsilon_{t,locQ}$, of a UHPC mixture shall be determined from a minimum of 15 tension response test results classified as Type H-1 or H-2, as defined in AASHTO T 397 (AASHTO 2022b).

Specimens shall be produced, tested, and evaluated in accordance with AASHTO T 397 (AASHTO 2022b) with the following restrictions:

- Specimens shall have a square cross section with 2-in. minimum dimension.

- Deformation shall be recorded over a minimum gauge length of 4 in.

A test result shall not be discarded, except that if any sample shows evidence of improper sampling, molding, or testing, said specimen shall be discarded and the tensile parameters shall be determined from the remaining specimens. A properly sampled, molded, and tested specimen exhibiting a tensile behavior of types other than H-1 or H-2, as defined in AASHTO T 397 (AASHTO 2022b), shall not be considered discarded, but its test results shall not be used to determine the tensile properties.

C2.6.4.3

The tensile qualification described in this Article pertains to UHPC mixtures exhibiting a strain-hardening stress-strain tensile behavior of Types H-1, H-2, H-3, and H-4, as defined in AASHTO T 397 (AASHTO 2022b). However, only test results where the localization crack occurs within the gauge length, i.e., tensile behavior of Types H-1 and H-2, are permitted to be used to determine the tensile properties.

A minimum of 30 tension test results, with tensile behavior of Type H-1 or H-2, are recommended to establish the variation (i.e., mean and sample standard deviation) in the tensile properties of a particular UHPC mixture.

To enable testing of both cast and extracted test specimens, AASHTO T 397 (AASHTO 2022b) does not stipulate strict restrictions on specimen geometry. To facilitate consistency in qualification testing, restrictions on test specimen geometry are provided in this Article.

A test specimen geometry with a 2-in.-square cross section and a 17-in. length has been commonly used in the execution of AASHTO T 397. This geometry allows for fiber reinforcement that is up to 0.8-in. long. It also provides for a 4-in. gauge length that is more than 2.5-in. away from the gripped portion of the test specimen.

Specimens shall be sampled from at least three separate batches. Each test result shall be classified based on the tensile behaviors described in Section 9.0 of AASHTO T 397 (AASHTO 2022b) and reported to the owner. A minimum of two but not more than half of the tested specimens used for qualification, i.e., exhibiting tensile behavior of Type H-1 or H-2, as defined in AASHTO T 397 (AASHTO 2022b), shall be obtained from a single batch.

If more than one out of five tested specimens from a single batch result in tension responses classified as Type S, as defined in AASHTO T 397 (AASHTO 2022b), all specimens sampled from the same batch shall not be used for qualification.

A UHPC mixture shall be disqualified if more than one out of five tested specimens from two or more batches result in a tension response of Type S or if any tested specimen from any batch results in a tension response of Type N, as defined in AASHTO T 397 (AASHTO 2022b).

Given that the localized crack of a tested specimen might occur outside the gauge length, i.e., tensile behavior of Type H-3 or H-4, as defined in AASHTO T 397 (AASHTO 2022b), a minimum of 10 to 14 specimens are recommended to be sampled from each batch. The testing of the sampled specimens may be halted when the minimum or required number of test results with tensile behaviors of Type H-1 or H-2 is achieved.

UHPC mixtures exhibiting a tensile response of Type S, as defined in AASHTO T 397 (AASHTO 2022b), are strain-softening materials and are not for use in structures designed according to the provisions of Section 1 of this Appendix.

If more than one out of five tested specimens from a single batch result in tension responses of Type S, it can indicate a problem with the batching procedure or with the production of the samples. Steps must be taken to correct the circumstances that resulted in such incompliant behavior.

When stress-strain responses of Type S are manifested in the test results of specimens sampled from more than one batch, the tension response of the mixture should be classified as strain softening, and the mixture is not for use in structures designed according to the provisions of Section 1 of this Appendix. Mixture design improvement shall be undertaken before qualification testing is repeated.

Tensile stress-strain results of Type N indicate regions of the specimens without fibers and with no resistance to postcracking tensile loads. Mixtures exhibiting behaviors of Type N are not for use in structures designed according to the provisions of Section 1 of this Appendix. Mixture design improvement shall be undertaken before qualification testing is repeated.

The average and sample standard deviation of the effective cracking strength, $\bar{f}_{t,crQ}$ and $s_{t,crQ}$, respectively, the crack localization strength, $\bar{f}_{t,locQ}$ and $s_{t,locQ}$, respectively, and the crack localization strain, $\bar{\varepsilon}_{t,locQ}$ and $s_{\varepsilon t,locQ}$, respectively, shall be calculated based on the total number of tested specimens exhibiting Type H-1 or H-2 tension responses (AASHTO T 397 in AASHTO 2022b) as follows:

$$\bar{f}_{t,crQ} = \frac{1}{n_{tQ}} \sum_{i=1}^{n_{tQ}} f_{t,cr,i} \qquad (2.6.4.3\text{-}1)$$

$$s_{t,crQ} = \sqrt{\frac{\sum_{i=1}^{n_{tQ}} \left(f_{t,cr,i} - \bar{f}_{t,crQ}\right)^2}{n_{tQ} - 1}} \qquad (2.6.4.3\text{-}2)$$

$$\bar{f}_{t,locQ} = \frac{1}{n_{tQ}} \sum_{i=1}^{n_{tQ}} f_{t,loc,i} \qquad (2.6.4.3\text{-}3)$$

$$s_{t,locQ} = \sqrt{\frac{\sum_{i=1}^{n_{tQ}} \left(f_{t,loc,i} - \bar{f}_{t,locQ}\right)^2}{n_{tQ} - 1}} \qquad (2.6.4.3\text{-}4)$$

$$\bar{\varepsilon}_{t,locQ} = \frac{1}{n_{tQ}} \sum_{i=1}^{n_{tQ}} \varepsilon_{t,loc,i} \qquad (2.6.4.3\text{-}5)$$

$$s_{\varepsilon t,locQ} = \sqrt{\frac{\sum_{i=1}^{n_{tQ}} \left(\varepsilon_{t,loc,i} - \bar{\varepsilon}_{t,locQ}\right)^2}{n_{tQ} - 1}} \qquad (2.6.4.3\text{-}6)$$

where:

n_{tQ} = total number of tensile test results exhibiting tension responses of Types H-1 or H-2 (AASHTO T 397 in AASHTO 2022b) obtained from qualification testing

$f_{t,cr,i}$ = effective cracking strength value obtained from tension test specimen i (ksi)

Similar to the statistical treatments of the compressive strength test results described in Article C2.6.4.2 of this Appendix, the results of each of the tensile parameters, namely, the effective cracking strength, the crack localization strength, and the crack localization strain, are assumed to follow a normal distribution. The probability density function for each of the three aforementioned property test results is established from the average and standard deviation calculated from a sample assumed to be large enough to provide sufficient data for statistical analysis.

112

$f_{t,loc,i}$ = crack localization strength value obtained from tension test specimen i (ksi)

$\varepsilon_{t,loc,i}$ = crack localization strain value obtained from tension test specimen i (in./in.)

The qualified design value of the effective cracking strength, $f_{t,crQ}$, of the UHPC mixture shall be determined as the lesser of the following:

$$f_{t,crQ} = \overline{f}_{t,crQ} - 1.34\, k_{tQ}\, s_{t,crQ} \qquad (2.6.4.3\text{-}7)$$

$$f_{t,crQ} = 1.11\, \overline{f}_{t,crQ} - 2.59\, k_{tQ}\, s_{t,crQ} \qquad (2.6.4.3\text{-}8)$$

where:

k_{tQ} = modification factor for the total number of tension test results, n_{tQ}, considered in calculating the sample standard deviation determined from Table 2.6.4.2-1 of this Appendix

The qualified design value of the crack localization strength, $f_{t,locQ}$, of the UHPC mixture shall be determined as the lesser of the following:

$$f_{t,locQ} = \overline{f}_{t,locQ} - 1.34\, k_{tQ}\, s_{t,locQ} \qquad (2.6.4.3\text{-}9)$$

$$f_{t,locQ} = 1.11\, \overline{f}_{t,locQ} - 2.59\, k_{tQ}\, s_{t,locQ} \qquad (2.6.4.3\text{-}10)$$

The qualified design value of the crack localization strain, $\varepsilon_{t,locQ}$, of the UHPC mixture shall be determined as the lesser of the values obtained from Eqs. 2.6.4.3-11 and 2.6.4.3-12 but need not be taken less than $0.80\overline{\varepsilon}_{t,locQ}$:

$$\varepsilon_{t,locQ} = \overline{\varepsilon}_{t,locQ} - 1.34\, k_{tQ}\, s_{\varepsilon t,locQ} \qquad (2.6.4.3\text{-}11)$$

$$\varepsilon_{t,locQ} = 1.11\overline{\varepsilon}_{t,locQ} - 2.59\, k_{tQ}\, s_{\varepsilon t,locQ} \qquad (2.6.4.3\text{-}12)$$

Following the same statistical considerations used to compute the qualified design value of the compressive strength, f'_{cQ}, described in Article C2.6.4.2 of this Appendix, the qualified values of each of the tensile properties are computed such that the two criteria defined in Article C2.6.4.1 of this Appendix are satisfied.

Given the variability that may be observed in crack localization strain test results, a maximum reduction of 20 percent from the average qualification result is stated in this Article.

2.6.4.4. Modulus of Elasticity

The qualified design value of the modulus of elasticity of a UHPC mixture, E_{cQ}, shall be determined from the results of a minimum of 15 cylinders produced, tested, and evaluated in accordance with ASTM C469/C469M (ASTM 2022g) as modified by ASTM C1856 (ASTM 2017a).

A test result shall not be discarded, except that if any cylinder shows evidence of improper sampling, molding, or testing, said cylinder shall be discarded, and the modulus of elasticity shall be determined from the remaining cylinders.

Specimens shall be sampled from at least three separate batches. A minimum of two but not more than half of the tested cylinders shall be obtained from a single batch.

The average and sample standard deviation of the modulus of elasticity, $\bar{E}_{cQ}$ and s_{EQ}, respectively, shall be calculated based on the total number of tested specimens as follows:

$$\bar{E}_{cQ} = \frac{1}{n_{EQ}} \sum_{i=1}^{n_{EQ}} E_{c,i} \qquad (2.6.4.4\text{-}1)$$

$$s_{EQ} = \sqrt{\frac{\sum_{i=1}^{n_{EQ}} \left(E_{c,i} - \bar{E}_{cQ} \right)^2}{n_{EQ} - 1}} \qquad (2.6.4.4\text{-}2)$$

where:

n_{EQ} = total number of modulus of elasticity test results obtained from qualification testing

$E_{c,i}$ = modulus of elasticity test result of specimen i (ksi)

C2.6.4.4

As indicated in Article 2.6.1 of this Appendix, qualification testing of the modulus of elasticity is optional. However, when the modulus of elasticity is assessed during the qualification phase, a minimum of 15 test results are to be included to establish the statistical parameters of this property. Similar to the suggested number of compression strength and tensile response tests, a minimum of 30 modulus of elasticity test results are recommended to establish confidence in the statistical parameters.

When determined from physical tests, the design value of the modulus of elasticity, E_c, should be selected considering its statistical variability and should lead to conservative designs of the UHPC component or structure. When a lower bound of the modulus of elasticity value is desired for design, the qualified value can be obtained using the same statistical considerations adopted for the qualification of the compression strength property described in Article 2.6.4.2 of this Appendix.

114

2.6.5. Durability

Unless otherwise approved by the owner, the durability of UHPC shall be assessed based on electrical resistivity, as described in Article 2.6.5.1 of this Appendix.

2.6.5.1. Electrical Resistivity

The electrical resistivity of a UHPC mixture shall be determined from the results of a minimum of six cylinders produced, tested, and evaluated in accordance with AASHTO TP 119-22 (AASHTO 2022a) and as amended herein.

The testing shall be conducted at 28 days after mixing or as approved by the owner.

Specimens shall be produced, tested, and evaluated in accordance with AASHTO TP 119-22 (AASHTO 2022a) with the following amendments and/or restrictions:

- The UHPC mixture being evaluated shall be proportioned and mixed according to the predefined procedure provided by the product developer or supplier. Fiber reinforcement shall be excluded from the mixture.

- The default conditioning option described in Section 10.2 of AASHTO TP 119-22 shall be used.

C2.6.5.1

AASHTO TP 119-22 is entitled, *Standard Method of Test for Electrical Resistivity of a Concrete Cylinder Tested in a Uniaxial Resistance Test* (AASHTO 2022a). Electrical resistivity provides information on how easily electrical charges move through a material when an electric field is applied. This property is commonly used as an indicator of concrete durability (Snyder 2001; Rajabipour, Sant, and Weiss 2007; McCarter et al. 2015; and Spragg et al. 2016). The amendments to AASHTO TP 119-22 listed in this Article are based on the work of Spragg et al. (2022).

The standard test specimen is a 4-in.-diameter by 8-in.-high cylinder. Three-inch-diameter by 6-in.-high cylinders can also be used for evaluating resistivity.

The cementitious composite material, inclusive of any binders, admixtures, and inert granular constituents and aggregates, shall be mixed without modification of the product batch proportions or the mixing process. Fiber reinforcement is excluded from the mixture because it can act as a secondary conductive phase within the UHPC matrix, resulting in increased conductivity.

The use of a different conditioning solution will affect the results of the test.

The use of the required conditioning solution may prove challenging for some laboratories. Owner approval is required for the use of an alternate conditioning solution. Spragg et al. (2022) have investigated the use of a saturated limewater solution in accordance with Section

7 of AASHTO M 201-21 (AASHTO 2021). This alternate conditioning solution will necessitate a revision to the UHPC qualification threshold; Spragg et al. (2022) suggest a uniaxial resistivity, ρ_Q, threshold value of 1,400 $\Omega \cdot$m.

- The specimens shall be demolded within 48 hours from the time of mixing and immediately placed into the conditioning solution as specified in AASHTO TP 119-22 (AASHTO 2022a). The specimens shall be continuously submerged in the conditioning solution until immediately before resistivity testing.

- The test equipment shall be capable of reading electrical resistance values across a range from 10 to 10,000 Ω.

Equipment capable of measuring a large resistance range is necessary, given the large range of values that are observed in conventional concrete and UHPC-class materials.

A test result shall not be discarded, except that if any cylinder shows evidence of improper sampling, molding, or testing, said cylinder shall be discarded, and the electrical resistivity shall be determined from the remaining cylinders.

Specimens shall be sampled from at least three separate batches. A minimum of two but not more than half of the tested cylinders shall be obtained from a single batch.

The uniaxial resistivity obtained from each tested specimen, ρ_i, shall be calculated as:

$$\rho_i = R_i k_i \tag{2.6.5.1-1}$$

in which:

$$k_i = \frac{A_{u,i}}{L_{u,i}} \tag{2.6.5.1-2}$$

where:

R_i = electrical resistance obtained from test specimen i (Ω)

Some resistivity devices report resistance in ohms (Ω), while others report uniaxial resistivity in ohm-meters ($\Omega \cdot$m). Devices that report uniaxial resistivity have integrated a specimen geometry factor into their measurement process. Confirmation of the appropriateness of an integrated specimen geometry factor is required.

116

k_i = specimen geometry factor of test specimen i (m)

$A_{u,i}$ = cross-sectional area test specimen i, measured with an accuracy of less than 1 percent (m^2)

$L_{u,i}$ = length of test specimen i, measured with an accuracy of less than 1 percent (m)

The average and sample standard deviation of the uniaxial resistivity, $\bar{\rho}_Q$ and $s_{\rho Q}$, respectively, shall be calculated and reported to the owner based on the total number of tested specimens as follows:

$$\bar{\rho}_Q = \frac{1}{n_{\rho Q}} \sum_{i=1}^{n_{\rho Q}} \rho_i \qquad (2.6.5.1\text{-}3)$$

$$s_{\rho Q} = \sqrt{\frac{\sum_{i=1}^{n_{\rho Q}} (\rho_i - \bar{\rho}_Q)^2}{n_{\rho Q} - 1}} \qquad (2.6.5.1\text{-}4)$$

where:

$n_{\rho Q}$ = total number of uniaxial resistivity test results obtained from qualification testing

The qualified value of the uniaxial resistivity, ρ_Q, of the UHPC mixture shall be determined as the lesser of the following:

$$\rho_Q = \bar{\rho}_Q - 1.34\, k_{\rho Q}\, s_{\rho Q} \qquad (2.6.5.1\text{-}3)$$

$$\rho_Q = 1.11\, \bar{\rho}_Q - 2.59\, k_{\rho Q}\, s_{\rho Q} \qquad (2.6.5.1\text{-}4)$$

where:

$k_{\rho Q}$ = modification factor for the total number of uniaxial resistivity test results, $n_{\rho Q}$, considered in calculating the sample standard deviation determined from Table 2.6.4.2-1 of this Appendix

To be classified as a UHPC-class material, the qualified value of the uniaxial resistivity, ρ_Q,

Similar to the statistical treatments of the compressive strength test results described in Article C2.6.4.2 of this Appendix, the results of the electrical resistivity tests are assumed to follow a normal distribution, in which their probability density function is established from the average and standard deviation calculated from a sample assumed to be large enough to provide sufficient data for statistical analysis.

The qualified values of each of the tensile properties are computed such that the two criteria defined in Article C2.6.4.1 of this Appendix are satisfied.

Refer to Spragg et al. (2022) for information on determination of the threshold value.

117

shall meet or exceed a threshold value of 1,500 Ω·m.

2.6.5.2. Alternative Testing

UHPC mixtures may contain conductive inclusions apart from steel fiber reinforcement. The use of other durability test methods may be acceptable for defining the durability of a material containing conductive inclusions.

The use of alternative testing methods shall be approved by the owner.

C2.6.5.2

Conductive inclusions will affect the results of the AASHTO TP 119-22 test method (AASHTO 2022a). If these inclusions cannot be excluded from the mix design of the product being tested, the test result may indicate an electrical conductivity greater than what can be attributed to the cementitious matrix. Water absorption performed in accordance with ASTM C1585 (ASTM 2020f), chloride migration performed in accordance with NT BUILD 492 (Nordtest 1999), and chloride ponding performed in accordance with ASTM C1556 (ASTM 2022f) are alternative test methods to consider when evaluating durability performance. Threshold limits for UHPC durability classification based on alternative durability tests have not yet been established.

2.6.6. Supplemental Flexural Testing Supporting Alternative Tensile Response Acceptance Methods

C2.6.6

Article 2.7.3.3.2 of this Appendix allows the use of a modified version of ASTM C1609 Revision A (ASTM 2019c) for tensile property material acceptance through flexural response testing. The testing described in this Article shall be completed prior to the engagement of Article 2.7.3.3.2 of this Appendix.

The qualification testing requirements of this Article are optional, unless acceptance testing based on the provisions of Article 2.7.3.3.2 of this Appendix is desired. The test results obtained from flexural response testing are not used in structural design.

The procedures described in this Article establish the qualified load-deflection response of a beam made of a particular UHPC mixture and tested according to the method described in this Article. The qualified load deflection is established such that the two criteria defined in Article C2.6.4.1 of this Appendix are satisfied and is used as the basis for acceptance testing when Article 2.7.3.3.2 is engaged.

The applicability of the procedures of this Article is limited to flexural test results showing small statistical variability. A large scatter in

The qualified flexural response of a particular UHPC mixture shall be defined by the qualified value of the peak load, P_{pQ}, and the qualified values of the loads, $P_{\delta Q}$, from the load-deflection responses of at least 15 tested specimens. The qualified values of the loads, $P_{\delta Q}$, shall be obtained at 0.005-in. increments of net midspan deflection up to the average value of net midspan deflection at peak load, $\overline{\delta}_{pQ}$, rounded up to the next 0.005 in.

Specimens shall be produced, tested, and evaluated in accordance with ASTM C1609 Revision A (ASTM 2019c) with the following modifications:

- Specimens shall be cast following the procedure described in AASHTO T 397 Section 7.3 (AASHTO 2022b).

- Specimens shall have a 4-in. by 4-in. cross section and shall be 14-in. long.

- The test machine shall be operated such that the net midspan deflection increases at a constant rate between 0.001 and 0.003 in./min until the peak load has been reached and the load subsequently decreased to less than 50 percent of the maximum load attained.

As described in ASTM C1609 Revision A (ASTM 2019c), test specimens shall be supported on rollers that are free to rotate on their axes in accordance with ASTM C1812 (ASTM 2015a).

the individual load-deflection responses will result in objectionably low qualified load-deflection responses that should not be used for acceptance.

The qualified values of the loads, $P_{\delta Q}$, obtained from flexural testing are intended to fall within the pre-peak portion of the load-deflection response to avoid the variability expected during the post-peak response after the development of the localized crack. The last load value of $P_{\delta Q}$ must be taken at the next incremental value of net midspan deflection that is greater than the average net midspan deflection at peak load, $\overline{\delta}_{pQ}$.

A minimum of 30 flexural response test results are recommended to establish the variation (i.e., mean and sample standard deviation) in the test results of a particular UHPC mixture.

The UHPC prismatic test specimen fabrication procedures in AASHTO T 397 (AASHTO 2022b) describes a consistent casting method of the test specimens.

The results obtained from an ASTM C1609 Revision A (ASTM 2019c) test are dependent on the test specimen geometry. A prescribed geometry is necessary to ensure that test results represent data points in the same population.

Specimens shall be sampled from at least three separate batches. A minimum of two but not more than half of the tested specimens shall be obtained from a single batch.

The load-deflection response of each tested specimen shall be measured and recorded. The load, $P_{\delta,i}$, of each tested specimen i shall be recorded at 0.005-in. increments of net midspan deflection, until the peak load has been reached and the load has subsequently decreased to less than 50 percent of the maximum load attained.

The peak load resisted by each specimen, $P_{p,i}$, and its corresponding net midspan deflection, $\delta_{p,i}$, shall be measured and recorded. This load may occur at a net midspan deflection other than the prescribed increments.

The average and standard deviation of the load recorded at each net midspan deflection increment, $\bar{P}_{\delta Q}$ and $s_{\delta Q}$, respectively, shall be calculated based on the total number of tested specimens from all batches as follows:

$$\bar{P}_{\delta Q} = \frac{1}{n_{fQ}} \sum_{i=1}^{n_{fQ}} P_{\delta,i} \qquad (2.6.6\text{-}1)$$

$$s_{\delta Q} = \sqrt{\frac{\sum_{i=1}^{n_{fQ}} \left(P_{\delta,i} - \bar{P}_{\delta Q}\right)^2}{n_{fQ} - 1}} \qquad (2.6.6\text{-}2)$$

where:

n_{fQ} = total number of flexural test results obtained from qualification testing

The average and sample standard deviation of the peak load, $\bar{P}_{pQ}$ and s_{pQ}, respectively, shall be calculated based on the total number of tested specimens as follows:

$$\bar{P}_{pQ} = \frac{1}{n_{fQ}} \sum_{i=1}^{n_{fQ}} P_{p,i} \qquad (2.6.6\text{-}3)$$

The load, $P_{\delta,i}$, should be recorded at a large number of 0.005-in. increments so that the total net midspan deflection of each tested specimen surpasses the expected average net midspan deflection at peak load, $\bar{\delta}_{pQ}$.

Similar to the statistical treatments of the compressive strength test results described in Article 2.6.4.2 of this Appendix and the tensile response test results described in Article 2.6.4.3 of this Appendix, the loads captured at the prescribed midspan deflection increments, $P_{\delta,i}$, as well as the peak loads, $P_{p,i}$, are assumed to follow a normal distribution. The probability density functions of $P_{\delta,i}$ and $P_{p,i}$ are established from their average and sample standard deviation, $\bar{P}_{\delta Q}$ and $s_{\delta Q}$, and $\bar{P}_{pQ}$ and s_{pQ}, respectively, calculated from a sample assumed to be large enough to provide sufficient data for statistical analysis.

$$s_{pQ} = \sqrt{\frac{\sum_{i=1}^{n_{fQ}} \left(P_{p,i} - \bar{P}_{pQ} \right)^2}{n_{fQ} - 1}} \qquad (2.6.6\text{-}4)$$

The average of the net midspan deflection at peak load, $\bar{\delta}_{pQ}$, shall be calculated based on the total number of tested specimens as follows:

$$\bar{\delta}_{pQ} = \frac{1}{n_{fQ}} \sum_{i=1}^{n_{fQ}} \delta_{p,i} \qquad (2.6.6\text{-}5)$$

The qualified value of the loads, $P_{\delta Q}$, at each increment of net midspan deflection shall be determined as the lesser of the following:

$$P_{\delta Q} = \bar{P}_{\delta Q} - 1.34 \, k_{fQ} \, s_{\delta Q} \qquad (2.6.6\text{-}6)$$

$$P_{\delta Q} = 1.11 \bar{P}_{\delta Q} - 2.59 \, k_{fQ} \, s_{\delta Q} \qquad (2.6.6\text{-}7)$$

where:

k_{fQ} = modification factor for the total number of flexural test results, n_{fQ}, considered in calculating the sample standard deviation determined from Table 2.6.4.2-1 of this Appendix

The qualified value of the peak load, P_{pQ}, shall be determined as the lesser of the following:

$$P_{pQ} = \bar{P}_{pQ} - 1.34 \, k_{fQ} \, s_{pQ} \qquad (2.6.6\text{-}8)$$

$$P_{pQ} = 1.11 \bar{P}_{pQ} - 2.59 \, k_{fQ} \, s_{pQ} \qquad (2.6.6\text{-}9)$$

Following the same statistical considerations used to compute the design compressive strength, f'_{cQ}, described in Article C2.6.4.2 of this Appendix, and the design tensile parameters, $f_{t,crQ}$, $f_{t,locQ}$, and $\varepsilon_{t,locQ}$, the qualified values of each of the captured loads are computed such that the two criteria defined in Article C2.6.4.1 of this Appendix are satisfied.

2.7. MATERIAL ACCEPTANCE

2.7.1. General

Material acceptance testing shall be conducted on the UHPC material being used to construct structural components.

Test specimens shall be fabricated according to ASTM C31 (ASTM 2012) or ASTM C192 (ASTM 2019a), as modified by ASTM C1856 (ASTM 2017a), AASHTO T 397 (AASHTO

2022b), and accompanying articles in this Appendix.

Test specimen curing shall match the curing process implemented during material qualification and specified for structural product manufacture.

Hardened property testing shall be conducted at the same age that the associated material qualification testing was completed.

Testing method and sampling frequency shall be in accordance with Table 2.7.1-1.

Table 2.7.1-1. Material acceptance testing methods and sampling frequency.

Property	Article	Minimum Frequency
Flow	2.7.2.1	Every batch.
Fiber segregation	2.7.2.2	First batch each day. Whenever compression or tension test specimens are cast.
Temperature	2.7.2.3	Every batch.
Compressive strength	2.7.3.2	One set per element cast. If element volume exceeds 25 yd^3, once per 25 yd^3 cast.
Tensile response: *Option 1*	2.7.3.3.1	One set per element cast. If element volume exceeds 25 yd^3, once per 25 yd^3 cast.
Tensile response: *Option 2*	2.7.3.3.2	One set per element cast. If element volume exceeds 25 yd^3, once per 25 yd^3 cast.

2.7.2. Plastic Properties

2.7.2.1. Flow

The flow shall be measured and reported for each batch. Flow shall be measured in accordance with ASTM C1856/1856M (ASTM 2017a) which provides direction on the use of ASTM C1437 (ASTM 2020e) when testing UHPC.

Flow shall be measured after the addition and mixing of all constituent materials. If water or admixture dosages are adjusted to achieve a

target flow property, flow shall be measured after the adjustments are implemented.

Flow shall be not more than 10 minutes from the start of component casting. For batches whose casting lasts for more than 30 minutes, flow shall be measured and reported at 30-minute intervals.

2.7.2.2. Fiber Segregation

Susceptibility to fiber segregation shall be measured and reported at the frequency defined in Table 2.7.1-1.

The test shall be completed according to ASTM C1712 (ASTM 2020g) with the modifications and procedures described in Article 2.6.3.3.

2.7.2.3. Temperature

The temperature of each batch shall be measured and reported in accordance with ASTM C1064 (ASTM 2017b). The temperature shall be measured in the mixer after the conclusion of mixing, in a convenance device transporting the UHPC to the placement forms, or in a sample container.

The temperature shall be measured no more than 5 minutes prior to the start of component casting.

Additional measurement times and locations may be defined by the owner.

2.7.3. Hardened Properties

2.7.3.1. General

The material acceptance of the hardened properties used for design—namely, design compressive strength, design effective cracking strength, design crack localization stress, and design crack localization strain—shall be established based on the required values

C2.7.3.1

The material acceptance procedures described herein establish required values of each property based on information particular to each UHPC mixture assessed in the qualification phase.

To optimize use of UHPC in structural components and to achieve efficient and

obtained following the provisions of this Article.

economical designs, the value of each hardened property used in design should be equal to the qualified value obtained from the qualification phase of a particular UHPC mixture according to the provisions of Article 2.6.4 of this Appendix. If the values of the hardened properties used in design, particularly the values of the tensile properties, are significantly lower than the qualified values of the UHPC mixture selected for the project, significant reduction in the UHPC component size and steel reinforcement may be achieved through design refinements based on the qualified properties.

Each hardened property shall be acceptable if both of the following criteria are met:

- Every average of three consecutive test results equals or exceeds their respective required value.

- No single property test result falls below their respective required value by more than 10 percent.

The acceptance criteria for each hardened property specified in this Article are based on the acceptance criteria for the compressive strength of conventional concrete stated in Article 26.12.3.1 of *Building Code Requirements for Structural Concrete* (ACI Committee 318 2019).

Given that the qualified value of each hardened property is computed based on the provisions of Article 2.6.4 of this Appendix, the acceptance criteria are expected to be satisfied with a probability of failure of 1 percent. Allowance should be made for statistically expected variations in deciding whether the hardened property of the UHPC mixture being produced is adequate, particularly when the qualified value of the hardened property is equal to the design value.

2.7.3.2. Compressive Strength

C2.7.3.2

The compressive strength for acceptance of a UHPC mixture shall consist of the compressive strength test results of at least three cylinders fabricated from material taken from a single batch of UHPC. A minimum of four cylinders shall be fabricated for each compressive strength acceptance requirement. The cylinders shall be produced, tested, and evaluated in

accordance with ASTM C1856/C1856M (ASTM 2017a).

A test result shall not be discarded, except that if any cylinder shows evidence of improper sampling, molding, or testing, said cylinder shall be discarded and the strength shall be determined from the remaining cylinders.

The required value of the compressive strength shall be taken as the greater of the following:

$$f'_{cR} = f'_c + 1.34\, k_{cQ}\, s_{cQ} \leq f'_{cQ} \qquad (2.7.3.2\text{-}1)$$

$$f'_{cR} = 0.90\, f'_c + 2.33\, k_{cQ}\, s_{cQ} \leq f'_{cQ} \qquad (2.7.3.2\text{-}2)$$

where:

f'_{cR} = required average value of the compressive strength obtained from acceptance testing (ksi)

f'_c = compressive strength of UHPC for use in design (ksi)

k_{cQ} = modification factor for the total number of compression strength test results, n_{cQ}, considered in calculating s_{cQ} according to Article 2.6.4.2 of this Appendix

s_{cQ} = sample standard deviation of the compressive strength for the mixture obtained from the qualification testing according to Article 2.6.4.2 of this Appendix (ksi)

f'_{cQ} = qualified design value of the compressive strength obtained from qualification testing according to Article 2.6.4.2 of this Appendix (ksi)

When the value of the compressive strength used in design, f'_c, is lower than the qualified value of a particular UHPC mixture, Eqs. 2.7.3.2-1 and 2.7.3.2-2 establish a required value greater than the design value based on the statistical variability of the UHPC mixture. This consideration is intended to restrict the average compression strength values obtained from acceptance testing from being significantly lower than their qualified values obtained during qualification of the same UHPC mixture.

The specified value of the compressive strength required for acceptance is recommended to be set equal to its qualified value, f'_{cQ}, when both the design value, f'_c, and the required value f'_{cR} are less than the qualified value, f'_{cQ}. This requirement ensures that the UHPC mixture being produced on the project is identical to the UHPC mixture qualified based on the provisions of Article 2.6.4.2 of this Appendix. When the acceptance value of the compressive strength is specified to be equal to the required value, f'_{cQ}, the acceptance criteria are expected to be satisfied with a probability of failure of 1 percent.

2.7.3.3. Tensile Response

Acceptance testing for the tension response shall be performed according to either of the two procedures described in this Article.

2.7.3.3.1. Option 1: Evaluation by Tension Testing

The tensile properties for acceptance of a UHPC mixture shall consist of the effective cracking strength, crack localization stress, and the crack localization strain obtained from the tension response test results of at least three specimens fabricated from material taken from a single batch of UHPC. The tension response test result of each specimen used to determine the tensile properties must be classified as Type H-1 or H-2 as defined in AASHTO T 397 (AASHTO 2022b). A minimum of six specimens shall be sampled for each tension response acceptance requirement. The specimens shall be produced, tested, and evaluated in accordance with AASHTO T 397 (AASHTO 2022b) with the modifications described in Article 2.6.4.3 of this Appendix.

A test result shall not be discarded, except that if any specimen shows evidence of improper sampling, molding, or testing, said specimen shall be discarded, and the tensile parameters shall be determined from the remaining specimens. A properly sampled, molded, and tested specimen exhibiting a tensile behavior of types other than H-1 or H-2, as defined in AASHTO T 397 (AASHTO 2022b), shall not be considered discarded, but its test results shall not be used for acceptance.

Each test result shall be classified based on the tensile behaviors described in Section 9.0 of AASHTO T 397 (AASHTO 2022b) and reported to the owner.

The minimum number of specimens considered for acceptance may be reduced, if, after testing all the sampled specimens, the tension response

C2.7.3.3.1

The acceptance testing for the tensile response verifies that the produced UHPC mixture exhibits a strain-hardening, stress-strain tensile behavior of Types H-1, H-2, H-3, and H-4 as defined in AASHTO T 397 (AASHTO 2022b). However, only test results where the localization crack occurs within the gauge length, i.e., tensile behavior of Types H-1 and H-2, are permitted to be used to determine the tensile properties.

The minimum number of the specimens considered for acceptance can be reduced only after the testing of at least the six specimens

of less than three specimens resulted in Type H-1 or H-2 response as defined in AASHTO T 397 (AASHTO 2022b).

If more than one out of every six tested specimens from a single batch result in a tension response of Type S, or if any tested specimen resulted in a tension response of Type N as defined in AASHTO T 397 (AASHTO 2022b), the mixture shall be considered as not meeting the acceptance criteria.

The required value for the effective cracking strength, $f_{t,crR}$, shall be taken as the greater of the following:

$$f_{t,crR} = f_{t,cr} + 1.34 \, k_{tQ} \, s_{t,crQ} \leq f_{t,crQ}$$

$$(2.7.3.3.1\text{-}1)$$

$$f_{t,crR} = 0.90 \, f_{t,cr} + 2.33 \, k_{tQ} \, s_{t,crQ} \leq f_{t,crQ}$$

$$(2.7.3.3.1\text{-}2)$$

where:

$f_{t,cr}$ = effective cracking strength for use in design (ksi)

k_{tQ} = modification factor for the total number of tension test results, n_{tQ}, considered in calculating the sample standard deviation according to Article 2.6.4.3 of this Appendix

required to be sampled for each acceptance requirement.

When tensile behaviors of Type S are manifested in the test results of sampled specimens, the tension response of the mixture is classified as strain softening, and the mixture shall not be used in design according to this Appendix.

Tensile behaviors of Type N indicate regions of the specimens without fibers and with no resistance to postcracking tensile loads. Mixtures exhibiting behaviors of Type N are not for use in structures designed according to the provisions of Section 1 of this Appendix.

When tensile behaviors of Type S are manifested at a frequency greater than one out of every six tested specimens from a single batch or when tensile behaviors of Type N are manifested, UHPC production must be halted until corrective action is taken to improve the fabrication procedures.

When the values of the tensile properties used in design are lower than their respective qualified values of a particular UHPC mixture, Eqs. 2.7.3.3.1-1 through 2.7.3.3.1-6 establish a required value greater than the design value for each tensile property based on the statistical variability of the selected UHPC mixture. This consideration is intended to restrict the average tensile property values obtained during acceptance testing from being significantly lower that their corresponding qualified property values obtained during qualification of the same UHPC mixture.

The specified value for acceptance of each tensile property is recommended to be set equal to its qualified value when both the design and required values are less than the qualified value. This requirement ensures that the UHPC mixture being produced on the project is identical to the UHPC mixture qualified based on the provisions of Article 2.6.4.3 of this

$s_{t,crQ}$ = sample standard deviation of the effective crack localization strength test results for a UHPC mixture obtained from qualification testing according to Article 2.6.4.3 of this Appendix (ksi)

$f_{t,crQ}$ = qualified design value of the effective cracking strength from qualification testing according to Article 2.6.4.3 of this Appendix (ksi).

The required value for the crack localization strength, $f_{t,locR}$, shall be taken as the greater of the following:

$$f_{t,locR} = f_{t,loc} + 1.34\, k_{tQ}\, s_{t,locQ} \le f_{t,locQ}$$

$$(2.7.3.3.1\text{-}3)$$

$$f_{t,locR} = 0.90\, f_{t,loc} + 2.33\, k_{tQ}\, s_{t,locQ} \le f_{t,locQ}$$

$$(2.7.3.3.1\text{-}4)$$

where:

$f_{t,loc}$ = crack localization strength for use in design (ksi)

$s_{t,locQ}$ = sample standard deviation of the crack localization strength test results for a UHPC mixture obtained from qualification testing according to Article 2.6.4.3 of this Appendix (ksi)

$f_{t,locQ}$ = qualified design value of the crack localization strength from qualification testing according to Article 2.6.4.3 of this Appendix (ksi).

The required value for the crack localization strain, $\varepsilon_{t,locR}$, shall be taken as the greater of the values obtained from Eqs. 2.7.3.3.1-5 and 2.7.3.3.1-6 but not greater than the lesser of $1.25\varepsilon_{t,loc}$ and $\varepsilon_{t,locQ}$:

Appendix. When the acceptance value of each tensile property is specified to be equal to the qualified value, the acceptance criteria are expected to be satisfied with a probability of failure of 1 percent.

As described in Article 2.6.4.3 of this Appendix, the qualified values of crack localization strain test results are capped to a maximum reduction of 20 percent from the average qualification result. In this case, the qualified value of the crack localization strain

128

$$\varepsilon_{t,locR} = \varepsilon_{t,loc} + 1.34 \, k_{tQ} \, s_{\varepsilon t,locQ} \qquad (2.7.3.3.1\text{-}5)$$

$$\varepsilon_{t,locR} = 0.90 \, \varepsilon_{t,loc} + 2.33 \, k_{tQ} \, s_{\varepsilon t,locQ}$$

$$(2.7.3.3.1\text{-}6)$$

where:

$\varepsilon_{t,loc}$ = crack localization strain for use in design (in./in.)

$s_{\varepsilon t,locQ}$ = sample standard deviation of the crack localization strain test results for a UHPC mixture obtained from qualification testing according to Article 2.6.4.3 of this Appendix (in./in.)

$\varepsilon_{t,locQ}$ = qualified design value of the crack localization strain from qualification testing according to Article 2.6.4.3 of this Appendix (in./in.).

2.7.3.3.2. Option 2: Evaluation by Flexural Testing

The acceptance of the tensile response of a UHPC mixture by flexural testing shall consist of the flexural responses defined by the peak loads and the loads corresponding to the same net midspan deflection increments determined during qualification testing of the mixture according to Article 2.6.6 of this Appendix. The flexural responses shall be obtained from the load-deflection test results of at least three specimens fabricated from a single batch of UHPC. A minimum of four specimens shall be sampled for each tension response acceptance criteria. The test specimens shall be produced, tested, and evaluated in accordance with ASTM C1609 Revision A (ASTM 2019c) with the modifications described in Article 2.6.6 of this Appendix.

may be expected to be satisfied with a probability of failure of more than 1 percent. Therefore, allowance may be made for variations in deciding whether the average value of the crack localization being produced is adequate, particularly when the required design value is equal to the qualified value and when the qualified value was determined by the 20 percent reduction cap from the average qualification result.

C2.7.3.3.2

Given that the load-deflection results of specimens tested in flexure are not a direct measurement of the uniaxial tensile properties used in structural design, the acceptance criteria based on flexural testing must be evaluated with respect to the qualified values of the peak load, P_{pQ}, and the loads, $P_{\delta Q}$, at the same net midspan deflection increments determined during qualification testing of the mixture.

The applicability of the procedures of this Article are limited to flexural test results showing small statistical variability during qualification testing. A large scatter in the individual load-deflection responses during qualification will result in objectionably low qualified load-deflection responses that should not be used for acceptance.

A test result shall not be discarded, except that, if any specimen shows evidence of improper sampling, molding, or testing, said specimen shall be discarded, and the tensile test shall consist of the remaining specimens.

The tensile response of a UHPC mixture shall be acceptable if the two criteria specified in Article 2.7.3.1 of this Appendix are met for each of the loads recorded at the prescribed net midspan deflection increments and at peak load.

ADDENDUM A1. TYPICAL MATERIAL PROPERTIES OF ULTRA-HIGH PERFORMANCE CONCRETE

Typical UHPC mechanical properties and associated test methods are presented in Table A1-1. Additionally, minimum properties as defined in Article 1.1.1 of this Appendix are also provided.

Table A1-1. Typical and minimum mechanical properties for UHPC.

Property	Test Method	Typical Values	Minimum Value
Modulus of elasticity, E_c (ksi)	ASTM C1856/C1856M (ASTM 2017a)	6,500–9,400	N/A
Compressive strength, f'_c (ksi)	ASTM C1856/C1856M (ASTM 2017a)	20.0–36.0	17.5
Ultimate compressive strain, ε_{cu}	ASTM C1856/C1856M (ASTM 2017a)	0.003–0.005	N/A
Poisson's ratio	ASTM C1856 (ASTM 2017a)	0.1–0.2	N/A
Effective cracking strength, $f_{t,cr}$ (ksi)	AASHTO T 397 (AASHTO 2022b)	0.90–1.80	0.75
Crack localization strength, $f_{t,loc}$ (ksi)	AASHTO T 397 (AASHTO 2022b)	0.90–1.80	$\geq f_{t,cr}$
Crack localization strain, $\varepsilon_{t,loc}$	AASHTO T 397 (AASHTO 2022b)	0.003–0.008	0.0025

N/A = not applicable.

ADDENDUM A2. SHEAR DESIGN TABLES FOR θ AND $f_{v,\alpha}$

A2.1. GENERAL

In lieu of the general method of Article 1.7.3.4.1 of this Appendix, the shear design parameters θ and $f_{v,\alpha}$ may be obtained from the tables provided in this Article as specified in Article 1.7.3.4.2 of this Appendix.

The provisions of this Addendum are applicable for members made of UHPC with or without transverse steel reinforcement having $E_c \geq$ 6,500 ksi and $f_{t,loc} \leq 1.80$ ksi.

A2.2. MEMBERS WITHOUT TRANSVERSE STEEL REINFORCEMENT

For members without transverse steel reinforcement (i.e., $\rho_{v,\alpha} = 0.0$ percent), the values of θ may be determined from Table A2.2-1 at a specific value of $\gamma_u\varepsilon_{t,loc}$ and ε_s.

Interpolations to calculate θ between the values of ε_s and $\gamma_u\varepsilon_{t,loc}$ in Table A2.2-1 shall not be permitted.

Table A2.2-1. Values of θ (degrees) for sections without transverse reinforcement (i.e., $\rho_{v,\alpha} = 0.0$ percent).

$\varepsilon_s \times$ 1,000	$\gamma_u\varepsilon_{t,loc} \times$ 1,000											
	$\geq$2.5	$\geq$3.0	$\geq$3.5	$\geq$4.0	$\geq$4.5	$\geq$5.0	$\geq$5.5	$\geq$6.0	$\geq$6.5	$\geq$7.0	$\geq$7.5	$\geq$8.0
≤ -1.0	30.8	30.0	29.3	28.7	28.2	27.7	27.2	26.8	26.5	26.1	25.8	25.5
≤ -0.5	32.5	31.5	30.7	30.0	29.3	28.8	28.3	27.8	27.4	27.0	26.6	26.3
$\leq$0.0	34.5	33.2	32.2	31.4	30.6	30.0	29.4	28.9	28.4	27.9	27.5	27.2
$\leq$0.5	36.7	35.2	33.9	32.9	32.0	31.3	30.6	30.0	29.4	28.9	28.5	28.1
$\leq$1.0	39.2	37.3	35.8	34.6	33.6	32.7	31.9	31.2	30.5	30.0	29.5	29.0
$\leq$1.5	42.1	39.7	37.9	36.4	35.2	34.1	33.2	32.4	31.7	31.1	30.5	30.0
$\leq$2.0	45.4	42.4	40.1	38.4	36.9	35.7	34.7	33.8	33.0	32.3	31.6	31.0
$\leq$2.5	49.1	45.3	42.6	40.5	38.8	37.4	36.2	35.2	34.3	33.5	32.8	32.1
$\leq$3.0	–	48.6	45.3	42.8	40.8	39.2	37.9	36.7	35.7	34.8	34.0	33.2
$\leq$3.5	–	–	48.2	45.3	43.0	41.1	39.6	38.2	37.1	36.1	35.2	34.4
$\leq$4.0	–	–	–	47.9	45.3	43.1	41.4	39.9	38.6	37.5	36.5	35.6
$\leq$4.5	–	–	–	–	47.7	45.2	43.2	41.6	40.2	38.9	37.8	36.9
$\leq$5.0	–	–	–	–	–	47.5	45.2	43.4	41.8	40.4	39.2	38.2
$\leq$5.5	–	–	–	–	–	–	47.5	45.2	43.5	42.0	40.6	39.5
$\leq$6.0	–	–	–	–	–	–	–	47.1	45.2	43.5	42.1	40.9
$\leq$6.5	–	–	–	–	–	–	–	–	47.0	45.2	43.6	42.3
$\leq$7.0	–	–	–	–	–	–	–	–	–	46.9	45.2	43.7
$\leq$7.5	–	–	–	–	–	–	–	–	–	–	46.8	45.2
$\leq$8.0	–	–	–	–	–	–	–	–	–	–	–	46.7

Note: Values for θ where ε_s is greater than $\gamma_u\varepsilon_{t,loc}$ are not relevant. These combinations are indicated by cells containing the "–" symbol.

A2.3. MEMBERS WITH TRANSVERSE STEEL REINFORCEMENT

For members with transverse steel reinforcement having $f_y \leq 75.0$ ksi, $\rho_{v,\alpha} \leq 3.0$ percent, and $\alpha = 90$ degrees, the values of the upper limit of $f_{v,\alpha}$ and θ may be determined from Table A2.3-1 through Table A2.3-6 based on the value of $\rho_{v,\alpha}$ and at a specific value of $\gamma_u\varepsilon_{t,loc}$ and ε_s.

Interpolations to calculate θ and $f_{v,\alpha}$ between the values of $\rho_{v,\alpha}$, ε_s, and $\gamma_u\varepsilon_{t,loc}$ in Table A2.3-1 through Table A2.3-6 shall not be permitted.

CA2.3

As specified in Article 1.7.3.4.2 of this Appendix, the value of $f_{v,\alpha}$ used in Eq. 1.7.3.3-4 shall be determined as the lesser of the value obtained from the tables of this Addendum and the specified minimum yield strength of the transverse steel, f_y.

Table A2.3-1. Values of θ (degrees) and upper limit of $f_{v,a}$ (ksi) for sections with transverse reinforcement with $\rho_{v,a} \leq 0.5$ percent.

$\varepsilon_s \times$ 1,000	Para-meter	$\gamma_u \varepsilon_{t,loc} \times$ 1,000											
		≥2.5	≥3.0	≥3.5	≥4.0	≥4.5	≥5.0	≥5.5	≥6.0	≥6.5	≥7.0	≥7.5	≥8.0
≤ −1.0	θ (deg)	31.8	31.2	30.8	30.4	29.9	29.3	28.8	28.4	28.0	27.6	27.3	27.0
	$f_{v,a}$ (ksi)	≤39.0	≤49.6	≤60.4	≤71.2	≤75.0	≤75.0	≤75.0	≤75.0	≤75.0	≤75.0	≤75.0	≤75.0
≤ −0.5	θ (deg)	33.5	32.7	32.1	31.6	31.0	30.4	29.9	29.4	28.9	28.5	28.1	27.7
	$f_{v,a}$ (ksi)	≤37.6	≤48.1	≤58.7	≤69.4	≤75.0	≤75.0	≤75.0	≤75.0	≤75.0	≤75.0	≤75.0	≤75.0
≤0.0	θ (deg)	35.4	34.4	33.6	32.9	32.3	31.6	30.9	30.4	29.9	29.4	29.0	28.6
	$f_{v,a}$ (ksi)	≤35.9	≤46.2	≤56.8	≤67.4	≤75.0	≤75.0	≤75.0	≤75.0	≤75.0	≤75.0	≤75.0	≤75.0
≤0.5	θ (deg)	37.5	36.2	35.2	34.3	33.6	32.8	32.1	31.5	30.9	30.4	29.9	29.4
	$f_{v,a}$ (ksi)	≤33.9	≤44.2	≤54.6	≤65.2	≤75.0	≤75.0	≤75.0	≤75.0	≤75.0	≤75.0	≤75.0	≤75.0
≤1.0	θ (deg)	40.0	38.3	37.0	35.9	35.0	34.1	33.3	32.6	32.0	31.4	30.8	30.3
	$f_{v,a}$ (ksi)	≤31.7	≤41.8	≤52.2	≤62.8	≤73.4	≤75.0	≤75.0	≤75.0	≤75.0	≤75.0	≤75.0	≤75.0
≤1.5	θ (deg)	42.8	40.6	38.9	37.6	36.6	35.6	34.6	33.8	33.1	32.4	31.8	31.3
	$f_{v,a}$ (ksi)	≤29.1	≤39.2	≤49.5	≤60.0	≤70.7	≤75.0	≤75.0	≤75.0	≤75.0	≤75.0	≤75.0	≤75.0
≤2.0	θ (deg)	45.9	43.1	41.1	39.5	38.2	37.1	36.0	35.1	34.3	33.5	32.9	32.3
	$f_{v,a}$ (ksi)	≤26.2	≤36.2	≤46.5	≤57.0	≤67.7	≤75.0	≤75.0	≤75.0	≤75.0	≤75.0	≤75.0	≤75.0
≤2.5	θ (deg)	49.5	45.9	43.4	41.5	39.9	38.7	37.5	36.5	35.5	34.7	34.0	33.3
	$f_{v,a}$ (ksi)	≤22.8	≤32.8	≤43.2	≤53.7	≤64.4	≤75.0	≤75.0	≤75.0	≤75.0	≤75.0	≤75.0	≤75.0
≤3.0	θ (deg)	–	49.1	45.9	43.6	41.8	40.4	39.0	37.9	36.8	35.9	35.1	34.4
	$f_{v,a}$ (ksi)	–	≤29.1	≤39.6	≤50.1	≤60.8	≤71.7	≤75.0	≤75.0	≤75.0	≤75.0	≤75.0	≤75.0
≤3.5	θ (deg)	–	–	48.7	46.0	43.8	42.1	40.7	39.4	38.2	37.2	36.3	35.5
	$f_{v,a}$ (ksi)	–	–	≤35.6	≤46.2	≤57.0	≤67.9	≤75.0	≤75.0	≤75.0	≤75.0	≤75.0	≤75.0
≤4.0	θ (deg)	–	–	–	48.5	46.0	44.0	42.4	40.9	39.6	38.5	37.5	36.7
	$f_{v,a}$ (ksi)	–	–	–	≤42.1	≤52.9	≤63.9	≤74.9	≤75.0	≤75.0	≤75.0	≤75.0	≤75.0
≤4.5	θ (deg)	–	–	–	–	48.3	46.0	44.1	42.5	41.1	39.9	38.8	37.9
	$f_{v,a}$ (ksi)	–	–	–	–	≤48.6	≤59.6	≤70.7	≤75.0	≤75.0	≤75.0	≤75.0	≤75.0
≤5.0	θ (deg)	–	–	–	–	–	48.1	46.0	44.2	42.7	41.3	40.1	39.1
	$f_{v,a}$ (ksi)	–	–	–	–	–	≤55.1	≤66.3	≤75.0	≤75.0	≤75.0	≤75.0	≤75.0
≤5.5	θ (deg)	–	–	–	–	–	–	47.9	46.0	44.3	42.8	41.5	40.4
	$f_{v,a}$ (ksi)	–	–	–	–	–	–	≤61.7	≤73.0	≤75.0	≤75.0	≤75.0	≤75.0
≤6.0	θ (deg)	–	–	–	–	–	–	–	47.8	46.0	44.3	42.9	41.7
	$f_{v,a}$ (ksi)	–	–	–	–	–	–	–	≤68.2	≤75.0	≤75.0	≤75.0	≤75.0
≤6.5	θ (deg)	–	–	–	–	–	–	–	–	47.7	45.9	44.4	43.0
	$f_{v,a}$ (ksi)	–	–	–	–	–	–	–	–	≤74.8	≤75.0	≤75.0	≤75.0
≤7.0	θ (deg)	–	–	–	–	–	–	–	–	–	47.5	45.9	44.4
	$f_{v,a}$ (ksi)	–	–	–	–	–	–	–	–	–	≤75.0	≤75.0	≤75.0
≤7.5	θ (deg)	–	–	–	–	–	–	–	–	–	–	47.4	45.8
	$f_{v,a}$ (ksi)	–	–	–	–	–	–	–	–	–	–	≤75.0	≤75.0
≤8.0	θ (deg)	–	–	–	–	–	–	–	–	–	–	–	46.6
	$f_{v,a}$ (ksi)	–	–	–	–	–	–	–	–	–	–	–	≤75.0

Note: Values for θ and $f_{v,a}$ where ε_s is greater than $\gamma_u \varepsilon_{t,loc}$ are not relevant. These combinations are indicated by cells containing the "–" symbol.

Table A2.3-2. Values of θ (degrees) and upper limit of $f_{v,a}$ (ksi) for sections with transverse reinforcement with $\rho_{v,a} \leq 1.0$ percent.

$\varepsilon_s \times$ 1,000	Para-meter	$\gamma_u \varepsilon_{t,loc} \times$ 1,000											
		≥2.5	≥3.0	≥3.5	≥4.0	≥4.5	≥5.0	≥5.5	≥6.0	≥6.5	≥7.0	≥7.5	≥8.0
≤ −1.0	θ (deg)	32.7	32.3	31.9	31.6	31.3	30.8	30.2	29.8	29.3	28.9	28.6	28.2
	$f_{v,a}$ (ksi)	≤36.7	≤46.6	≤56.5	≤66.5	≤75.0	≤75.0	≤75.0	≤75.0	≤75.0	≤75.0	≤75.0	≤75.0
≤ −0.5	θ (deg)	34.3	33.7	33.2	32.8	32.4	31.8	31.2	30.7	30.2	29.8	29.4	29.0
	$f_{v,a}$ (ksi)	≤35.3	≤45.1	≤54.9	≤64.8	≤74.8	≤75.0	≤75.0	≤75.0	≤75.0	≤75.0	≤75.0	≤75.0
≤0.0	θ (deg)	36.2	35.3	34.6	34.1	33.6	32.9	32.3	31.7	31.2	30.7	30.2	29.8
	$f_{v,a}$ (ksi)	≤33.8	≤43.4	≤53.1	≤63.0	≤72.9	≤75.0	≤75.0	≤75.0	≤75.0	≤75.0	≤75.0	≤75.0
≤0.5	θ (deg)	38.2	37.1	36.2	35.4	34.8	34.2	33.4	32.7	32.1	31.6	31.1	30.6
	$f_{v,a}$ (ksi)	≤32.0	≤41.4	≤51.1	≤60.9	≤70.8	≤75.0	≤75.0	≤75.0	≤75.0	≤75.0	≤75.0	≤75.0
≤1.0	θ (deg)	40.6	39.1	37.9	36.9	36.2	35.4	34.6	33.9	33.2	32.6	32.0	31.5
	$f_{v,a}$ (ksi)	≤29.9	≤39.3	≤48.9	≤58.6	≤68.4	≤75.0	≤75.0	≤75.0	≤75.0	≤75.0	≤75.0	≤75.0
≤1.5	θ (deg)	43.3	41.3	39.7	38.6	37.6	36.8	35.9	35.0	34.3	33.6	33.0	32.4
	$f_{v,a}$ (ksi)	≤27.4	≤36.8	≤46.4	≤56.1	≤65.9	≤75.0	≤75.0	≤75.0	≤75.0	≤75.0	≤75.0	≤75.0
≤2.0	θ (deg)	46.4	43.7	41.8	40.3	39.2	38.2	37.2	36.3	35.4	34.7	34.0	33.4
	$f_{v,a}$ (ksi)	≤24.7	≤34.0	≤43.6	≤53.3	≤63.2	≤73.1	≤75.0	≤75.0	≤75.0	≤75.0	≤75.0	≤75.0
≤2.5	θ (deg)	49.9	46.4	44.0	42.2	40.8	39.7	38.6	37.6	36.6	35.8	35.0	34.4
	$f_{v,a}$ (ksi)	≤21.5	≤30.9	≤40.6	≤50.3	≤60.2	≤70.1	≤75.0	≤75.0	≤75.0	≤75.0	≤75.0	≤75.0
≤3.0	θ (deg)	–	49.5	46.5	44.3	42.6	41.3	40.1	38.9	37.9	37.0	36.1	35.4
	$f_{v,a}$ (ksi)	–	≤27.5	≤37.2	≤47.0	≤56.9	≤66.9	≤75.0	≤75.0	≤75.0	≤75.0	≤75.0	≤75.0
≤3.5	θ (deg)	–	–	49.2	46.5	44.5	42.9	41.6	40.4	39.2	38.2	37.3	36.5
	$f_{v,a}$ (ksi)	–	–	≤33.5	≤43.5	≤53.4	≤63.5	≤73.5	≤75.0	≤75.0	≤75.0	≤75.0	≤75.0
≤4.0	θ (deg)	–	–	–	48.9	46.6	44.7	43.2	41.8	40.6	39.5	38.5	37.6
	$f_{v,a}$ (ksi)	–	–	–	≤39.6	≤49.7	≤59.8	≤70.0	≤75.0	≤75.0	≤75.0	≤75.0	≤75.0
≤4.5	θ (deg)	–	–	–	–	48.7	46.6	44.9	43.4	42.0	40.8	39.7	38.7
	$f_{v,a}$ (ksi)	–	–	–	–	≤45.7	≤55.9	≤66.2	≤75.0	≤75.0	≤75.0	≤75.0	≤75.0
≤5.0	θ (deg)	–	–	–	–	–	48.6	46.6	45.0	43.5	42.2	41.0	39.9
	$f_{v,a}$ (ksi)	–	–	–	–	–	≤51.8	≤62.1	≤72.5	≤75.0	≤75.0	≤75.0	≤75.0
≤5.5	θ (deg)	–	–	–	–	–	–	48.5	46.6	45.0	43.6	42.3	41.1
	$f_{v,a}$ (ksi)	–	–	–	–	–	–	≤57.9	≤68.4	≤75.0	≤75.0	≤75.0	≤75.0
≤6.0	θ (deg)	–	–	–	–	–	–	–	48.3	46.6	45.0	43.6	42.4
	$f_{v,a}$ (ksi)	–	–	–	–	–	–	–	≤64.1	≤74.6	≤75.0	≤75.0	≤75.0
≤6.5	θ (deg)	–	–	–	–	–	–	–	–	48.3	46.6	45.0	43.7
	$f_{v,a}$ (ksi)	–	–	–	–	–	–	–	–	≤70.2	≤75.0	≤75.0	≤75.0
≤7.0	θ (deg)	–	–	–	–	–	–	–	–	–	48.1	46.5	45.0
	$f_{v,a}$ (ksi)	–	–	–	–	–	–	–	–	–	≤75.0	≤75.0	≤75.0
≤7.5	θ (deg)	–	–	–	–	–	–	–	–	–	–	48.0	46.4
	$f_{v,a}$ (ksi)	–	–	–	–	–	–	–	–	–	–	≤75.0	≤75.0
≤8.0	θ (deg)	–	–	–	–	–	–	–	–	–	–	–	47.8
	$f_{v,a}$ (ksi)	–	–	–	–	–	–	–	–	–	–	–	≤75.0

Note: Values for θ and $f_{v,a}$ where ε_s is greater than $\gamma_u \varepsilon_{t,loc}$ are not relevant. These combinations are indicated by cells containing the "–" symbol.

Table A2.3-3. Values of θ (degrees) and upper limit of $f_{v,a}$ (ksi) for sections with transverse reinforcement with $\rho_{v,a} \leq 1.5$ percent.

$\varepsilon_s \times$ 1,000	Parameter	$\gamma_u \varepsilon_{t,loc} \times$ 1,000											
		≥2.5	≥3.0	≥3.5	≥4.0	≥4.5	≥5.0	≥5.5	≥6.0	≥6.5	≥7.0	≥7.5	≥8.0
≤ −1.0	θ (deg)	33.4	33.1	32.8	32.6	32.5	32.0	31.5	31.0	30.5	30.1	29.7	29.4
	$f_{v,a}$ (ksi)	≤34.7	≤43.9	≤53.2	≤62.5	≤71.9	≤75.0	≤75.0	≤75.0	≤75.0	≤75.0	≤75.0	≤75.0
≤ −0.5	θ (deg)	35.0	34.5	34.1	33.8	33.5	33.0	32.4	31.9	31.4	30.9	30.5	30.1
	$f_{v,a}$ (ksi)	≤33.4	≤42.5	≤51.7	≤60.9	≤70.2	≤75.0	≤75.0	≤75.0	≤75.0	≤75.0	≤75.0	≤75.0
≤0.0	θ (deg)	36.8	36.1	35.5	35.0	34.6	34.2	33.5	32.9	32.3	31.8	31.3	30.9
	$f_{v,a}$ (ksi)	≤31.9	≤40.9	≤50.0	≤59.2	≤68.4	≤75.0	≤75.0	≤75.0	≤75.0	≤75.0	≤75.0	≤75.0
≤0.5	θ (deg)	38.8	37.8	37.0	36.3	35.8	35.3	34.6	33.9	33.3	32.7	32.2	31.7
	$f_{v,a}$ (ksi)	≤30.2	≤39.1	≤48.1	≤57.2	≤66.4	≤75.0	≤75.0	≤75.0	≤75.0	≤75.0	≤75.0	≤75.0
≤1.0	θ (deg)	41.1	39.7	38.6	37.8	37.1	36.5	35.7	35.0	34.3	33.6	33.1	32.5
	$f_{v,a}$ (ksi)	≤28.2	≤37.0	≤46.0	≤55.1	≤64.2	≤73.4	≤75.0	≤75.0	≤75.0	≤75.0	≤75.0	≤75.0
≤1.5	θ (deg)	43.8	41.8	40.4	39.3	38.5	37.8	36.9	36.1	35.3	34.6	34.0	33.4
	$f_{v,a}$ (ksi)	≤26.0	≤34.7	≤43.7	≤52.7	≤61.9	≤71.1	≤75.0	≤75.0	≤75.0	≤75.0	≤75.0	≤75.0
≤2.0	θ (deg)	46.7	44.2	42.4	41.0	39.9	39.1	38.2	37.3	36.4	35.7	35.0	34.4
	$f_{v,a}$ (ksi)	≤23.4	≤32.2	≤41.1	≤50.2	≤59.3	≤68.5	≤75.0	≤75.0	≤75.0	≤75.0	≤75.0	≤75.0
≤2.5	θ (deg)	50.2	46.8	44.5	42.9	41.5	40.5	39.6	38.5	37.6	36.8	36.0	35.3
	$f_{v,a}$ (ksi)	≤20.4	≤29.3	≤38.3	≤47.4	≤56.6	≤65.8	≤75.0	≤75.0	≤75.0	≤75.0	≤75.0	≤75.0
≤3.0	θ (deg)	–	49.8	46.9	44.8	43.2	42.0	40.9	39.9	38.8	37.9	37.1	36.3
	$f_{v,a}$ (ksi)	–	≤26.1	≤35.1	≤44.3	≤53.6	≤62.8	≤72.2	≤75.0	≤75.0	≤75.0	≤75.0	≤75.0
≤3.5	θ (deg)	–	–	49.5	47.0	45.1	43.6	42.4	41.2	40.1	39.1	38.2	37.4
	$f_{v,a}$ (ksi)	–	–	≤31.7	≤41.0	≤50.3	≤59.7	≤69.1	≤75.0	≤75.0	≤75.0	≤75.0	≤75.0
≤4.0	θ (deg)	–	–	–	49.3	47.0	45.3	43.9	42.7	41.4	40.3	39.3	38.4
	$f_{v,a}$ (ksi)	–	–	–	≤37.4	≤46.9	≤56.3	≤65.8	≤75.0	≤75.0	≤75.0	≤75.0	≤75.0
≤4.5	θ (deg)	–	–	–	–	49.2	47.1	45.4	44.1	42.8	41.6	40.5	39.5
	$f_{v,a}$ (ksi)	–	–	–	–	≤43.2	≤52.7	≤62.3	≤71.8	≤75.0	≤75.0	≤75.0	≤75.0
≤5.0	θ (deg)	–	–	–	–	–	49.0	47.1	45.6	44.2	42.9	41.7	40.7
	$f_{v,a}$ (ksi)	–	–	–	–	–	≤48.9	≤58.6	≤68.2	≤75.0	≤75.0	≤75.0	≤75.0
≤5.5	θ (deg)	–	–	–	–	–	–	48.9	47.2	45.7	44.3	43.0	41.9
	$f_{v,a}$ (ksi)	–	–	–	–	–	–	≤54.7	≤64.4	≤74.1	≤75.0	≤75.0	≤75.0
≤6.0	θ (deg)	–	–	–	–	–	–	–	48.8	47.2	45.7	44.3	43.1
	$f_{v,a}$ (ksi)	–	–	–	–	–	–	–	≤60.4	≤70.2	≤75.0	≤75.0	≤75.0
≤6.5	θ (deg)	–	–	–	–	–	–	–	–	48.7	47.2	45.7	44.3
	$f_{v,a}$ (ksi)	–	–	–	–	–	–	–	–	≤66.2	≤75.0	≤75.0	≤75.0
≤7.0	θ (deg)	–	–	–	–	–	–	–	–	–	48.6	47.1	45.6
	$f_{v,a}$ (ksi)	–	–	–	–	–	–	–	–	–	≤72.0	≤75.0	≤75.0
≤7.5	θ (deg)	–	–	–	–	–	–	–	–	–	–	48.5	47.0
	$f_{v,a}$ (ksi)	–	–	–	–	–	–	–	–	–	–	≤75.0	≤75.0
≤8.0	θ (deg)	–	–	–	–	–	–	–	–	–	–	–	48.4
	$f_{v,a}$ (ksi)	–	–	–	–	–	–	–	–	–	–	–	≤75.0

Note: Values for θ and $f_{v,a}$ where ε_s is greater than $\gamma_u \varepsilon_{t,loc}$ are not relevant. These combinations are indicated by cells containing the "–" symbol.

Table A2.3-4. Values of θ (degrees) and upper limit of $f_{v,a}$ (ksi) for sections with transverse reinforcement with $\rho_{v,a} \le 2.0$ percent.

$\varepsilon_s \times$ 1,000	Para-meter	$\gamma_u \varepsilon_{t,loc} \times$ 1,000											
		≥2.5	≥3.0	≥3.5	≥4.0	≥4.5	≥5.0	≥5.5	≥6.0	≥6.5	≥7.0	≥7.5	≥8.0
≤ −1.0	θ (deg)	34.0	33.8	33.6	33.5	33.3	33.1	32.6	32.1	31.6	31.2	30.7	30.4
	$f_{v,a}$ (ksi)	≤32.9	≤41.6	≤50.3	≤59.0	≤67.8	≤75.0	≤75.0	≤75.0	≤75.0	≤75.0	≤75.0	≤75.0
≤ −0.5	θ (deg)	35.6	35.2	34.8	34.6	34.3	34.2	33.5	33.0	32.4	32.0	31.5	31.1
	$f_{v,a}$ (ksi)	≤31.7	≤40.2	≤48.9	≤57.5	≤66.2	≤74.9	≤75.0	≤75.0	≤75.0	≤75.0	≤75.0	≤75.0
≤0.0	θ (deg)	37.4	36.7	36.2	35.8	35.4	35.1	34.5	33.9	33.3	32.8	32.3	31.9
	$f_{v,a}$ (ksi)	≤30.3	≤38.7	≤47.3	≤55.8	≤64.5	≤73.2	≤75.0	≤75.0	≤75.0	≤75.0	≤75.0	≤75.0
≤0.5	θ (deg)	39.3	38.4	37.6	37.1	36.6	36.2	35.6	34.9	34.3	33.7	33.1	32.7
	$f_{v,a}$ (ksi)	≤28.6	≤37.0	≤45.5	≤54.0	≤62.6	≤71.3	≤75.0	≤75.0	≤75.0	≤75.0	≤75.0	≤75.0
≤1.0	θ (deg)	41.6	40.2	39.2	38.4	37.8	37.3	36.7	35.9	35.2	34.6	34.0	33.5
	$f_{v,a}$ (ksi)	≤26.8	≤35.1	≤43.5	≤52.0	≤60.6	≤69.2	≤75.0	≤75.0	≤75.0	≤75.0	≤75.0	≤75.0
≤1.5	θ (deg)	44.2	42.3	41.0	40.0	39.2	38.5	37.9	37.1	36.3	35.6	34.9	34.3
	$f_{v,a}$ (ksi)	≤24.7	≤32.9	≤41.3	≤49.8	≤58.4	≤67.0	≤75.0	≤75.0	≤75.0	≤75.0	≤75.0	≤75.0
≤2.0	θ (deg)	47.1	44.6	42.9	41.6	40.6	39.8	39.1	38.2	37.4	36.6	35.9	35.2
	$f_{v,a}$ (ksi)	≤22.2	≤30.5	≤38.9	≤47.4	≤56.0	≤64.6	≤73.3	≤75.0	≤75.0	≤75.0	≤75.0	≤75.0
≤2.5	θ (deg)	50.4	47.2	45.0	43.4	42.1	41.1	40.3	39.4	38.5	37.6	36.9	36.2
	$f_{v,a}$ (ksi)	≤19.4	≤27.8	≤36.2	≤44.8	≤53.4	≤62.1	≤70.8	≤75.0	≤75.0	≤75.0	≤75.0	≤75.0
≤3.0	θ (deg)	–	50.1	47.3	45.3	43.8	42.6	41.6	40.7	39.7	38.7	37.9	37.1
	$f_{v,a}$ (ksi)	–	≤24.8	≤33.3	≤42.0	≤50.6	≤59.3	≤68.1	≤75.0	≤75.0	≤75.0	≤75.0	≤75.0
≤3.5	θ (deg)	–	–	49.9	47.4	45.6	44.1	43.0	42.0	40.9	39.9	39.0	38.2
	$f_{v,a}$ (ksi)	–	–	≤30.1	≤38.9	≤47.6	≤56.4	≤65.2	≤74.0	≤75.0	≤75.0	≤75.0	≤75.0
≤4.0	θ (deg)	–	–	–	49.7	47.5	45.8	44.4	43.3	42.2	41.1	40.1	39.2
	$f_{v,a}$ (ksi)	–	–	–	≤35.5	≤44.4	≤53.2	≤62.1	≤71.0	≤75.0	≤75.0	≤75.0	≤75.0
≤4.5	θ (deg)	–	–	–	–	49.5	47.5	45.9	44.7	43.5	42.3	41.2	40.3
	$f_{v,a}$ (ksi)	–	–	–	–	≤40.9	≤49.9	≤58.9	≤67.8	≤75.0	≤75.0	≤75.0	≤75.0
≤5.0	θ (deg)	–	–	–	–	–	49.4	47.6	46.1	44.9	43.6	42.4	41.4
	$f_{v,a}$ (ksi)	–	–	–	–	–	≤46.4	≤55.4	≤64.5	≤73.5	≤75.0	≤75.0	≤75.0
≤5.5	θ (deg)	–	–	–	–	–	–	49.3	47.6	46.2	44.9	43.7	42.5
	$f_{v,a}$ (ksi)	–	–	–	–	–	–	≤51.8	≤60.9	≤70.0	≤75.0	≤75.0	≤75.0
≤6.0	θ (deg)	–	–	–	–	–	–	–	49.2	47.6	46.3	44.9	43.7
	$f_{v,a}$ (ksi)	–	–	–	–	–	–	–	≤57.2	≤66.4	≤75.0	≤75.0	≤75.0
≤6.5	θ (deg)	–	–	–	–	–	–	–	–	49.1	47.7	46.3	44.9
	$f_{v,a}$ (ksi)	–	–	–	–	–	–	–	–	≤62.7	≤71.9	≤75.0	≤75.0
≤7.0	θ (deg)	–	–	–	–	–	–	–	–	–	49.1	47.6	46.2
	$f_{v,a}$ (ksi)	–	–	–	–	–	–	–	–	–	≤68.1	≤75.0	≤75.0
≤7.5	θ (deg)	–	–	–	–	–	–	–	–	–	–	49.0	47.5
	$f_{v,a}$ (ksi)	–	–	–	–	–	–	–	–	–	–	≤73.6	≤75.0
≤8.0	θ (deg)	–	–	–	–	–	–	–	–	–	–	–	48.8
	$f_{v,a}$ (ksi)	–	–	–	–	–	–	–	–	–	–	–	≤75.0

Note: Values for θ and $f_{v,a}$ where ε_s is greater than $\gamma_u \varepsilon_{t,loc}$ are not relevant. These combinations are indicated by cells containing the "–" symbol.

Table A2.3-5. Values of θ (degrees) and upper limit of $f_{v,α}$ (ksi) for sections with transverse reinforcement with $ρ_{v,α} ≤ 2.5$ percent.

$ε_s ×$ 1,000	Para-meter	$γ_u ε_{t,loc} ×$ 1,000											
		≥2.5	≥3.0	≥3.5	≥4.0	≥4.5	≥5.0	≥5.5	≥6.0	≥6.5	≥7.0	≥7.5	≥8.0
≤ −1.0	θ (deg)	34.5	34.4	34.2	34.1	34.1	34.0	33.6	33.0	32.6	32.1	31.7	31.3
	$f_{v,α}$ (ksi)	≤31.3	≤39.5	≤47.7	≤56.0	≤64.2	≤72.5	≤75.0	≤75.0	≤75.0	≤75.0	≤75.0	≤75.0
≤ −0.5	θ (deg)	36.1	35.7	35.5	35.2	35.1	34.9	34.5	33.9	33.4	32.9	32.4	32.0
	$f_{v,α}$ (ksi)	≤30.1	≤38.2	≤46.4	≤54.5	≤62.7	≤70.9	≤75.0	≤75.0	≤75.0	≤75.0	≤75.0	≤75.0
≤0.0	θ (deg)	37.8	37.2	36.8	36.4	36.1	35.9	35.5	34.9	34.3	33.7	33.2	32.8
	$f_{v,α}$ (ksi)	≤28.8	≤36.8	≤44.8	≤52.9	≤61.1	≤69.3	≤75.0	≤75.0	≤75.0	≤75.0	≤75.0	≤75.0
≤0.5	θ (deg)	39.8	38.9	38.2	37.7	37.2	36.9	36.5	35.8	35.2	34.6	34.0	33.5
	$f_{v,α}$ (ksi)	≤27.3	≤35.1	≤43.2	≤51.2	≤59.3	≤67.4	≤75.0	≤75.0	≤75.0	≤75.0	≤75.0	≤75.0
≤1.0	θ (deg)	42.0	40.7	39.8	39.0	38.4	38.0	37.6	36.9	36.1	35.5	34.9	34.3
	$f_{v,α}$ (ksi)	≤25.5	≤33.3	≤41.3	≤49.3	≤57.4	≤65.5	≤73.7	≤75.0	≤75.0	≤75.0	≤75.0	≤75.0
≤1.5	θ (deg)	44.5	42.7	41.5	40.5	39.7	39.1	38.6	37.9	37.1	36.4	35.8	35.2
	$f_{v,α}$ (ksi)	≤23.5	≤31.3	≤39.2	≤47.2	≤55.3	≤63.4	≤71.6	≤75.0	≤75.0	≤75.0	≤75.0	≤75.0
≤2.0	θ (deg)	47.4	45.0	43.3	42.1	41.1	40.4	39.7	39.1	38.2	37.4	36.7	36.1
	$f_{v,α}$ (ksi)	≤21.2	≤29.0	≤37.0	≤45.0	≤53.1	≤61.2	≤69.4	≤75.0	≤75.0	≤75.0	≤75.0	≤75.0
≤2.5	θ (deg)	50.7	47.5	45.4	43.8	42.6	41.7	40.9	40.3	39.3	38.4	37.7	37.0
	$f_{v,α}$ (ksi)	≤18.5	≤26.4	≤34.4	≤42.5	≤50.7	≤58.8	≤67.0	≤75.0	≤75.0	≤75.0	≤75.0	≤75.0
≤3.0	θ (deg)	–	50.4	47.6	45.7	44.2	43.1	42.1	41.4	40.4	39.5	38.7	37.9
	$f_{v,α}$ (ksi)	–	≤23.6	≤31.7	≤39.8	≤48.0	≤56.2	≤64.5	≤72.7	≤75.0	≤75.0	≤75.0	≤75.0
≤3.5	θ (deg)	–	–	50.1	47.7	46.0	44.6	43.5	42.6	41.6	40.6	39.7	38.9
	$f_{v,α}$ (ksi)	–	–	≤28.7	≤36.9	≤45.2	≤53.5	≤61.8	≤70.0	≤75.0	≤75.0	≤75.0	≤75.0
≤4.0	θ (deg)	–	–	–	50.0	47.8	46.2	44.9	43.8	42.9	41.8	40.8	39.9
	$f_{v,α}$ (ksi)	–	–	–	≤33.8	≤42.2	≤50.5	≤58.9	≤67.2	≤75.0	≤75.0	≤75.0	≤75.0
≤4.5	θ (deg)	–	–	–	–	49.8	47.9	46.4	45.1	44.1	43.0	41.9	40.9
	$f_{v,α}$ (ksi)	–	–	–	–	≤38.9	≤47.4	≤55.9	≤64.3	≤72.7	≤75.0	≤75.0	≤75.0
≤5.0	θ (deg)	–	–	–	–	–	49.7	47.9	46.5	45.3	44.2	43.1	42.0
	$f_{v,α}$ (ksi)	–	–	–	–	–	≤44.1	≤52.6	≤61.2	≤69.6	≤75.0	≤75.0	≤75.0
≤5.5	θ (deg)	–	–	–	–	–	–	49.6	48.0	46.7	45.5	44.3	43.2
	$f_{v,α}$ (ksi)	–	–	–	–	–	–	≤49.2	≤57.8	≤66.4	≤75.0	≤75.0	≤75.0
≤6.0	θ (deg)	–	–	–	–	–	–	–	49.5	48.0	46.8	45.5	44.3
	$f_{v,α}$ (ksi)	–	–	–	–	–	–	–	≤54.4	≤63.1	≤71.7	≤75.0	≤75.0
≤6.5	θ (deg)	–	–	–	–	–	–	–	–	49.5	48.1	46.8	45.5
	$f_{v,α}$ (ksi)	–	–	–	–	–	–	–	–	≤59.5	≤68.3	≤75.0	≤75.0
≤7.0	θ (deg)	–	–	–	–	–	–	–	–	–	49.4	48.1	46.7
	$f_{v,α}$ (ksi)	–	–	–	–	–	–	–	–	–	≤64.7	≤73.5	≤75.0
≤7.5	θ (deg)	–	–	–	–	–	–	–	–	–	–	49.4	48.0
	$f_{v,α}$ (ksi)	–	–	–	–	–	–	–	–	–	–	≤69.9	≤75.0
≤8.0	θ (deg)	–	–	–	–	–	–	–	–	–	–	–	49.3
	$f_{v,α}$ (ksi)	–	–	–	–	–	–	–	–	–	–	–	≤75.0

Note: Values for θ and $f_{v,α}$ where $ε_s$ is greater than $γ_u ε_{t,loc}$ are not relevant. These combinations are indicated by cells containing the "–" symbol.

Table A2.3-6. Values of θ (degrees) and upper limit of $f_{v,α}$ (ksi) for sections with transverse reinforcement with $\rho_{v,α} \leq 3.0$ percent.

$\varepsilon_s \times$ 1,000	Para-meter	$\gamma_u \varepsilon_{t,loc} \times$ **1,000**											
		≥2.5	**≥3.0**	**≥3.5**	**≥4.0**	**≥4.5**	**≥5.0**	**≥5.5**	**≥6.0**	**≥6.5**	**≥7.0**	**≥7.5**	**≥8.0**
≤ −1.0	θ (deg)	35.0	34.9	34.8	34.7	34.7	34.6	34.5	33.9	33.4	33.0	32.5	32.1
	$f_{v,α}$ (ksi)	≤29.9	≤37.6	≤45.4	≤53.2	≤61.0	≤68.8	≤75.0	≤75.0	≤75.0	≤75.0	≤75.0	≤75.0
≤ −0.5	θ (deg)	36.5	36.2	36.0	35.8	35.7	35.5	35.4	34.8	34.3	33.7	33.3	32.8
	$f_{v,α}$ (ksi)	≤28.8	≤36.4	≤44.1	≤51.9	≤59.6	≤67.4	≤75.0	≤75.0	≤75.0	≤75.0	≤75.0	≤75.0
≤0.0	θ (deg)	38.2	37.7	37.3	37.0	36.7	36.5	36.3	35.7	35.1	34.6	34.0	33.6
	$f_{v,α}$ (ksi)	≤27.5	≤35.0	≤42.7	≤50.3	≤58.0	≤65.8	≤73.5	≤75.0	≤75.0	≤75.0	≤75.0	≤75.0
≤0.5	θ (deg)	40.2	39.3	38.7	38.2	37.8	37.5	37.2	36.7	36.0	35.4	34.8	34.3
	$f_{v,α}$ (ksi)	≤26.0	≤33.5	≤41.1	≤48.7	≤56.4	≤64.1	≤71.8	≤75.0	≤75.0	≤75.0	≤75.0	≤75.0
≤1.0	θ (deg)	42.3	41.1	40.2	39.5	39.0	38.5	38.2	37.7	37.0	36.3	35.7	35.1
	$f_{v,α}$ (ksi)	≤24.3	≤31.8	≤39.3	≤46.9	≤54.5	≤62.2	≤69.9	≤75.0	≤75.0	≤75.0	≤75.0	≤75.0
≤1.5	θ (deg)	44.8	43.1	41.9	41.0	40.2	39.7	39.2	38.7	37.9	37.2	36.6	35.9
	$f_{v,α}$ (ksi)	≤22.4	≤29.8	≤37.3	≤45.0	≤52.6	≤60.3	≤68.0	≤75.0	≤75.0	≤75.0	≤75.0	≤75.0
≤2.0	θ (deg)	47.6	45.3	43.7	42.5	41.6	40.9	40.3	39.8	39.0	38.2	37.5	36.8
	$f_{v,α}$ (ksi)	≤20.2	≤27.7	≤35.2	≤42.8	≤50.5	≤58.2	≤65.9	≤73.6	≤75.0	≤75.0	≤75.0	≤75.0
≤2.5	θ (deg)	50.9	47.8	45.7	44.2	43.1	42.1	41.4	40.8	40.0	39.2	38.4	37.7
	$f_{v,α}$ (ksi)	≤17.7	≤25.2	≤32.8	≤40.5	≤48.2	≤55.9	≤63.7	≤71.4	≤75.0	≤75.0	≤75.0	≤75.0
≤3.0	θ (deg)	–	50.6	47.9	46.1	44.6	43.5	42.6	41.9	41.2	40.2	39.4	38.6
	$f_{v,α}$ (ksi)	–	≤22.5	≤30.2	≤38.0	≤45.7	≤53.5	≤61.3	≤69.1	≤75.0	≤75.0	≤75.0	≤75.0
≤3.5	θ (deg)	–	–	50.4	48.1	46.3	45.0	43.9	43.0	42.3	41.3	40.4	39.6
	$f_{v,α}$ (ksi)	–	–	≤27.4	≤35.2	≤43.1	≤50.9	≤58.7	≤66.6	≤74.4	≤75.0	≤75.0	≤75.0
≤4.0	θ (deg)	–	–	–	50.2	48.1	46.5	45.3	44.2	43.4	42.4	41.5	40.6
	$f_{v,α}$ (ksi)	–	–	–	≤32.3	≤40.2	≤48.1	≤56.0	≤63.9	≤71.8	≤75.0	≤75.0	≤75.0
≤4.5	θ (deg)	–	–	–	–	50.1	48.2	46.7	45.5	44.5	43.6	42.5	41.6
	$f_{v,α}$ (ksi)	–	–	–	–	≤37.1	≤45.2	≤53.2	≤61.1	≤69.1	≤75.0	≤75.0	≤75.0
≤5.0	θ (deg)	–	–	–	–	–	50.0	48.3	46.9	45.8	44.8	43.7	42.6
	$f_{v,α}$ (ksi)	–	–	–	–	–	≤42.0	≤50.1	≤58.2	≤66.2	≤74.2	≤75.0	≤75.0
≤5.5	θ (deg)	–	–	–	–	–	–	49.9	48.3	47.0	46.0	44.9	43.7
	$f_{v,α}$ (ksi)	–	–	–	–	–	–	≤46.9	≤55.1	≤63.2	≤71.3	≤75.0	≤75.0
≤6.0	θ (deg)	–	–	–	–	–	–	–	49.8	48.4	47.1	46.1	44.9
	$f_{v,α}$ (ksi)	–	–	–	–	–	–	–	≤51.8	≤60.0	≤68.2	≤75.0	≤75.0
≤6.5	θ (deg)	–	–	–	–	–	–	–	–	49.8	48.4	47.3	46.0
	$f_{v,α}$ (ksi)	–	–	–	–	–	–	–	–	≤56.7	≤65.0	≤73.2	≤75.0
≤7.0	θ (deg)	–	–	–	–	–	–	–	–	–	49.7	48.4	47.2
	$f_{v,α}$ (ksi)	–	–	–	–	–	–	–	–	–	≤61.6	≤69.9	≤75.0
≤7.5	θ (deg)	–	–	–	–	–	–	–	–	–	–	49.7	48.5
	$f_{v,α}$ (ksi)	–	–	–	–	–	–	–	–	–	–	≤66.5	≤74.9
≤8.0	θ (deg)	–	–	–	–	–	–	–	–	–	–	–	49.6
	$f_{v,α}$ (ksi)	–	–	–	–	–	–	–	–	–	–	–	≤71.4

Note: values for θ and $f_{v,α}$ where ε_s is greater than $\gamma_u \varepsilon_{t,loc}$ are not relevant. These combinations are indicated by cells containing the "–" symbol.

APPENDIX B. ANALYSIS OF A RECTANGULAR, MILD STEEL REINFORCED UHPC BEAM

Appendix B is based on the content presented in Appendix A of this report.

LIST OF NOTATIONS

A_{ct} = area of UHPC on the flexural tension side of the member (in.^{2})

A_g = gross area of section (in.^{2})

A_{ps} = area of prestressing steel on the flexural tension side of the member (in.^{2}), as shown in AASHTO LRFD BDS Figure 5.7.3.4.2-1 (AASHTO 2020)

A_s = area of nonprestressed steel on the flexural tension side of the member at the section under consideration (in.^{2}), as shown in AASHTO LRFD BDS Figure 5.7.3.4.2-1 (AASHTO 2020) (in.^{2})

$A_{s,bar}$ = area of one nonprestressed steel bar (in.^{2})

A_v = area of transverse reinforcement to resist shear within a distance s (in.^{2})

b_v = effective web width taken as the minimum web width within the depth d_v (in.)

b_w = web width (in.)

c = distance from the extreme compression fiber to the neutral axis (in.)

c_L = distance from the extreme compression fiber of the member to the neutral axis when the UHPC tensile strain limit, $\gamma_u\varepsilon_{t,loc}$, at extreme tension fiber is reached (in.)

d_b = nominal diameter of reinforcing bar (in.)

d_e = effective depth taken as taken as the distance, measured perpendicular to the neutral axis, between the extreme compression fiber to the centroid of the flexural tensile reinforcement (in.)

d_v = effective shear depth taken as the distance, measured perpendicular to the neutral axis, between the resultants of the tensile and compressive forces due to flexure (in.)

E_c = modulus of elasticity of UHPC for use in design (ksi)

E_s = modulus of elasticity of the mild steel reinforcement (ksi)

f'_c = compressive strength of UHPC for use in design (ksi)

f_{po} = a parameter taken as modulus of elasticity of prestressing steel multiplied by the locked-in difference in strain between the prestressing steel and the surrounding UHPC (ksi)

f_{pu} = specified tensile strength of prestressing steel (ksi)

$f_{s\ell}$ = stress limit in steel at service loads after losses (ksi)

$f_{t,cr}$ = effective cracking strength of UHPC for use in design (ksi)

$f_{t,loc}$ = crack localization strength of UHPC for use in design (ksi)

f_v = stress in the transverse steel reinforcement at nominal shear resistance (ksi)

$f_{v,Check}$ = value of f_v at the end of an iteration step during analysis of nominal shear resistance (ksi)

f_y = specified minimum yield strength of reinforcement (ksi)

h	=	overall depth of the member (in.)
L	=	span length measured between center of supports (in.)
M	=	nominal flexural moment (kip-ft)
M_c	=	nominal crushing moment (kip-ft)
M_{cr}	=	nominal cracking moment (kip-ft)
M_L	=	nominal crack localization moment (kip-ft)
M_n	=	nominal flexural resistance (kip-ft)
M_r	=	factored flexural resistance (kip-ft)
$M_{s\ell}$	=	nominal flexural moment when the steel stress in the extreme tension steel is equal to the steel service stress limit, $f_{s\ell}$ (kip-ft)
M_{su}	=	nominal flexural moment at the rupture of tension steel (kip-ft)
M_{sy}	=	nominal flexural moment when the steel stress in the extreme tension steel is equal to the steel yield strength, f_{sy} (kip-ft)
M_u	=	factored moment at the section (kip-ft)
N_u	=	factored axial force, taken as positive if tensile and negative if compressive (kip)
s	=	spacing of transverse reinforcement measured in a direction parallel to the longitudinal reinforcement (in.)
V_n	=	nominal shear resistance (kip)
$V_{n,max}$	=	upper limit on factored shear force at critical shear section (kip)
V_p	=	component of prestressing force in the direction of the shear force (kip)
V_s	=	shear resistance provided by transverse reinforcement (kip)
V_u	=	factored shear force (kip)
V_{UHPC}	=	nominal shear resistance of the UHPC (kip)
V_{u1}	=	factored shear force at a distance d_v from face of support (kip)
$V_{u,max}$	=	maximum factored shear force applied on the beam (kip)
$w_{u,max}$	=	maximum factored applied load that the beam can carry (kip/ft)
y_{bs}	=	distance between centroid of steel reinforcement and extreme tension fiber of the beam (in.)
α	=	angle of inclination of transverse reinforcement to longitudinal axis (degrees)
α_u	=	reduction factor to account for the nonlinearity of the UHPC compressive stress-strain response
γ_u	=	factor to allow for the reduction of UHPC tensile parameter values; it shall not be taken greater than 1.0
ε_2	=	strain in the UHPC diagonal compressive strut (in./in.)

ε_c	=	compressive strain in extreme compression fiber of the UHPC section (in./in.)
ε_{cp}	=	elastic compressive strain limit of UHPC (in./in.)
ε_{cu}	=	ultimate compressive strain of UHPC for use in design (in./in.)
ε_s	=	net longitudinal tensile strain in the section at the centroid of the tension reinforcement (in./in.)
ε_{su}	=	ultimate tensile strain capacity of steel reinforcement
$\varepsilon_{s\ell}$	=	net tensile strain in the extreme tension steel when the steel service stress limit, $f_{s\ell}$, is reached (in./in.)
ε_t	=	net tensile strain in extreme tension fiber of the UHPC section (in./in.)
$\varepsilon_{t,cr}$	=	elastic tensile strain limit of UHPC corresponding to a tensile stress of $\gamma_u f_{t,cr}$ (in./in.)
$\varepsilon_{t,loc}$	=	crack localization strain of UHPC for use in design (in./in.)
ε_v	=	strain in the transverse steel reinforcement at nominal shear resistance (in./in.)
ε_y	=	strain in the steel reinforcement corresponding to f_y (in./in.)
θ	=	angle of inclination of diagonal compressive stresses (degrees)
μ	=	curvature ductility ratio
μ_ℓ	=	curvature ductility ratio limit
$\mu_{s\ell}$	=	curvature ductility ratio at steel service limit
ρ_v	=	ratio of area of transverse shear reinforcement to area of gross UHPC area of a horizontal section
ϕ	=	resistance factor
ϕ_f	=	resistance factor for flexure
ψ	=	sectional curvature at nominal flexural moment, M (1/in.)
ψ_c	=	sectional curvature at nominal crushing moment, M_c (1/in.)
ψ_{cr}	=	sectional curvature at nominal cracking moment, M_{cr} (1/in.)
ψ_L	=	sectional curvature at nominal crack localization moment, M_L (1/in.)
ψ_n	=	sectional curvature at nominal flexural strength (1/in.)
$\psi_{s\ell}$	=	baseline sectional curvature at $M_{s\ell}$ (1/in.)
ψ_{sy}	=	sectional curvature at nominal steel yielding moment, M_{sy} (1/in.)
ω_c	=	unit weight of UHPC

CHAPTER B1. INTRODUCTION

The example in this Appendix illustrates the flexural and shear analysis of a beam made of ultra-high performance concrete (UHPC). The beam is rectangular in shape with a width of 12 in. and a height of 24 in.; it is simply supported over a span of 30 ft (center-to-center of supports) and subjected to a uniformly distributed total factored load of 4.55 kip/ft (including self-weight). The width of each support is 1 ft. The beam is reinforced with one layer of three No. 11 Grade 60 steel reinforcing bars (ASTM A615/A615M (ASTM 2020a)) in the longitudinal direction and No. 4 Grade 60 steel two-legged stirrups at 6-in. spacing, as shown in Figure B1-1. This analysis example explains in detail the flexural behavior of the reinforced UHPC beam at cracking, yield, crack localization, and compression failure, and presents the shear capacity calculations at one location within the beam's span. The analysis is accomplished in accordance with the *AASHTO LRFD Bridge Design Specifications*, 9th edition (AASHTO 2020), hereafter referred to "AASHTO LRFD BDS," and Appendix A of this document, entitled, "Guide Specification for Structural Design with Ultra-High Performance Concrete." Appendix A, hereafter referred to as the "UHPC Guide," has been proposed to AASHTO T-10 for their consideration by the Federal Highway Administration's Turner-Fairbank Highway Research Center.
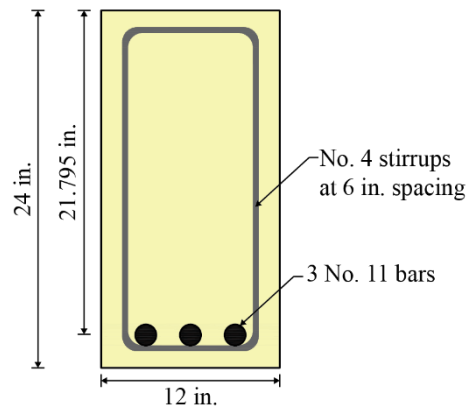
Source: FHWA.

Figure B1-1. Illustration. Cross-section detail.

CHAPTER B2. MATERIALS

The material properties for the UHPC in the beam are as follows:

- Compressive strength for use in design, $f'_c = 22.0$ ksi.

- Ultimate compressive strain for use in design, $\varepsilon_{cu} = 0.0035$.

- UHPC unit weight, $\omega_c = 0.155$ kip/ft^3.

- Modulus of elasticity for use in design, $E_c = 2,500(f'_c)^{0.33} = 6,933$ ksi.

  [UHPC Guide Article 1.4.2.3]

- Cracking strength for use in design, $f_{t,cr} = 1.00$ ksi.

- Crack localization stress for use in design, $f_{t,loc} = 1.00$ ksi.

- Ultimate tension strain for use in design, $\varepsilon_{t,loc} = 0.003$.

- Reduction factor on tensile parameters, $\gamma_u = 1.00$.

The material properties for the steel reinforcement are as follows:

- Modulus of elasticity, $E_s = 29,000$ ksi.

- Yield strength, $f_y = 60$ ksi.

- Yield strain for use in design, $\varepsilon_y = 0.00207$.

- Service stress limit, $f_{s\ell} = 0.80 f_y = 48$ ksi.   [UHPC Guide Article 1.5.2]

- Ultimate strain for use in design, $\varepsilon_{su} = 0.09$.   [ASTM A615/A615M (ASTM 2020a)]

- No. 11 bar diameter, $d_b = 1.41$ in.

- No. 11 bar area, $A_{s,bar} = 1.56$ in.^{2}.

- No. 4 bar area, $A_{s,bar} = 0.20$ in.^{2}.

CHAPTER B3. FLEXURAL ANALYSIS

According to UHPC Guide Article 1.6.3.1, the flexural behavior of UHPC beams shall be determined from a strain compatibility approach by employing representative stress-strain models to determine the stresses based on strains in any cross-sectional layer of UHPC or steel reinforcement.

The nominal flexural moment is taken as the moment corresponding to the lesser of (1) the sectional curvature values calculated when the compressive strain at the extreme compression fiber of the UHPC section is equal to the compression strain limit, i.e., $\varepsilon_{cu} = 0.0035$; (2) the net tensile strain at extreme tension fiber of the UHPC section is equal to the UHPC tensile strain limit, i.e., $\gamma_u \varepsilon_{t,loc} = 0.003$; and (3) the strain in the extreme tension steel is equal to the minimum total elongation strain of the reinforcing steel, i.e., $\varepsilon_{su} = 0.09$ [UHPC Guide Article 1.6.3.2.2].

The resistance factor for flexural capacity is based on a sectional curvature ductility ratio, where a minimum ratio, $\mu_{s\ell} = \psi_n/\psi_{s\ell}$, of 3.0 is specified in UHPC Guide Article 1.6.2. The baseline sectional ductility is calculated at equilibrium when the stress in the extreme layer of steel is equal to the steel service limit stress, $f_{s\ell} = 48$ ksi, which corresponds to a strain, $\varepsilon_{s\ell}$, of $\varepsilon_{s\ell} = f_{s\ell}/E_s = 0.00166$. The sectional curvature at steel service stress limit, $\psi_{s\ell}$, shall also be calculated from a strain compatibility analysis [UHPC Guide Article 1.6.3.1].

In many cases, the nominal capacity of a UHPC beam occurs when the strain in the extreme tension layer of UHPC reaches the UHPC tensile strain limit, i.e., $\varepsilon_t = \gamma_u \varepsilon_{t,loc}$, while the strain in the extreme compression layer, ε_c, is less than the compression strain limit, $\varepsilon_{cu} = 0.0035$. Therefore, a good practice is to first determine the moment at crack localization from a strain compatibility analysis and assess the state of strain in the section compared with the strain limits of each material. If none of the strains in UHPC and steel layers is greater than its respective strain limit, then the nominal moment, M_n, is the crack localization moment, M_L. The next step would be to determine the sectional curvature, $\psi_{s\ell}$, when the extreme steel layer strain reaches $\varepsilon_{s\ell}$ from a second run of the strain compatibility analysis. $\psi_{s\ell}$ will be used to determine the flexural resistance factor, as described in UHPC Guide Article 1.5.4.2.

Note that the case where the compression strain limit is reached before the tensile strain limit of UHPC, $\gamma_u \varepsilon_{t,loc}$, may generally occur in compression members or heavily reinforced beams with a shallow compression zone and/or made from a UHPC material with a high localization strain capacity. The third strain limit described in UHPC Guide Article 1.6.3.2.2 pertains to the rupture of tensile reinforcement and may generally occur in heavily prestressed members.

In the analysis of the rectangular beam described in Chapter B1 of this Appendix, a full strain compatibility analysis is performed in accordance with UHPC Guide Article 1.6.3.1. The objective is to illustrate the full moment-curvature diagram of the beam and better demonstrate the flexural behavior under various loading conditions.

B3.1. STRAIN COMPATIBILITY ANALYSIS

The strain compatibility analysis of the beam shown in Figure B1-1 was initiated by discretizing the beam's cross section into 0.1-in.-thick horizontal layers through the height and assuming constant strains within each layer. In calculating the moment corresponding to each possible strain profile, various neutral axis depths were assumed for a chosen extreme compression strain value, ε_c, until equilibrium of forces was established, at which point the flexural bending moment at this value was calculated. The process was repeated for 110 values of ε_c ranging from 0 to $\varepsilon_{cu} = 0.0035$.

B3.1.1. Material Models for UHPC and Reinforcing Steel

In calculating the moment and forces at equilibrium, the compression and tension stress-strain models specified in UHPC Guide Articles 1.4.2.4.3 and 1.4.2.5.4 for UHPC were employed, respectively, as shown in Figure B3.1.1-1-A and Figure B3.1.1-1-B.

| A. UHPC in compression. | B. UHPC in tension. | C. Conventional steel bars in tension. |
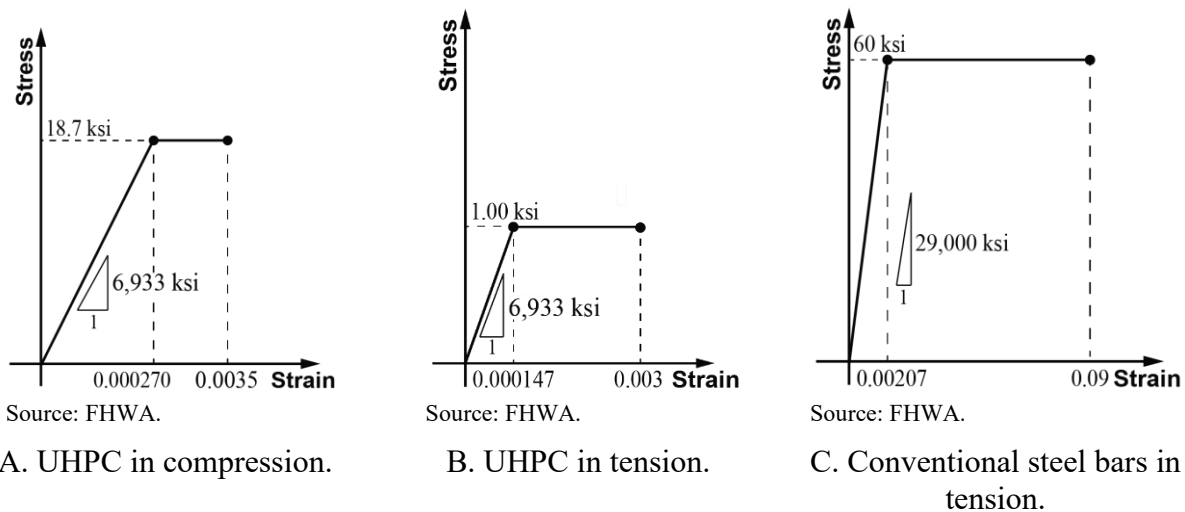
Figure B3.1.1-1. Graphs. Idealized uniaxial stress-strain relationships.

The idealized uniaxial stress-strain model of UHPC under compression is defined by the modulus of elasticity of UHPC, $E_c = 6{,}933$ ksi, a reduced value of the compressive strength, $\alpha_u f'_c = 18.7$ ksi, where $\alpha_u = 0.85$ [UHPC Guide Article 1.4.2.4.2], the elastic compressive strain limit, $\varepsilon_{cp} = \alpha_u f'_c/E_c = 0.00270$, and the ultimate compressive strain of UHPC, $\varepsilon_{cu} = 0.0035$ [UHPC Guide Article 1.4.2.4.2]. Note that α_u is a reduction factor to account for the nonlinearity of the UHPC compressive stress-strain response.

The idealized elastic, perfectly plastic uniaxial stress-strain model of UHPC defined in UHPC Guide Figure 1.4.2.5.4-1 is employed in this analysis since the UHPC material used to make the beam has an effective cracking strength, $f_{t,cr}$, equal to or less than $1.2f_{t,loc}$ (i.e., $f_{t,cr} = f_{t,loc} = 1.00$ ksi) [UHPC Guide Article 1.4.2.5.4]. The tensile stress-strain model of Figure B3.1.1-1-B is defined by the modulus of elasticity of UHPC, $E_c = 6{,}933$ ksi, the effective cracking and crack localization strength limits, $\gamma_u f_{t,cr} = \gamma_u f_{t,loc} = 1.00$ ksi, the cracking strain, $\varepsilon_{t,cr} = \gamma_u f_{t,cr}/E_c = 0.000144$, and the and the tensile strain limit, $\gamma_u f_{t,loc} = 0.003$. Note that $\gamma_u = 1.00$.

For the tensile steel reinforcement, an elastic, perfectly plastic stress-strain model was implemented as shown in Figure B3.1.1-1-C, where E_s = 29,000 ksi, f_{sy} = 60 ksi, ε_{sy} = 0.00207, and ε_{su} = 0.09.

B3.2. MOMENT CURVATURE DIAGRAM

The flexural moment-sectional curvature ($M - \psi$) diagram obtained from strain compatibility is shown in Figure B3.2-1 and includes the intermediate and final behaviors of the beam, such as first cracking, service steel stress limit, yielding of reinforcement, UHPC crack localization, and UHPC crushing. Note that the $M - \psi$ diagram of Figure B3.2-1 includes the moments and curvatures corresponding to strain profiles in which the crack localization strain of UHPC is exceeded. This information is provided to illustrate sectional behaviors after crack localization.
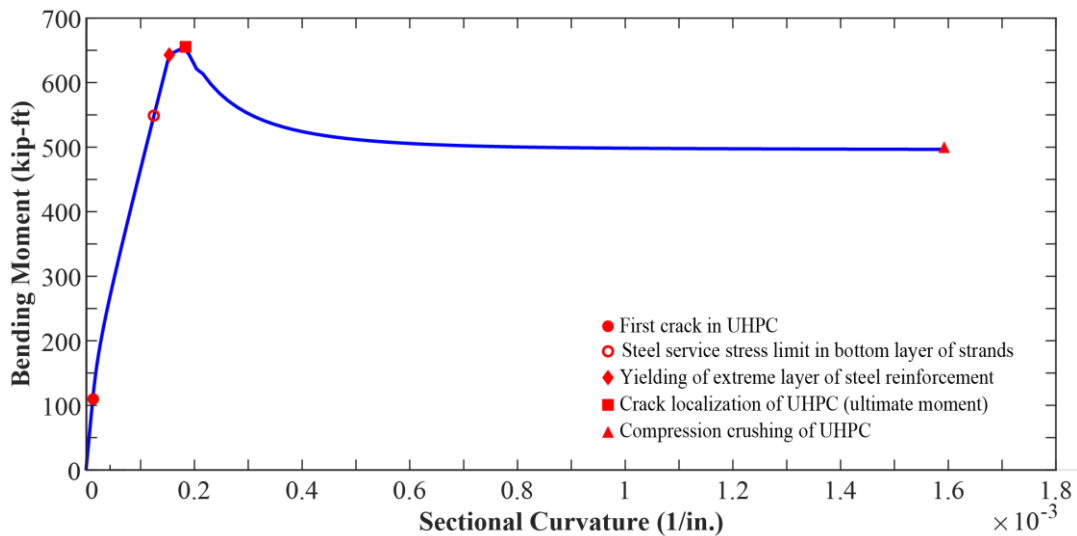
Source: FHWA.

Figure B3.2-1. Graph. Flexural moment-sectional curvature ($M - \psi$) diagram of the UHPC cross section.

The first key point (M_{cr}, ψ_{cr}) in the $M - \psi$ diagram of the UHPC section represents the initiation of cracking, which occurs when the strain in the extreme tension fiber of the section reaches the UHPC effective cracking strain limit, $\varepsilon_{t,cr} = \gamma_u f_{t,cr}/E_c = 0.000144$ (tension). At this point, the compressive and tensile stresses of the UHPC and steel remained within the elastic region of their respective constitutive models. The strain and stress profiles obtained at the end of this analysis are shown in Figure B3.2-2. The details of the results are presented in Table B3.2-1.
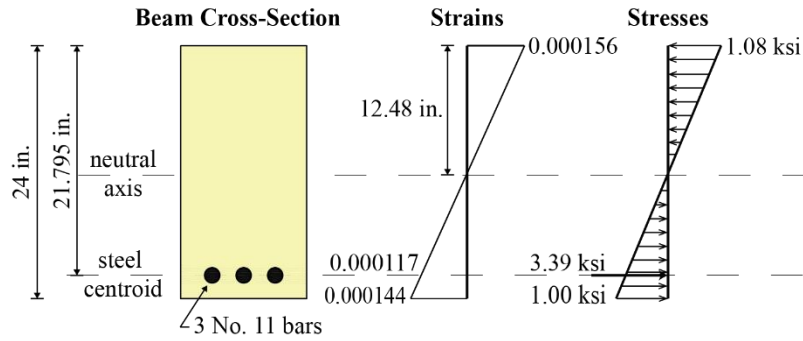
Source: FHWA.

Figure B3.2-2. Illustration. Strain and stress profiles at first crack in UHPC.

Table B3.2-1. Summary of the moment-curvature analysis.

Parameter	(M_{cr}, ψ_{cr}) First Crack	$(M_{s\ell}/\psi_{s\ell})$ Steel Service	(M_{sy}, ψ_{sy}) Steel Yield	(M_L, ψ_L) Localization	(M_c, ψ_c) Crushing
M (kip-ft)	109.8	548.8	642.8	655.3	496.5
c (in.)	12.48	8.69	8.43	7.78	2.20
ε_c	0.000156	0.00110	0.00130	0.00144	$\varepsilon_{cu} = 0.0035$
ε_t	$\varepsilon_{t,cr} = 0.000144$	0.00193	0.00241	$\gamma_u \varepsilon_{t,loc} = 0.00300$	0.0348
ε_s	0.000117	$\varepsilon_{s\ell} = 0.00166$	$\varepsilon_{sy} = 0.00207$	0.00259	0.0312
ψ (1/in.) $\times$ 10^{-3}	0.0125	0.127	0.154	0.185	1.591

Note: See List of Notations for variable definitions.

The second point ($M_{s\ell}/\psi_{s\ell}$) shown in the $M - \psi$ diagram of Figure B3.2-1 corresponds to the baseline sectional curvature for ductility calculations in which the extreme tension layer of the steel reinforcement reached the steel service stress and strain limits, $\varepsilon_{s\ell}$ and $f_{s\ell}$, of 0.00166 and 48 ksi, respectively. The strain and stress profiles obtained at the end of this analysis are shown in Figure B3.2-3. At this point, the compressive stresses and strains remained within the elastic portions of their constitutive law, while the tensile strains reached a strain of 0.00193 within the plastic zone. The details of the results are presented in Table B3.2-1 in which the sectional curvature was calculated as follows: $\psi_{s\ell} = 0.00110/8.69 = 0.127 \times 10^{-3}$ [UHPC Guide Eq. 1.6.3.2.3-2].
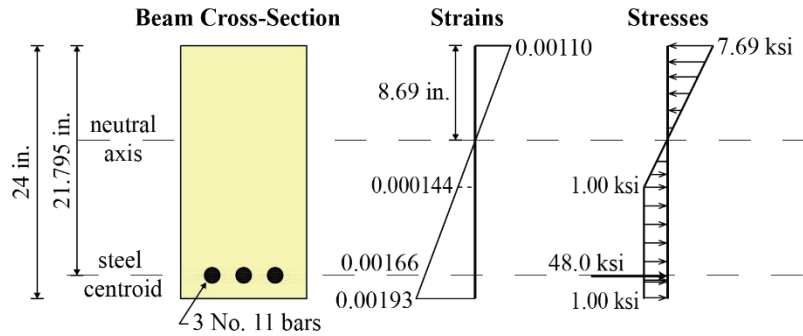
Source: FHWA.

Figure B3.2-3. Illustration. Strain and stress profiles when the steel reinforcement reaches steel service limit.

The third point (M_{sy}, ψ_{sy}) corresponds to the yielding of reinforcement when the strain in the extreme tension steel layer reaches the steel yield strain, $\varepsilon_y = 0.00207$.
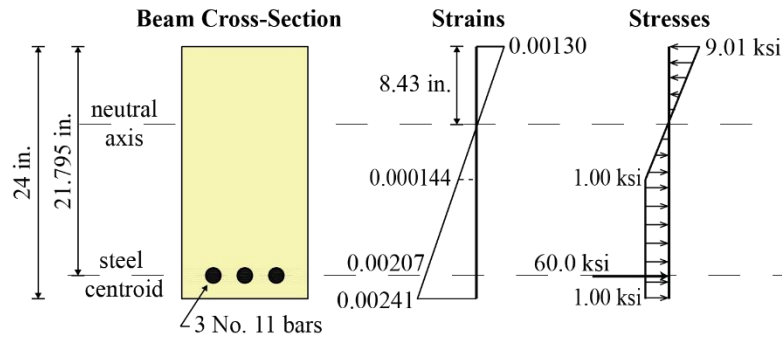
Source: FHWA.

Figure B3.2-4. Illustration. Strain and stress profiles at yielding of steel reinforcement.

The fourth point (M_L, ψ_L) shown in the $M - \psi$ diagram of Figure B3.2-1 corresponds to the UHPC crack localization. At this point, the tensile contribution of the UHPC is exhausted and the strain in the extreme tension fiber of the section is equal to the UHPC tensile strain limit, $\gamma_u\varepsilon_{t,loc} = 0.003$. The strain and stress profiles obtained at the end of this analysis are shown in Figure B3.2-5, and the details of the results are presented in Table B3.2-1. The moment corresponding to this point shall be taken as the nominal moment capacity of the section, i.e., $M_n = M_L = 655.3$ kip-ft, because the tensile strain limit of UHPC was reached before the strains in the steel or the compressed UHPC reached their ultimate limits (i.e., $\varepsilon_s = 0.00259 < \varepsilon_{su} = 0.09$ and $\varepsilon_c = 0.00144 < \varepsilon_{cu} = 0.0035$ [UHPC Guide Article 1.6.3.2.2]. The nominal curvature ductility can be calculated as follows:

$$\psi_n = \psi_L = 0.00144/7.78 = 0.185 \times 10^{-3} \qquad \text{[UHPC Guide Eq. 1.6.3.2.3-3]}$$
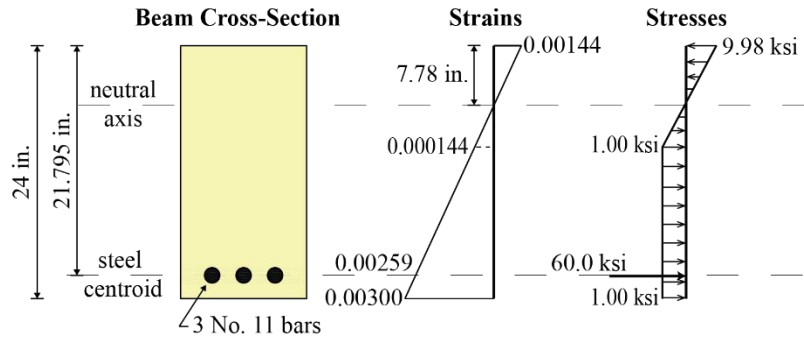
Source: FHWA.

Figure B3.2-5. Illustration. Strain and stress profiles at UHPC crack localization.

The fifth and final point (M_c, ψ_c) shown in the $M - \psi$ diagram of Figure B3.2-1 corresponds to the crushing of the UHPC and is calculated herein for illustration purposes. The crushing of UHPC in compression occurs when the strain in the extreme compression fiber of the section reaches the ultimate compression strain limit of UHPC, $\varepsilon_{cu} = 0.0035$. The portion of the UHPC within the tension zone with a strain lower than the UHPC localization strain is assumed to resist tension, as shown in Figure B3.2-6. Note that for all points in the $M - \psi$ diagram of Figure B3.2-1 calculated after the localization of cracks in UHPC (i.e., all points with sectional curvature greater than the sectional curvature at UHPC crack localization, $\psi > \psi_L$), the sectional behavior violates UHPC Guide Article 1.6.3.2.2, because the strain in the UHPC at the extreme tension layer at each of these points is greater than the UHPC crack localization capacity. The flexural behavior after UHPC crack localization is not recommended to be considered in the design, because the loss of UHPC fiber bridging capacity may result in the hinging of the beam at the localized crack section and the straining of the tensile reinforcement over a short distance, increasing the risk of reinforcement rupture [UHPC Guide Article C1.6.3.2.2]. Note that the hinging and local straining of the tensile reinforcement might occur in cases where the calculated postcrack localization moment (or moment at crushing or rupture of tension steel) is greater than the localization moment capacity (i.e., $M_c > M_L$ or $M_{su} > M_L$). Regardless of the moment capacity calculated after UHPC crack localization, the provisions of Article 1.6.3.2.2 limit the flexural capacity to the moment calculated at the UHPC crack localization.
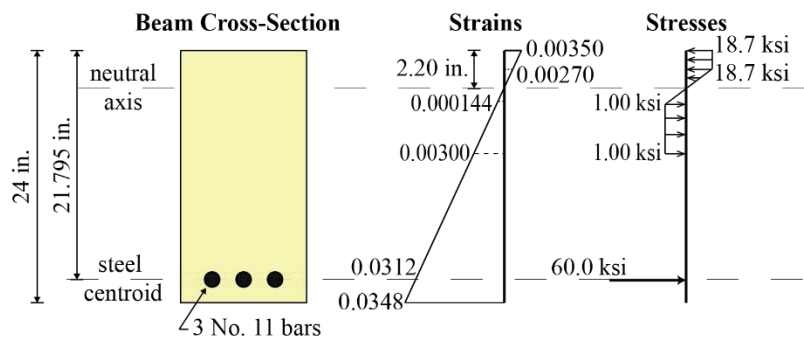
Source: FHWA.

Figure B3.2-6. Illustration. Strain and stress profiles at the crushing of UHPC in compression.

156

B3.3. FACTORED FLEXURAL RESISTANCE

The factored flexural resistance shall be taken as:

$$M_r = \phi M_n \qquad \text{[UHPC Guide Eq. 1.6.3.2.1-1]}$$

where:
    M_n = nominal flexural resistance (kip-ft.)
    ϕ = resistance factor specified in UHPC Guide Article 1.5.4.2

The resistance factor for flexural capacity is based on a ductility performance threshold expressed in terms of a curvature ductility ratio.   [UHPC Guide Article 1.5.4.2]

The curvature ductility ratio is defined as:

$$\mu = \frac{\psi_n}{\psi_{s\ell}} \qquad \text{[UHPC Guide Eq. 1.6.3.2.3-1]}$$

where:
    ψ_n = sectional curvature at nominal flexural strength
    $\psi_{s\ell}$ = sectional curvature when the steel stress in the extreme tension steel is equal to the steel service stress limit, $f_{s\ell}$

in which $f_{s\ell}$ = stress limit in reinforcing steel = $0.80 f_{sy}$ = 48 ksi.

The resistance factor can be calculated in accordance with UHPC Guide Articles 1.5.4.2 and 1.6.3.2.3:

    Ultimate moment: $M_n = M_L = 659.0$ kip-ft

    Curvature ductility ratio limit: $\mu_\ell = 3.0$ [UHPC Guide Article 1.6.2]

    Curvature ductility ratio: $\mu = \dfrac{\psi_L}{\psi_{s\ell}} = \dfrac{0.000185}{0.000127} = 1.464$

    Resistance factor: $\phi_f = 0.75 + 0.15 \dfrac{\mu - 1.0}{\mu_\ell - 1.0} = 0.785$

Therefore:

$$\phi_f M_n = \phi_f M_L = (0.785)(655.3) = 514.4 \text{ kip-ft}$$

B3.4. FLEXURE DEMAND VS. CAPACITY CHECK

The simply supported beam in this example is subjected to a uniformly distributed total factored load of 4.55 kip/ft (including self-weight) over a span of 30 ft. Therefore, the maximum total factored moment the beam is subjected is calculated at midspan as follows:

$M_{u,max} = w_u L^2/8 = 4.55 (30)^2/8 = 511.9$ kip-ft

Since $\phi M_n = 514.4$ kip-ft is less than the maximum applied moment $M_{u,max} = 511.9$ kip-ft, the beam passes the ultimate limit state check in flexure.

CHAPTER B4. SHEAR ANALYSIS

The area and spacing of shear reinforcement must be determined at regular intervals along the length of the beam. Transverse reinforcement shall be provided where:

$$V_u > \phi(V_{UHPC} + V_p)$$
[UHPC Guide Eq. 1.7.2.3-1]

where:

V_u	=	factored shear force	
ϕ	=	resistance factor = 0.9	[UHPC Guide Article 1.5.4.2]
V_{UHPC}	=	nominal shear resistance of the UHPC	
V_p	=	component of prestressing force in the direction of shear force; positive if resisting the applied shear	
V_p	=	0 kips for this nonprestressed example	

or where consideration of torsion is required.

In this example, torsion is not being considered, and the ultimate limit state check in shear is only performed at the critical section for shear located at a distance equal to the effective shear depth, d_v, from the internal face of support [UHPC Guide Article 1.7.3.2]. Note that the factored shear capacity must be verified not to exceed the factored demand force at each section within the length of the beam.

B4.1. CONTRIBUTION OF UHPC TO SHEAR RESISTANCE

The effective shear depth, d_v, is taken as the distance, measured perpendicular to the neutral axis, between the resultants of the tensile and compressive forces due to flexure. It need not be taken to be less than the greater of $0.9d_e$ or $0.72h$ [AASHTO LRFD BDS Article 5.7.2.8]. In this design example, it is taken at the specified maximum limit shown as follows:

$$d_e = h - y_{bs} = 24 - 2.205 = 21.795 \text{ in.}$$

$$d_v = \max(0.9d_e, 0.72h) = 19.62 \text{ in.} = 1.64 \text{ ft}$$

For a simply supported span of 30 ft subjected to 4.55 kip/ft uniformly distrusted factored load:

Factored shear at the end of the beam:

$$V_{u,max} = w_u \, L/2 = 4.55(30)/2 = 68.25 \text{ kip}$$

Factored shear demand at the critical shear section (distance d_v from internal face of support with a support width, $W_{sup} = 1$ ft):

$$V_{u1} = \frac{V_u}{L/2} \times \left(\frac{L}{2} - d_v - \frac{W_{sup}}{2}\right) = 58.54 \text{ kip}$$

Factored moment at critical shear section:

$$M_u = V_{u1}(d_v + (w_{sup}/2)) = 125.0 \text{ kip-ft}$$

The net longitudinal tensile strain at the centroid of tensile reinforcement at the critical shear section is determined by:

$$\varepsilon_s = \frac{\dfrac{|M_u|}{d_v} + 0.5N_u + |V_u| - A_{ps}f_{po} - \gamma_u f_{t,cr} A_{ct}}{E_s A_s + E_p A_{ps}}$$

[UHPC Guide Eq. 1.7.3.4.1-6]

where:

N_u	=	factored axial force = 0 kip
f_{po}	=	parameter equal to modulus of elasticity multiplied by the locked-in difference in strain and surrounding concrete
	=	$0.7f_{pu}$ = 0 ksi for a nonprestressed beam
A_{ct}	=	area of UHPC on the flexural tension side of the member
	=	$(A_g/2) - A_s = (12(24)/2) - 3(1.56) = 139.32$ in.^{2}
A_{ps}	=	area of prestressing steel on the flexural tension side of the member
	=	0 in.^{2}
A_s	=	area of nonprestressed steel on the flexural tension side of the member
	=	$33(1.56) = 4.68$ in.^{2}

Therefore:

$$\varepsilon_s = \frac{\dfrac{|125.0|}{1.64} + 0 + |58.54| - (0) - (1.00)(1.00)(139.32)}{(29,000)(4.68)} = -0.0000336$$

Since the value of ε_s calculated from UHPC Guide Eq. 1.7.3.4.1-6, is less than $\varepsilon_{t,cr} = 0.000144$, Eq. 1.7.3.4.1-7 of the UHPC Guide shall be used to determine ε_s:

$$\varepsilon_s = \frac{\dfrac{|M_u|}{d_v} + 0.5N_u + |V_u| - A_{ps}f_{po}}{E_s A_s + E_p A_{ps} + E_c A_{ct}}$$

[UHPC Guide Eq. 1.7.3.4.1-7]

$$\varepsilon_s = \frac{\dfrac{|125.0|}{1.64} + 0 + |58.54| - (0)}{(29,000)(4.68) + (6,933)(139.32)} = 0.000123$$

B4.2. CALCULATION OF INCLINATION ANGLE AND STRESS IN TRANSVERSE STEEL

B4.2.1. General Approach

The general approach for determining shear resistance parameters, θ and f_v, involves solving UHPC Guide Eqs. 1.7.3.4.1-1 through 1.7.3.4.1-4 iteratively. For sections with transverse steel reinforcement perpendicular to the longitudinal axis ($\alpha = 90$ degrees), Eqs. 1.7.3.4.1-1 and 1.7.3.4.1-2 reduce to:

$$\gamma_u \varepsilon_{t,loc} = \frac{\varepsilon_s}{2}(1 + \cot(\theta)^2) + \frac{2f_{t,loc}}{E_c}\cot(\theta)^4 + \frac{2\rho_v f_v}{E_c}\cot(\theta)^2[1 + \cot(\theta)^2]$$

[UHPC Guide Eq. C1.7.3.4.1-3]

$$\varepsilon_2 = -\frac{2f_{t,loc}}{E_c}\cot(\theta)^2 - \frac{2\rho_v f_v}{E_c}[1 + \cot(\theta)^2]$$

[UHPC Guide Eq. C1.7.3.4.1-4]

Strain in vertical steel: $\varepsilon_v = \gamma_u \varepsilon_{t,loc} - 0.5\varepsilon_s + \varepsilon_2$ [UHPC Guide Eq. 1.7.3.4.1-3]

Stress in vertical steel: $f_v = E_s \varepsilon_v \le f_y$ [UHPC Guide Eq. 1.7.3.4.1-4]

in which: $\rho_v = \dfrac{A_v}{b_w s}$ [UHPC Guide Eq. 1.7.3.4.1-5]

For this design example, the beam is reinforced with two legs of No. 4 stirrups at a spacing of 6 in.:

Spacing of transverse reinforcement	$s = 6$ in.
Area of transverse reinforcement	$A_v = 2(0.20) = 0.40$ in.^{2}
Yield stress of transverse steel	$f_y = 60$ ksi
Modulus of elasticity of transverse steel	$E_s = 29,000$ ksi
Shear reinforcement ratio	$\rho_v = 0.40/(12(6)) = 0.0056 = 0.56$ percent

The solution to Eq. C1.7.3.4.1-3 shown in the preceding equations can be solved by setting $\varepsilon_{t,loc} = 0.0030$ and assuming a value of f_v. Eqs. C1.7.3.4.1-4, 1.7.3.4.1-3, and 1.7.3.4.1-4 are then evaluated using the assumed value of f_v and the calculated value of θ. This process is repeated until the assumed and calculated value of f_v converges.

Trial 1:

Assume $f_v = f_y = 60$ ksi.

By solving Eq. C1.7.3.4.1-3 with $f_v = 60$ ksi, the inclination angle θ is determined to be 31.98 degrees.

Using $\theta = 31.98$ degrees and $f_v = f_y = 60$ ksi:

$$\gamma_u \varepsilon_{t,loc} = \frac{0.000123}{2}(1+\cot(31.98)^2) + \frac{2(1.2)}{6{,}933}\cot(31.98)^4 + \frac{2(0.0056)(60)}{6{,}933}\cot(31.98)^2\,[1+\cot(31.98)^2]$$

$$= 0.00300$$

$$\varepsilon_2 = -\frac{2(1.00)}{6{,}933}\cot(31.98)^2 - \frac{2(0.0056)(60)}{6{,}933}(1+\cot(31.98)^2)$$

$$= -0.00108$$

$$\varepsilon_v = \gamma_u \varepsilon_{t,loc} - 0.5\varepsilon_s + \varepsilon_2 = 0.00186$$

Check f_v: $f_{v,Check} = \min(E_s\,\varepsilon_v, f_y) = 53.8$ ksi. Repeat with $f_v = 53.8$ ksi.

Trial 2:

Assume $f_v = 53.8$ ksi.

By solving Eq. C1.7.3.4.1-3 with $f_v = 53.8$ ksi, the inclination angle θ is determined to be 31.75 degrees.

Using $\theta = 31.75$ degrees and $f_v = 53.8$ ksi:

$$\gamma_u \varepsilon_{t,loc} = \frac{0.000123}{2}(1+\cot(31.75)^2) + \frac{2(1.00)}{6{,}933}\cot(31.75)^4 + \frac{2(0.0056)(53.8)}{6{,}933}\cot(31.75)^2\,[1+\cot(31.75)^2]$$

$$= 0.00300$$

$$\varepsilon_2 = -\frac{2(1.00)}{6{,}933}\cot(31.75)^2 - \frac{2(0.0056)(53.8)}{6{,}933}(1+\cot(31.75)^2)$$

$$= -0.00106$$

$$\varepsilon_v = \gamma_u \varepsilon_{t,loc} - 0.5\varepsilon_s + \varepsilon_2 = 0.00187$$

Check f_v: $f_{v,Check} = \min(E_s\,\varepsilon_v, f_y) = 54.3$ ksi. Repeat with $f_v = 53.8$ ksi.

Trial 3:

Assume $f_v = 54.3$ ksi.

By solving Eq. C1.7.3.4.1-3 with $f_v = 54.3$ ksi, the inclination angle θ is determined to be 31.76 degrees.

Using $\theta = 31.76°$ and $f_v = 54.3$ ksi:

$$\gamma_u \varepsilon_{t,loc} = \frac{0.000123}{2}(1+\cot(31.76)^2) + \frac{2(1.00)}{6{,}933}\cot(31.76)^4 + \frac{2(0.0056)(54.3)}{6{,}933}\cot(31.76)^2\,[1+\cot(31.76)^2]$$

$$= 0.00300$$

$$\varepsilon_2 \quad = -\frac{2(1.00)}{6,933}\cot(31.76)^2 - \frac{2(0.0056)(54.3)}{6,933}(1+\cot(31.76)^2)$$

$$= -0.00107$$

$$\varepsilon_v \quad = \gamma_u\varepsilon_{t,loc} - 0.5\varepsilon_s + \varepsilon_2 = 0.00187$$

Check f_v: $f_{v,Check} = \min(E_s\,\varepsilon_v, f_y) = 54.3$ ksi.
OK.

The angle of inclination of diagonal compressive stresses and the stress in the steel at nominal flexural resistance are:

$f_v = 54.3$ ksi and $\theta = 31.8$ degrees

B4.2.2. Simplified Approach

The simplified approach detailed in UHPC Guide Article 1.7.3.4.2 was developed to provide a conservative alternative procedure for determining shear resistance parameters, θ and f_v, without the need for iteratively solving Eqs. 1.7.3.4.1-1 through 1.7.3.4.1-4 [UHPC Guide Article C1.7.3.4.2]. The shear capacity determined from the simplified approach yields to a lower estimate of the shear capacity of the beam compared to the general approach.

To use the simplified approach, the following should apply:

- A UHPC modulus of elasticity: $E_c \geq 6,500$ ksi: $E_c = 6,933$ ksi > 6,500 ksi.　　　　　OK.
- A UHPC localization stress: $f_{t,loc} \leq 1.8$ ksi: $f_{t,loc} = 1.00$ ksi < 1.8 ksi.　　　　OK.
- A transverse steel yield stress: $f_y \leq 75.0$ ksi: $f_y = 60.0$ ksi < 75.0 ksi.　　　　OK.
- A transverse steel reinforcement ratio: $\rho_v \leq 3.0$ percent: $\rho_v = 0.56$ percent < 3.0 percent.　　　　OK.

[UHPC Guide Article 1.7.3.4.2]

Therefore, the tables of Addendum A2 of the UHPC Guide may be used to estimate θ and f_v.

Note that the beam is reinforced with vertical transverse bars, and thus, $\alpha = 90°$ and no modification factor for ρ_v need be applied [UHPC Guide Article 1.7.3.4.2]. For $\rho_v = 0.56$ percent ≤ 1.0 percent, Table A2.3-2 of Addendum A2 of the UHPC Guide can be used to determine θ and f_v.

For $\varepsilon_s = 0.000123 \leq 0.5 \times 10^{-3}$ and $\gamma_u\varepsilon_{t,loc} = 0.003 \geq 0.003$, and using UHPC Guide Table A2.3-2, $\theta = 37.1°$ and $f_v \leq 41.4$ ksi (maximum stress lower than yield). Therefore, the shear capacity can be calculated with $\theta = 37.1°$ and $f_v = 41$ ksi. Note that if the value of f_v in the table is greater than f_y, it must be taken equal to f_y [UHPC Guide Article 1.7.3.4.2].

B4.3. TOTAL SHEAR RESISTANCE

UHPC shear resistance based on the shear resistance parameters calculated from the general method:

$$V_{UHPC} = \gamma_u f_{t,loc}\, d_v\, b_v \cot\theta = 1.00(1.00)(19.62)(12)\cot(31.8) = 379.6 \text{ kips}$$

[UHPC Guide Eq. 1.7.3.3-3]

Transverse reinforcement shear contribution based on the shear resistance parameters calculated from the general method:

$$V_s = \frac{A_v f_y d_v \cot\theta}{s} = \frac{(0.40)(54.3)(19.62)\cot(31.8)}{6} = 114.5 \text{ kips} \qquad \text{[UHPC Guide Eq. 1.7.3.3-4]}$$

Total shear resistance: $V_n = V_{UHPC} + V_s = 494.1$ kips   [UHPC Guide Eq. 1.7.3.3-1]

Factored shear resistance: $\phi V_n = (0.9)494.1 = 444.7$ kips

Maximum shear resistance:

$$V_{n,max} = 0.25 f'_c\, d_v\, b_v = 0.25(22)(19.62)(12) = 1{,}294.9 \text{ kips} > V_n = 494.1 \text{ kip} \qquad\qquad \text{OK.}$$

[UHPC Guide Eq. 1.7.3.3-2]

Using the shear resistance parameters obtained from the simplified approach, the total factored shear resistance can be calculated as:

$$\phi V_n = 0.9\left[1.00(1.00)(19.62)(12)\cot(37.1) + \frac{(0.40)(41.4)(19.62)\cot(37.1)}{6}\right]$$

$$= 0.9\,[311.3 + 71.6]$$

$$= 344.6 \text{ kips}$$

B4.4. SHEAR DEMAND VS. CAPACITY CHECK

The shear demand at the critical shear location (i.e., distance $d_v = 1.64$ ft from internal face of support) is $V_u = 58.5$ kips. Given that $\phi V_n = 494.1$ kips (or 344.6 kips if using the simplified approach) is greater than $V_u = 58.5$ kips, the beam can sustain the applied shear load at this location.

The maximum shear spacing at the critical shear location, s_{max}, can be calculated using UHPC Guide Eq. 1.7.2.6-1 as follows:

Using $\theta = 31.8$ degrees obtained from the general approach
$$s_{max} = 0.25 d_v \cot\theta = 0.25(19.62)\cot(31.8) = 7.92 \text{ in.} \leq 24.0 \text{ in.}$$

Using $\theta = 37.1$ degrees obtained from the simplified approach

$$s_{max} = 0.25d_v \cot \theta = 0.25(19.62)\cot(37.1) = 6.48 \text{ in.} \leq 24.0 \text{ in.}$$

Given that the provided spacing of transverse reinforcement, $s = 6$ in., is less than $s_{max} = 7.92$ in. (or 6.48 in. if using the simplified approach), the reinforcement spacing is compliant with the provisions of UHPC Guide Article 1.7.2.6.

Note that the shear demand, capacity calculations, and maximum spacing of transverse reinforcement checks presented herein are shown at one location for illustration purposes. To complete the ultimate limit state check in shear, the factored shear capacity and the maximum spacing of transverse reinforcement must be determined at regular intervals along the length of the beam and compared to the factored shear demand and the provided spacing at the same location, respectively. The factored shear capacity must be greater than the factored demand at each section along the length of the beam. The spacing of transverse reinforcement must also be lower than the provided spacing at each section.

APPENDIX C. DESIGN EXAMPLE OF A PRETENSIONED UHPC I-BEAM BRIDGE WITH A CONVENTIONAL CONCRETE DECK

Appendix C is based on the content presented in Appendix A of this report.

LIST OF NOTATIONS

A	=	area of a portion of the cross section (in.^{2})
A_c	=	total area of the composite section (in.^{2})
A_{ct}	=	area of UHPC on the flexural tension side of the member (in.^{2})
A_{cv}	=	area of UHPC considered to be engaged in interface shear transfer (in.^{2})
A_d	=	area of conventional concrete deck (in.^{2})
A_g	=	gross area of cross section of the UHPC girder (in.^{2})
A_p	=	area of one prestressing strand (in.^{2})
A_{ps}	=	total area of prestressing strands (in.^{2})
$A_{ps,crs}$	=	total area of prestressing strands on the flexural tension side at critical shear location (in.^{2})
A_{psE}	=	total area of prestressing strands at girder ends (in.^{2})
A_s	=	area of nonprestressed reinforcement (in.^{2})
$A_{s,crs}$	=	area of nonprestressed steel on the flexural tension side of the member at critical shear location (in.^{2})
$A_{s,r}$	=	total area of pretensioned anchorage zone reinforcement located within the distance $h/4$ from the end of the beam (in.^{2})
A_{tc}	=	area of composite transformed section at midspan at final time (in.^{2})
A_{tf}	=	area of noncomposite transformed section at midspan at final time (in.^{2})
A_{ti}	=	area of transformed section at midspan at time of prestressing (in.^{2})
A_{tiE}	=	area of transformed section at girder ends at time of prestressing (in.^{2})
A_v	=	area of transverse reinforcement to resist shear within a distance s (in.^{2})
A_{vf}	=	area of interface reinforcement crossing the shear plane within the area A_{cv} (in.^{2})
$A_{vf,min}$	=	minimum required area of interface reinforcement crossing the shear plane within the area A_{cv} (in.^{2})
a	=	distance from the girder end to the harp point of strands (in.)
b_e	=	effective flange width in composite girder system (in.)
b_h	=	width of haunch (in.)
b_v	=	effective web width taken as the minimum web width within the depth d_v (in.)
b_{vi}	=	interface width considered to be engaged in shear transfer (in.)
b_w	=	web width (in.)
c	=	depth of the compression zone measured from the extreme compression fiber of the composite section at the completion of strain compatibility analysis (in.)

169

c_i	=	cohesion factor for interface shear resistance calculation (ksi)
DC	=	dead load of structural components and nonstructural attachments
DFD	=	distribution factor for deflection
DFM	=	distribution factor for bending moment for interior girder
DFV	=	distribution factor for shear force for interior girder
DL_{ws}	=	dead load of future wearing surface (kip/in.^{2})
D_p	=	diameter of prestressing strand (in.)
DW	=	dead load of wearing surfaces and utilities
d_{crack}	=	horizontal distance from the girder end to the location where the critical shear crack plane crosses the centroid of the bottom strands (in.)
d_e	=	effective depth taken as the distance, measured perpendicular to the neutral axis, between the extreme compression fiber of the UHPC section to the resultant of the forces in the tensile reinforcement (in.)
d_{end}	=	distance between the centroid of the strands in a row and the bottom of the section at girder ends (in.)
d_{mid}	=	distance between the centroid of the strands in a row and the bottom of the section at midspan (in.)
d_v	=	effective shear depth taken as the distance, measured perpendicular to the neutral axis, between the resultants of the tensile and compressive forces due to flexure (in.)
d_{vi}	=	distance between the centroid of the tension steel and the midthickness of the deck (in.)
$d_{v,limit}$	=	maximum value of d_v in composite sections made of a UHPC girder and a conventional concrete deck (in.)
E_c	=	modulus of elasticity of UHPC for use in design (ksi)
E_{cD}	=	modulus of elasticity of conventional concrete deck for use in design (ksi)
E_{ci}	=	modulus of elasticity of UHPC at the time of prestressing for use in design (ksi)
E_p	=	modulus of elasticity of prestressing steel for use in design (ksi)
E_s	=	modulus of elasticity of the mild steel reinforcement (ksi)
e'	=	difference between eccentricity of the prestressing strand at midspan and at end of the girder
e_d	=	eccentricity to centroid of the conventional concrete deck with respect to the gross composite section (in.)
e_g	=	distance between the centers of gravity of the UHPC girder and the conventional concrete deck (in.)
e_{pc}	=	eccentricity of strands with respect to the centroid of composite section (in.)

e_{pg}	$=$	eccentricity of strands in noncomposite section at midspan (in.)
e_{pgE}	$=$	eccentricity of strands in noncomposite section at ends (in.)
e_{tc}	$=$	eccentricity of strands in composite transformed section at midspan at final time (in.)
e_{tf}	$=$	eccentricity of strands in noncomposite transformed section at midspan at final time (in.)
e_{ti}	$=$	eccentricity of strands in noncomposite transformed section at midspan at time of prestressing (in.)
e_{tiE}	$=$	eccentricity of strands in noncomposite transformed section at girder ends at time of prestressing (in.)
f_{bi}	$=$	stress in the extreme bottom fiber of UHPC girder at prestress transfer at midspan (ksi)
f_{biE}	$=$	stress in the extreme bottom fiber of UHPC girder at prestress transfer at transfer length section (ksi)
f'_c	$=$	compressive strength of UHPC for use in design (ksi)
f'_{cD}	$=$	compressive strength of conventional concrete for use in design (ksi)
f'_{cDi}	$=$	compressive strength of conventional concrete deck at initial loading (ksi)
f'_{cd}	$=$	UHPC girder compressive strength at time of deck placement (ksi)
f_{cgp}	$=$	sum of stresses at the center of gravity of prestressing strands due to prestressing force at transfer and the self-weight of the member at maximum moment sections (ksi)
f_{ci}	$=$	stress in conventional concrete layer as obtained by stress-strain constitutive model (ksi)
f'_{ci}	$=$	compressive strength of UHPC at time of prestressing for use in design (ksi)
f_{cpe}	$=$	compressive stress in UHPC due to effective prestress forces only at extreme fiber section, where tensile stress is caused by externally applied loads
$f_{in,1}$	$=$	initial stress in conventional concrete at top of the deck at the start of strain compatibility analysis (ksi)
$f_{in,2}$	$=$	initial stress in conventional concrete at bottom of the haunch at the start of strain compatibility analysis (ksi)
$f_{in,3}$	$=$	initial stress in UHPC at top of the girder at the start of strain compatibility analysis (ksi)
$f_{in,4}$	$=$	initial stress in UHPC at bottom of the girder at the start of strain compatibility analysis (ksi)
f_{min}	$=$	minimum principal stress in the web with the tension taken as a negative value (ksi)
f_{pcx}	$=$	horizontal stress in the web (ksi)
f_{pcy}	$=$	vertical stress in the web (ksi)

f_{pe}	=	stress in prestressing steel after all losses and permanent gains (ksi)
f_{pee}	=	effective prestress in strands after allowance of all losses (ksi)
$f_{pe,ng}$	=	stress in prestressing steel after all losses (no gains) (ksi)
f_{peS}	=	stress in prestressing steel at service after all losses and gains (ksi)
f_{pi}	=	stress limit in prestressing steel at time of prestressing (ksi)
f_{po}	=	a parameter taken as modulus of elasticity of prestressing steel multiplied by the locked-in difference in strain between the prestressing steel and the surrounding UHPC (ksi)
f_{ps}	=	average stress in prestressing steel at the time for which the nominal resistance of the member is required (ksi)
$f_{psT,j}$	=	total stress in prestressing steel layer j at the completion of strain compatibility analysis (ksi)
f_{pt}	=	stress in prestressing strands immediately after transfer (ksi)
f_{pu}	=	specified tensile strength of prestressing steel (ksi)
f_{py}	=	specified yield strength of prestressing steel (ksi)
$f_{s\ell}$	=	stress limit in prestressing steel at service loads after losses (ksi)
$f_{s,r}$	=	stress in the interface steel reinforcement not to exceed 20.0 ksi (ksi)
$f_{T,i}$	=	total stress in UHPC or conventional concrete layer i at the completion of strain compatibility analysis (ksi)
f_{ti}	=	stress in the extreme top fiber of the UHPC girder at prestress transfer at midspan (ksi)
$f_{t,cr}$	=	effective cracking strength of UHPC for use in design (ksi)
$f_{t,cri}$	=	effective cracking strength of UHPC at time of prestressing for use in design (ksi)
f_{tiE}	=	stress in the extreme top fiber of the UHPC girder at prestress transfer at transfer length section (ksi)
$f_{t,loc}$	=	crack localization strength of UHPC for use in design (ksi)
f_v	=	stress in the transverse steel reinforcement at nominal shear resistance (ksi)
$f_{v,Check}$	=	value of f_v at the end of an iteration step during analysis of nominal shear resistance (ksi)
$f_{v,max}$	=	maximum value of f_v determined according to UHPC Guide Article 1.7.3.4.2 (ksi)
f_y	=	specified minimum yield strength of reinforcement (ksi)
H	=	average annual ambient relative humidity (percent)
h	=	overall depth of the UHPC beam (in.)
h_c	=	overall depth of the composite section (in.)
I	=	moment of inertia of a portion of the cross section (in.^{4})

I_c = moment of inertia of the composite section (in.^{4})

I_g = moment of inertia about the centroid of the noncomposite UHPC girder (in.^{4})

IM = dynamic allowance applied to the design truck load

I_{tc} = composite transformed section moment of inertia at midspan at final time (in.^{4})

I_{te} = transformed flange moment of inertia (in.^{4})

I_{tf} = noncomposite transformed section moment of inertia at midspan at final time (in.^{4})

I_{th} = transformed haunch moment of inertia (in.^{4})

I_{ti} = noncomposite transformed section moment of inertia at midspan at time of prestressing (in.^{4})

I_{tiE} = noncomposite transformed section moment of inertia at girder ends at time of prestressing (in.^{4})

K = limiting interface shear resistance (ksi)

K_{df} = transformed section coefficient that accounts for time-dependent interaction between UHPC and bonded steel in the section considered for the time period between deck placement and final time

K_g = longitudinal stiffness parameter (in.^{4})

K_{id} = transformed section coefficient that accounts for time-dependent interaction between UHPC and bonded steel in the section considered for the time period between prestress transfer and deck placement

K_L = factor accounting for the type of steel taken as 30 for low-relaxation strands and 7 for other prestressing steel, unless more accurate manufacturer's data are available

K_1 = correction factor for modulus of elasticity of UHPC

K_{1D} = correction factor for modulus of elasticity of conventional concrete

K_3 = correction factor for creep of UHPC

K_4 = correction factor for shrinkage of UHPC

k = factor for conventional concrete stress-strain constitutive model

k_f = factor for the effect of UHPC strength

$k_{f,D}$ = factor for the effect of conventional concrete strength

k_{hc} = humidity factor for creep of UHPC

$k_{hc,D}$ = humidity factor for creep of conventional concrete deck

k_{hs} = humidity factor for shrinkage of UHPC

$k_{hs,D}$ = humidity factor for shrinkage of conventional concrete deck

$k_{\ell d}$ = factor for the effect of loading age at time of deck placement

$k_{\ell i}$ = factor for the effect of loading age at time of prestress transfer

k_s = factor for the effect of the volume-to-surface ratio of the UHPC girder

$k_{s,D}$ = factor for the effect of the volume-to-surface ratio of the conventional concrete deck

k_{tdd} = time development factor between prestress transfer and deck placement

k_{tdf} = time development factor between prestress transfer and final time

$k_{td,D}$ = time development factor for conventional concrete deck between deck placement and final time

L = design span of UHPC girder (ft)

LL = vehicular live load

L_T = overall length of UHPC girder (ft)

L_{vi} = interface length considered to be engaged in shear transfer (in.)

ℓ_d = development length of the prestressing strand (in.)

ℓ_t = transfer length of the prestressing strand (in.)

M_b = bending moment due to barrier weight (kip-ft)

$M_{b,crs}$ = bending moment at critical shear location due to barrier weight (kip-ft)

$M_{b,m}$ = bending moment at midspan due to barrier weight (kip-ft)

M_{cr} = nominal cracking moment (kip-in.)

M_D = bending moment due to deck and haunch weight (kip-ft)

$M_{D,crs}$ = bending moment at critical shear location due to deck and haunch weight (kip-ft)

$M_{D,m}$ = bending moment at midspan due to deck and haunch weight (kip-ft)

M_{dnc} = total unfactored dead load moment acting on the monolithic or noncomposite section (kip-in.)

M_{FI} = moment due to Fatigue I load combination (kip-ft)

M_f = bending moment due to fatigue truck (kip-ft)

$M_{f,m}$ = bending moment at midspan due to fatigue truck (kip-ft)

M_g = bending moment due to UHPC girder self-weight based on girder span length, L (kip-ft)

$M_{g,crs}$ = bending moment at critical shear location due to UHPC girder self-weight based on girder span length, L (kip-ft)

$M_{g,m}$ = bending moment at midspan due to UHPC girder self-weight based on girder span length, L (kip-ft)

$M_{gT,m}$ = bending moment at midspan due to UHPC girder self-weight based on overall length of girder, L_T (kip-ft)

$M_{gT,tr}$ = bending moment at transfer length section due to UHPC girder self-weight based on overall length of girder, L_T (kip-ft)

M_L	=	bending moment when the strain in the extreme tension layer of UHPC is equal to the UHPC tensile strain limit, $\gamma_u \varepsilon_{t,loc}$ (kip-ft)
M_{LL}	=	bending moment due to lane load (kip-ft)
$M_{LL,crs}$	=	bending moment at critical shear location due to lane load (kip-ft)
$M_{LL,m}$	=	bending moment at midspan due to lane load (kip-ft)
M_{LT}	=	bending moment due to truck load (kip-ft)
$M_{LT,crs}$	=	bending moment at critical shear location due to truck load (kip-ft)
$M_{LT,m}$	=	bending moment at midspan due to truck load (kip-ft)
M_n	=	nominal flexural resistance (kip-in.)
M_r	=	factored flexural resistance (kip-in.)
M_{SIDL}	=	bending moment at midspan due to superimposed dead load (kip-ft)
M_{SL}	=	bending moment at midspan due to service load (kip-ft)
$M_{s\ell}$	=	nominal flexural moment when the steel stress in the extreme tension layer is equal to the steel service stress limit, $f_{s\ell}$ (kip-in.)
M_u	=	factored bending moment at a location along the span of the beam (kip-in.)
$M_{u,crs}$	=	factored moment at the critical shear location due to dead load and live load (kip-in.)
$M_{u,m}$	=	factored moment at midspan due to dead load and live load (kip-in.)
M_{ws}	=	bending moment due to wearing surface weight (kip-ft)
$M_{ws,crs}$	=	bending moment at critical shear location due to wearing surface weight (kip-ft)
$M_{ws,m}$	=	bending moment at midspan due to wearing surface weight (kip-ft)
M_x	=	bending moment of a simply supported beam at distance x along the span (kip-in.)
N_b	=	number of girders in the bridge
N_{end}	=	quantity of strands per row at girder ends
N_{mid}	=	quantity of strands per row at girder ends
$N_{u,crs}$	=	factored axial force at the critical shear location (kip)
n	=	modular ratio between UHPC and prestressing strands
n_{bD}	=	modular ratio between UHPC and conventional concrete
n_c	=	factor for conventional concrete stress-strain constitutive model
n_{Db}	=	modular ratio between conventional concrete and UHPC
n_{tf}	=	modular ratio modular ratio between UHPC and conventional concrete at final time
n_{ti}	=	modular ratio modular ratio between UHPC and conventional concrete at time of prestressing
P_c	=	permanent net compressive force, normal to the shear plane (kip)

P_{pe}	=	force in prestressing steel after all losses and permanent gains (ksi)
P_{pee}	=	force in prestressing steel due to effective prestress only (kips)
P_{pi}	=	total prestressing force before transfer at midspan (kip)
P_{piE}	=	total prestressing force before transfer at girder ends (kip)
P_{pt}	=	total prestressing force after transfer at midspan (kips)
P_r	=	factored splitting resistance of pretensioned anchorage zones (kip)
$P_{r,UHPC}$	=	splitting resistance of pretensioned anchorage zones provided by the UHPC (kip)
Q	=	total factored load for a particular load combination
Q_g	=	first moment of area about the centroid of the gross concrete area above or below the height of the web where the principal tension is being calculated (in.^{3})
Q_{gc}	=	first moment of area about the centroid of the composite nontransformed section above or below the height of the web where the principal tension is being calculated (in.^{3})
Q_i	=	force effects from specified loads for case i
S	=	spacing of girders in a bridge (ft)
S_b	=	section modulus for the extreme bottom fiber of the noncomposite UHPC section (in.^{3})
S_{bc}	=	section modulus for the extreme bottom fiber of the composite section (in.^{3})
S_{btc}	=	section modulus for the extreme bottom fiber of the composite transformed at midspan at final time (in.^{3})
S_{btf}	=	section modulus for the extreme bottom fiber of the noncomposite transformed section at midspan at final time (in.^{3})
S_{bti}	=	section modulus for the extreme bottom fiber of the noncomposite transformed section at midspan at time of prestressing (in.^{3})
S_{btiE}	=	section modulus for the extreme bottom fiber of the noncomposite transformed section at girder ends at time of prestressing (in.^{3})
S_{dtc}	=	section modulus for extreme top fiber of the composite transformed section at midspan at final time (in.^{3})
S_t	=	section modulus for the extreme top fiber of the noncomposite UHPC section (in.^{3})
S_{tc}	=	section modulus for the extreme top fiber of composite section (in.^{3})
S_{tg}	=	section modulus for the extreme top fiber of the noncomposite UHPC girder (in.^{3})
S_{ttc}	=	section modulus for extreme top fiber of the UHPC section in the composite transformed section at midspan at final time (in.^{3})
S_{ttf}	=	section modulus for extreme top fiber of the noncomposite section at midspan at final time (in.^{3})

S_{tti}	=	section modulus for extreme top fiber of the noncomposite section at midspan at time of prestressing (in.^{3})
S_{ttiE}	=	section modulus for extreme top fiber of the noncomposite section at girder ends at time of prestressing (in.^{3})
s	=	spacing of transverse reinforcement measured in a direction parallel to the longitudinal reinforcement (in.)
s_{max}	=	maximum spacing of transverse reinforcement (in.)
T_s	=	total number of prestressing strands at midspan
T_{sE}	=	total number of prestressing strands at girder ends
t	=	maturity of conventional concrete or UHPC, taken as the time being considered for creep or shrinkage effects (days)
t_D	=	thickness of deck at time of placement (days)
t_d	=	UHPC age at time of deck placement (days)
t_f	=	UHPC age at final time (days)
t_h	=	structural thickness of haunch (in.)
t_i	=	age of UHPC at time of prestress transfer (days)
t_{iD}	=	age of conventional concrete deck at time of loading (days)
t_s	=	structural thickness of cast-in-place conventional concrete deck (in.)
V	=	shear force from Service III load combination (kips)
V_b	=	shear force due to barrier weight (kip)
$V_{b,crs}$	=	shear force at critical shear location due to barrier weight (kip)
V_D	=	shear force due to deck and haunch weight (kip)
$V_{D,crs}$	=	shear force at critical shear location due to deck and haunch weight (kip)
V_g	=	shear force due to girder weight based on girder span length, L (kip)
V_{g1}	=	shear force applied to the UHPC gross section at the critical shear location at service (kip)
V_{g2}	=	shear force applied to the composite nontransformed gross section at the critical shear location at service (kip)
$V_{g,crs}$	=	shear force at critical shear location due to girder weight based on girder span length, L (kip)
V_{hi}	=	horizontal factored shear force per unit length of girder (kip/in.)
V_{LL}	=	shear force due to lane load (kip)
$V_{LL,crs}$	=	shear force at critical shear location due to lane load (kip)
V_{LT}	=	shear force due to truck load (kip)
$V_{LT,crs}$	=	shear force at critical shear location due to truck load (kip)

V_n	=	nominal shear resistance (kip)
V_{ni}	=	nominal interface shear resistance (kip)
V_p	=	component of prestressing force in the direction of the shear force (kip)
V/S	=	volume to surface ratio of the conventional concrete deck (in.)
V_s	=	shear resistance provided by transverse reinforcement (kip)
V_{UHPC}	=	nominal shear resistance of the UHPC (kip)
V_u	=	factored shear force (kip)
$V_{u,crs}$	=	factored shear force at the critical shear section (kip)
V_{ui}	=	horizontal factored shear force per unit length of the girder (kip)
$V_{u,max}$	=	maximum nominal shear resistance (kip)
V_{ws}	=	shear due to wearing surface weight (kip)
$V_{ws,crs}$	=	shear due to wearing surface weight (kip)
V_x	=	shear force of a simply supported beam at distance x along the span (kip)
W_R	=	clear roadway width between curbs of a bridge (ft)
w	=	uniform distributed load (kip/ft)
w_b	=	linear weight of the barrier (kip/ft)
w_D	=	linear weight of the conventional concrete deck (kip/ft)
$w_{d\ell}$	=	design lane load for live load deflection calculations per girder (kip/ft)
w_g	=	linear weight of the noncomposite UHPC girder (kip/ft)
w_h	=	linear weight of the conventional concrete haunch (kip/ft)
w_p	=	nominal weight of 0.7-in.-diameter prestressing strand per unit length (kip/ft)
w_s	=	total linear weight of conventional concrete deck and haunch (kip/ft)
w_{ws}	=	linear weight of future wearing surface (kip/ft)
x	=	distance along span of a simply supported beam where sectional analysis is completed (ft)
y_b	=	distance from the centroid to the extreme bottom fiber of the UHPC girder (in.)
$y_b{}^*$	=	distance from the centroid of a portion of the cross section to the extreme bottom fiber of the composite section (in.)
y_{bc}	=	distance from the centroid of the composite section to the extreme bottom fiber of the UHPC girder (in.)
y_{bcb}	=	distance between the extreme tension fiber and the centroid of the strands on the flexural tension side at beam ends and within the debonded length (in.)

y_{bs}	=	distance between the centroid of the strands and the extreme bottom fiber of the UHPC girder at midspan (in.)
y_{bsE}	=	distance between the centroid of the strands and the extreme bottom fiber of the UHPC girder at ends (in.)
y_{btc}	=	distance from centroid of composite transformed section to extreme bottom fiber of composite section at midspan at final time (in.)
y_{btf}	=	distance from centroid of noncomposite transformed section to extreme bottom fiber of UHPC section at midspan at final time (in.)
y_{bti}	=	distance from centroid of noncomposite transformed section to extreme bottom fiber of UHPC section at midspan at time of prestressing (in.)
y_{btiE}	=	distance from centroid of noncomposite transformed section to extreme bottom fiber of UHPC section at girder ends at time of prestressing (in.)
y_t	=	distance from the centroid to the extreme top fiber of the UHPC girder (in.)
y_{tc}	=	distance from the centroid of the composite section to the extreme top fiber of the structural deck (in.)
y_{tg}	=	distance from the centroid of the composite section to the extreme top fiber of the UHPC section (in.)
y_{ttc}	=	distance from centroid of composite transformed section to extreme top fiber of composite section at midspan at final time (in.)
y_{ttf}	=	distance from centroid of noncomposite transformed section to extreme top fiber of UHPC section at midpan at final time (in.)
y_{tti}	=	distance from centroid of noncomposite transformed section to extreme top fiber of UHPC section at midpan at time of prestressing (in.)
y_{ttiE}	=	distance from centroid of noncomposite transformed section to extreme top fiber of UHPC section at girder ends at time of prestressing (in.)
α	=	angle of inclination of transverse reinforcement to the longitudinal axis (degrees)
γ	=	load factor specified in AASHTO LRFD BDS Table 3.4.1-1 for Fatigue I load combination
γ_i	=	load factor for case i
γ_{LL}	=	load factor for live load for Service III load combination
γ_u	=	factor to allow for the reduction of UHPC tensile parameter values
γ_1	=	flexural cracking variability factor
γ_2	=	prestress variability factor
γ_3	=	steel yield to ultimate strength factor
Δ_{b+ws}	=	deflection due to barrier and future wearing surface weights (in.)
Δc	=	depth of the compression zone measured from the extreme compression fiber of the composite section during strain compatibility analysis (in.)

Δ_D	=	deflection due to deck and haunch weights (in.)
$(\Delta F)_{TH}$	=	constant-amplitude fatigue threshold, as specified in AASHTO LRFD BDS Article 5.5.3.3 for prestressing steel (ksi)
Δf	=	force effect, live load stress range at the bottom layer of strands due to the passage of the fatigue load as specified AASHTO LRFD BDS Article 3.6.1.4 (ksi)
Δf_{bD}	=	change in stress at bottom of UHPC girder due to conventional concrete deck weight (ksi)
Δf_{bLDF}	=	change in stress at bottom of UHPC girder between deck placement and final time (ksi)
Δf_{bLTD}	=	change in stress at bottom of UHPC girder between transfer and deck placement (ksi)
Δf_{bSIDL}	=	change in stress at bottom of UHPC girder due to superimposed dead load (ksi)
Δf_{bSL}	=	change in stress at bottom of UHPC girder due to service load (ksi)
Δf_{bSS}	=	change in stress at bottom of the UHPC girder due to shrinkage of conventional concrete deck at final time (ksi)
Δf_{cD}	=	change in stress in UHPC at the level of the centroid of prestressing steel due to conventional concrete weight (ksi)
Δf_{cd}	=	change in UHPC stress at the centroid of the prestressing strands due to long-term losses between transfer and deck placement, combined with deck weight and superimposed loads (ksi)
Δf_{cdf}	=	change in UHPC stress at the centroid of the prestressing strands due to shrinkage of the conventional concrete deck (ksi)
Δf_{cSIDL}	=	change in UHPC stress at level of the centroid of prestressing steel due to superimposed dead load (ksi)
Δf_{cSL}	=	change in stress in UHPC at the level of the centroid of prestressing steel due to the service load (ksi)
Δf_{dbLDF}	=	change in stress at bottom of the conventional concrete deck between deck placement and final time (ksi)
Δf_{dbSIDL}	=	change in stress at bottom of the concrete deck due to superimposed dead load (ksi)
Δf_{dbSL}	=	change in stress at bottom of conventional concrete deck due to the service load (ksi)
Δf_{dtLDF}	=	change in stress at top of the concrete deck between deck placement and final time (ksi)
Δf_{dtSL}	=	change in stress at top of conventional concrete deck due to the service load (ksi)
Δf_{dtSIDL}	=	change in stress at top of the concrete deck due to superimposed dead load (ksi)
Δf_{dtSS}	=	change in stress at top of conventional concrete deck due to shrinkage at final time (ksi)

Δf_{pCD} = prestress loss due to creep of girder UHPC between the time of deck placement and final time (ksi)

Δf_{pCR} = prestress loss due to creep of UHPC girder between the time of prestress transfer and deck placement (ksi)

Δf_{pD} = prestress gain in prestressing steel due to conventional concrete deck weight (ksi)

Δf_{pES} = sum of all prestress losses or gains due to elastic shortening or extension at the time of prestressing (ksi)

Δf_{pi} = total prestress loss after transfer (ksi)

Δf_{pLDF} = change in steel stress due to long-term effects between deck placement and final time, exclusive of deck shrinkage (ksi)

Δf_{pLT} = long-term prestress losses due to shrinkage and creep of UHPC and conventional concrete, and relaxation of steel after transfer (ksi)

Δf_{pLTD} = change in steel stress due to long-term effects between transfer and deck placement (ksi)

Δf_{pR1} = prestress loss due to relaxation of prestressing strands between prestress transfer and deck placement (ksi)

Δf_{pR2} = prestress loss due to relaxation of prestressing strands between deck placement and final time (ksi)

Δf_{pSD} = prestress loss due to shrinkage of UHPC between time of deck placement and final time (ksi)

Δf_{pSIDL} = prestress gain in steel due to superimposed dead load (ksi)

Δf_{pSL} = prestress gain in steel due to the service load (ksi)

Δf_{pSR} = prestress loss due to shrinkage of UHPC girder between the time of prestress transfer and deck placement

Δf_{pSS} = prestress gain due to shrinkage of the conventional concrete deck between initial loading and final time (ksi)

Δf_{pT} = total prestress loss in prestressing steel (ksi)

Δf_{tD} = change in stress at top of UHPC girder due to conventional concrete deck weight (ksi)

Δf_{tLDF} = change in stress at top of UHPC girder between deck placement and final time (ksi)

Δf_{tLTD} = change in stress at top of UHPC girder between transfer and deck placement (ksi)

Δf_{tSIDL} = change in stress at top of UHPC girder due to superimposed dead load (ksi)

Δf_{tSL} = change in stress at top of UHPC girder due to service load (ksi)

Δf_{tSS} = change in stress at top of the UHPC girder due to shrinkage of conventional concrete deck at final time (ksi)

Δ_g = deflection due to the beam self-weight (in.)

Δ_{LL}	=	deflection due to live load and impact (in.)
Δ_{LT}	=	deflection due to truck load (in.)
ΔP_{ds}	=	restraining force due to shrinkage of conventional concrete deck (kips)
ΔP_{pLDF}	=	change in steel force between deck placement and final time (ksi)
ΔP_{pLTD}	=	change in steel force between transfer and deck placement (kip)
Δ_p	=	camber due to prestressing force at transfer (in.)
$\Delta\varepsilon_{cs}$	=	change in strain in UHPC at centroid of prestressing steel during strain compatibility analysis (in./in.)
$\Delta\varepsilon_{cs,j}$	=	change in strain in prestressing steel layer j during strain compatibility analysis (in./in.)
$\Delta\varepsilon_i$	=	change in strain in UHPC or conventional concrete layer i during strain compatibility analysis (in./in.)
$\Delta\varepsilon_1$	=	change in strain in conventional concrete at top of the deck during strain compatibility analysis (in./in.)
$\Delta\varepsilon_2$	=	change in strain in conventional concrete at bottom of the haunch during strain compatibility analysis (in./in.)
$\Delta\varepsilon_3$	=	change in strain in UHPC at top of the girder during strain compatibility analysis (in./in.)
$\Delta\varepsilon_4$	=	change in strain in UHPC at bottom of the girder during strain compatibility analysis (in./in.)
ε_{bdf}	=	UHPC shrinkage strain for the period between deck placement and final time (in./in.)
ε_{bid}	=	UHPC shrinkage strain for the period between prestress transfer and deck placement (in./in.)
ε_{bif}	=	UHPC shrinkage strain for the period between prestress transfer and final time (in./in.)
ε'_c	=	strain at peak strength for use conventional concrete stress-strain constitutive model (in./in.)
$\varepsilon_{csin,j}$	=	initial strain in UHPC at prestressing steel layer j at the start of strain compatibility analysis (in./in.)
$\varepsilon_{csT,b}$	=	total strain in UHPC at extreme bottom prestressing steel layer at the completion of strain compatibility analysis (in./in.)
$\varepsilon_{csT,i}$	=	total strain in UHPC at prestressing steel layer j at the completion of strain compatibility analysis (in./in.)
ε_{cu}	=	ultimate compressive strain of UHPC for use in design (in./in.)
ε_{ddf}	=	shrinkage strain of conventional concrete deck for the time period between deck placement and final time (in./in.)

$\varepsilon_{in,i}$	=	initial strain in UHPC or conventional concrete layer i at the start of strain compatibility analysis (in./in.)
$\varepsilon_{in,1}$	=	initial strain in conventional concrete at top of the deck at the start of strain compatibility analysis (in./in.)
$\varepsilon_{in,2}$	=	initial strain in conventional concrete at bottom of the haunch at the start of strain compatibility analysis (in./in.)
$\varepsilon_{in,3}$	=	initial strain in UHPC at top of girder at the start of strain compatibility analysis (in./in.)
$\varepsilon_{in,4}$	=	initial strain in UHPC at bottom of girder at the start of strain compatibility analysis (in./in.)
$\varepsilon_{pin,j}$	=	initial strain in prestressing steel layer j at the start of strain compatibility analysis (in./in.)
$\varepsilon_{psT,j}$	=	total strain in prestressing steel layer j at the completion of strain compatibility analysis (in./in.)
ε_s	=	net longitudinal tensile strain in the section at the centroid of the tension reinforcement (in./in.)
ε_{sh}	=	UHPC shrinkage strain at a given time (in./in.)
$\varepsilon_{sh,D}$	=	conventional concrete deck shrinkage strain at final time (in./in.)
$\varepsilon_{s\ell}$	=	tensile strain in the extreme tension steel when the steel service stress limit, $f_{s\ell}$, is reached (in./in.)
$\varepsilon_{T,i}$	=	total strain in UHPC or conventional concrete layer i at the completion of strain compatibility analysis (in./in.)
$\varepsilon_{T,1}$	=	total strain in conventional concrete at top of the deck at the completion of strain compatibility analysis (in./in.)
$\varepsilon_{T,2}$	=	total strain in conventional concrete at bottom of haunch at the completion of strain compatibility analysis (in./in.)
$\varepsilon_{T,3}$	=	total strain in UHPC at top of girder at the completion of strain compatibility analysis (in./in.)
$\varepsilon_{T,4}$	=	total strain in UHPC at bottom of girder at the completion of strain compatibility analysis (in./in.)
$\varepsilon_{t,cr}$	=	elastic tensile strain limit of UHPC corresponding to a tensile stress of $\gamma_u f_{t,cr}$ (in./in.)
$\varepsilon_{t,loc}$	=	crack localization strain of UHPC for use in design (in./in.)
ε_v	=	strain in the transverse steel reinforcement at nominal shear resistance (in./in.)
η_i	=	load modification factor for case i relating to ductility, redundancy, and operational importance
θ	=	angle of inclination of diagonal compressive stresses (degrees)
μ	=	curvature ductility ratio

μ_i	=	friction factor for interface shear resistance calculation
μ_ℓ	=	curvature ductility ratio limit
ξ	=	multiplier for transfer length of prestressing strand
ρ_v	=	ratio of area of transverse shear reinforcement to area of gross UHPC area of a horizontal section
τ	=	shear stress in web (ksi)
ϕ_c	=	resistance factor for axial resistance
ϕ_f	=	resistance factor for flexure
ϕ_v	=	resistance factor for shear
$\Psi(t_d,t_i)$	=	creep coefficient of UHPC at time of deck placement, t_d, due to loading at prestress transfer, t_i
$\Psi(t_f,t_d)$	=	creep coefficient of UHPC at final time, t_f, due to loading at deck placement, t_d
$\Psi(t_f,t_i)$	=	creep coefficient of UHPC at final time, t_f, due to loading at prestress transfer, t_i
$\Psi_D(t_f,t_d)$	=	creep coefficient of conventional concrete deck at the final time, t_f, due to loading shortly after deck placement, t_d
ψ	=	sectional curvature at nominal flexural moment (1/in.)
ψ_L	=	sectional curvature when the strain at extreme tension layer of UHPC is equal to the UHPC tensile strain limit, $\gamma_u\varepsilon_{t,loc}$ (1/in.)
ψ_n	=	sectional curvature at nominal flexural strength (1/in.)
$\psi_{s\ell}$	=	sectional curvature when the steel stress in the extreme tension steel is equal to the steel service stress limit, $f_{s\ell}$ (1/in.)
ω_c	=	unit weight of UHPC in girder (kip/ft^3)
ω_{cD}	=	unit weight of conventional concrete in deck (kip/ft^3)

CHAPTER C1. INTRODUCTION

The example in this Appendix illustrates the design of a pretensioned girder for a 150-ft-long, single-span bridge with no skew (overall beam length is 151 ft). The bulb tee girder of this example is a modified Minnesota Department of Transportation (MnDOT) "MN54" beam made of ultra-high performance concrete (UHPC) in which the web and flange widths are decreased by sliding the forms inward and utilizing a 27-in. soffit width and 5-in.-wide blocks in the top flange, as shown in Figure C1-1. This design example explains in detail the design of a typical interior beam at the critical sections in positive flexure, shear, and deflection due to prestress, dead loads, and live load. The bridge dimensions are adapted from the design example for a MnDOT "MN63" beam from the MnDOT (2018) *LRFD Bridge Design Manual*.

The superstructure of the bridge consists of six beams spaced at 9-ft centers. A typical transverse superstructure section is provided in Figure C1-2. The roadway section is composed of two 12-ft traffic lanes and two 12-ft shoulders. Beams are designed to act compositely with the 9-in.-thick cast-in-place conventional concrete deck to resist all superimposed dead loads, live loads, and impact. A ½-in.-thick wearing surface is assumed. A deck thickness of 8.5 in. is used for composite section properties. The haunch is assumed to have an average thickness of 2½ in. for dead load computations and 1½ in. for section property computations. The design live load is HL-93. Elastic stresses from external loads are calculated using transformed sections.

The design is accomplished in accordance with the *AASHTO LRFD Bridge Design Specification*, 9th edition, hereafter referred to as "AASHTO LRFD BDS," and Appendix A of this document, entitled, "Guide Specifications for Structural Design with Ultra-High Performance Concrete," which has been proposed to AASHTO T-10 for their consideration by the Federal Highway Administration's Turner-Fairbank Highway Research Center, hereafter referred to as the "UHPC Guide" (AASHTO 2020).
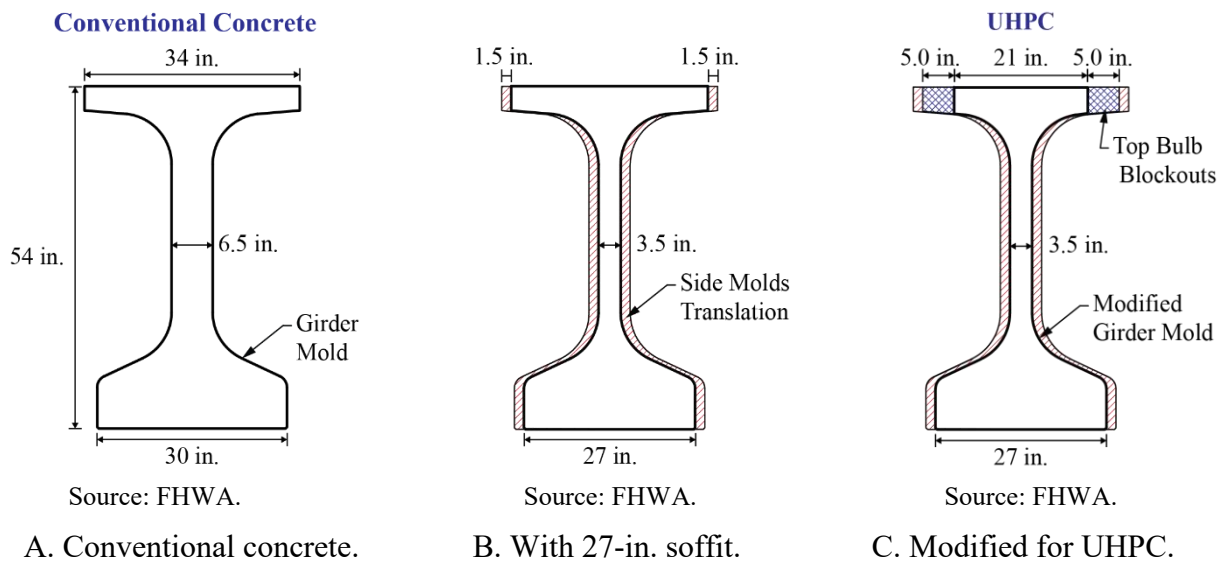
Figure C1-1. Illustrations. MnDOT "MN54" cross sections.
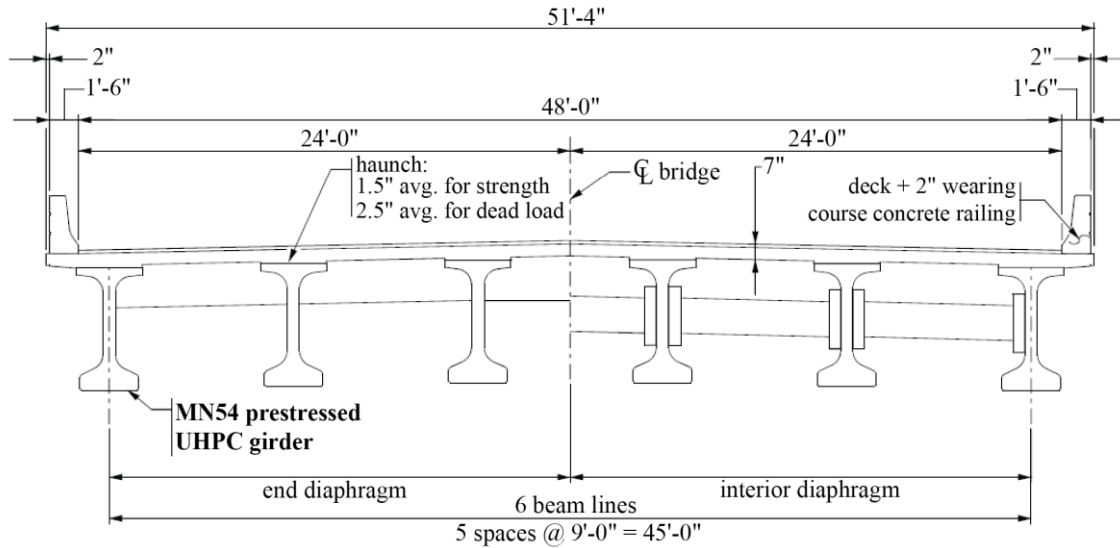
Original illustration: © 2018 Minnesota Department of Transportation. Modified by FHWA to show
new annotations and dimensions.

Figure C1-2. Illustration. Bridge cross section (MnDOT 2018).

C1.1. TERMINOLOGY

The following terminology is used to describe cross sections in this design example:

- *Noncomposite Section*—The UHPC beam cross section.

- *Noncomposite, Nontransformed Section*—The UHPC beam cross section without the strands transformed (also called the gross section).

- *Noncomposite, Transformed Section*—The UHPC beam cross section with the strands transformed to provide cross-sectional properties equivalent to the UHPC used in the girder.

- *Composite Section*—The UHPC beam plus the conventional concrete deck and haunch transformed to provide cross-sectional properties equivalent to the UHPC used in the girder.

- *Composite, Nontransformed Section*—The UHPC beam plus the conventional concrete deck and haunch transformed to provide cross-sectional properties equivalent to the UHPC used in the girder but without the strands transformed.

- *Composite, Transformed Section*—The UHPC beam plus the conventional concrete deck and haunch and the strands transformed to provide cross-sectional properties equivalent to the UHPC used in the girder.

The term "composite" implicitly includes the transformation of the conventional concrete deck and haunch. The term "transformed" generally refers to transformation of the strands.

186

CHAPTER C2. MATERIALS

The material properties and key geometric details for the bridge being designed are listed below.

Cast-in-place conventional concrete deck:

- Actual thickness, $t_D = 9.0$ in.

- Structural thickness, $t_s = 8.5$ in.
  (Note: a ½-in. wearing surface is considered to be part of the 9-in.-thick deck.)

- Specified concrete compressive strength for use in design: $f'_{cD} = 4.0$ ksi.

- Concrete unit weight, $\omega_{cD} = 0.145$ kip/ft³.

- Aggregate correction factor, $K_{1D} = 1.0$.

- Modulus of elasticity for use in design,
  $E_{cD} = 120{,}000 K_{1D}(\omega_{cD})^{2.0}(f'_{cD})^{0.33} = 3{,}987$ ksi.   [AASHTO LRFD BDS Eq. 5.4.2.4-1]

- Average thickness of haunch = 2.5 in.

- Structural thickness of haunch, $t_h = 1.5$ in.

- Width of haunch, $b_h = 21$ in.

Precast UHPC girder—Modified MN54 bulb tee, as shown in Figure C1-1-C:

- UHPC compressive strength at transfer, $f'_{ci} = 14.0$ ksi.

- Compressive strength for use in design, $f'_c = 22.0$ ksi.

- Ultimate compressive strain for use in design, $\varepsilon_{cu} = 0.0035$.

- UHPC unit weight, $\omega_c = 0.160$ kip/ft³.
  (Note: Includes 0.005 kip/ft³ to account for the steel strands.)

- Overall girder length, $L_T = 151$ ft.

- Girder design span, $L = 150$ ft.

- Correction factor for modulus of elasticity, $K_1 = 1.0$.

- Modulus of elasticity at transfer, $E_{ci} = 2{,}500 K_1 f'^{0.33}_{ci} = 5{,}973$ ksi.

[UHPC Guide Article 1.4.2.3]

- Modulus of elasticity for use in design, $E_c = 2,500K_1 f_c'^{0.33} = 6,933$ ksi.

- Cracking strength for use in design, $f_{t,cr} = 1.00$ ksi.

- Cracking strength at transfer, $f_{t,cri} = 0.75 f_{t,cr} = 0.75$ ksi.   [UHPC Guide Article 1.9.1.2]

- Ultimate tension strength for use in design, $f_{t,loc} = 1.00$ ksi.

- Ultimate tension strain for use in design, $\varepsilon_{t,loc} = 0.0040$.

- Reduction factor on tensile parameters, $\gamma_u = 1.00$.

- Correction factor for creep, $K_3 = 0.62$.

- Correction factor for shrinkage, $K_4 = 0.41$.

Prestressing strands: 0.7-in.-diameter, seven-wire, low-relaxation:

- Diameter of strand, $D_p = 0.7$ in.

- Area of one strand, $A_p = 0.294$ in.^{2}.

- Specified tensile strength, $f_{pu} = 270$ ksi.

- Yield strength, $f_{py} = 0.9 \cdot f_{pu} = 243.0$ ksi.

- Stress limit at transfer, $f_{pi} = 0.75 \cdot f_{pu} = 202.5$ ksi.

- Stress limit at service after losses, $f_{s\ell} = 0.80 \cdot f_{py} = 194.4$ ksi.

- Ultimate tension strain for use in design, $\varepsilon_{ps} = 0.035$.

- Modulus of elasticity, $E_p = 28,500$ ksi.

- Nominal weight, $\omega_p = 0.001$ kip/ft.

Future wearing surface: 2 in. of additional concrete, unit weight = 0.145 kcf.

New Jersey-type barrier: unit weight = 0.300 kips/ft/side.

CHAPTER C3. CROSS-SECTIONAL PROPERTIES FOR A TYPICAL INTERIOR GIRDER

C3.1. NONCOMPOSITE, NONTRANSFORMED GIRDER SECTION

The noncomposite, nontransformed cross-sectional properties of the UHPC girder section are as follows:

- Gross cross-sectional area of UHPC girder, A_g = 544.35 in.^{2}.

- Overall depth of girder, h = 54 in.

- Moment of inertia about the centroid of the noncomposite girder, I_g = 209,570.6 in.^{4}.

- Distance from the centroid to extreme bottom fiber of the noncomposite beam, y_b = 21.89 in.

- Distance from the centroid to extreme top fiber of the noncomposite beam, y_t = 32.11 in.

- Section modulus for extreme bottom fiber of the noncomposite beam, $S_b = \dfrac{I_g}{y_b} = 9{,}573.8$ in.^{3}.

- Section modulus for extreme top fiber of the noncomposite beam, $S_t = \dfrac{I_g}{y_t} = 6{,}526.6$ in.^{3}.

- Beam weight per unit length, w_g = (544.35 in.^{2})(1 ft^2/144 in.^{2})(0.160 kip/ft^3) = 0.6048 kip/ft.

C3.2. COMPOSITE GIRDER SECTION

C3.2.1. Effective Flange Width

Article 4.6.2.6 of AASHTO LRFD BDS states the deck effective flange width in composite girder systems may be taken as one-half the distance to the adjacent girder on each side of the component (AASHTO 2020).

Therefore, the effective flange width, b_e = 2(9/2) = 9.0 ft = 108 in.

C3.2.2. Modular Ratio Between Deck and Girder UHPC

Modular ratio between concrete deck and UHPC girder, $n_{Db} = \dfrac{E_c(\text{slab})}{E_c(\text{beam})} = 0.575$.

C3.2.3. Section Properties

To obtain cross-sectional properties equivalent to the girder UHPC, the effective flange width must be transformed by the modular ratio. Only the structural thickness of the deck, 8.5 in., is considered.

Transformed flange width = $n_{Db} \cdot b_e$ = (0.575)(108) = 62.10 in.

Transformed flange area = $n_{Db} \cdot b_e \cdot t_s$ = (0.575)(108)(8.5) = 527.84 in.^{2}.

Transformed flange moment of inertia = $(62.1)(8.5^3)/12$ = 3,178.0 in.^{4}.

The width of the haunch must also be transformed by the modular ratio.

Transformed width of haunch = (0.575)(21.00) = 12.07 in.

Transformed area of haunch = (0.575)(21.00)(1.5) = 18.11 in.^{2}.

Transformed moment of inertia of haunch = $(12.07)(1.5^3)/12$ = 3.40 in.^{4}.

Note that the haunch should only be considered to contribute to section properties if it is required to be provided in the complete structure. For this example, haunch contributions to section properties will be used.

Figure C3.2.3-1 illustrates the dimensions of the composite UHPC/conventional concrete section. Table C3.2.3-1 provides calculated properties.
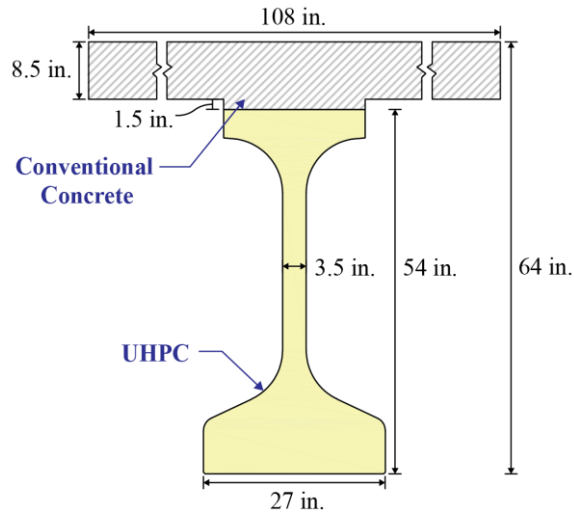
Source: FHWA.

Figure C3.2.3-1. Illustration. Dimensions of the composite UHPC/conventional concrete section.

Table C3.2.3-1. Properties of the composite UHPC/conventional concrete section.

	Area, A (in.^{2})	y_b* (in.)	Ay_b* (in.^{3})	$A(y_{bc} - y_b$*$)^2$ (in.^{4})	I (in.^{4})	$I + A(y_{bc} - y_b$*$)^2$ (in.^{4})
Girder	544.35	21.89	11,915.8	193,927.3	209,570.6	403,497.9
Haunch	18.11	54.75	991.6	3,542.5	3.4	3,545.9
Deck	527.84	59.75	31,538.3	190,254.4	3,178.0	193,432.4
Summation	1,090.30	—	44,445.7	—	—	600,476.2

—Not calculated.
Note: See List of Notations for variable definitions.

Total area of the composite section, $A_c = 1,090.30$ in.^{2}.

Overall depth of the composite section, $h_c = 64.00$ in.

Moment of inertia of the composite section, $I_c = 600,476.2$ in.^{4}.

Distance from the centroid of the composite section to the extreme bottom fiber of the UHPC girder,

$$y_{bc} = 44,445.7 \text{ in.}^3/1,090.30 \text{ in.}^2 = 40.76 \text{ in.}$$

Distance from the centroid of the composite section to the extreme top fiber of the UHPC girder,

$$y_{tg} = h - y_{bc} = 13.24 \text{ in.}$$

Distance from the centroid of the composite section to the extreme top fiber of the structural deck,

$$y_{tc} = h_c - y_{bc} = 23.24 \text{ in.}$$

Composite section modulus for the extreme bottom fiber of the UHPC girder,

$$S_{bc} = \frac{I_c}{y_{bc}} = \frac{600,476.2}{40.76} = 14,730.3 \text{ in.}^3$$

Composite section modulus for the extreme top fiber of the UHPC girder,

$$S_{tg} = \frac{I_c}{y_{tg}} = \frac{600,476.2}{13.24} = 45,369.3 \text{ in.}^3$$

Composite section modulus for extreme top fiber of the structural deck,

$$S_{tc} = \left(\frac{1}{n}\right)\left(\frac{I_c}{y_{tc}}\right) = \left(\frac{1}{0.575}\right)\left(\frac{600,476.2}{23.24}\right) = 44,945.9 \text{ in.}^3$$

CHAPTER C4. SHEAR FORCES AND BENDING MOMENTS

C4.1. SHEAR FORCES AND BENDING MOMENTS DUE TO DEAD LOADS

C4.1.1. Dead Loads

The dead loads acting on the structure are as follows. Note that the haunch thickness is taken as 2.5 in. for load calculations.

Dead loads acting on the noncomposite structure:

- Girder self-weight, $w_g = 0.6048$ kip/ft.

- 9-in. deck weight, $w_D = (9\ \text{in.}/(12\ \text{in.}/\text{ft}))(9\ \text{ft.})(0.145\ \text{kip/ft}^3) = 0.9788$ kip/ft.

- Haunch weight, $w_h = (2.5\ \text{in.}/(12\ \text{in.}/\text{ft}))(21\ \text{in.}/(12\ \text{in.}/\text{ft}))(0.145\ \text{kip/ft}^3) = 0.0529$ kip/ft.

- Total weight of deck and haunch, $w_s = w_D + w_h = 1.0316$ kip/ft.

Dead loads acting on the composite structure:

AASHTO LRFD BDS Article 4.6.2.2.1 (AASHTO 2020) specifies that permanent loads may be distributed uniformly among the girders if the following criteria are met:

- Width of deck is constant.
  OK.

- Number of girders is not less than four.
  ($N_b = 6$).
  OK.

- Beams are parallel and have approximately the same stiffness.
  OK.

- The roadway part of the overhang is less than or equal to 3.0 ft.
  $(3.0 - 1.5 - 0.5(3.5/12) = 1.854$ ft$)$.
  OK.

- Curvature is less than specified in the AASHTO LRFD BDS (AASHTO 2020).
  (curvature = 0.0 degrees).
  OK.

- Cross section of the bridge is consistent with one of the cross-sections given in Table 4.6.2.2.1-1 of AASHTO LRFD BDS (AASHTO 2020). For precast concrete I-beams or bulb-tee beams with cast-in-place concrete deck, the bridge is type (k).
  OK.

This example meets the criteria, and, therefore, the permanent loading is distributed uniformly.

- Barrier weight,

  $w_b = (2)(3 \text{ kip/ft})/6 = 0.1000 \text{ kip/ft/beam}$

- Dead load of future wearing surface,

  $DL_{ws} = (2 \text{ in.})(0.145 \text{ kip/ft}^3) = 0.1678 \text{ kip/in.}^2$

- Future wearing surface weight,

  $w_{ws} = (DL_{ws})(48 \text{ ft})/6 = 0.1933 \text{ kip/ft/beam}$

C4.1.2. Unfactored Shear Forces and Bending Moments

For the simply supported beam of length, L, under a uniform distributed load, w, shear force, V_x, and bending moment, M_x, at any distance, x, from the support are given as:

$V_x = w (0.5L - x)$

$M_x = 0.5wx (L - x)$

Shear forces and bending moments for a typical interior beam under self-weight, weight of slab and haunch, and weight of barriers and wearing surface are calculated and shown in Table C4.1.2-1. A span length of 150 ft is used for these calculations, but the total span length of 151 ft will be used for stress and deflection calculations at the time of prestress transfer.

Table C4.1.2-1. Unfactored shear forces and bending moments due to dead loads for a typical interior girder.

Distance x (ft)	Section x /L	Girder Weight		Deck + Haunch Weight		Barrier Weight		Wearing Surface Weight	
		Shear V_g (kip)	Moment M_g (kip-ft)	Shear V_D (kip)	Moment M_D (kip-ft)	Shear V_b (kip)	Moment M_b (kip-ft)	Shear V_{ws} (kip)	Moment M_{ws} (kip-ft)
4.60*	0.031	42.6	202.3	72.6	345	7.0	33.4	13.6	64.7
0	0.0	45.4	0.0	77.4	0.0	7.5	0.0	14.5	0.0
15	0.1	36.3	612.4	61.9	1,044.5	6.0	101.3	11.6	195.8
30	0.2	27.2	1088.7	46.4	1,856.9	4.5	180.0	8.7	348.0
45	0.3	18.1	1428.9	30.9	2,437.2	3.0	236.3	5.8	456.8
60	0.4	9.1	1633.1	15.5	2,785.4	1.5	270.0	2.9	522.0
75	0.5	0.0	1701.1	0.0	2,901.4	0.0	281.3	0.0	543.8

*Critical section for shear according to Section C11.1 of this Appendix.
Note: See List of Notations for variable definitions.

C4.2. Shear Forces and Bending Moments Due to Live Loads

C4.2.1. Live Loads

The design live load is HL-93, which consists of:

1. Design truck or design tandem with dynamic allowance: The design truck consists of 8.0-, 32.0-, and 32.0-kip axles, with the first pair spaced at 14 ft and the second pair spaced at 14–30 ft. The design tandem consists of a pair of 25.0-kip axles spaced at 4 ft.

2. Design lane load of 0.64 kips/ft without dynamic allowance.

[AASHTO LRFD BDS Article 3.6.1.2.1-4]

C4.2.2. Live Load Distribution Factors for a Typical Interior Beam

The live load bending moments and shear forces are determined by using the simplified distribution factor formulas specified in AASHTO LRFD BDS (AASHTO 2020) Article 4.6.2.2. To use the simplified live load distribution factor formulas, the following conditions must be met:

- Width of deck is constant.
  OK.

- Number of beams is not less than four ($N_b = 6$).
  OK.

- Beams are parallel and have approximately the same stiffness.
  OK.

- The roadway part of the overhang is less than or equal to 3.0 ft.
  $(3.0 – 1.5 – 0.5(9/12) = 1.854$ ft).
  OK.

- Curvature is less than specified in the AASHTO LRFD BDS (AASHTO 2020).
  (curvature $= 0.0°$).
  OK.

- Cross section of the bridge is consistent with one of the cross-sections given in Table 4.6.2.2.1-1 of AASHTO LRFD BDS (AASHTO 2020). For precast concrete I-beams or bulb-tee beams with cast-in-place concrete deck, the bridge is type (k).
  OK.

The number of design lanes = the integer part of the ratio of $W_R/12$, where W_R is the clear roadway width, in feet, between the curbs. From Figure C1-2, $W_R = 48$ ft. Number of design lanes = integer part of $(48/12) = 4$ lanes.

C4.2.2.1. Distribution Factor for Bending Moment

For all limit states except fatigue limit state, the distribution factor for bending moment is calculated as follows.

- For two or more lanes loaded:

$$DFM = 0.075 + \left(\frac{S}{9.5}\right)^{0.6} \left(\frac{S}{L}\right)^{0.2} \left(\frac{K_g}{12.0Lt_s^3}\right)^{0.1}$$

provided:

$3.5 \le S \le 16.0$; $S = 9.0$ ft	OK.
$4.5 \le t_s \le 12.0$; $t_s = 8.5$ in. or 9.0 in. with wearing surface	OK.
$20 \le L \le 240$; $L = 150$ ft	OK.
$N_b \ge 4$; $N_b = 6$	OK.
$10,000 \le K_g \le 7,000,000$	OK.

Where:
DFM = distribution factor for bending moment for interior girder
S = girder spacing, ft
L = design span, ft
t_s = structural depth of concrete deck, in.
K_g = longitudinal stiffness parameter, in.^{4} = $n_{bD}(I_g + A_g e_g^2)$

[AASHTO LRFD BDS Eq. 4.6.2.2.1-1]

in which:
n_{bD} = modular ratio between UHPC girder and conventional concrete deck
  = $E_c / E_{cD} = 1.739$
A_g = gross area of UHPC girder = 544.35 in.^{2}
I_g = moment of inertia of the UHPC girder = 209,570.6 in.^{4}
e_g = distance between the centers of gravity of the UHPC girder and conventional concrete deck
  = 9 in./2 + 2.5 in. + 32.11 in. = 39.11 in.
(Note: e_g is conservatively calculated using the total thickness of deck including the wearing surface and the average thickness of the haunch.)

Therefore:

$$K_g = n_{bD}(I_g + A_g e_g^2) = 1.739\,(209,570.6 + 544.35(39.11^2)) = 1,812,572 \text{ in.}^4$$

$$DFM = 0.075 + \left(\frac{9.0}{9.5}\right)^{0.6} \left(\frac{9.0}{150}\right)^{0.2} \left(\frac{1,812,572}{12.0(150)(8.5)^3}\right)^{0.1} = 0.654 \text{ lanes/beam}$$

(Note: DFM is conservatively calculated using the structural thickness of deck.)

- For one design lane loaded:

$$DFM = 0.06 + \left(\frac{S}{14}\right)^{0.4} \left(\frac{S}{L}\right)^{0.3} \left(\frac{K_g}{12.0Lt_s^3}\right)^{0.1}$$

$$= 0.06 + \left(\frac{9.0}{14}\right)^{0.4} \left(\frac{9.0}{150}\right)^{0.3} \left(\frac{1,812,572}{12.0(150)(8.5)^3}\right)^{0.1} = 0.439 \text{ lanes/beam}$$

(Note: *DFM* is conservatively calculated using the structural thickness of deck.)

The situation where two or more lanes are loaded controls; therefore, $DFM = 0.654$ lanes/beam.

For the fatigue limit state, AASHTO LRFD BDS Article C3.4.1 (AASHTO 2020) states that a single design truck should be used and that the live load distribution factors take into consideration the multiple presence factor, m. The multiple presence factor for one design lane loaded is 1.2. Therefore, the distribution factor for one design lane loaded with the multiple presence factor removed should be used. The distribution factor for fatigue limit state is $DFM = 0.439/1.2 = 0.365$ lanes/beam.

C4.2.2.2. Distribution Factor for Shear Force

The distribution factor for shear is calculated as follows.

- For two or more lanes loaded:

$$DFV = 0.2 + \left(\frac{S}{12}\right) - \left(\frac{S}{35}\right)^2$$

provided:

$3.5 \leq S \leq 16.0$; $S = 9.0$ ft	OK.
$4.5 \leq t_s \leq 12.0$; $t_s = 8.5$ in. or 9.0 in. with wearing surface	OK.
$20 \leq L \leq 240$; $L = 150$ ft	OK.
$N_b \geq 4$; $N_b = 6$	OK.

Where:
DFV = distribution factor for shear force for interior girder
S = girder spacing, ft

Therefore:

$$DFV = 0.2 + \left(\frac{9.0}{12}\right) - \left(\frac{9.0}{35}\right)^2 = 0.884 \text{ lanes/beam}$$

- For one design lane loaded:

$$DFV = 0.36 + \left(\frac{S}{25}\right) = 0.36 + \left(\frac{9.0}{25}\right) = 0.720 \text{ lanes/beam}$$

The situation where two or more lanes are loaded controls, with $DFM = 0.884$ lanes/beam.

C4.2.3. Dynamic Allowance

The dynamic allowance parameters are as follows, where *IM* is the dynamic allowance, applied to the design truck load only.

IM = 15 percent for fatigue limit state.
IM = 33 percent for all other limit states.

C4.2.4. Unfactored Shear Forces and Bending Moments

C4.2.4.1. Due to Truck Load: V_{LT} and M_{LT}

For all limit states except for the fatigue limit state, shear force and bending moment envelopes per lane are calculated at tenth points of the span using commercially available computer software that analyzes moving loads. The values of the truck load shear forces, V_{LT}, and the bending moments, M_{LT}, at selected locations along the girder length are given in Table C4.2.4.1-1 and calculated as follows:

$$V_{LT} = \text{(shear force per lane)}(DFV)(1 + IM).$$
$$= \text{(shear force per lane)}(0.884)(1 + 0.33).$$
$$= \text{(shear force per lane)}(1.176).$$
$$M_{LT} = \text{(bending moment per lane)}(DFM)(1 + IM).$$
$$= \text{(bending moment per lane)}(0.654)(1 + 0.33).$$
$$= \text{(bending moment per lane)}(0.869).$$

For the fatigue limit state, AASHTO LRFD BDS Article 3.6.1.4.1 states that fatigue load is a single truck that has the same axle weight used in all other limit states but with a constant spacing of 30 ft between the 32-kip axles. The bending moment envelope per lane is calculated using computer software. The values of the bending moment of the fatigue truck, M_f, at selected locations along the girder's length are given in Table C4.2.4.1-1 and calculated as follows:

$$M_f = \text{(bending moment per lane)}(DFM)(1 + IM).$$
$$= \text{(bending moment per lane)}(0.365)(1 + 0.15).$$
$$= \text{(bending moment per lane)}(0.420).$$

Table C4.2.4.1-1. Unfactored shear forces and bending moments due to live loads for a typical interior girder.

| Distance, x, ft | Section x/L | Truckload with Impact | | Lane Load | | Fatigue I Truck with Impact |
		Shear V_{LT} (kips)	Moment M_{LT} (kip-ft)	Shear V_{LL} (kips)	Moment M_{LL} (kip-ft)	Moment M_f (kip-ft)
4.60*	0.031	76.6	260.7	39.9	140.1	117.7
0	0.0	78.8	0.0	42.4	0.0	0.0
15	0.1	70.3	787.6	34.4	424.1	353.4
30	0.2	61.9	1387.1	27.2	753.9	616.0
45	0.3	53.4	1798.6	20.8	989.5	787.8
60	0.4	45.0	2022.1	15.3	1130.9	868.9
75	0.5	36.5	2106.4	10.6	1178.0	909.6

*Critical section for shear according to Section C11.1 of this Appendix.
Note: See List of Notations for variable definitions.

C4.2.4.2. Due to Design Lane Load: V_{LL} and M_{LL}

To obtain the maximum shear force at a section located at a distance (x) from the left support under a uniformly distributed load of 0.64 kips/ft, the member should be loaded to the right of the section under consideration. Therefore, the maximum shear force per lane at location x along the girder's length is:

$$V_x = \frac{0.32(L - x)^2}{L} \text{ for } x \leq 0.5L$$

where:

$$
\begin{aligned}
V_{LL} &= \text{(shear force per lane)}(DFV) \\
&= \text{(shear force per lane)}(0.884)
\end{aligned}
$$

For all limit states except for the fatigue limit state:

$$
\begin{aligned}
M_{LL} &= \text{(bending moment per lane)}(DFM) \\
&= \text{(bending moment per lane)}(0.654)
\end{aligned}
$$

The values of V_{LL} and M_{LL} are given along selected location of the girder's length in Table C4.2.4.1-1.

C4.3. LOAD COMBINATIONS

Total factored load is taken as:

$$Q = \Sigma \eta_i \gamma_i Q_i \qquad\qquad \text{[AASHTO LRFD BDS Eq. 3.4.1-1]}$$

where:

η_i = a load modifier relating to ductility, redundancy, and operational importance (here η_i is taken as 1.0 for typical bridges)   [AASHTO LRFD BDS Article 1.3.2]

γ_i = load factor   [AASHTO LRFD BDS Table 3.4.1-1]

Q_i = force effects from specified loads

The following limit states given in AASHTO LRFD BDS Article 3.4.1 are applicable:

- Service I: Check compressive stresses in prestressed UHPC components and tensile stress limits for prestressed UHPC components subject to fatigue loads:

$$Q = 1.00(DC + DW) + 1.00(LL + IM)$$ [AASHTO LRFD BDS Table 3.4.1-1]

where:

DC = dead load of structural components and nonstructural attachments
DW = dead load of wearing surfaces and utilities
LL = vehicular live load
IM = dynamic allowance

This load combination is the general combination for service limit state stress checks and applies to all conditions other than Service III.

- Service III: Check tensile stresses in prestressed UHPC components:

$$Q = 1.00(DC + DW) + \gamma_{LL}(LL + IM)$$ [AASHTO LRFD BDS Table 3.4.1-1]

where:

γ_{LL} = load factor for live load for Service III load combination

In prestressed conventional concrete, this load combination is a special combination for service limit state stress checks that applies only in tension to control cracks. However, γ_{LL} for UHPC is always equal to 1.0 because only the refined estimates of time-dependent losses are allowed.

[AASHTO LRFD BDS Table 3.4.1-4; UHPC Guide Article 1.9.1.1]

Note that, in this design example, the bending stresses due to Service I and Service III load combinations are assumed to be similar.

- Strength I: Check ultimate strength:

Maximum $Q = 1.25(DC) + 1.50(DW) + 1.75(LL + IM)$

[AASHTO LRFD BDS Table 3.4.1-1 and Table 3.4.1-2]

Minimum $Q = 0.90(DC) + 0.65(DW) + 1.75(LL + IM)$

This combination is the general load combination for strength limit state design.

Note: For simple span bridges, the maximum load factors produce maximum effects. However, use minimum load factors for dead load (*DC*) and wearing surface (*DW*) when dead load and wearing surface stresses are opposite to those of live load.

- Fatigue I: Check the stress range in strands and UHPC compression stresses:

$$Q = 1.75(LL + IM) \hspace{2cm} \text{[AASHTO LRFD BDS Table 3.4.1-1]}$$

This load combination is a special load combination to check tensile stress range in the strands due to live load and dynamic allowance.

CHAPTER C5. REQUIRED PRESTRESSING

UHPC Guide Article 1.9.1 states prestressing strands shall satisfy requirements at service, fatigue, strength, and extreme event limit states, as specified in Articles 1.5 and 1.9.2. For this design example, a strand profile has been predetermined.

C5.1. STRAND PATTERN

Fifty 0.7-in.-diameter, Grade 270 low-relaxation strands are selected to reinforce the girder. Forty-eight strands are placed in the bottom flange at a horizontal and vertical spacing of 2 in. center-to-center, as shown in Figure C5.1-1. Two strands are placed in the top flange at a distance of 2 in. between the top of the girder and the center of the strands; the top strands were placed at a horizontal spacing of 4 in. center to center. At each end of the girder, 14 strands are debonded near girder ends to satisfy stress limit requirement at release at the transfer length section, as described in Section C7.2 of this Appendix, and to adequately reinforce the girder at the pretensioned anchorage zones, as described in Section C14.1 of this Appendix. The strand pattern at the girder ends is selected following the provisions of UHPC Guide Article 1.9.4.3.3 and is shown in Figure C5.1-2.

Total area of prestressing strands at midspan, $A_{ps} = T_s A_p = 14.700$ in.^{2}.

Total area of prestressing strands at girder ends, $A_{psE} = T_{sE} A_p = 10.584$ in.^{2}.

Distance between the centroid of the strands and the extreme bottom fiber of the UHPC girder at midspan, $y_{bs} = \dfrac{\sum N_{mid} d_{mid}}{T_s} = 6.64$ in.

Distance between the centroid of the strands and the extreme bottom fiber of the UHPC girder at ends, $y_{bsE} = \dfrac{\sum N_{end} d_{end}}{T_{sE}} = 7.44$ in.

where:
- N_{mid} = quantity of strands per row at midspan = [2, 9, 13, 13, 13]
- d_{mid} = distance between the centroid of the strands in a row and the bottom of the section at midspan = [52, 8, 6, 4, 2]
- T_s = total number of prestressing strands at midspan = 50
- T_{sE} = total number of prestressing strands at girder ends = 36
- N_{end} = quantity of strands per row at girder ends = [2, 7, 9, 9, 9]
- d_{end} = distance between the centroid of the strands in a row and the bottom of the section at girder ends = d_{mid}

Strand eccentricity in noncomposite section at midspan, $e_{pg} = y_b - y_{bs} = 21.89 - 6.64 = 15.25$ in.

Strand eccentricity in noncomposite section at ends, $e_{pgE} = y_b - y_{bsE} = 21.89 - 7.44 = 14.45$ in.

Total prestressing force before transfer at midspan, $P_{pi} = T_s A_p f_{pi} = 2,976.75$ kip.

Total prestressing force before transfer at girder ends, $P_{piE} = T_{sE} A_p f_{pi} = 2{,}143.26$ kip.

Number of strands	Distance from bottom (in.)
2	52
9	8
13	6
13	4
13	2
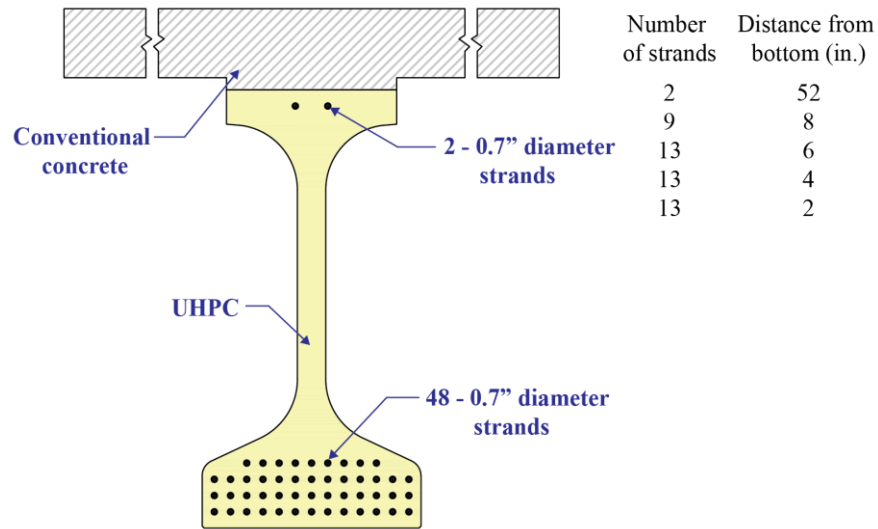
Source: FHWA.

Figure C5.1-1. Illustration. Strand pattern at midspan.

Number of strands	Distance from bottom (in.)
2	52
7	8
9	6
9	4
9	2
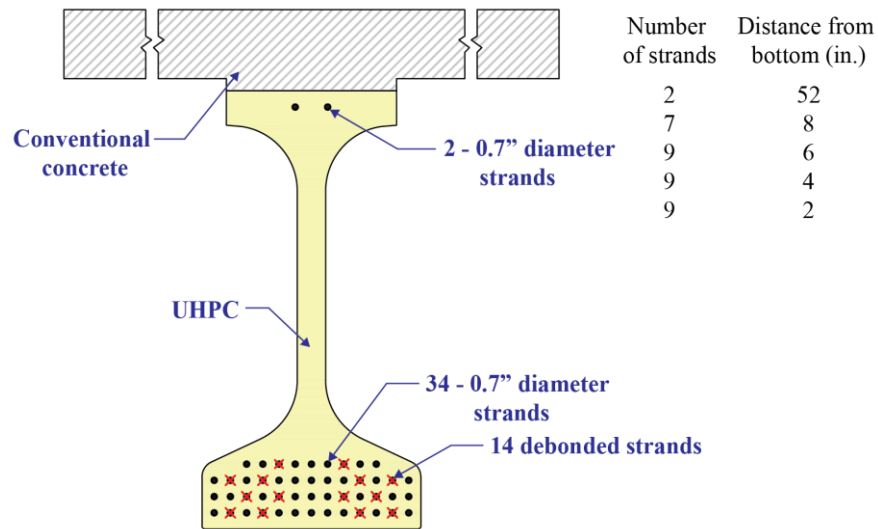
Source: FHWA.

Figure C5.1-2. Illustration. Strand pattern at beam ends.

C5.2. STEEL TRANSFORMED SECTION PROPERTIES

Transformed sections are obtained from the gross sections by adding the transformed area of steel. Transformed sectional analysis yields more accurate results of prestressing forces than does the gross section analysis. To obtain the transformed area of the reinforcing steel, the steel area in each row of prestressing strands shown in Figure C5.1-1 is multiplied by $(n - 1)$, where n is the modular ratio between UHPC and prestressing strands. The modulus of elasticity of UHPC is different at

transfer and final time; therefore, the transformed section properties are calculated separately for the two periods.

C5.2.1. Noncomposite Transformed Section at Transfer at Midspan

The noncomposite transformed section properties at transfer at midspan are as follows:

$n - 1$ at transfer, denoted by n_{ti}, $n_{ti} = \dfrac{E_p}{E_{ci}} - 1 = 3.772$

Area of transformed section, $A_{ti} = A_g + \sum n_{ti} N_{mid} A_p = 599.8 \text{ in.}^2$

Distance from centroid to bottom of section, $y_{bti} = \dfrac{\sum d_{mid}\, n_{ti}\, N_{mid}\, A_p + A_g\, y_b}{A_{ti}} = 20.48 \text{ in.}$

Moment of inertia, $I_{ti} = I_g + A_g\,(y_{bti} - y_b)^2 + \sum n_{ti}\, N_{mid}\, A_p\,(y_{bti} - d_{mid})^2$

$I_{ti} = 226{,}271.6 \text{ in.}^4$

Distance from centroid to top of section, $y_{tti} = h - y_{bti} = 33.52 \text{ in.}$

Eccentricity of strands, $e_{ti} = y_{bti} - y_{bs} = 13.84 \text{ in.}$

Section modulus for the bottom of section, $S_{bti} = \dfrac{I_{ti}}{y_{bti}} = 11{,}048 \text{ in.}^3$

Section modulus for the top of section, $S_{tti} = \dfrac{I_{ti}}{y_{tti}} = 6{,}750 \text{ in.}^3$

C5.2.2. Noncomposite Transformed Section at Girder Ends at Transfer (14 Strands Debonded)

The noncomposite transformed section properties at girder ends at transfer are as follows:

$n - 1$ at transfer, denoted by n_{ti}, $n_{ti} = 3.772$

Area of transformed section, $A_{tiE} = A_g + \sum n_{ti} N_{end} A_p = 584.3 \text{ in.}^2$

Distance from centroid to bottom of section, $y_{btiE} = \dfrac{\sum d_{end}\, n_{ti}\, N_{end}\, A_p + A_g\, y_b}{A_{tiE}} = 20.90 \text{ in.}$

Moment of inertia, $I_{tiE} = I_g + A_g\,(y_{btiE} - y_b)^2 + \sum n_{ti} N_{end} A_p (y_{btiE} - d_{end})^2$

$$I_{tiE} = 222{,}172.1 \text{ in.}^4$$

Distance from centroid to top of section, $\quad y_{ttiE} = h - y_{btiE} = 33.10$ in.

Eccentricity of strands, $\quad e_{tiE} = y_{btiE} - y_{bsE} = 13.46$ in.

Section modulus for bottom of section, $\quad S_{btiE} = \dfrac{I_{tiE}}{y_{btiE}} = 10{,}629 \text{ in.}^3$

Section modulus for top of section, $\quad S_{ttiE} = \dfrac{I_{tiE}}{y_{ttiE}} = 6{,}713 \text{ in.}^3$

C5.2.3. Noncomposite Transformed Section at Midspan at Final Time

The noncomposite transformed section properties at midspan at final time are as follows:

$n - 1$ at transfer, denoted by n_{tf}, $\quad n_{tf} = \dfrac{E_p}{E_c} - 1 = 3.111$

Area of transformed section, $\quad A_{tf} = A_g + \sum n_{tf} N_{mid} A_p = 590.1 \text{ in.}^2$

Distance from centroid to bottom of section, $\quad y_{btf} = \dfrac{\sum d_{mid}\, n_{tf}\, N_{mid}\, A_p + A_g\, y_b}{A_{tf}} = 20.71$ in.

Moment of inertia, $\quad I_{tf} = I_g + A_g\,(y_{btf} - y_b)^2 + \sum n_{tf} N_{mid} A_p (y_{btf} - d_{mid})^2$

$$I_{tf} = 223{,}502.9 \text{ in.}^4$$

Distance from centroid to top of section, $\quad y_{ttf} = h - y_{btf} = 33.29$ in.

Eccentricity of strands, $\quad e_{tf} = y_{btf} - y_{bs} = 14.07$ in.

Section modulus for bottom of section, $\quad S_{btf} = \dfrac{I_{tf}}{y_{btf}} = 10{,}793 \text{ in.}^3$

Section modulus for top of section, $\quad S_{ttf} = \dfrac{I_{tf}}{y_{ttf}} = 6{,}713 \text{ in.}^3$

C5.2.4. Composite Transformed Section at Midspan at Final Time

The composite transformed section properties at midspan at final time are as follows:

$n - 1$ at transfer, denoted by n_{tf}, $\quad n_{tf} = \dfrac{E_p}{E_c} - 1 = 3.111$

Area of transformed section, $\quad A_{tc} = A_c + \sum n_{tf} N_{mid} A_p = 1{,}136.0 \text{ in.}^2$

Distance from centroid to bottom of section, $\quad y_{btc} = \dfrac{\sum d_{mid}\, n_{tf}\, N_{mid}\, A_p + A_c\, y_{bc}}{A_{tc}} = 39.39 \text{ in.}$

Moment of inertia, $\quad I_{tc} = I_{te} + I_{th} + I_g + A_{tc}(y_{btc} - y_{bc})^2 + \sum n_{tf} N_{mid} A_p(y_{btc} - d_{mid})^2$

$I_{tc} = 655{,}702.7 \text{ in.}^4$

Distance from centroid to top of composite section, $\quad y_{ttc} = h_c - y_{btc} = 24.61 \text{ in.}$

Eccentricity of strands, $\quad e_{tc} = y_{btc} - y_{bs} = 32.75 \text{ in.}$

Section modulus for the bottom of composite section, $\quad S_{btc} = \dfrac{I_{tc}}{y_{btc}} = 16{,}646 \text{ in.}^3$

Section modulus for the top of UHPC section, $\quad S_{ttc} = \dfrac{I_{tc}}{\left(y_{ttc} - t_s - t_h\right)} = 44{,}884 \text{ in.}^3$

Section modulus for the top of composite section, $\quad S_{dtc} = \dfrac{1}{n_{Db}} \dfrac{I_{tc}}{y_{ttc}} = 46{,}340 \text{ in.}^3$

CHAPTER C6. PRESTRESS LOSSES

The total prestress loss is calculated as follows.

$$\Delta f_{pT} = \Delta f_{pES} + \Delta f_{pLT}$$
$\hspace{4cm}$ [AASHTO LRFD BDS Eq. 5.9.5.1-1]

where:

Δf_{pT} = total prestress loss in prestressing steel (ksi)

Δf_{pES} = sum of all prestress losses or gains due to elastic shortening or extension at time of prestressing (ksi)

Δf_{pLT} = long-term prestress losses due to shrinkage and creep of UHPC and conventional concrete, and relaxation of steel after transfer (ksi)

C6.1. ELASTIC SHORTENING

The prestress loss due to elastic shortening is calculated as follows:

$$\Delta f_{pES} = \frac{E_p}{E_{ci}} f_{cgp}$$

where:

E_p = modulus of elasticity of prestressing strands = 28,500 ksi

E_{ci} = modulus of elasticity of beam UHPC at transfer = 5,973 ksi

f_{cgp} = sum of stresses at the center of gravity of prestressing strands due to prestressing force at transfer and the self-weight of the member at maximum moment sections (ksi)

When gross section properties are used, the elastic loss, Δf_{pES}, is usually assumed to be 10 percent of the initial prestress to calculate f_{cgp} to calculate a more refined Δf_{pES}. This iteration continues until the values of Δf_{pES} and f_{cgp} converge.

By using transformed properties to calculate stress, effects of losses and gains due to elastic deformations are accounted for. Therefore, for this example, Δf_{pES} will not be included in calculating f_{cgp}.

Force per strand before transfer = area of strand × prestress before transfer = (0.294)(202.5) = 59.54 kips.

$$f_{cpg} = \frac{P_{pi}}{A_{ti}} + \frac{P_{pi}\,e_{ti}^2}{I_{ti}} - \frac{M_{gT,m}\,e_{ti}}{I_{ti}}$$

where:

e_{ti} = eccentricity of strands at midspan with respect to the transformed section at transfer
$\hspace{0.9cm}$ = 13.84 in.

P_{pi} = total prestressing force before transfer
$\hspace{0.9cm}$ = 2,976.8 kips

$M_{gT,m}$ = unfactored bending at midspan moment due to UHPC girder self-weight, which is calculated based on overall girder length 151 ft
= 1,723.9 kip-ft

$$f_{cpg} = \frac{2,976.8}{599.8} + \frac{(2,976.8)(13.84)^2}{226,271.6} - \frac{(1,723.9)(12)(13.84)}{226,271.6} = 6.218 \text{ ksi}$$

Therefore, prestress loss due to elastic shortening:

$$\Delta f_{pES} = \frac{28,500}{5,973}(6.218) = 29.669 \text{ ksi}$$

AASHTO LRFD BDS Article C5.9.5.3 (AASHTO 2020) indicates that the loss due to elastic shortening at transfer should be added to the time-dependent losses to determine total losses. However, this loss at transfer is directly accounted for when transformed properties are used in stress analysis.

C6.2. TIME-DEPENDENT LOSSES BETWEEN TRANSFER AND DECK PLACEMENT

The time-dependent prestress loss between prestress transfer and deck placement is calculated as follows:

The following construction schedule is assumed for calculating time-dependent losses:

- UHPC age at time of prestress transfer: t_i = 1 day.
- UHPC age at time of deck placement: t_d = 90 days.
- UHPC age at final time: t_f = 20,000 days.

The total time-dependent losses between transfer and deck placement are the sum of prestress losses incurred during all stages listed above.

C6.2.1. Creep of UHPC

The prestress loss due to creep of UHPC girder between the time of prestress transfer, t_i, and deck placement, t_d, is:

$$\Delta f_{pCR} = \frac{E_p}{E_{ci}} f_{cgp} \Psi(t_d, t_i) K_{id}$$

where:
$\Psi(t_d,t_i)$ = creep coefficient of UHPC at time of deck placement, t_d, due to loading at prestress transfer, t_i
K_{id} = transformed section coefficient that accounts for time-dependent interaction between UHPC and bonded steel in the section considered for the time period between prestress transfer and deck placement

The creep coefficient $\Psi(t_d, t_i)$ is taken as:

$$\Psi(t_d,t_i) = 1.2 k_s\, k_{hc}\, k_f\, k_{tdd}\, k_{\ell i}\, K_3 \qquad\qquad \text{[AASHTO LRFD BDS Eq. 1.4.2.8.2-1]}$$

where:

k_s = factor for the effect of volume-to-surface ratio of the UHPC girder = 1.0

k_{hc} = humidity factor for creep of UHPC = $1.12 - 0.0024H = 0.945$

k_f = factor for the effect of UHPC strength

$$= \frac{18}{1.5 f'_{ci} - 3} = 1.0$$

k_{tdd} = time development factor between prestress transfer and deck placement

$$= \frac{t}{\left(\dfrac{300}{f'_{ci}+30}\right) + 0.8 t^{0.98}} = \frac{(90-1)}{\left(\dfrac{300}{14+30}\right) + 0.8(90-1)^{0.98}} = 1.238$$

$k_{\ell i}$ = factor for the effect of loading age at prestress transfer = 1.0, because $t_i < 7$

K_3 = correction factor for creep of UHPC = 0.62

in which:

H = average annual ambient relative humidity = 73 percent

f'_{ci} = compressive strength of UHPC at the time of prestressing for use in design = 14 ksi

t = maturity of UHPC in days, taken as the time being considered for analysis of creep or shrinkage effects = $t_d - t_i = 90 - 1 = 89$ days

Therefore:

$$\Psi(t_d,t_i) = 1.2(1.0)(0.945)(1.0)(1.238)(1.0)(0.62) = 0.870$$

The transformed section coefficient is taken as:

$$K_{id} = \frac{1}{1 + \dfrac{E_p}{E_{ci}}\dfrac{A_{pT}}{A_g}\left(1 + \dfrac{A_g\left(e_{pg}\right)^2}{I_g}\right)\left[1 + 0.7\Psi\left(t_f,t_i\right)\right]}$$

where:

e_{pg} = eccentricity of strands in noncomposite section at midspan = 15.25 in.

$\Psi(t_f,t_i)$ = girder creep coefficient at final time, t_f, due to loading at prestress transfer, t_i

          = $1.2 k_s\, k_{hc}\, k_f\, k_{tdf}\, k_{\ell i}\, K_3 = 1.071$

in which:

k_{tdf} = time development factor between prestress transfer and final time

$$= \frac{t}{\left(\dfrac{300}{f'_{ci}+30}\right) + 0.8 t^{0.98}} = \frac{(20{,}000-1)}{\left(\dfrac{300}{14+30}\right) + 0.8(20{,}000-1)^{0.98}} = 1.523$$

t = maturity of UHPC in days, taken as the time being considered for analysis of creep or shrinkage effects = $t_f - t_i$ = 20,000 − 1 = 19,999 days.

Therefore:

$$K_{id} = \cfrac{1}{1 + \cfrac{28{,}500}{5{,}973} \cdot \cfrac{14.70}{544.35}\left(1 + \cfrac{544.35(15.25)^2}{209{,}570.6}\right)[1 + 0.7(1.071)]} = 0.734$$

and

$$\Delta f_{pCR} = \frac{28{,}500}{5{,}973}(6.218)(0.870)(0.734) = 18.958 \text{ ksi}$$

C6.2.2. Shrinkage of UHPC

The prestress loss due to shrinkage of UHPC girder between the time of prestress transfer, t_i, and the time of deck placement, t_d, is calculated as:

$$\Delta f_{pSR} = \varepsilon_{sh} E_p K_{id} \qquad\qquad \text{[AASHTO LRFD BDS Eq. 5.9.5.4.2a-1]}$$

where the strain due to shrinkage, ε_{sh}, is taken as:

$$\varepsilon_{sh} = \varepsilon_{bid} = 0.6 \times 10^{-3}\, k_s\, k_{hs}\, k_f\, k_{tdd}\, K_4 \qquad\qquad \text{[AASHTO LRFD BDS Eq. 1.4.2.8.3-1]}$$

in which:
- ε_{bid} = UHPC shrinkage strain for the period between prestress transfer and deck placement (in./in.)
- k_{hs} = humidity factor for shrinkage of UHPC = $1.5 - 0.01H = 0.770$
- K_4 = correction factor for shrinkage = 0.41
- k_{tdd} = 1.238

Therefore:

$$\varepsilon_{bid} = (0.6 \times 10^{-3})(1.0)(0.770)(1.0)(1.238)(0.41) = 0.000234$$

Prestress losses due to shrinkage between transfer and deck placement is:

$$\Delta f_{pSR} = (0.000234)(28{,}500)(0.734) = 4.907 \text{ ksi}$$

C6.2.3. Relaxation of Prestressing Strands

Prestress loss due to the relaxation of prestressing strands between prestress transfer and deck placement is calculated by:

$$\Delta f_{pR1} = \frac{f_{pt}}{K_L}\left(\frac{f_{pt}}{f_{py}} - 0.55\right) \qquad\qquad \text{[AASHTO LRFD BDS Eq. 5.9.5.4.2c-1]}$$

where:

   f_{pt} =   stress in prestressing strands immediately after transfer, taken as not less than $0.55f_y$ (ksi)

   K_L =   factor accounting for the type of steel taken as 30 for low-relaxation strands and 7 for other prestressing steel, unless more accurate manufacturer's data are available

Therefore:

$$\Delta f_{pR1} = \frac{(202.5 - 29.669)}{30}\left(\frac{(202.5 - 29.669)}{243} - 0.55\right) = 0.929 \text{ ksi}$$

C6.3. TIME-DEPENDENT LOSSES BETWEEN DECK PLACEMENT AND FINAL TIME

The total time-dependent losses between deck placement and final time are the sum of prestress losses due to shrinkage and creep of the UHPC beam, relaxation of prestressing strands, and shrinkage of the deck concrete. The calculation of each of these prestress losses are detailed here in sections C6.3.1 to C6.3.4.

C6.3.1. Creep of UHPC

The prestress loss due to creep of the girder UHPC between the time of deck placement, t_d, and final time, t_f, is determined as:

$$\Delta f_{pCD} = \frac{E_p}{E_{ci}} f_{cgp} \left[\Psi(t_f,t_i) - \Psi(t_d,t_i)\right] K_{df} + \frac{E_p}{E_c} \Delta f_{cd} \Psi(t_f,t_d) K_{df}$$

[AASHTO LRFD BDS Eq. 5.9.3.4.3b-1]

where:

   K_{df} =   transformed section coefficient that accounts for time-dependent interaction between UHPC and bonded steel in the section considered for the time period between deck placement and final time

   $\Psi(t_f,t_d)$ =   girder creep coefficient at final time, t_f, due to loading at time of deck placement, t_d

   Δf_{cd} =   change in UHPC stress at the centroid of the prestressing strands due to long-term losses between transfer and deck placement, combined with deck weight and superimposed loads (ksi)

The UHPC girder creep coefficient $\Psi(t_f,t_d)$ is calculated as follows:

$$\Psi(t_f,t_d) = 1.2 k_s \, k_{hc} \, k_f \, k_{tdfd} \, k_{\ell d} \, K_3 \qquad \text{[AASHTO LRFD BDS Eq. 5.4.2.3.2-1]}$$

where:

   $k_{\ell d}$ =   factor for the effect of loading age at time of deck placement, $t_d \geq 7$ days

213

$$= (t_d - 6)^{-0.15} = 0.5145 \geq 0.5 \qquad\qquad \text{[UHPC Guide Eq. 1.4.2.8.2-7]}$$

k_{tdfd} = time development factor between deck placement and final time

$$= \frac{t}{\left(\dfrac{300}{f'_{cd} + 30}\right) + 0.8t^{0.98}} = \frac{(20{,}000 - 90)}{\left(\dfrac{300}{18 + 30}\right) + 0.8(20{,}000 - 90)^{0.98}} = 1.523$$

in which:

    t = maturity of UHPC in days, taken as the time being considered for analysis of creep or shrinkage effects = $t_f - t_d = 20{,}000 - 90 = 19{,}910$ days

    f'_{cd} = UHPC girder strength at time of deck loading placement = 18 ksi

Therefore:

$$\Psi(t_f, t_d) = 1.2(1.0)(0.945)(1.0)(1.523)(0.5145)(0.62) = 0.551.$$

The change in UHPC stress at the centroid of the prestressing strands, Δf_{cd}, can be calculated as follows:

$$\Delta f_{cd} = -\left(\Delta f_{pSR} + \Delta f_{pCR} + \Delta f_{pR1}\right)\frac{A_{ps}}{A_g}\left(1 + \frac{A_g e_{pg}^2}{I_g}\right) - \left(\frac{M_{D,m}e_{tf}}{I_{tf}} + \frac{(M_{b,m} + M_{ws,m})e_{tc}}{I_{tc}}\right)$$

where:

    $M_{D,m}$ = unfactored bending moment at midspan due to deck and haunch weight = 2,901.4 kip-ft

    $M_{b,m}$ = unfactored bending moment at midspan due to barrier weight = 281.3 kip-ft

    $M_{ws,m}$ = unfactored bending moment at midspan due to wearing surface weight = 543.8 kip-ft

Therefore:

$$\Delta f_{cd} = -(4.907 + 18.958 + 0.929)\frac{14.70}{544.35}\left(1 + \frac{(544.35)(15.25)^2}{209{,}570.6}\right)$$
$$- \left(\frac{(2{,}901.4)(12)(14.07)}{223{,}502.9} + \frac{(281.3 + 543.8)(12)(32.75)}{655{,}702.7}\right)$$

$$= -3.760 \text{ ksi.}$$

The transformed section coefficient of the UHPC girder, K_{df}, can be calculated according to the following equation:

$$K_{df} = \frac{1}{1 + \dfrac{E_p}{E_{ci}}\dfrac{A_{ps}}{A_c}\left(1 + \dfrac{A_c(e_{pc})^2}{I_c}\right)[1 + 0.7\Psi(t_f, t_i)]} \qquad \text{[AASHTO LRFD BDS Eq. 5.9.3.4.3a-2]}$$

214

where:

e_{pc} = eccentricity of strands with respect to the centroid of composite section (in.)

$\quad\quad = y_{bc} - y_{bs} = 34.13$ in.

Therefore:

$$K_{df} = \cfrac{1}{1 + \cfrac{28{,}500}{5{,}973} \cfrac{14.70}{1{,}090.30} \left(1 + \cfrac{1{,}090.30(34.13)^2}{600{,}476.2}\right) [1 + 0.7(1.071)]} = 0.740$$

The prestress loss due to creep, Δf_{pCD}, can be calculated as:

$$\Delta f_{pCD} = \frac{28{,}500}{5{,}973}(6.218)[1.071 - 0.870](0.740) + \frac{28{,}500}{6{,}933}(-3.760)(0.551)(0.740)$$

$$= -1.898 \text{ ksi}$$

Note that the negative sign indicates a prestress gain.

C6.3.2. Shrinkage of UHPC

The prestress loss due to shrinkage of UHPC between time of deck placement, t_d, and final time, t_f, can be computed based on the following equation:

$$\Delta f_{pSD} = \varepsilon_{bdf} E_p K_{df} \quad\quad\quad\quad \text{[AASHTO LRFD BDS Eq. 5.9.3.4.3a-1]}$$

where:
$\quad \varepsilon_{bdf} = \varepsilon_{bif} - \varepsilon_{bid}$

in which:

$\quad \varepsilon_{bdf} \quad = \quad$ UHPC shrinkage strain for the period between deck placement and final time
$\quad \varepsilon_{bif} \quad = \quad$ UHPC shrinkage strain for the period between prestress transfer and final time (in./in.)
$\quad\quad\quad = \quad 0.6 \times 10^{-3} k_s k_{hs} k_f k_{tdf} K_4$

Therefore:

$\quad \varepsilon_{bif} \quad = \quad 0.6 \times 10^{-3}(1.0)(0.770)(1.0)(1.523)(0.41) = 0.000288$

$\quad \varepsilon_{bdf} \quad = \quad \varepsilon_{bif} - \varepsilon_{bid} = 0.000054$

$\quad \Delta f_{pSD} \quad = \quad (0.000054)(28{,}500)(0.740) = 1.140 \text{ ksi}$

C6.3.3. Relaxation of Prestressing Strands

The prestress loss due to relaxation of the prestressing strands in the composite section between time of deck placement and final time is taken equal to the loss due to the relaxation between time of prestress transfer and deck placement. Therefore:

$$\Delta f_{pR2} = \Delta f_{pR1} = 0.929 \text{ ksi} \qquad \text{[AASHTO LRFD BDS Eq. 5.9.3.4.3c-1]}$$

C6.3.4. Shrinkage of Deck Concrete

The prestress gain due to shrinkage of deck concrete is:

$$\Delta f_{pSS} = \frac{E_p}{E_c} \Delta f_{cdf} K_{df} \left[1 + 0.7 \Psi\left(t_f, t_d\right)\right] \qquad \text{[AASHTO LRFD BDS Eq. 5.9.3.4.3d-1]}$$

where Δf_{cdf} is the change in UHPC stress at the centroid of prestressing strands due to shrinkage of conventional concrete deck (ksi), calculated according to the following equation:

$$\Delta f_{cdf} = \frac{\varepsilon_{ddf} A_d E_{cD}}{1 + 0.7 \Psi_D\left(t_f, t_d\right)} \left(\frac{1}{A_c} - \frac{e_{pc} e_d}{I_c}\right) \qquad \text{[AASHTO LRFD BDS Eq. 5.9.3.4.3d-2]}$$

in which:

$\varepsilon_{ddf,D}$ = shrinkage strain of conventional concrete deck for the period between deck placement and final time (in./in.)

A_d = area of conventional concrete deck = 9 in. × 108 in. = 972 in.^{2}

$\Psi_D(t_f, t_d)$ = creep coefficient of conventional concrete at the final time, t_f, due to loading shortly after deck placement, t_d

e_d = eccentricity to the centroid of the conventional concrete deck with respect to the gross composite section (in.)

= $y_{tc} - (t_D/2) = 23.24 - (9.0/2) = 18.74$ in.

Assuming that the strength of the concrete at initial loading, f'_{cDi}, is 0.8(4.0) = 3.2 ksi, the strain due to shrinkage for the conventional concrete deck at final time, $\varepsilon_{sh,D}$, can be calculated as follows:

$$\varepsilon_{sh,D} = k_{s,D} \, k_{hs,D} \, k_{f,D} \, k_{td,D} \, 0.48 \times 10^{-3} \qquad \text{[AASHTO LRFD BDS Eq. 5.4.2.3.3-1]}$$

where:

$k_{s,D}$ = factor for the effect of the volume to surface ratio of the deck, calculated according to AASHTO LRFD BDS Eq. 5.4.2.3.2-2

= $1.45 - 0.13(V/S) = 1.45 - 0.13(3.940) = 0.938 \geq 1.0$, thus $k_{s,D} = 1.0$

$k_{hs,D}$ = humidity factor for shrinkage of conventional concrete deck, calculated according to AASHTO LRFD BDS Eq. 5.4.2.3.3-2

= $2 - 0.014 H = 2 - 0.014 \times 73 = 0.978$

$k_{f,D}$ = factor for the effect of conventional concrete strength, calculated according to AASHTO LRFD BDS Eq. 5.4.2.3.2-4

= $\dfrac{5}{1 + f'_{cDi}} = \dfrac{5}{1 + 3.2} = 1.190$

$k_{td,D}$ = time development factor for the conventional concrete deck between deck placement and final time, calculated according to AASHTO LRFD BDS Eq. 5.4.2.3.2-5

$$= \frac{t}{12\left(\frac{100-4f'_{cDi}}{f'_{cDi}+20}\right)+t} = \frac{19,910}{12\left(\frac{100-4(3.2)}{3.2+20}\right)+19,910} = 0.998$$

in which:

V/S = volume to surface ratio of the conventional concrete deck (in.)

$$= \frac{b_e\, t_D}{2b_e+2t_D} = 4.154 \text{ in.}$$

t = maturity of conventional concrete in days, taken as the time being considered for analysis of creep or shrinkage effects $= t_f - t_d = 20,000 - 90 = 19,910$ days

Therefore:

$$\varepsilon_{sh,D} = (1.0)(0.978)(1.190)(0.998)(0.48 \times 10^{-3}) = 0.000558$$

The creep coefficient of the conventional concrete deck at final time due to loading shortly after deck placement, $\Psi_D(t_f, t_d)$, can be calculated according to the following equation:

$$\Psi_D(t_f, t_d) = 1.9 k_{s,D}\, k_{hc,D}\, k_f\, k_{td,D}\, t_{iD}^{-0.118} \qquad \text{[AASHTO LRFD BDS Eq. 5.4.2.3.2-1]}$$

where:

$k_{hc,D}$ = humidity factor for creep of conventional concrete deck, calculated according to AASHTO LRFD BDS Eq. 5.4.2.3.2-3
$= 2 - 0.008\, H = 2 - 0.008(73) = 0.976$

t_{iD} = age of conventional concrete deck at time of loading, taken as 1 day after casting

Therefore:

$$\Psi_D(t_f, t_d) = 1.9(1.0)(0.976)(1.190)(0.998)(1^{-0.118}) = 2.203.$$

The change in UHPC stress at the centroid of prestressing strands, Δf_{cdf}, can now be calculated as:

$$\Delta f_{cdf} = \frac{(0.000558)(972)(3,987)}{1+0.7(2.203)}\left(\frac{1}{1,090.30} - \frac{(34.13)(18.74)}{600,476.2}\right)$$

$$= -0.125 \text{ ksi}$$

Note that the negative sign indicates a prestress gain.

Finally, the prestress gain due to shrinkage of the deck can be computed as follows:

$$\Delta f_{pSS} = \frac{28,500}{6,933}(-0.125)(0.740)[1+0.7(0.551)] = -0.529 \text{ ksi}$$

The effect of deck shrinkage on the UHPC stresses should be analyzed by considering it as an external force applied to the composite nontransformed section. One hundred percent of the effect due to deck shrinkage on the prestress losses and UHPC stresses is considered according to AASHTO LRFD BDS Eq. 5.9.3.4.3d-2.

C6.4. TOTAL TIME-DEPENDENT LOSSES

The total time-dependent loss is:

$$\Delta f_{pLT} = (\Delta f_{pSR} + \Delta f_{pCR} + \Delta f_{pR1}) + (\Delta f_{pSD} + \Delta f_{pCD} + \Delta f_{pR2} + \Delta f_{pSS})$$

[AASHTO LRFD BDS Eq. 5.9.3.4.1-1]

$$= (4.907 + 18.958 + 0.929) + (1.140 - 1.898 + 0.929 - 0.529)$$

$$= 24.44 \text{ ksi}$$

C6.5. TOTAL LOSSES AT PRESTRESS TRANSFER

AASHTO LRFD BDS Articles C5.9.5.2.3a and C5.9.5.3 state that the losses or gains due to elastic deformation must be taken equal to zero if transformed section properties are used in stress analysis. However, the losses or gains due to elastic deformation must be included in determining the total prestress losses and effective stress in the prestressing strands.

The stresses and forces in the prestressing strand immediately after transfer are as follows:

Total prestress loss: $\Delta f_{pi} = \Delta f_{pES} = 29.67$ ksi.

Stress in strands: $f_{pt} = f_{pi} - \Delta f_{pi} = 202.5 - 29.67 = 172.83$ ksi.

Force in one strand $= (f_{pt})(A_s) = 172.83(0.294) = 50.81$ kips.

Total prestressing force after transfer, $P_{pt} = 50.81(50) = 2{,}540.6$ kips.

Initial loss, in percent $= (\Delta f_{pi})/f_{pi} = 29.67/202.5 = 14.65$ percent.

For determining concrete stresses using transformed section properties, strand force is the force before transfer:

Force per strand $= (202.5)(0.294) = 59.54$ kips.

Total prestressing force before transfer, $P_{pi} = 2{,}976.75$ kips.

C6.6. TOTAL LOSSES AT SERVICE LOADS

The total prestress loss due to elastic shortening and long-term losses is:

$$\Delta f_{pT} = \Delta f_{pES} + \Delta f_{pLT} = 29.67 + 24.44 = 54.11 \text{ ksi}$$

The elastic gain due to deck weight, superimposed dead load, and live load is:

$$\left(\frac{M_{D,m}e_{tf}}{I_{tf}} + \frac{(M_{b,m}+M_{ws,m})e_{tc}}{I_{tc}}\right)\frac{E_p}{E_c} + \left(\frac{(M_{LT,m}+M_{LL,m})e_{tc}}{I_{tc}}\right)\frac{E_p}{E_c}$$

$$= \left(\frac{(2{,}901.4)(12)(14.07)}{223{,}502.9} + \frac{(281.3+543.8)(12)(32.75)}{655{,}702.7}\right)\frac{28{,}500}{6{,}933}$$

$$+ \left(\frac{(2{,}106.4+1{,}178.0)(12)(32.75)}{655{,}702.7}\right)\frac{28{,}500}{6{,}933}$$

$$= 11.04 + 8.09 = 19.13 \text{ ksi}$$

in which:

$M_{LT,m}$ = bending moment at midspan due to truck load = 2,106.4 kip-ft
$M_{LL,m}$ = bending moment at midspan due to lane load = 1,178.0 kip-ft

The stresses and forces in the prestressing strand after all losses and permanent gains (gains due to M_D, M_b, and M_{ws}) are as follows:

Effective prestress: $f_{pe} = f_{pi} - \Delta f_{pT} + 11.04 = 202.5 - 54.11 + 11.04 = 159.43$ ksi.

Force per strand = $(f_{pe})(A_s) = (159.43)(0.294) = 46.87$ kips.

Total prestressing force, $P_{pe} = 46.87(50) = 2{,}343.6$ kips.

Final loss, in percent = (*total losses and permanent gains*)/(f_{pi}) = (202.5 − 159.43)/(202.5) = 21.27 percent.

Final loss without consideration of prestressing gain at deck placement = $\Delta f_{pT}/f_{pi}$ = 54.11/202.5 = 26.72 percent.

CHAPTER C7. UHPC STRESSES AT PRESTRESS TRANSFER

C7.1. STRESS LIMITS FOR UHPC AT PRESTRESS TRANSFER, BEFORE LOSSES

The stress limits for UHPC at transfer and before losses are defined as follows:

Compression: $0.65\,f'_{ci} = 0.65(14) = +9.100$ ksi   [UHPC Guide Article 1.9.2.3.1a]

Tension: $-\gamma_u f_{t,cri} = -1.00(0.750) = -0.750$ ksi   [UHPC Guide Article 1.9.2.3.1b]

C7.2. STRESSES AT TRANSFER LENGTH SECTION

Stresses at the transfer length section will only be checked at transfer in this example because this stage almost always controls.

Transfer length, $\ell_t = \xi 24 D_p = 0.75(24)(0.7) = 12.6$ in. $= 1.05$ ft

where ξ is the factor for transfer length, taken as 0.75 because shorter transfer lengths result in more severe stress states within the section.   [UHPC Guide Eq. 1.9.4.3.1-1]

The moment due to self-weight of the beam at the transfer length section is:

$$M_{gT,tr} = 0.5 w_g\, \ell_t\, (L_T - \ell_t) = (0.5)(0.6048)(1.05)(151-1.05) = 47.61 \text{ kip-ft}$$

where:
$w_g = \omega_c\, A_g = 0.6048$ kip/ft.

The stress in the extreme top fiber of the UHPC girder, assuming all strands are bonded at the ends:

$$\frac{P_{pi}}{A_{ti}} - \frac{P_{pi}\, e_{ti}}{S_{tti}} + \frac{M_{g,tr}}{S_{tti}} = \frac{2{,}976.75}{599.8} - \frac{(2{,}976.75)(13.84)}{6{,}750} + \frac{(47.61)(12)}{6{,}750} = -1.056 \text{ ksi}$$

Tensile stress limit for UHPC is −0.750 ksi.
Not acceptable.

The stress in the extreme bottom fiber of the UHPC girder, assuming all strands are bonded at the ends:

$$\frac{P_{pi}}{A_{ti}} + \frac{P_{pi}\, e_{ti}}{S_{bti}} - \frac{M_{g,tr}}{S_{bti}} = \frac{2{,}976.75}{599.8} + \frac{(2{,}976.75)(13.84)}{11{,}048} - \frac{(47.61)(12)}{11{,}048} = +8.640 \text{ ksi}$$

Compressive stress limit for UHPC is +9.100 ksi.
OK.

Since the stresses at the top of the beam exceed the tensile stress limit of −0.750 ksi, a number of strands must be debonded to reduce the top tensile stresses. In this example, six strands must be

debonded in the girder bottom flange near the ends to meet the tensile stress limit at release at the transfer length section. However, 14 strands are debonded to lower the bursting stresses and adequately reinforce the girder at the pretensioned anchorage zones, as described in Section C14.1 of Appendix C.

C7.3. RECOMPUTED STRESSES AT TRANSFER LENGTH SECTION WITH 14 STRANDS DEBONDED

The stress at extreme top fiber of the UHPC girder, after debonding 14 strands at ends:

$$f_{tiE} = \frac{P_{piE}}{A_{tiE}} - \frac{P_{piE}\,e_{tiE}}{S_{ttiE}} + \frac{M_{g,tr}}{S_{ttiE}} = \frac{2{,}143.26}{584.3} - \frac{(2{,}143.26)(13.46)}{6{,}713} + \frac{(47.61)(12)}{6{,}713} = -0.544 \text{ ksi}$$

Tensile stress limit for UHPC is −0.750 ksi
OK.

Compute stress in the bottom of the beam:

$$f_{biE} = \frac{P_{piE}}{A_{tiE}} + \frac{P_{piE}\,e_{tiE}}{S_{btiE}} - \frac{M_{g,tr}}{S_{btiE}} = \frac{2{,}143.26}{584.3} + \frac{(2{,}143.26)(13.46)}{10{,}629} - \frac{(47.61)(12)}{10{,}629} = +6.328 \text{ ksi}$$

Compressive stress limit for UHPC is +9.100 ksi
OK.

C7.4. STRESSES AT MIDSPAN

The stress in the extreme top fiber of the UHPC girder is calculated as follows:

$$f_{ti} = \frac{P_{pi}}{A_{ti}} - \frac{P_{pi}\,e_{ti}}{S_{tti}} + \frac{M_{gT,m}}{S_{tti}}$$

where $M_{gT,m}$ is the moment due to self-weight of the beam at midspan, calculated as:

$$M_{gT,m} = 0.5 w_g\, x(L_T - x) = (0.5)(0.6048)(75.5)(151 - 75.5) = 1{,}724 \text{ kip-ft.}$$

Therefore:

$$f_{ti} = \frac{P_{pi}}{A_{ti}} - \frac{P_{pi}\,e_{ti}}{S_{tti}} + \frac{M_{gT,m}}{S_{tti}} = \frac{2{,}976.75}{599.8} - \frac{(2{,}976.75)(13.84)}{6{,}750} + \frac{(1{,}724)(12)}{6{,}750} = +1.924 \text{ ksi}$$

Tensile stress limit for UHPC is −0.750 ksi.
OK.

The compressive stress in the bottom of the beam is calculated as follows:

$$f_{bi} = \frac{P_{pi}}{A_{ti}} + \frac{P_{pi}\,e_{ti}}{S_{bti}} - \frac{M_{gT,m}}{S_{bti}} = \frac{2{,}976.75}{599.8} + \frac{(2{,}976.75)(13.84)}{11{,}048} - \frac{(1{,}724)(12)}{11{,}048} = +6.820 \text{ ksi}$$

Compressive stress limit for UHPC is +9.100 ksi.
OK.

C7.5. SUMMARY OF STRESSES AT TRANSFER

Table C7.5-1 shows a summary of the stresses at transfer.

Table C7.5-1. Stresses at transfer.

Location	Top Fiber Stresses (ksi)	Bottom Fiber Stresses (ksi)
At transfer length	−0.544	6.328
At midspan	1.924	6.820

C7.6. PRINCIPAL TENSILE STRESS IN THE WEB OF THE GIRDER

The provisions of UHPC Guide Article 1.9.2.3.3 and AASHTO LRFD BDS Article 5.9.2.3.3 state that the maximum principal stress at any location along the height of the web shall not exceed $\gamma_u f_{t,cr}$ when the superstructure element is subject to the loadings of Service III limit state of AASHTO LRFD BDS Article 3.4.1, both before and after all losses.

The principal tensile stress limit before losses is $\gamma_u f_{t,cri} = 1.00(-0.750) = -0.750$ ksi.

The principal stress determination may be based on the analysis using Mohr's circle:

$$f_{min} = \frac{1}{2}\left[\left(f_{pcx} + f_{pcy}\right) - \sqrt{\left(f_{pcx} + f_{pcy}\right)^2 + (2\tau)^2}\right] \qquad \text{[AASHTO LRFD BDS Article 5.9.2.3.3-4]}$$

where:
  f_{min} = minimum principal stress in the web with the tension taken as a negative value (ksi)
  f_{pcx} = horizontal stress in the web (ksi)
  f_{pcy} = vertical stress in the web = 0 ksi
  τ = shear stress in web (ksi)

For open sections that may be considered thin walled, such as typical I-girders and bulb-tee girders:

$$\tau = \frac{VQ_g}{I_g b_w} \qquad \text{[AASHTO LRFD BDS Article 5.9.2.3.3-1]}$$

where:
  V = shear force for Service III load combination (kip)
  Q_g = first moment about the neutral axis of the gross concrete area above or below the height of the web where the principal tension is being checked (in.^{3})
  b_w = web width at the height of the web where principal tension is being checked (in.)

AASHTO LRFD BDS Article 5.9.2.3.3 recommends calculating the principal stress at multiple locations in the web.

In this design example, the principal tensile stress check will only be computed at the transfer length section and at two locations in the web:(1) at the centroid of the UHPC gross section (location of maximum shear stress); and (2) at the top of the web are computed (location of maximum longitudinal tensile stress in the web). Note that principal tensile stress calculations are presented herein for illustration purposes. To complete the principal tensile stress check at transfer of prestress, the principal stresses in the web must be computed at multiple locations within the web and at regular intervals along the length of the beam.

C7.6.1. Principal Stress at the Centroid of the UHPC Gross Section

The first moment of the area is calculated using the UHPC area below or above the centroid of the gross UHPC area (y_b = 21.89 in.): Q_g = 4,892.91 in.^{3}.

The applied shear force at the transfer length section at release is conservatively computed at beam ends such as $V = 0.5w_g\,L_T = (0.5)(0.6048)(151) = 45.66$ kips.

The shear stress in the web at the centroid of the UHPC gross section, y_b = 21.89 in., can be calculated as follows:

$$\tau = \frac{VQ_g}{I_g b_w} = \frac{(45.66)(4,892.91)}{(209,570.6)(3.5)} = 0.305 \text{ ksi}$$

The horizontal stress in the web at the neutral axis of the gross UHPC section, y_b = 21.89 in., can be determined from elastic analysis as follows:

$$f_{pcx} = f_{biE} - \frac{-f_{tiE} + f_{biE}}{h} y_b = 6.328 - \frac{0.544 + 6.328}{54}(21.89) = 3.542 \text{ ksi}$$

The maximum principal tension stress is:

$$f_{min} = \frac{1}{2}\left[(3.542+0) - \sqrt{(3.542+0)^2 + (2\times0.305)^2}\right] = -0.026 \text{ ksi}$$

Tensile stress limit for UHPC is −0.750 ksi.
OK.

C7.6.2. Principal Stress at Top of the Web

The top of the web is located at a distance of 41.44 in. from the bottom of the girder. The first moment of area at this location is calculated using the UHPC area of the section above or below the top of the web: Q_g = 4,223.99 in.^{3}.

$$\tau = \frac{VQ_g}{I_g b_w} = \frac{(45.66)(4,223.99)}{(209,570.6)(3.5)} = 0.263 \text{ ksi}$$

$$f_{pcx} = f_{biE} - \frac{-f_{tiE} + f_{biE}}{h}(41.44) = 6.328 - \frac{0.544 + 6.328}{54} \times 41.44 = +1.054 \text{ ksi}$$

The maximum principal tension stress is:

$$f_{min} = \frac{1}{2}\left[(1.054+0) - \sqrt{(1.054+0)^2 + (2(0.263))^2}\right] = -0.062 \text{ ksi}$$

Tensile stress limit for UHPC is −0.750 ksi.
OK.

CHAPTER C8. CONCRETE STRESSES AT SERVICE LOADS

C8.1. STRESS LIMITS FOR UHPC GIRDER AND CONVENTIONAL CONCRETE DECK AT FINAL TIME, AFTER LOSSES

The stress limits for UHPC girder and conventional concrete deck at final time after losses are calculated as follows:

- Compression:

  Due to the sum of effective prestress and permanent loads, for load combination Service I the following values area selected.

  For precast beams: $0.45 f'_c = 0.45(22) = +9.900$ ksi.
  For deck: $0.45 f'_{cD} = 0.45(4) = +1.800$ ksi.

  Due to permanent and transient loads, for load combination Service I the following values are selected.

  For precast beams: $0.60 f'_c = 0.60(22) = +13.20$ ksi.
  For deck: $0.60 f'_{cD} = 0.60(4) = +2.400$ ksi.

- Tension:

  For components with bonded prestressing tendons the following values are selected.

  For load combination Service III: $- \gamma_u f_{t,cr}$.
  For precast beam: $-1.00(1.00) = -1.00$ ksi.

  For deck concrete, a stress limit of 0.000 ksi is selected.

  Note that for members subject to fatigue loads, the UHPC tensile stress due to Service I load combination must not exceed $0.95\gamma_u f_{t,cr} = 0.95(1.00)(1.00) = 0.95$ ksi, as described in Section C9.2.2 of this Appendix and UHPC Guide Article 1.5.3. In this design example, the tensile stresses due to Service I and Service III are identical; therefore, the tension stress due to Service III must not exceed 0.95 ksi for the member to pass the fatigue limit state requirements of UHPC Guide Article 1.5.3.

C8.2. STRESSES AT MIDSPAN

UHPC stresses at service loads are found by superposition of the following components:

- Instantaneous elastic stresses at transfer, using the precast transformed section properties.

- Long-term effects between transfer and deck placement, applied to the precast gross section properties.

- Instantaneous elastic stresses at deck placement using precast transformed section properties.

- Instantaneous elastic stresses due to superimposed dead loads, using composite transformed section properties.

- Long-term effects between deck placement and final time, except for effects of deck shrinkage, applied to the composite section properties.

- Long-term effects of deck shrinkage.

- Instantaneous elastic stresses due to live loads using composite transformed section properties.

The calculations for each of these items are detailed as follows.

A. At transfer, as previously calculated in Section C7.4 of this Appendix:

Stress at top of UHPC girder $= f_{ti} = +1.924$ ksi.

Stress at bottom of UHPC girder $= f_{bi} = +6.820$ ksi.

Stress in UHPC at the level of the steel centroid, $f_{cgp} = 6.218$ ksi.

Instantaneous prestress losses at transfer, $\Delta f_{pi} = 29.67$ ksi.

Stress in steel at transfer, $f_{pt} = f_{pi} - \Delta f_{pi} = 173.83$ ksi.

B. Between transfer and deck placement:

Long-term loss of steel stress, $\Delta f_{pLTD} = \Delta f_{pSR} + \Delta f_{pCR} + \Delta f_{pR1} = 24.80$ ksi.

Long-term loss of steel force, $\Delta P_{pLTD} = \Delta f_{pLTD} (A_{ps}) = 364.5$ kips.

This force is applied as a negative prestress to the precast UHPC section.

Change in stress at top of UHPC girder, $\Delta f_{tLTD} = (-\Delta P_{pLTD})/A_g + \Delta P_{pLTD} (e_{pg})/S_t = +0.182$ ksi.

Change in stress at bottom of UHPC girder,
$\Delta f_{bLTD} = (-\Delta P_{pLTD})/A_g - \Delta P_{pLTD} (e_{pg})/S_b = -1.250$ ksi.

C. At deck placement:

$M_{D,m} = 2{,}901.4$ kip-ft.

The moment due to deck weight is applied to the noncomposite transformed section at the final time.

Change in stress at top of UHPC girder, $\Delta f_{tD} = M_{D,m}/S_{ttf} = 2{,}901.4(12)/6{,}713 = +5.186$ ksi.

Change in stress at bottom of UHPC girder,
$\Delta f_{bD} = -M_{D,m}/S_{btf} = -2,901.4(12)/10,793 = -3.226$ ksi.

Change in stress in UHPC at the level of steel, $\Delta f_{cD} = (-M_{D,m} \, e_{tf})/I_{tf} = -2.192$ ksi.

Prestress gain at centroid of prestressing steel, $\Delta f_{pD} = \Delta f_{cD} \, E_p/E_c = -9.01$ ksi.

D. Due to superimposed dead load:

$M_{SIDL} = M_{b,m} + M_{ws,m} = 825.0$ kip-ft.

Moment due to superimposed dead load is applied to the composite transformed section at final time.

Change in stress at top of UHPC girder, $\Delta f_{tSIDL} = M_{SIDL}/S_{ttc} = +0.221$ ksi.

Change in stress at bottom of UHPC girder, $\Delta f_{bSIDL} = -M_{SIDL}/S_{btc} = -0.595$ ksi.

Change in stress in UHPC at the level of steel, $\Delta f_{cSIDL} = -M_{SIDL} \, e_{tc}/I_{tc} = -0.494$ ksi.

Prestress gain in steel at centroid, $\Delta f_{pSIDL} = \Delta f_{cSIDL} \, E_p/E_c = -2.033$ ksi.

Change in stress at top of the concrete deck, $\Delta f_{dtSIDL} = M_{SIDL}/S_{dtc} = 0.214$ ksi.

Change in stress at bottom of the concrete deck,
$\Delta f_{dbSIDL} = (E_{cD}/E_c)(M_{SIDL} \, (y_{ttc} - t_s - t_h)/I_{tc}) = 0.127$ ksi.

E. Long-term effects between deck placement and final time, except for deck shrinkage:

Change in steel stress due to shrinkage and creep of girder and relaxation strand,
$\Delta f_{pLDF} = \Delta f_{pSD} + \Delta f_{pCD} + \Delta f_{pR2} = 0.172$ ksi.

Long term loss of prestress force, $\Delta P_{pLDF} = \Delta f_{pLDF} \, A_{ps} = 2.524$ kip.

This force is applied as a positive prestress to the composite section.

Change in stress at top of UHPC girder,
$\Delta f_{tLDF} = -\Delta P_{pLDF}/A_c - (-\Delta P_{pLDF}) \, (y_{bc} - y_{bs})/S_{tc} = -0.00040$ ksi.

Change in stress at bottom of UHPC girder,
$\Delta f_{bLDF} = -\Delta P_{pLDF}/A_c + (-\Delta P_{pLDF})(y_{bc} - y_{bs})/S_{bc} = -0.008$ ksi.

Change in stress at top of the concrete deck,

$$\Delta f_{dtLDF} = \frac{E_{cD}}{E_c}\left(\frac{-\Delta P_{pLDF}}{A_c} - \frac{-\Delta P_{pLDF}\left(y_{bc} - y_{bs}\right)y_{tc}}{I_c}\right) = 0.001 \text{ ksi.}$$

Change in stress at bottom of the concrete deck,

$$\Delta f_{dbLDF} = \frac{E_{cD}}{E_c}\left(\frac{-\Delta P_{pLDF}}{A_c} - \frac{-\Delta P_{pLDF}(y_{bc} - y_{bs})(y_{tc} - t_s - t_h)}{I_c}\right) = -0.00024 \text{ ksi.}$$

F. Long-term effect of deck shrinkage:

The change in steel stress due to deck shrinkage is a stress gain. The deck shrinkage creates a sagging of the girder. Effects on the girder are represented by a compressive force acting at the center of the deck. AASHTO LRFD BDS Eq. 5.9.5.4.3d-2 can be used to calculate the stress at the top and bottom fibers by replacing eccentricity of prestressing steel with those of the top and bottom fibers of the girder.

Restraining force due to shrinkage of conventional concrete is calculated as:

$$\Delta P_{ds} = \frac{\varepsilon_{ddf} A_d E_{cD}}{1 + 0.7 \Psi_D(t_f, t_d)} = \frac{(0.0006)(972)(3,987)}{1 + 0.7(2.203)} = 850.0 \text{ kip}$$

This force is applied at the center of the deck with an eccentricity from the center of the deck to the composite center, $e_d = y_{tc} - t_D/2 = 18.74$ in.

The corresponding change in top and bottom fiber stresses in the UHPC girder, Δf_{tSS} and Δf_{bSS}, respectively, are calculated below using composite nontransformed section and assuming the force is 100 percent effective:

$$\Delta f_{tSS} = \frac{\Delta P_{ds}}{A_c} + \frac{\Delta P_{ds} e_d}{S_{tg}} = 1.131 \text{ ksi}$$

$$\Delta f_{bSS} = \frac{\Delta P_{ds}}{A_c} - \frac{\Delta P_{ds} e_d}{S_{bc}} = -0.302 \text{ ksi}$$

Change in stress at level of steel centroid, $\Delta f_{cdf} = -0.125$ ksi.

Stress gain in steel at centroid from Section C6.3.4 of this Appendix, $\Delta f_{pSS} = -0.529$ ksi.

The change in stresses in the deck due to deck shrinkage are considered in this design example.

G. Due to live load (service load):

Bending moment due to service load is applied to the composite transformed section at final time,

$$M_{SL} = M_{LT,m} + M_{LL,m} = 3,284.4 \text{ kip-ft}$$

Change in stress at top of UHPC girder $\Delta f_{tSL} = M_{SL}/S_{ttc} = 0.878$ ksi.

Change in stress at bottom of UHPC girder $\Delta f_{bSL} = -M_{SL}/S_{btc} = -2.368$ ksi.

Change in stress in UHPC at the level of steel, $\Delta f_{cSL} = (-M_{SL}\,e_{tc})/I_{tc} = -1.969$ ksi.

Stress gain in steel at centroid, $\Delta f_{pSL} = (\Delta f_{cSL}\,E_p)/E_c = -8.092$ ksi.

Change in stress at top of the concrete deck, $\Delta f_{dtSL} = M_{SL}/S_{dtc} = 0.851$ ksi.

Change in stress at bottom of concrete deck,

$$\Delta f_{dbSL} = \frac{E_{cD}}{E_c}\left(\frac{(M_{SL})(y_{ttc} - t_s - t_h)}{I_{tc}}\right) = 0.505 \text{ ksi}$$

C8.2.1. Net UHPC Girder Stresses

Based on these calculations, the net UHPC girder stresses at midspan are as follows.

At deck placement:	Top fiber stress $= f_{ti} + \Delta f_{tLTD} + \Delta f_{tD} = +7.292$ ksi	
	Bottom fiber stress $= f_{bi} + \Delta f_{bLTD} + \Delta f_{bD} = +2.344$ ksi	
	No stress limits need to be checked for this loading stage.	

At service (no live load):

Top fiber stress $= f_{ti} + \Delta f_{tLTD} + \Delta f_{tD} + \Delta f_{tSIDL} + \Delta f_{tLDF} + \Delta f_{tSS}$

$\qquad = +8.643$ ksi $< +9.900$ ksi   OK.

Bottom fiber stress $= f_{bi} + \Delta f_{bLTD} + \Delta f_{bD} + \Delta f_{bSIDL} + \Delta f_{bLDF} + \Delta f_{bSS}$

$\qquad = +1.439$ ksi > -1.00 ksi   OK.

At service (including live load):

Top fiber stress $= f_{ti} + \Delta f_{tLTD} + \Delta f_{tD} + \Delta f_{tSIDL} + \Delta f_{tLDF} + \Delta f_{tSS} + f_{tSL}$

$\qquad = +9.521$ ksi $< +13.20$ ksi   OK.

Bottom fiber stress $= f_{bi} + \Delta f_{bLTD} + \Delta f_{bD} + \Delta f_{bSIDL} + \Delta f_{bLDF} + \Delta f_{bSS} + f_{bSL}$

$\qquad = -0.929$ ksi > -1.00 ksi   OK.

Tensile stress limit due to Service I for members subjected to fatigue loads is -0.95 ksi (see Section C9.2.2 of this Appendix for details).   OK.

C8.2.2. Net Conventional Concrete Deck Stresses

Based on these calculations, the net conventional concrete deck stresses at midspan are as follows.

At service (no live load):

Stress at top of deck, $\Delta f_{dtSIDL} + \Delta f_{dtLDF} = +0.215$ ksi $< +1.800$ ksi   OK.

Stress at bottom of deck/haunch,

$\Delta f_{dbSIDL} + \Delta f_{dbLDF} = +0.127$ ksi > 0.000 ksi; $< +1.800$ ksi   OK.

At service
(including live
load):

Stress at top of deck,

$\Delta f_{dtSIDL} + \Delta f_{dtLDF} + f_{dtSL} = +1.066 \text{ ksi} < +2.400 \text{ ksi}$ OK.

Stress at bottom of deck/haunch,

$\Delta f_{dbSIDL} + \Delta f_{dbLDF} + f_{dbSL} = +0.632 \text{ ksi} > 0.000 \text{ ksi}$ OK.

C8.3. PRINCIPAL TENSILE STRESS IN WEBS

The provisions of UHPC Guide Article 1.9.2.3.3 and AASHTO LRFD BDS Article 5.9.2.3.3 state that the maximum principal stress at any location along the height of the web shall not exceed $\gamma_u f_{t,cr}$ when the superstructure element is subject to the loadings of Service III limit state of AASHTO LRFD BDS Article 3.4.1, both before and after all losses.

The principal tensile stress limit at service limit state after losses is:

$\gamma_u f_{t,cr} = 1.00(-1.00) = -1.00 \text{ ksi}$

For precast sections made composite with a cast-in-place deck, AASHTO LRFD BDS Article C5.9.2.3.3 recommends calculating the principal tensile stress at both the noncomposite and the composite neutral axes using the shear stress and axial stress at each location.

In this design example, the principal tensile stress check will only be computed at the critical shear location (location of highest shear force per UHPC Guide Article 1.7.3.2; See Section C11.1 of this Appendix for critical shear force location calculations) and at two locations in the web: (1) at the centroid of the noncomposite gross section; and (2) at the centroid of the noncomposite, nontransformed cross section. Note that principal tensile stress calculations are presented herein for illustration purposes. To complete the principal tensile stress check at transfer of prestress, the principal stresses in the web must be computed at multiple locations within the web and at regular intervals along the length of the beam.

C8.3.1. Principal Stress at the Centroid of the Noncomposite Gross Section

The first moment of area of the composite nontransformed section at the centroid of the noncomposite UHPC gross section ($y_b = 21.89$ in.) is $Q_{gc} = 11,021.13 \text{ in.}^3$.

The shear force applied to the UHPC gross section at the critical shear location at service (see Table C4.1.2-1) is:

$V_{g1} = V_{g,crs} + V_{D,crs} = 42.6 + 72.6 = 115.2 \text{ kip}$

The shear force applied to the composite nontransformed gross section at the critical shear location at service (see Table C4.1.2-1 and Table C4.2.4.1-1) is:

$V_{g2} = V_{b,crs} + V_{ws,crs} + V_{LT,crs} + V_{LL,crs} = 7.0 + 13.6 + 76.6 + 39.9 = 137.1 \text{ kip}$

The shear stress at the centroid of the noncomposite UHPC gross section, $y_b = 21.89$ in., is as follows:

$$\tau = \frac{V_{g1}Q_g}{I_g b_w} + \frac{V_{g2}Q_{gc}}{I_c b_w} = \frac{(115.2)(4,892.91)}{(209,570.6)(3.5)} + \frac{(137.1)(11,021.13)}{(600,476.2)(3.5)} = 0.768 + 0.719 = 1.487 \text{ ksi}$$

The horizontal stress in the web at $y_b = 21.89$ in. at the critical shear location at service can be determined from an elastic analysis following the procedures of Section C8.2.1 of this Appendix but using the applied moments at the critical shear location given in Table C4.1.2-1 and Table C4.2.4.1-1.

Assuming that (1) all 14 strands are debonded at the critical shear section (see Section C11.1 of this Appendix for details), (2) the change in stresses due to all prestress losses and gain due to conventional concrete deck shrinkage at the critical shear location is the same as those calculated at midspan in Section C8.2.1, and (3) that using the gross section properties of the girder and composite sections to determine the stresses due to the applied loads is sufficiently adequate (instead of transformed section properties at ends at final time), the top and bottom fiber stresses at the critical shear location can be calculated as follows:

Top fiber stress:

$$= \frac{P_{piE}}{A_{tiE}} - \frac{P_{piE}\, e_{tiE}}{S_{ttiE}} + \frac{M_{g,crs}}{S_{ttiE}} + \Delta f_{tLTD} + \frac{M_{D,crs}}{S_t} + \frac{M_{b,crs} + M_{ws,crs}}{S_{tc}} + \Delta f_{tLDF} + \Delta f_{tSS}$$

$$+ \frac{M_{LT,crs} + M_{LL,crs}}{S_{tc}}$$

$$= \frac{2,143.26}{584.3} - \frac{(2,143.26)(13.46)}{6,713} + \frac{202.3(12)}{6,713} + 0.182 + \frac{345.0(12)}{6,526.6} + \frac{(33.4 + 64.7)(12)}{44,945.9}$$

$$-0.00040 + 1.131 + \frac{(260.7 + 140.1)(12)}{44,945.9}$$

$$= 3.668 - 4.297 + 0.362 + 0.182 + 0.634 + 0.026 - 0.00040 + 1.131 + 0.107$$

$$= 1.812 \text{ ksi (compressive stress)}$$

Bottom fiber stress:

$$= \frac{P_{piE}}{A_{tiE}} + \frac{P_{piE}\, e_{tiE}}{S_{btiE}} - \frac{M_{g,crs}}{S_{btiE}} + \Delta f_{bLTD} - \frac{M_{D,crs}}{S_b} - \frac{M_{b,crs} + M_{ws,crs}}{S_{bc}} + \Delta f_{bLDF} + \Delta f_{bSS}$$

$$- \frac{M_{LT,crs} + M_{LL,crs}}{S_{bc}}$$

$$= \frac{2,143.26}{584.3} + \frac{(2,143.26)(13.46)}{10,629} - \frac{202.3(12)}{10,629} - 1.250 - \frac{345.0(12)}{9,573.8} - \frac{(33.4 + 64.7)(12)}{14,730.3}$$

$$-0.008 - 0.302 - \frac{(260.7 + 140.1)(12)}{14{,}730.3}$$

$$= 3.668 + 2.714 - 0.228 - 1.250 - 0.432 - 0.080 - 0.008 - 0.302 - 0.327$$

$$= 3.755 \text{ ksi (compressive stress)}$$

Horizontal stress at $y_b = 21.89$ in.:

$$f_{pcx} = 1.812 + \frac{(3.755 - 1.812)}{54}(54 - 21.89) = +2.967 \text{ ksi (compressive stress)}$$

The principal tension stress is:

$$f_{min} = \frac{1}{2}\left[(2.967 + 0) - \sqrt{(2.967 + 0)^2 + (2 \times 1.487)^2}\right] = -0.617 \text{ ksi}$$

Tensile stress limit for UHPC is -1.00 ksi.

Tensile stress limit due to Service I for members subjected to fatigue loads is -0.95 ksi (See Section C9.2.2 of this Appendix for details).
OK.

Note that for sections controlled by the principal tension stress limit in webs at Service III load combination or at Service I for members subjected to fatigue loads, the transformed section properties at ends at final time are recommended be used to calculate the horizontal stress, f_{pcx}, when the overall section is subjected to compression stresses. Such calculation will result in lower values of compression stresses in the section leading to lower values of f_{pcx}, and thus a more conservative prediction of principal tension stresses in webs.

C8.3.2. Principal Stress at the Centroid of the Composite Nontransformed Section

The principal tensile stress at the location of the centroid of the composite nontransformed section ($y_{bc} = 40.76$ in.) may control since it is closer to the top fiber of the UHPC section where the horizontal compression stress is lower than the stress at the bottom fiber.

At $y_{bc} = 40.76$ in.: $Q_{gc} = 11{,}644.55$ in.^{3}, and $Q_g = 4{,}269.71$ in.^{3}

$$f_{pcx} = 1.812 + \frac{(3.755 - 1.812)}{54}(54 - 40.76) = +2.288 \text{ ksi (compressive stress)}$$

$$\tau = \frac{V_{g1}Q_g}{I_g b_w} + \frac{V_{g2}Q_{gc}}{I_c b_w} = \frac{(115.2)(4{,}269.71)}{(209{,}570.6)(3.5)} + \frac{(137.1)(11{,}644.55)}{(600{,}476.2)(3.5)} = 0.670 + 0.760 = 1.430 \text{ ksi}$$

$$f_{min} = \frac{1}{2}\left[(2.288 + 0) - \sqrt{(2.288 + 0)^2 + (2 \times 1.430)^2}\right] = -0.687 \text{ ksi}$$

Tensile stress limit for UHPC is −1.00 ksi.

Tensile stress limit due to Service I for members subjected to fatigue loads is −0.95 ksi (see Section C9.2.2 of this Appendix for details).

OK.

Note that if the tension zone at service due to Service III extends to the web, checking the principal stresses at that location is recommended as well (i.e., location of maximum longitudinal stress in the web). In this example, the section at critical shear location is under compressive stresses over the whole depth.

CHAPTER C9. STEEL STRESS AT SERVICE LOADS

C9.1. SERVICE LIMIT STATE

The prestress limit at service is as follows:

For bonded prestressing tendons, for load combination Service I:

$0.80f_{py} = 0.80(243 \text{ ksi}) = 194.4 \text{ ksi}$

Stress in prestressing strands after all losses and gains at Service I limit state at level of steel centroid is as follows:

$$
\begin{aligned}
f_{peS} &= f_{pi} - \Delta f_{pES} - \Delta f_{pLTD} - \Delta f_{pD} - \Delta f_{pSIDL} - \Delta f_{pLDF} - \Delta f_{pSS} - \Delta f_{pSL} \\
&= 202.5 - 29.67 - 24.80 - (-9.01) - (-2.03) - 0.172 - (-0.529) - (-8.09) \\
&= 167.51 \text{ ksi}
\end{aligned}
$$

$f_{peS} = 167.51 \text{ ksi} \leq 194.4 \text{ ksi}$ OK.

Note that in this example Service I and Service III load combinations are identical.

C9.2. FATIGUE LIMIT STATE

C9.2.1. UHPC Compression Stress Check

UHPC Guide Article 1.5.3 states that the compressive stress due to Fatigue I load combination and one-half the sum of effective prestress and permanent loads shall not exceed $0.40f'_c$ after losses.

$0.4f'_c = 0.4(22) = 8.800 \text{ ksi}$

Compression stress due to Fatigue I load combination is calculated at midspan as follows:

Moment due to Fatigue I load combination is applied to the composite transformed section at the final time.

$M_{FI} = 1.75M_{f,m} = 1.75(909.6) = 1,591.7 \text{ kip-ft}$

Change in stress in at top of UHPC girder $= M_{FI}/S_{ttc} = +0.426 \text{ ksi}$

The compression stress due to one-half of effective prestress and permanent loads is taken as half of the net stresses at service with no live load summarized in Section C8.2.1 of this Appendix, such as:

Top fiber stress $= 0.5 (f_{ti} + \Delta f_{tLTD} + \Delta f_{tD} + \Delta f_{tSIDL} + \Delta f_{tLDF} + \Delta f_{tSS}) = 0.5(+8.643) = +4.322$

Total stress for fatigue limit state requirement for compression stress is calculated as follows:

Top fiber stress = 0.426 + 4.322 = +4.747 < 8.800 ksi
OK.

C9.2.2. UHPC Tension Stress Check

For tension stresses, UHPC Guide Article 1.5.3 states that regions of members subjected to fatigue loads shall be designed such that the UHPC tensile stress due to Service I load combination does not exceed $0.95\gamma_u f_{t,cr} = 0.95(1.00)(1.00) = 0.95$ ksi.

In this design example, the tensile stresses due to Service I and Service III are identical, and the maximum tensile stresses at midspan due to Service III calculated in Section C8.2.1 of this Appendix, i.e. 0.929 ksi, and Section C8.3 of this Appendix, i.e., 0.696 ksi, are lower than the fatigue limit of 0.95 ksi. Therefore, the stress requirement for fatigue is satisfied.

C9.2.3. Fatigue of Reinforcement Check

Given that UHPC tensile stress is greater than conventional concrete, UHPC Guide Article 1.5.3 states that discrete steel elements embedded in UHPC should be checked for fatigue in accordance with AASHTO LRFD BDS Eq. 5.5.3.1-1 and Articles 5.5.3.2, 5.5.3.3, and 5.5.3.4. This provision ensures that the fatigue limit on the steel reinforcement in UHPC is met even when the UHPC girder is uncracked.

For fatigue considerations, the prestressing steel in UHPC members shall satisfy:

$\gamma(\Delta f) \leq (\Delta F)_{TH}$ [UHPC Guide Article 1.5.3; AASHTO LRFD BDS Article 5.5.3.1]

where:

γ = load factor specified in AASHTO LRFD BDS Table 3.4.1-1 for Fatigue I load combination = 1.75

Δf = force effect, live load stress range at the bottom layer of strands due to the passage of the fatigue load as specified in AASHTO LRFD BDS Article 3.6.1.4 (ksi)

$$= \frac{M_{f,m}\left(y_{btc} - 2 \text{ in.}\right)}{I_{tc}} \cdot \frac{E_p}{E_c} = \frac{909.6(12)(39.39 - 2)}{655,702.7} \cdot \frac{28,500}{6,933} = 2.56 \text{ ksi}$$

$(\Delta F)_{TH}$ = constant-amplitude fatigue threshold, as specified in AASHTO LRFD BDS Articles 5.5.3.3 for prestressing steel

        = 18.0 ksi because the radius of the curvature of the girder exceeds 30.0 ft

$\gamma(\Delta f) = 1.75(2.56) = 4.48$ ksi $< (\Delta F)_{TH} = 18.0$ ksi
OK.

CHAPTER C10. STRENGTH LIMIT STATE

The factored bending moment at midspan due to dead load and live load is computed as follows:

$$M_{u,m} = 1.25(M_{g,m} + M_{D,m} + M_{b,m}) + 1.5(M_{ws,m}) + 1.75(M_{LL.m} + M_{LT,m}) = 12{,}668 \text{ kip-ft}$$

In this design example, strain compatibility between the conventional concrete deck, UHPC girder, and prestressing steel is assumed; the strain compatibility analysis, specified in UHPC Guide Article 1.6.3.1, is utilized to determine the ultimate flexural capacity. Figure C10-1 shows the steps followed in the strain compatibility analysis.
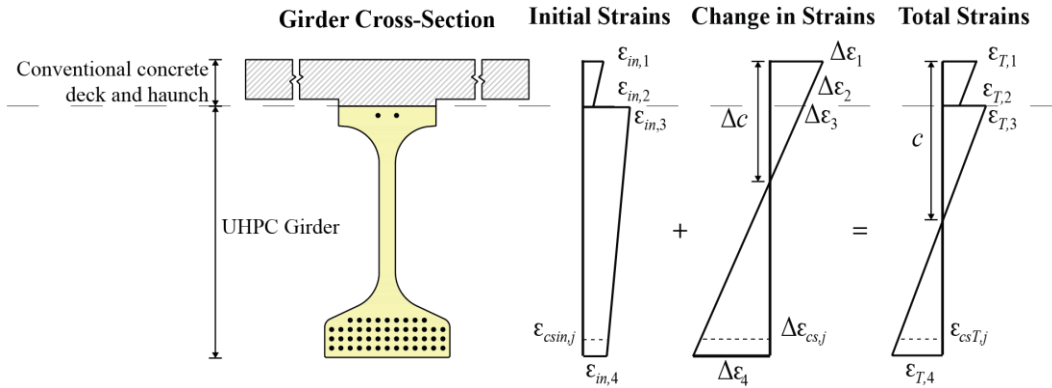
Source: FHWA.
Note: See List of Notations for variable definitions.

Figure C10-1. Illustration. Strain compatibility analysis of composite section.

Note that in strain compatibility of conventional concrete girders, the locked-in stress between the top of the UHPC girder and the concrete deck is sometimes ignored. The final strain diagram in the composite section is then assumed to be linear (i.e., no discontinuity at the top of the girder), and the precompression strain is added to the change in the steel strain in the final calculations of stresses. This assumption may be acceptable in some cases where the neutral axis is in the deck. However, in UHPC girders, this assumption will not be made because the neutral axis may not be in the deck at ultimate flexural strength.

Given the stresses in the UHPC girder at the deck placement may be significant, the initial strains due to girder self-weight and all losses and gains are calculated in this example. The strain compatibility analysis is performed by assuming a strain profile due to applied load and adding it to the initial strain profile to obtain the total strains as shown in Figure C10-1.

The initial stress profile in the UHPC can be found by calculating the stresses at the top and bottom of the conventional concrete deck (denoted by the subscripts 1 and 2, respectively) and at top and bottom of the UHPC girder (denoted by the subscripts 3 and 4, respectively) (Figure C10-1). The initial strain in the UHPC at each of these four locations and the initial tensile strain at the centroid of the strands due to prestressing can be found by the superposition of the following components:

- Instantaneous elastic stresses at transfer, using the precast transformed section properties.

- Long-term effects between transfer and deck placement, applied to the precast gross section properties.

- Instantaneous elastic stresses at deck placement due to deck self-weight, using precast transformed section properties.

- Long-term effects between deck placement and final time, except for effects of deck shrinkage, applied to the composite section properties.

- Long-term effects of deck shrinkage.

Note that the calculation of each of the preceding listed stresses can be found in Section C8.2.

Stresses and strains in the composite section for strain compatibility calculations are calculated as follows:

At the top of deck,
$$f_{in,1} = \Delta f_{dtLDF} = 0.001 \text{ ksi}$$
$$\varepsilon_{in,1} = f_{in,1}/E_{cD} = 0.0000001$$

At the bottom of the deck/haunch,
$$f_{in,2} = \Delta f_{dbLDF} = -0.00024 \text{ ksi}$$
$$\varepsilon_{in,2} = f_{in,2}/E_{cD} = 0.0000000$$

At the top of the girder,
$$f_{in,3} = f_t + \Delta f_{tLTD} + \Delta f_{tD} + \Delta f_{tLDF} + \Delta f_{tSS} = 8.423 \text{ ksi}$$
$$\varepsilon_{in,3} = f_{in,3}/E_c = 0.0012148$$

At the bottom of the girder,
$$f_{in,4} = f_b + \Delta f_{bLTD} + \Delta f_{bD} + \Delta f_{bLDF} + \Delta f_{bSS} = 2.034 \text{ ksi}$$
$$\varepsilon_{in,4} = f_{in,4}/E_c = 0.0002933$$

In each layer of prestressing strands (taken equal to initial strain at centroid),
$$f_{pin,j} = f_{pi} - \Delta f_{pES} - \Delta f_{pLTD} - \Delta f_{pD} - \Delta f_{pLDF} - \Delta f_{pSS} = 157.4 \text{ ksi}$$
$$\varepsilon_{pin,j} = f_{pin}/E_p = 0.0055230$$

In calculating the bending moment at a desired strain profile, the section is discretized into 0.5-in.-thick horizontal layers (denoted by i) through the overall height of the composite section; the stress and strain in each layer are assumed to be constant. The strains in each layer are inferred from the strain profiles of Figure C10-1. The total strain in each layer of steel, UHPC, and conventional concrete is calculated as follows:

$\varepsilon_{T,i} = \varepsilon_{in,i} + \Delta\varepsilon_i$ at each layer i of the UHPC or conventional concrete
$\varepsilon_{psT,j} = \varepsilon_{pin,j} + \Delta\varepsilon_{cs,j}$ at each layer j of prestressing steel

240

The stresses in each of the conventional concrete, UHPC, and steel layers are calculated by employing the mechanical models of conventional concrete, UHPC, and steel and utilizing the total strains of Figure C10-1:

- For UHPC, the mechanical models described in UHPC Guide Articles 1.4.2.4.3 and 1.4.2.5.4 are employed.

- For conventional concrete, the model suggested by Popovics (1973) and later modified by Thorenfeldt, Tomaszewicz, and Jensen (1987), with the curve fitting parameters proposed by Collins and Mitchell (1991), is utilized to determine the stress in each of the layers in the deck, f_{ci}:

$$f_{T,i} = f'_{cD} \left[\frac{n_c(\varepsilon_{T,i}/\varepsilon'_c)}{n_c - 1 + (\varepsilon_{T,i}/\varepsilon'_c)^{nk}} \right]$$

where:

$$n_c = 0.8 + \frac{f'_{cD}}{2{,}500} = 0.8 + \frac{4{,}000}{2{,}500} = 2.4$$

$$\varepsilon'_c = \frac{f'_{cD}}{E_{cD}} \cdot \frac{n_c}{n_c - 1} = \frac{4}{3{,}986} \cdot \frac{2.4}{2.4 - 1} = 0.00172$$

$$k = 0.67 + \frac{f'_{cD}}{9{,}000} = 0.67 + \frac{4{,}000}{9{,}000} = 1.114$$

- For prestressing steel, the power formula recommended by the *PCI Bridge Design Manual* is utilized to determine the total stress in each layer of strands (PCI 2014):

$$f_{psT,j} = \varepsilon_{psT,j} \left| 887 + \frac{27{,}613}{(1 + (112.4\varepsilon_{psT,j})^{7.36})^{\frac{1}{7.36}}} \right| \leq 270 \text{ ksi}$$

The stresses in each of the conventional concrete, UHPC, and steel are then converted into compression and tension forces, which are summed to check force equilibrium in the section. The process is repeated, assuming different change in strain profiles, until equilibrium is established, after which the flexural moment is computed.

In this design example, four failure modes exist for the prestressed UHPC girder with a conventional concrete deck:

- Mode I: Deck concrete crushing, $\varepsilon_{T,1} = 0.003$.
- Mode II: UHPC crushing, $\varepsilon_{T,3} = \varepsilon_{cu} = 0.0035$.
- Mode III: UHPC tensile strain limit, $\varepsilon_{T,4} = \gamma_u \varepsilon_{t,loc} = -0.0040$.
- Mode IV: Steel strand rupture at bottom steel layer, $\varepsilon_{psT} = -0.035$.

In prestressed UHPC girders, the third mode of failure (i.e., UHPC crack localization) typically controls; therefore, the strain compatibility analysis is first performed to find the stress and strain profiles at this failure mode. Figure C10-2 shows the results of this analysis.
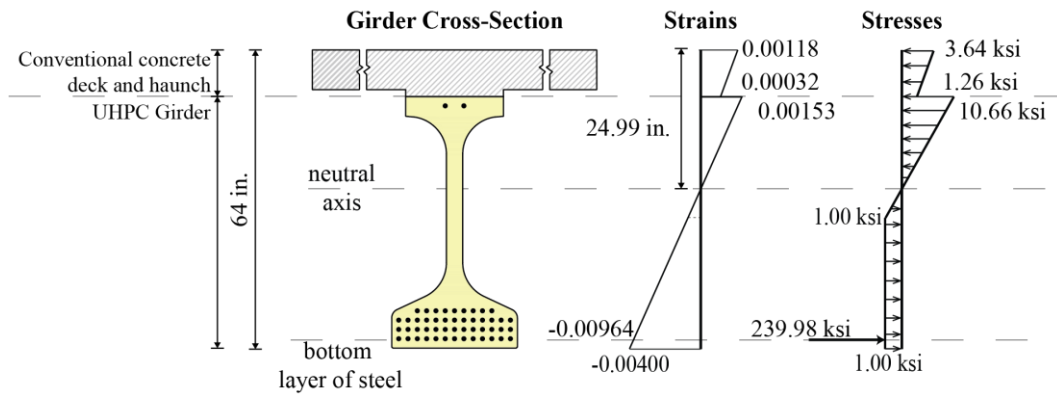
Source: FHWA.

Figure C10-2. Illustration. Mode III: UHPC crack localization.

As shown in Figure C10-2, when the UHPC strain in the extreme tensile layer reaches the UHPC tensile strain limit ($\varepsilon_{T,4} = \gamma_u \varepsilon_{t,loc} = -0.0040$), the values of the tensile strains in the extreme compression layer of the conventional concrete deck ($\varepsilon_{T,1} = +0.00118$) and the UHPC girder ($\varepsilon_{T,3} = +0.00153$) are lower than their respective ultimate limit compression strain of 0.003 and 0.0035, respectively. Therefore, the nominal bending capacity of the section is equal to the moment at UHPC crack localization ($M_n = M_L$). Note that any further increases in the top strain will cause the strains in the tension to increase beyond the localization strain capacity of UHPC, which is not allowed per UHPC Guide Article 1.6.3.2.2. The postlocalization behavior is not recommended to be considered in the design because the loss of UHPC fiber bridging capacity may cause hinging of the beam at the localized crack section and the straining of the tensile reinforcement over a short distance, thus increasing the risk of reinforcement rupture. The details of the strain compatibility analysis results and the bending moment at localization are presented in Table C10-1.

Table C10-1. Summary of the strain compatibility analysis.

Parameter	(M_{st}, ψ_{st}) Steel Service	(M_L, ψ_L) or (M_n, ψ_n) Crack Localization
M (kip-ft)	12,502	16,131
c (in.)	39.67	24.98
$\varepsilon_{T,1}$	0.00058	0.00118
$\varepsilon_{T,2}$	0.00026	0.00032
$\varepsilon_{T,3}$	0.00147	0.00153
$\varepsilon_{T,4}$	−0.00121	$\varepsilon_{t,loc} = -0.0040$
$\varepsilon_{psT,b}$ (bottom steel layer)	$\varepsilon_{s\ell} = -0.00696$	−0.00964
ψ (in.$^{-1}$) $\times 10^{-4}$	0.4965	1.0254

Note: Neutral axis, c, is measured from the top of the composite section.
Note: See List of Notations for variable definitions.

C10.1. FACTORED BENDING MOMENT CAPACITY

The resistance factor for flexural capacity is based on a ductility performance threshold expressed in terms of a curvature ductility ratio [UHPC Guide Article 1.5.4.2].

The curvature ductility ratio is defined as:

$$\mu = \frac{\psi_n}{\psi_{s\ell}}$$
[UHPC Guide Eq. 1.6.3.2.3-1]

where:

ψ_n = sectional curvature at nominal flexural strength

$\psi_{s\ell}$ = sectional curvature when the steel stress in the extreme tension steel is equal to the steel service stress limit, $f_{s\ell}$

in which $f_{s\ell}$ is the stress limit in steel at service loads after losses = $0.80\,f_{py}$ = 194.4 ksi.
[AASHTO LRFD BDS Table 5.9.2.2-1]

To determine the sectional curvature when the steel stress in the extreme tension steel is equal to the steel service stress limit, a strain compatibility analysis was performed to find the strain profile at equilibrium of forces when the total strain in the extreme prestressing steel layer is equal to $\varepsilon_{s\ell} = -0.00696$ (determined from the strand power formula equation presented above). The strain and stress profiles obtained at the end of this analysis are shown in Figure C10.1-1. The details of the results are presented in Table C10-1.
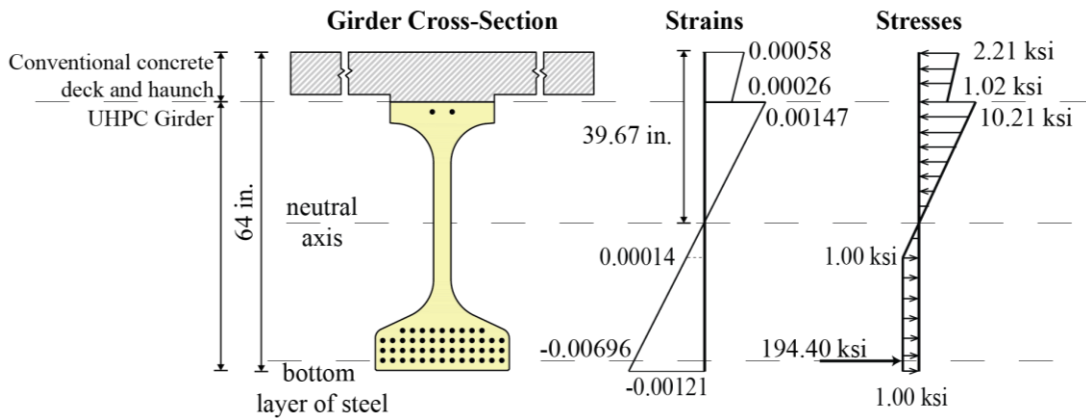
Source: FHWA.

Figure C10.1-1. Illustration. Strands reach steel service limit.

The resistance factor can be calculated in accordance with UHPC Guide Articles 1.5.4.2 and 1.6.3.2.3:

Ultimate moment:
$$M_n = M_L = 16{,}131 \text{ kip-ft}$$

| Curvature at localization: | $\Psi_n = \Psi_L = \dfrac{\varepsilon_{T,3}\,(\text{at }M_n)}{c\,(\text{at }M_n) - t_s - t_h} = \dfrac{0.00153}{24.98 - 8.5 - 1.5} = 1.0254 \times 10^{-4}\,\dfrac{1}{\text{in.}}$ |

| Curvature at steel service: | $\Psi_{s\ell} = \dfrac{\varepsilon_{T,3}\,(\text{at }M_{sl})}{c\,(\text{at }M_{sl}) - t_s - t_h} = \dfrac{0.00147}{39.67 - 8.5 - 1.5} = 0.4965 \times 10^{-4}\,\dfrac{1}{\text{in.}}$ |

Curvature ductility ratio limit: $\quad \mu_\ell = 3.0$ [UHPC Guide Article 1.6.2]

Curvature ductility ratio: $\quad \mu = \dfrac{\Psi_n}{\Psi_{s\ell}} = 2.065$

Resistance factor: $\quad \phi_f = 0.75 + 0.15\,\dfrac{\mu - 1.0}{\mu_\ell - 1.0} = 0.830$

Therefore:

$$\phi M_n = \phi_f M_L = (0.830)(16{,}131) = 13{,}387 \text{ kip-ft} > 12{,}668 \text{ kip-ft} \qquad \text{OK.}$$

C10.2. MINIMUM REINFORCEMENT

Article 1.6.3.3 of the proposed UHPC Guide and Article 5.6.3.3 of AASHTO LRFD BDS states that the amount of prestressed and nonprestressed tensile reinforcement shall be adequate to develop a factored flexural resistance, M_r, greater than or equal to the lesser of the following:

- 1.33 times the factored moment required by the applicable strength load combination, M_u.

- $M_{cr} = \gamma_3 \left[\left(\gamma_1 f_{t,cr} + \gamma_2 f_{cpe} \right) S_{btc} - M_{dnc} \left(\dfrac{S_{btc}}{S_{btf}} - 1 \right) \right].$

where:

M_{cr}	=	cracking moment (kip-ft)
$f_{t,cr}$	=	UHPC effective cracking strength = 1.00 ksi
f_{cpe}	=	compressive stress in UHPC due to effective prestress forces only at extreme fiber section, where tensile stress is caused by externally applied loads
	=	$\dfrac{P_{pee}}{A_{tf}} + \dfrac{P_{pee}\,e_{tf}}{S_{btf}}$
M_{dnc}	=	total unfactored dead load moment acting on the monolithic or noncomposite section
	=	$M_{g,m} + M_{D,m} = (1{,}701.1 + 2{,}901.4)(12) = 55{,}230$ kip-in.
γ_1	=	flexural cracking variability factor
	=	1.6 for concrete structures other than precast segmental structures
γ_2	=	prestress variability factor
	=	1.1 for bonded tendons
γ_3	=	ratio of specified minimum yield strength to ultimate tensile strength of the nonprestressed reinforcement

= 1.0 for prestressing steel

in which:

P_{pee} = force in prestressing strands due to effective prestress only
= $f_{pee} A_{pT}$ = (178.05)(14.70) = 2,617.3 kips

f_{pee} = effective prestress in strands after allowance of all losses
= $f_{pi} - \Delta f_{pLTD} - \Delta f_{pLDF} - \Delta f_{pSS}$ = 178.05 ksi

Therefore:

$$f_{cpe} = \frac{2{,}617.3}{590.1} + \frac{(2{,}617.3)(14.07)}{10{,}793} = 7.847 \text{ ksi}$$

$$M_{cr} = 1.0\left[\left(1.6(1.00) + 1.1(7.847)\right)(16{,}646) - (55{,}230)\left(\frac{16{,}646}{10{,}793} - 1\right)\right]$$

= 140,368 kip-in. = 11,698.4 kip-ft

and $1.33M_u$ = (1.33)(12,668) = 16,848.5 kip-ft

Since $1.33M_u$ = 16,848.5 kip-ft > M_{cr} = 11,697.3 kip-ft, the factored flexural resistance, M_r, must be greater than M_{cr} = 11,698.4 kip-ft.

In this design, M_r = 13,387 kip-ft is greater than M_{cr} = 11,698.4 kip-ft; therefore, the section satisfied the minimum reinforcement requirements.

CHAPTER C11. SHEAR DESIGN

The area and spacing of shear reinforcement must be determined at regular intervals along the length of the beam. Transverse reinforcement shall be provided where:

$$V_u > \phi_v \left(V_{UHPC} + V_p \right) \qquad \text{[UHPC Guide Eq. 1.7.2.3-1]}$$

where:

V_u = factored shear force (kip)
ϕ_v = resistance factor for shear = 0.9   [UHPC Guide Article 1.5.4.2]
V_{UHPC} = nominal shear resistance of the UHPC (kip)
V_p = component of prestressing force in the direction of shear force; positive if resisting the applied shear = 0 kips

or where consideration of torsion is required. In this design example, torsion is not considered and the shear design is only performed at the critical shear location.

C11.1. CONTRIBUTION OF UHPC TO SHEAR RESISTANCE

Effective shear depth, d_v, is taken as the distance, measured perpendicular to the neutral axis, between the resultants of the tensile and compressive forces due to flexure. It need not be taken less than the greater of $0.9d_e$ or $0.72h_c$, in which d_e is the distance between the extreme compression fiber of the UHPC section to the resultant of the forces in the tensile reinforcement.

[AASHTO LRFD BDS Article 5.7.2.8]

However, according to UHPC Guide Article 1.7.2.8, in composite sections made with UHPC beams and conventional concrete decks, the effective shear depth, d_v, shall not exceed the distance, $d_{v,limit}$, measured perpendicular to the neutral axis, between the resultant of the forces in the tensile reinforcement and the extreme UHPC fiber on the flexural compression side.

The distance from the extreme bottom fiber of the UHPC girder to resultant of the forces in the tensile reinforcement is $(9 \times 2 + 9 \times 4 + 9 \times 6 + 7 \times 8)/(9 + 9 + 9 + 7) = 4.82$ in. Note that this calculation only considers the strands in the flexural tensile zone and assumes all 14 strands are debonded at the critical shear location (which is a conservative estimation based on the debonding pattern of Figure C5.1-2.

Therefore, the effective shear depth, d_v, is calculated as follows:

$$d_e = h_c - y_{bsE} = 56.56 \text{ in.}$$

$$\max (0.9d_e, 0.72h_c) = 50.90 \text{ in.} = 4.24 \text{ ft}$$

$$d_{v,limit} = h - 4.82 = 49.18 \text{ in.} = 4.10 \text{ ft} \qquad \text{[UHPC Guide Article 1.7.2.8]}$$

The value of $d_{v,limit} = 4.10$ ft is less than the value of the greater of $0.9d_e$ and $0.72h_c$ and thus, the effective shear depth need not be less than 4.10 ft. Therefore, for shear calculations, $d_v = 4.10$ ft.

According to UHPC Guide Article 1.7.3.2, the location of the critical shear section is taken at $d_v = 4.10$ ft from the face of the support. Assuming a support width of 1 ft, the location of the critical section for shear is at 4.10 ft + 0.5 ft = 4.60 ft from the centerline of the beam's supports. The factored shear force due to dead load and live load at critical section is:

$$V_{u,crs} = 1.25(V_{g,crs} + V_{D,crs} + V_{b,crs}) + 1.5V_{ws,crs} + 1.75(V_{LL,crs} + V_{LT,crs})$$
$$= 1.25(42.6 + 72.6 + 7.0) + 1.5(13.6) + 1.75(39.9 + 76.6)$$
$$= 377.0 \text{ kips}$$

Factored moment due to dead load and live load at critical shear section is:

$$M_{u,crs} = 1.25(M_{g,crs} + M_{D,crs} + M_{b,crs}) + 1.5M_{ws,crs} + 1.75(M_{LL,crs} + M_{LT,crs})$$
$$= 1.25(202.3 + 345.0 + 33.4) + 1.5(64.7) + 1.75(140.1 + 260.7)$$
$$= 1{,}524.3 \text{ kip-ft}$$

The net longitudinal tensile strain at the centroid of tensile reinforcement at the critical shear section is determined by:

$$\varepsilon_s = \frac{\dfrac{|M_{u,crs}|}{d_v} + 0.5N_{u,crs} + |V_{u,crs} - V_p| - A_{ps,crs}f_{po} - \gamma_u f_{t,loc}A_{ct}}{E_s A_{s,crs} + E_p A_{ps,crs}} \qquad \text{[UHPC Guide Eq. 1.7.3.4.1-6]}$$

where:
$M_{u,crs}$ = factored bending moment at section at the critical shear location, not taken less than $|V_u - V_p| d_v = 377.0 \times 4.10 = 1{,}545.8$ kip-ft; thus, $M_{u,crs} = 1{,}545.8$ kip-ft
$N_{u,crs}$ = factored axial force at the critical shear location = 0 kip
f_{po} = parameter equal to modulus of elasticity multiplied by the locked-in difference in strain and surrounding UHPC which may be taken equal to $0.7f_{pu} = 189$ ksi for prestressed strands
A_{ct} = area of UHPC on the flexural tension side of the member
  = $360.05 - 48(0.294) = 345.94$ in.^{2}
$A_{ps,crs}$ = area of prestressing steel on the flexural tension side at the critical shear location
$A_{s,crs}$ = area of nonprestressed steel on the flexural tension side of the member at the critical shear location = 0 in.^{2}

According to UHPC Guide Article 1.7.3.4.1, if the location of the critical shear section is within the transfer length section, f_{po} in Eqs. 1.7.3.4.1-6 and 1.7.3.4.1-7 shall be increased linearly from zero at the location where the bond between the strands and UHPC commences to its full value at the end of the transfer length. Moreover, if the critical shear location falls within the development length of the prestressing strands, the area of the strands, $A_{ps,crs}$, shall be reduced in proportion of the strands' lack of development. This condition will be checked by calculating the transfer and development length of the strands.

Given that 14 strands are debonded at each end of the girder, a debonding pattern must be determined based on the restrictions of UHPC Guide Article 1.9.4.3.3 before the values of f_{po} and $A_{ps,crs}$ can be computed. The debonding pattern shown in Figure C11.1-1 is chosen for this example in which the debonding of six, four, and four strands is terminated at a longitudinal spacing equal to the transfer length for shear considerations, ℓ_t.
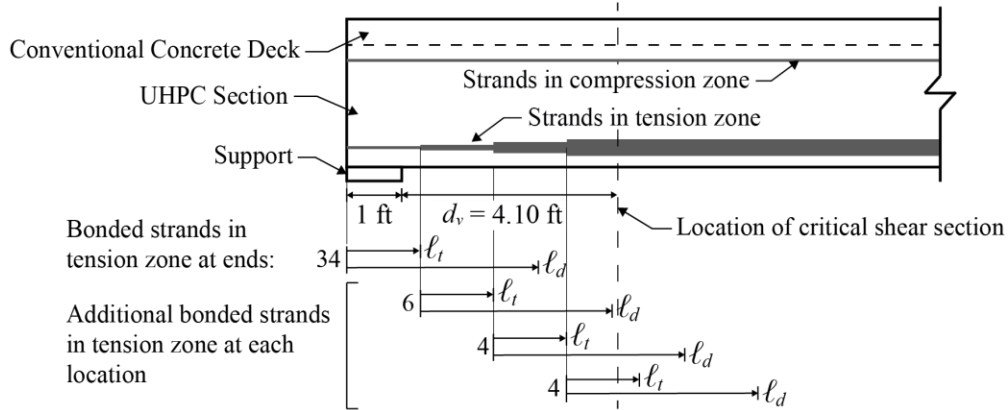
Source: FHWA.

Figure C11.1-1. Illustration. Debonding pattern of strands.

In calculating the transfer length for shear design considerations, longer transfer and development length values will result in more critical stress states generated by the applied shear demand. This result is because longer development length values will increase the likelihood of the critical shear location to fall at a location where the strands are not fully developed. Therefore, the factor for transfer length, ξ, should be taken as 1.0.

Transfer length, $\ell_t = \xi 24 D_p = 1.00(24)(0.7) = 16.8$ in. or 1.4 ft

[UHPC Guide Eq. 1.9.4.3.1-1]

As shown in Figure C11.1-1, the location of the critical shear section is within the transfer length of the last 4 bonded strands; therefore:

$$f_{po} = \frac{189(44) + \frac{189}{1.4}(5.10 - 3(1.4))(4)}{48} = 183.375 \text{ ksi}$$

The development length of the strands, ℓ_d, can be calculated according to UHPC Guide Article 1.9.4.3.2 as follows:

$$\ell_d \geq \ell_t + 0.30(f_{ps} - f_{pe,ng}) D_p \qquad \text{[UHPC Guide Eq. 1.9.4.3.2-1]}$$

where:
  f_{ps} = average stress in prestressing steel at the time for which the nominal resistance of the member is required, taken equal to the ultimate capacity of the strands = 270 ksi
  $f_{pe,ng}$ = effective stress in the prestressing steel after losses (no gains)
      = $f_{pi} - \Delta f_{pT} = 202.5 - 54.11 = 148.39$ ksi

Therefore:

$$\ell_d \geq \ell_t + 0.30(f_{ps} - f_{pe,ng}) D_p = 16.8 + 0.30(270 - 148.39)(0.7) = 42.34 \text{ in. or } 3.53 \text{ ft}$$

As shown in Figure C11.1-1, the location of the critical shear section is within various locations of the development length of the debonded strands; therefore:

$$A_{ps,crs} = 0.294(34) + (0.294)(6) + \frac{0.294}{3.53}(5.10 - 2(1.4))(4) + \frac{0.294}{3.53}(5.10 - 3(1.4))(4)$$

$$= 12.82 \text{ in.}^2$$

The value of the ε_s can be now calculated according to UHPC Guide Eq. 1.7.3.4.1-6 as:

$$\varepsilon_s = \frac{\frac{|1,545.8|}{4.24} + |377.025| - (12.82)(183.375) - (1.00)(1.00)(345.94)}{(28,500)(12.82)} = -0.00535$$

Note that in calculating ε_s according to Eq. 1.7.3.4.1-6, the limit on d_v in composite sections need not apply [UHPC Guide Article 1.7.3.4.1], and, thus, the value of d_v in the calculation above was taken equal to the greater of $0.9d_e$ or $0.72h_c$, i.e., 4.24 ft.

Since the value of ε_s calculated from UHPC Guide Eq. 1.7.3.4.1-6 is negative, it should be either taken as $\varepsilon_{t,cr}$, or recalculated using Eq. 1.7.3.4.1-7:

$$\varepsilon_s = \frac{\frac{|M_{u,crs}|}{d_v} + 0.5N_u + |V_{u,crs} - V_p| - A_{ps,crs}f_{po}}{E_s A_{s,crs} + E_p A_{ps,crs} + E_c A_{ct}} = -0.00058 \qquad \text{[UHPC Guide Eq. 1.7.3.4.1-7]}$$

C11.2. CONTRIBUTION OF STEEL REINFORCEMENT TO SHEAR RESISTANCE

C.11.2.1. General Approach to Determine θ and f_v

The general approach for determining shear resistance parameters θ and f_v is to iteratively solve UHPC Guide Eqs. 1.7.3.4.1-1 through 1.7.3.4.1-4. For sections with transverse steel reinforcement perpendicular to the longitudinal axis ($\alpha = 90$ degrees), equations reduce to:

$$\gamma_u \varepsilon_{t,loc} = \frac{\varepsilon_s}{2}(1 + \cot^2 \theta) + \frac{2f_{t,loc}}{E_c}\cot^4 \theta + \frac{2\rho_v f_v}{E_c}\cot^2 \theta (1 + \cot^2 \theta) \quad \text{[UHPC Guide Eq. C1.7.3.4.1-3]}$$

$$\varepsilon_2 = -\frac{2f_{t,loc}}{E_c}\cot^2 \theta - \frac{2\rho_v f_v}{E_c}(1 + \cot^2 \theta) \qquad \text{[UHPC Guide Eq. C1.7.3.4.1-2]}$$

Strain in vertical steel, $\varepsilon_v = \gamma_u \varepsilon_{t,loc} - 0.5\varepsilon_s + \varepsilon_2$ \qquad [UHPC Guide Eq. 1.7.3.4.1-3]

Stress in vertical steel, $f_v = E_s \varepsilon_v \leq f_y$ \qquad [UHPC Guide Eq. 1.7.3.4.1-4]

in which:

$$\rho_v = \frac{A_v}{b_v s} \qquad \text{[UHPC Guide Eq. 1.7.3.4.1-5]}$$

For this design example, try No. 4 Grade 60 reinforcing bars at a spacing of 6 in.:

Spacing of transverse reinforcement $\qquad s = 6$ in.

Area of transverse reinforcement $A_v = 0.20$ in.^{2}

Yield stress of transverse steel $f_y = 60$ ksi

Modulus of elasticity of transverse steel $E_s = 29{,}000$ ksi

Shear reinforcement ratio $\rho_v = \dfrac{0.20}{(3.5)(6)} = 0.0095$

Set the steel stress at shear failure to steel yield stress, $f_v = f_y = 60$ ksi.

Assume a principal angle direction and begin the iterative process to obtain a localization strain equal to the localization strain of UHPC.

Using $\theta = 29.13$ degrees:

$$\gamma_u \varepsilon_{t,loc} = \frac{-0.00058}{2}(1+\cot^2(29.13))+\frac{2(1.0)}{6{,}933}\cot^4(29.13)+\frac{2(0.0095)(60)}{6{,}933}\cot^2(29.13)(1+\cot^2(29.21))$$

$$= 0.00400 \qquad\qquad\qquad\qquad\qquad\qquad\qquad\text{OK.}$$

$$\varepsilon_2 = -\frac{2(1.0)}{6{,}933}\cot^2(29.13) - \frac{2(0.0095)(60)}{6{,}933}(1+\cot^2(29.13))$$

$$= -0.00162$$

$$\varepsilon_v = \varepsilon_{t,loc} - 0.5\varepsilon_s + \varepsilon_2 = 0.00267$$

Check f_v, $f_{v,Check} = \min(E_s\,\varepsilon_v,\,f_y) = 60.0$ ksi OK.

Note: If $f_{v,Check}$ was not equal to the assumed value of f_v, a new value of f_v should be assumed and the iteration process repeated until the assumed values of θ and f_v converge. Convergence occurs when both the pair of assumed values for θ and f_v results in a value of $\gamma_u\varepsilon_{t,loc}$ equal to 0.004 [UHPC Guide Eq. C1.7.3.4.1-3] and the assumed value of f_v is equal to the calculated value [UHPC Guide Eq. 1.7.3.4.1-4].

Transverse reinforcement shear contribution,

$$V_s = \frac{A_v f_v d_v \cot\theta}{s} = \frac{(0.20)(60.00)(49.18)\cot(29.13)}{6} = 176.5 \text{ kip}$$

[UHPC Guide Eq. 1.7.3.3-4]

251

C.11.2.2. Simplified Approach to Determine θ and f_v

If a simplified approach to determine the shear resistance parameters θ and $f_{v,\alpha}$ described in UHPC Guide Article 1.7.3.4.2 is used, the contribution of the steel reinforcement to the shear resistance can be calculated as follows:

- The reinforcement ratio $\rho_v = 0.0095 < 0.01$. Therefore, Table A2.3-2 of the UHPC Guide can be used to estimate the value of the inclination angle θ and the maximum allowable stress in steel, $f_{v,max}$. For $\gamma_u\varepsilon_{t,loc} = 0.004 \geq 0.004$ and $\varepsilon_s = -0.00058 \leq -0.0005$, $\theta = 32.8$ and $f_{v,max} = 64.8$ ksi. Since $f_v = 60.0$ ksi $< f_{v,max}$, use $f_v = 60.00$ ksi.

- Transverse reinforcement shear contribution,

$$V_s = \frac{A_v f_v \, d_v \cot\theta}{s} = \frac{(0.20)(60.00)(49.18)\cot(32.8)}{6} = 152.6 \text{ kip}$$

[UHPC Guide Eq. 1.7.3.3-4]

C.11.2.3. Maximum Spacing of Transverse Reinforcement

The maximum spacing of transverse reinforcement cannot exceed s_{max}, determined as:

$$s_{max} = 0.25 d_{v,limit} \cot\theta \leq 24.0 \text{ in.} \qquad \text{[UHPC Guide Eq. 1.7.2.5-1]}$$

Using $\theta = 29.13$ degrees obtained from the general approach:

$$s_{max} = 0.25(49.18)\cot(29.13) = 22.07 \text{ in.} \leq 24.0 \text{ in.}$$

Using $\theta = 32.8$ degrees obtained from the general approach:

$$s_{max} = 0.25(49.18)\cot(32.8) = 19.08 \text{ in.} \leq 24.0 \text{ in.}$$

Given that the provided spacing of transverse reinforcement, $s = 6$ in., is less than $s_{max} = 22.07$ in. using general approach or $s_{max} = 19.08$ in. from the simplified approach, the reinforcement spacing is compliant with the provisions of UHPC Guide Article 1.7.2.6.

C11.3. TOTAL SHEAR RESISTANCE

The total shear resistance of the beam is calculated from the general approach as follows:

UHPC shear resistance, $V_{UHPC} = \gamma_u f_{t,loc} \, d_{v,limit} \, b_v \cot\theta = 308.9$ kip   [UHPC Guide Eq. 1.7.3.3-3]

Total shear resistance, $V_n = V_{UHPC} + V_s = 485.3$ kip   [UHPC Guide Eq. 1.7.3.3-1]

Factored shear resistance, $\phi_v V_n = 436.8$ kip $> V_u = 377.0$ kip   OK.

Maximum shear resistance: $V_{u,max} = 0.25 f'_c \, d_v \, b_v = 946.6$ kip $> V_n = 485.3$ kip   OK.

[UHPC Guide Eq. 1.7.3.3-2]

The total shear resistance of the beam is calculated from the simplified approach as follows:

- UHPC shear resistance, $V_{UHPC} = \gamma_u f_{t,loc} d_v b_v \cot \theta = 267.1$ kip

  [UHPC Guide Eq. 1.7.3.3-3]

- Total shear resistance, $V_n = V_{UHPC} + V_s = 419.7$ kip $\quad$ [UHPC Guide Eq. 1.7.3.3-1]

- Factored shear resistance, $\phi_v V_n = 377.7$ kip $> V_u = 377.0$ kip
  OK.

CHAPTER C12. INTERFACE SHEAR TRANSFER

C12.1. FACTORED HORIZONTAL SHEAR

At the strength limit state, horizontal shear at a section per unit can be taken as:

$$V_{ui} = \frac{V_u}{d_v} \qquad \text{[AASHTO LRFD BDS Eq. C5.7.4.5-7]}$$

where:

- V_{ui} = horizontal factored shear force per unit length of the girder (kip/in.)
- V_u = factored shear force due to total load based on the applicable strength and extreme event load combinations, kip
- d_{vi} = distance between the centroid of the tension steel and the mid-thickness of the deck.
  = $d_e - t_s/2 = 56.56 - 8.5/2 = 52.31$ in.

The location of the critical section is assumed to be the same location as the critical section for vertical shear, 3.88 ft from face of support.

The factored shear force due to Strength I load combination at the critical shear section is:
$V_{u,crs} = 377.0$ kip

Applied factored horizontal shear is:

$V_{ui} = 377.0$ kip/52.31 in. = 7.21 kip/in.

C12.2. REQUIRED NOMINAL RESISTANCE

Required nominal shear resistance $V_{ni} = V_{ui}/\phi_v = 7.21/0.9 = 8.01$ kip/in.

[AASHTO LRFD BDS Eq. 5.7.4.3-1]

C12.3. REQUIRED INTERFACE SHEAR REINFORCEMENT

The nominal shear resistance of the surface is:

$$V_{ni} = c_i A_{cv} + \mu_i (A_{vf} f_y + P_c) \qquad \text{[UHPC Guide Eq. 1.7.4.3-4]}$$

where:

- c_i = cohesion factor (ksi)
- μ_i = friction factor
- A_{cv} = area of UHPC considered to be engaged in interface shear transfer (in.^{2})
- A_{vf} = area of interface reinforcement crossing the shear plane within the area A_{cv} (in.^{2})
- f_y = specified minimum yield strength of reinforcement; it shall not be taken greater than 60 ksi (ksi)
- P_c = permanent net compressive force normal to the horizontal shear plane; if force is tensile, $P_c = 0.0$ kip

The nominal shear resistance shall not exceed $V_{ni} \le K A_{cv}$ [UHPC Guide Eq. 1.7.4.3-5]

where: $A_{cv} = b_{vi} L_{vi}$ [UHPC Guide Eq. 1.7.4.3-6]

in which:
    A_{cv} = area of UHPC considered to be engaged in interface shear transfer
    b_{vi} = interface width considered to be engaged in shear transfer
    K = limiting interface shear resistance
    L_{vi} = interface length considered to be engaged in shear transfer

For this example:

    b_{vi} = 21 in.
    L_{vi} = 1 in.
    A_{cv} = 21 in.^{2}
    P_c = 0 kip

For conventional concrete placed against a clean UHPC substrate surface, free of laitance, with surface intentionally roughened to an amplitude of 0.25 in. or cast to have 0.25-in. amplitude roughness: [UHPC Guide Article 1.7.4.4]

    c_i = 0.075 ksi
    μ_i = 1.00
    K = 1.8 ksi

Solving UHPC Guide Eq. 1.7.4.3-4 for A_{vf}:

    8.01 kip/in. = (0.075)(21) + 1.00($A_{vf}f_y$ + 0) $\rightarrow A_{vf}f_y$ = 6.435 kip/in.

    A_{vf} (required) = (6.435 kip/in.)/60 ksi = 0.107 in.^{2}/in.

Provide two legs of No. 5 Grade 60 stirrup at 6-in. spacing and extend the No. 4 shear reinforcement bars across the interface zone.

Spacing of transverse reinforcement, s = 6 in.

Area of interface shear reinforcement = 2(0.31 in.^{2}) + 1(0.20 in.^{2}) = 0.82 in.^{2}

Therefore, A_{vf} (provided) = 0.82/6 = 0.137 in.^{2}/in. $\ge$ 0.107 in.^{2}/in.   OK.

Therefore, the nominal shear resistance of the interface plane is:

    V_{ni} = (0.075)(21) + 1.00((0.137)(60) + 0) = 9.775 kip/in. and $\phi_v V_{ni}$ = 8.79 kip/in.

    V_{ui} = 7.21 kip/in. < $\phi_v V_{ni}$ = 8.789 kip/in.   OK.

C12.4. MINIMUM AREA OF INTERFACE SHEAR REINFORCEMENT

For a cast-in-place concrete slab on clean concrete girder surfaces free of laitance, Article 1.7.4.2 of UHPC Guide and Article 5.7.4.2 of AASHTO LRFD BDS (AASHTO 2020) state that the minimum interface shear reinforcement, A_{vf}, need not exceed the lesser of the amount determined using Eq. 5.7.4.2-1 and the amount needed to resist $1.33V_{ui}/\phi_v$ as determined using Eq. 1.7.4.3-4.

The minimum shear resistance calculated according to Eq. 5.7.4.2-1 of AASHTO LRFD BDS (AASHTO 2020) is:

$A_{vf,min} = 0.05\ A_{cv}/f_y = 0.05(21)/60 = 0.0175$ in.^{2}/in.

The amount of reinforcement needed to resist $1.33V_{ui}/\phi_v = 1.33\ (7.21)/0.9 = 10.65$ kip/in. is calculated as follows:

10.65 kip/in. $= (0.075)(21) + 1.00(A_{vf}f_y + 0) \rightarrow A_{vf}f_y = 9.080$ kip/in.

$A_{vf} = 9.080$ kip/in. $/\,60$ ksi $= 0.151$ in.^{2}/in.

Therefore, the minimum area of interface shear reinforcement shall be $A_{vf,min} = 0.0175$ in.^{2}/in. The provided area of interface shear reinforcement, $A_{vf} = 0.151$ in.^{2}/in., exceeds the minimum and therefore the provisions of Article 1.7.4.2 of UHPC Guide are satisfied.

C12.5. MAXIMUM NOMINAL INTERFACE SHEAR RESISTANCE

The maximum nominal shear resistance is checked as follows:

$V_{ni} \leq KA_{cv}$

$V_{ni} = 8.789$ kip/in. $\leq K\ A_{cv} = (1.8)(21) = 37.80$ kip/in.   OK.

CHAPTER C13. MINIMUM LONGITUDINAL REINFORCEMENT REQUIREMENT

According to UHPC Guide Article 1.7.3.5, at each section, the tensile capacity of the longitudinal reinforcement on the flexural tension side shall be proportioned to satisfy:

$$A_{ps}f_{ps}+A_sE_s\gamma_u\varepsilon_{t,loc}+A_{ct}\gamma_u f_{t,cr} \geq \frac{|M_u|}{d_v\phi_f}+0.5\frac{N_u}{\phi_c}+\left(\left|\frac{V_u}{\phi_v}-V_p\right|-0.5V_s\right)\cot\theta$$

$$[\text{UHPC Guide Eq. 1.7.3.5-1}]$$

where:

ϕ_f, ϕ_c, ϕ_v = resistance factors taken from UHPC Guide Article 1.5.4.2 as appropriate for moment, axial resistance, and shear, respectively

V_s = shear resistance provided by transverse reinforcement at the section under investigation, as given by UHPC Guide Eq. 1.7.3.3-4, except V_s shall not be taken as greater than V_u/ϕ_v

θ = angle of inclination of diagonal compressive stresses used in determining the nominal shear resistance of the section under investigation

M_u = factored moment at the section corresponding to the factored shear force

V_p = component in the direction of the applied shear of the effective prestressing force

A_s = area of nonprestressed tensile reinforcement

Note that the term $E_s\,\varepsilon_{t,loc}$ shall not exceed the specified yield strength of reinforcing bars, f_y.

In this design example, the required longitudinal tensile reinforcement check is performed only at the inside edge of the bearing area of the supports. To complete the design, the longitudinal reinforcement requirement must be checked at regular intervals within the span of the beam.

According to UHPC Guide Article 1.7.3.5, at the inside edge of the bearing area of simple end supports to the section of critical shear, the longitudinal reinforcement on the flexural tension side of the member shall satisfy:

$$A_{ps}f_{ps}+A_sE_s\gamma_u\varepsilon_{t,loc}+0.6\,A_{ct}\gamma_u f_{t,cr} \geq \left(\frac{V_u}{\phi_v}-0.5V_s-V_p\right)\cot\theta \qquad [\text{UHPC Guide Eq. 1.7.3.5-2}]$$

Note that the term $E_s\,\varepsilon_{t,loc}$ shall not exceed the specified yield strength of reinforcing bars, f_y.

According to AASHTO LRFD BDS Article C5.7.3.5, the values of V_u, V_s, V_p, and θ calculated for the section located at d_v from the face of support may be used for determining the tensile force that the reinforcement is expected to resist at the inside edge of the bearing area. Therefore, $V_u = V_{u,crs}$ = 377.025 kip, $V_p = 0$ kip, $V_s = 176.57$ kip (using the general approach of Article C.11.2.1), and θ = 29.13 degrees.

When the required longitudinal reinforcement at the face of the bearing is checked, longer transfer lengths will necessitate the use of more reinforcement; therefore, the factor for transfer length, ξ, is taken equal to 1.0. Therefore, $\ell_t = 16.8$ in. [UHPC Guide Article 1.9.4.3.1]

Assuming a distance of 6 in. between the end of the girder and the center of the support (centerline of bearing), the horizontal distance from the end of the girder to the location where the critical shear crack plane crosses the centroid of the bottom strands (within the flexural tension zone) can be calculated as:

$$d_{crack} = 6 \text{ in.} + y_{bcb} \cot \theta = 6 + 4.82 \cot(29.13) = 14.65 \text{ in.}$$

where, $y_{bcb} = 4.82$ in. is the distance between the extreme tension fiber and the centroid of the strands on the flexural tension side at beam ends and within the debonded length (i.e., 14 debonded strands).

Therefore, the average stress in the prestressing strand at the time that nominal resistance is required can be taken as:

$$f_{ps} = \left(f_{pi} - \Delta f_{pT}\right)\frac{d_{crack}}{l_t} = (202.5 - 54.11)\frac{14.65}{16.8} = 129.4 \text{ ksi}$$

The right-hand side of UHPC Guide Eq. 1.7.3.5-2 can be computed as follows:

$$A_{ps} f_{ps} + A_s E_s \gamma_u \varepsilon_{t,loc} + 0.60 A_{ct} \gamma_u f_{t,cr} = (34)(0.294)(129.4) + 0 + 0.60(345.94)(1.00)(1.00)$$

$$= 1{,}501.58 \text{ kip}$$

The left-hand side of UHPC Guide Eq. 1.7.3.5-2 can be computed as follows:

$$\left(\frac{V_{u,crs}}{\phi_v} - 0.5V_s - V_p\right)\cot\theta = \left(\frac{377.0}{0.9} - 0.5(176.5) - 0\right)\cot(29.13) = 593.2 \text{ kips}$$

Given that, capacity of the tensile reinforcement and UHPC, i.e., right-hand side of UHPC Guide Eq. 1.7.3.5-2, is greater than the demand, i.e., the left hand side of UHPC Guide Eq. 1.7.3.5-2, additional flexural tensile steel reinforcements are not needed.

CHAPTER C14. PRETENSIONED ANCHORAGE ZONE

C14.1. ANCHORAGE ZONE REINFORCEMENT

The design of the anchorage zone reinforcement is computed using the force in the strands just before transfer:

$$P_{piE} = 2,143.26 \text{ kip}$$

The factored splitting resistance, P_r, should not be less than 4.0 percent of P_{pi}.

$$P_r = f_s A_{s,r} + P_{r,UHPC} \qquad \text{[UHPC Guide Eq. 1.9.4.4-1]}$$

in which:

$$P_{r,UHPC} = 0.25\gamma_u f_{t,cri} b_v h \qquad \text{[UHPC Guide Eq. 1.9.4.4-2]}$$

where:
$\quad f_{s,r}$ = stress in steel not to exceed 20.0 ksi
$\quad A_{s,r}$ = total area of reinforcement within the distance $h/4$ from the end of the beam
$\quad h$ = overall height of the member = 54 in.
$\quad b_v$ = effective web width taken as the minimum web width within the depth = 3.5 in.

Therefore:

$$P_r = 0.04 P_{piE} = 85.73 \text{ kip}$$

$$P_{r,UHPC} = 0.25(1.00)(0.75)(3.5)(54) = 35.44 \text{ kip}$$

$$A_s(\text{required}) = \frac{P_r - P_{r,UHPC}}{f_{s,r}} = 2.52 \text{ in.}^2$$

At least 2.52 in.^{2} of vertical transverse reinforcement should be provided within a distance of $h/4 = 13.5$ in. from the end of the beam.

Use five bundles of two No. 5 bars at 3 in. spacing center to center.

Provided $A_s = 5(2)(0.31) = 3.10$ in.$^2 > 2.52$ in.^{2} OK.

C14.2. CONFINEMENT REINFORCEMENT

For the distance of $1.5h = 81$ in. from the end of the beam, reinforcement shall be placed to confine the prestressing steel in the bottom flange. The reinforcement shall not be less than No. 3 deformed bars with spacing not exceeding 6.0 in. and shaped to enclose the strands.

[UHPC Guide Article 1.9.4.4.2; AASHTO LRFD BDS Article 5.9.4.4.2]

CHAPTER C15. DEFLECTION AND CAMBER

Deflections are calculated using the modulus of elasticity of UHPC and the gross section properties of the noncomposite girder section.   [UHPC Guide Article 1.6.3.5]

C15.1. DEFLECTION DUE TO PRESTRESSING FORCE AT TRANSFER

Force per strands after transfer, $P_p = f_{pt} A_p = 50.81$ kip.

$$\Delta_p = \frac{P_{pt}}{E_{ci} I_g} \left(\frac{e_{pg} L^2}{8} - \frac{e' a^2}{6} \right)$$

in which:

    e' = difference between eccentricity of the prestressing strand at midspan and at end of the beam $= e_{pg} - e_{pgE} = 15.25 - 14.45 = 0.80$ in.

where:

    Δ_p = camber due to prestressing force at transfer
    P_{pt} = total prestressing force after transfer at midspan $= 50\,(50.8) = 2{,}540.6$ kip
    E_{ci} = modulus of elasticity of UHPC at transfer $= 5{,}973$ ksi
    I_g = moment of inertia of the noncomposite precast beam $= 209{,}570.6$ in.^{2}
    e_{pg} = eccentricity of strands in noncomposite section at midspan $= 15.25$ in.^{2}
    a = distance from the girder end to the harp point of strands $= 0$ ft
    L_T = overall beam length $= 151$ ft

Therefore:

$$\Delta_p = \frac{2{,}546}{(5{,}973)(209{,}570.6)} \left(\frac{(15.25)(151 \times 12)^2}{8} - 0 \right) = 12.70 \text{ in. } \uparrow$$

C15.2. DEFLECTION DUE TO BEAM SELF-WEIGHT

The deflection due to the beam self-weight is calculated as follows:

$$\Delta_g = \frac{5 w_g L^4}{384 E_{ci} I_g}$$

where:

    Δ_g = deflection due to beam self-weight
    w_g = girder linear weight $= 0.6058$ kip/ft

Deflection due to beam self-weight after transfer is:

$$\Delta_g = \frac{5(0.6048)(151)^4}{384(5{,}973)(209{,}570.6)} = 5.65 \text{ in.} \downarrow$$

Deflection due to beam self-weight used to compute deflection at erection is:

$$\Delta_g = \frac{5(0.6048)(150)^4}{384(5,973)(209,570.6)} = 5.50 \text{ in.}\downarrow$$

C15.3. DEFLECTION DUE TO SLAB AND HAUNCH WEIGHT

The deflection due to the slab and haunch weight is calculated as follows:

$$\Delta_D = \frac{5(w_D + w_h)L^4}{384E_cI_g}$$

where:
Δ_D = deflection due to deck and haunch weights (in.)
w_D = deck linear weight = 0.9788 kip/ft
w_h = haunch linear weight = 0.0529 kip/ft
L = design span = 150 ft
E_c = modulus of elasticity of precast beam at service loads = 6,933 ksi

Therefore:

$$\Delta_D = \frac{5(0.9788 + 0.0529)(150)^4}{384(6,933)(209,570.6)} = 8.09 \text{ in.}\downarrow$$

C15.4. DEFLECTION DUE TO BARRIER AND FUTURE WEARING SURFACE WEIGHTS

The deflection due to barrier and future wearing surface weight is calculated as follows:

$$\Delta_{b+ws} = \frac{5(w_b + w_{ws})L^4}{384E_cI_c}$$

where:
Δ_{b+ws} = deflection due to barrier and future wearing surface weights (in.)
w_b = barrier weight = 0.100 kip/ft
w_{ws} = wearing surface weight = 0.1933 kip/ft
I_c = moment of inertia of the composite section = 600,476.2 in.^{2}

Therefore:

$$\Delta_{b+ws} = \frac{5(0.100 + 0.1933)(150)^4}{384(6,933)(600,476.2)} = 0.80 \text{ in.}\downarrow$$

C15.5. DEFLECTION AND CAMBER SUMMARY

After transfer, $\Delta_p - \Delta_g = 7.20$ in.↑.

The Precast/Prestressed Concrete Institute has proposed multipliers that are used to predict the long-term deflection of a pretensioned beam (PCI 2014). These multipliers are used herein to estimate the total long-term deflection of the girder.

Estimate of total long-term deflection calculated using PCI multipliers = 1.8(12.70) − 1.85(5.65) = 12.68 in.↑.

C15.6. DEFLECTION DUE TO LIVE LOAD AND IMPACT

Live load deflection limit = span/800 = 2.25 in.   [AASHTO LRFD BDS Article 2.5.2.6.2]

If the owner invokes the optional live load deflection criteria, the deflection is the greater of the value resulting from the design truck plus impact Δ_{LT}, or that resulting from 25 percent of the design truck plus impact Δ_{LT}, taken together with the design lane load, Δ_{LL}.

AASHTO LRFD BDS states that all beams should be assumed to deflect equally under the applied live load and impact. Therefore, the distribution factor for deflection is calculated as follows:

DFD = (number of lanes)/(number of beams) = 4/6 = 0.667
[AASHTO LRFD BDS Article C2.5.2.6.2]

Deflection due to lane load is as follows:

Design lane load, $w_{d\ell} = 0.64(DFD) = 0.4267$ kip/ft/girder

Therefore:

$$\Delta_{LL} = \frac{5w_{dl}L^4}{384E_cI_c} = \frac{5(0.4267)(150)^4}{384(6,933)(600,476.2)} = 1.17 \text{ in.↓}$$

C15.7. DEFLECTION DUE TO DESIGN TRUCK LOAD AND IMPACT

For maximum moment and deflection at the midspan due to the truck load, assume the centerline of the beam coincides with the middle point of the distance between the inner 32-kip axle and the resultant of the truck load.

Using elastic moment area or influence lines, deflection at midspan is:

$\Delta_{LT} = (1.044)(1 + IM)(DFD) = (1.044)(1.33)(0.667) = 0.93$ in.↓

Live load deflection is the larger of:

$\Delta_{LT} = 0.93$ in.↓

$0.25\Delta_{LT} + \Delta_{LL} = 0.25(0.93) + 1.17 = 1.40$ in.↓ (Controls)

Therefore:

Live load deflection = 1.40 in. < 2.25 in. allowable deflection.   OK.

CHAPTER C16. DESIGN SUMMARY

This example illustrated the design of a pretensioned I-beam for a 150-ft-long, single-span I-beam bridge with no skew (overall beam length is 151 ft). The I-beam cross section is modified from the MnDOT "MN54" beam and is made of UHPC. The superstructure of the bridge consists of six beams spaced at 9-ft centers. The roadway section is composed of two 12-ft traffic lanes and two 12-ft shoulders. Beams are designed to act compositely with the 9-in.-thick cast-in-place conventional concrete deck to resist all superimposed dead loads, live loads, and impact. A ½-in.-thick wearing surface is assumed. A deck thickness of 8.5 in. is used for composite section properties. The haunch is assumed to have an average thickness of 2½ in. for dead load computations and 1½ in. for section property computations. Design live load is HL-93. The conceptual reinforcement design drawing for the UHPC beam is shown in Figure C16-1. Note that the reinforcement of the deck is not shown.
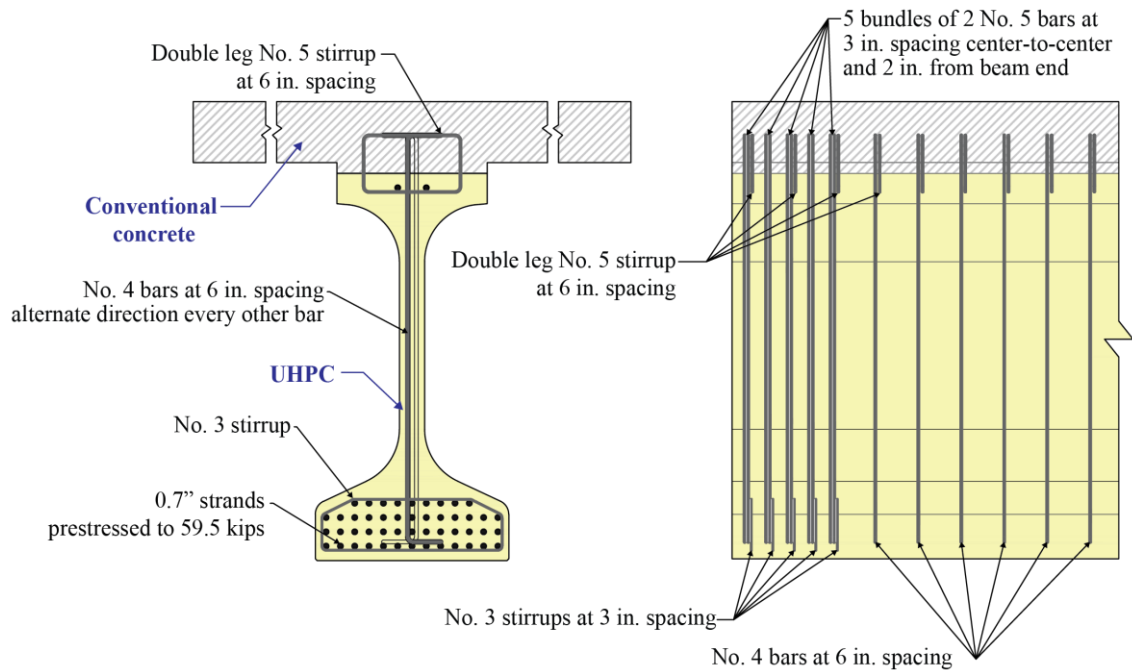
Source: FHWA.

Figure C16-1. Illustration. Conceptual design drawing showing the details of the girder reinforcement.

UHPC Guide Articles 1.10.1 and 1.10.3 state that the maximum fiber length associated with the minimum cover or reinforcement spacing requirements shall be shown in contract documents. The minimum cover and the clear distance between reinforcement bars shall not be less than the greater of 1.5 times the length of the longest fiber reinforcement included in the UHPC or 0.75 in. In this design example, the cover requirement to the transverse bars or the clear spacing between the vertical reinforcement at the interface between the girder and the deck at ends are critical to the fiber length requirement of the UHPC beam. Selecting a minimum cover of 0.75 in. would result in a maximum allowable fiber length of 0.5 in. in the UHPC mixture used to cast the girder.

267

ACKNOWLEDGMENTS

REFERENCES

AASHTO. 2019. *Standard Method of Test for Coefficient of Thermal Expansion of Hydraulic Cement Concrete*. T 336-15. Washington, DC: American Association of State Highway and Transportation Officials.

AASHTO. 2020. *AASHTO LRFD Bridge Design Specifications*, 9th ed. Washington, DC: American Association of State Highway and Transportation Officials.

AASHTO. 2021. *Standard Specification for Mixing Rooms, Moist Cabinets, Moist Rooms, and Water Storage Tanks Used in the Testing of Hydraulic Cements and Concretes*. M 201-21. Washington, DC: American Association of State Highway and Transportation Officials.

AASHTO. 2022a. *Standard Method of Test for Electrical Resistivity of a Concrete Cylinder Tested in a Uniaxial Resistance Test*. TP 119-22. Washington, DC: American Association of State Highway and Transportation Officials.

AASHTO. 2022b. *Standard Method of Test for Uniaxial Tensile Response of Ultra-High Performance Concrete*. T 397-22. Washington, DC: American Association of State Highway and Transportation Officials.

ACI Committee 214. 2011. *Guide to Evaluation of Strength Test Results of Concrete*. ACI 214R-11. Farmington Hills, MI: American Concrete Institute.

ACI Committee 301. 2020. *Specifications for Concrete Construction*. ACI 301-20. Farmington Hills, MI: American Concrete Institute.

ACI Committee 318. 2019. *Building Code Requirements for Structural Concrete*. ACI 318-19. Farmington Hills, MI: American Concrete Institute.

American Petroleum Institute. 2022. *Cements and Materials for Well Cementing*. API Specification 10A. Washington, DC: American Petroleum Institute.

Association Française de Normalisation. 2016. *French National Standard (NF) P18-710. National Addition to Eurocode 2—Design of Concrete Structures: Specific Rules for Ultra-High Performance Fiber-Reinforced Concrete*. Paris, France: Association Française de Normalisation (AFNOR).

ASTM. 2007. *Standard Specification for Cellulose Fibers for Fiber-Reinforced Concrete*. D7357-07. West Conshohocken, PA: ASTM International.

ASTM. 2008. *Standard Specification for Alkali Resistant (AR) Glass Fiber for GFRC and Fiber-Reinforced Concrete and Cement*. C1666/C1666M-08. West Conshohocken, PA: ASTM International.

ASTM. 2012. *Standard Practice for Making and Curing Concrete Test Specimens in the Field*. C31/C31M-12. West Conshohocken, PA: ASTM International.

ASTM. 2015a. *Standard Practice for Design of Journal Bearing Supports to be Used in Fiber Reinforced Concrete Beam Tests*. C1812/C1812M-15. West Conshohocken, PA: ASTM International.

ASTM. 2015b. *Standard Practice for Fabricating Test Specimens with Self-Consolidating Concrete*. C1758/C1758M-15. West Conshohocken, PA: ASTM International.

ASTM. 2015c. *Standard Test Method for Creep of Concrete in Compression*. C512/C512M-15. West Conshohocken, PA: ASTM International.

ASTM. 2017a. *Standard Practice for Fabricating and Testing Specimens of Ultra-High Performance Concrete*. C1856/C1856-17. West Conshohocken, PA: ASTM International.

ASTM. 2017b. *Standard Practice for Temperature of Freshly Mixed Hydraulic-Cement Concrete*. C1064/C1064M-17. West Conshohocken, PA: ASTM International.

ASTM. 2017c. *Standard Specification for Ground Calcium Carbonate and Aggregate Mineral Fillers for use in Hydraulic Cement Concrete*. C1797-17. West Conshohocken, PA: ASTM International.

ASTM. 2017d. *Standard Test Method for Density (Unit Weight), Yield, and Air Content (Gravimetric) of Concrete*. C138/C138M-17a. West Conshohocken, PA: ASTM International.

ASTM. 2017e. *Standard Test Method for Length Change of Hardened Hydraulic-Cement Mortar and Concrete*. C157/C157M-17. West Conshohocken, PA: ASTM International.

ASTM. 2018a. *Standard Specification for Aggregate for Masonry Mortar*. C144-18. West Conshohocken, PA: ASTM International.

ASTM. 2018b. *Standard Specification for Concrete Aggregates*. C33/C33M-18. West Conshohocken, PA: ASTM International.

ASTM. 2019a. *Standard Practice for Making and Curing Concrete Test Specimens in the Laboratory*. C192/C192M-19. West Conshohocken, PA: ASTM International.

ASTM. 2019b. *Standard Specification for Chemical Admixtures for Concrete*. C494/C494M-19. West Conshohocken, PA: ASTM International.

ASTM. 2019c. *Standard Test Method for Flexural Performance of Fiber-Reinforced Concrete (Using Beam With Third-Point Loading)*. C1609/C1609M-19a. West Conshohocken, PA: ASTM International.

ASTM. 2020a. *Standard Specification for Deformed and Plain Carbon-Steel Bars for Concrete Reinforcement*. A615/A615M. West Conshohocken, PA: ASTM International.

ASTM. 2020b. *Standard Specification for Polyolefin Chopped Strands for Use in Concrete*. D7508/D7508M-20. West Conshohocken, PA: ASTM International.

ASTM. 2020c. *Standard Specification for Silica Fume Used in Cementitious Mixtures*. C1240-20. West Conshohocken, PA: ASTM International.

ASTM. 2020d. *Standard Test Method for Compressive Strength of Cylindrical Concrete Specimens*. C39/C39M. West Conshohocken, PA: ASTM International.

ASTM. 2020e. *Standard Test Method for Flow of Hydraulic Cement Mortar*. C1437-20. West Conshohocken, PA: ASTM International.

ASTM. 2020f. *Standard Test Method for Measurement of Rate of Absorption of Water by Hydraulic-Cement Concretes.* C1585-20. West Conshohocken, PA: ASTM International.

ASTM. 2020g. *Standard Test Method for Rapid Assessment of Static Segregation Resistance of Self-Consolidating Concrete Using Penetration Test*. C1712-20. West Conshohocken, PA: ASTM International.

ASTM. 2021. *Standard Specification for Blended Hydraulic Cements.* C595/C595M-21. West Conshohocken, PA: ASTM International.

ASTM. 2022a. *Standard Specification for Coal Ash and Raw or Calcined Pozzolan for Use in Concrete*. C618-22. West Conshohocken, PA: ASTM International.

ASTM. 2022b. *Standard Specification for Mixing Water Used in the Production of Hydraulic Cement Concrete*. C1602/C1602M-22. West Conshohocken, PA: ASTM International.

ASTM. 2022c. *Standard Specification for Portland Cement*. C150/C150M-22. West Conshohocken, PA: ASTM International.

ASTM. 2022d. *Standard Specification for Slag Cement for Use in Concrete and Mortars*. C989/C989M-22. West Conshohocken, PA: ASTM International.

ASTM. 2022e. *Standard Specification for Steel Fibers for Fiber-Reinforced Concrete*. A820/A820M-22. West Conshohocken, PA: ASTM International.

ASTM. 2022f. *Standard Test Method for Determining the Apparent Chloride Diffusion Coefficient of Cementitious Mixtures by Bulk Diffusion*. C1556-22. West Conshohocken, PA: ASTM International.

ASTM. 2022g. *Standard Test Method for Static Modulus of Elasticity and Poisson's Ratio of Concrete in Compression*. C469/C469M-22. West Conshohocken, PA: ASTM International.

Baby, F., P. Marchand, and F. Toutlemonde. 2014. "Shear Behavior of Ultrahigh Performance Fiber-Reinforced Concrete Beams. Ⅰ: Experimental Investigation." *Journal of Structural Engineering* 140, no. 5.

Bertram, G., and J. Hegger. 2012. "Bond Behavior of Strands in UHPC—Tests and Design," in *Proceedings of Hipermat 2012 3rd International Symposium on UHPC and*

Nanotechnology for High Performance Construction Materials. Kassel, Germany: Kassel University Press, p. 525–532.

British Standards Institution. 2004. *Eurocode 2: EN 1992–Design of Concrete Structures*, 1st ed. Brussels, Belgium: British Standards Institution.

Canadian Standards Association. 2019. *Canadian Highway Bridge Design Code*, 12th ed. Toronto, Canada: CSA Group.

Chen, S., R. Zhang, L. Jia, and J. Wang. 2018. "Flexural Behaviour of Rebar-Reinforced Ultra-High-Performance Concrete Beams." *Magazine of Concrete Research* 70, no. 19: 997–1015.

Collins, M., and D. Mitchell. 1991. *Material Properties: Prestressed Concrete Structures*. Hoboken, NJ: Prentice-Hall.

Cook, J. E. 1989. "10,000 psi Concrete." *Concrete International*. 11, no. 10: 67–75.

Crane, C. 2010. "Shear and Shear Friction of Ultra-High Performance Concrete Bridge Girders." Ph.D. dissertation. Georgia Institute of Technology.

El-Helou, R., and B. Graybeal. 2022a. "Flexural Behavior and Design of Ultrahigh-Performance Concrete Beams." *Journal of Structural Engineering* 148, no. 4. doi: 10.1061/(ASCE)ST.1943-541X.0003246.

El-Helou, R., and B. Graybeal. 2022b. "Shear Behavior of Ultrahigh-Performance Concrete Pretensioned Bridge Girders." *Journal of Structural Engineering* 148, no. 4. doi: 10.1061/(ASCE)ST.1943-541X.0003279.

El-Helou, R., and B. Graybeal. 2023. "Shear Design of Strain-Hardening Fiber-Reinforced Concrete Beams." *Journal of Structural Engineering* 149, no. 2. doi: 10.1061/JSENDH.STENG-11065.

El-Helou, R., Z. Haber, and B. Graybeal. 2022. "Mechanical Behavior and Design Properties of Ultra-High Performance Concrete." *ACI Materials Journal* 119, no. 1: 181-194. doi: 10.14359/51734194.

FHWA. 2021. "Deployments of UHPC in Highway Bridge Construction. Interactive Map" (web page). https://highways.dot.gov/research/structures/ultra-high-performance-concrete/deployments, last accessed March 16, 2023.

Frosch, R. J. 2001. "Flexural Crack Control in Reinforced Concrete," in *Design and Construction Practices to Mitigate Cracking, SP-204*. Farmington Hills, MI: American Concrete Institute, p. 135–154.

Graybeal, B. 2006a. *Material Property Characterization of Ultra-High Performance Concrete*. Report No. FHWA-HRT-06-103. Washington, DC: Federal Highway Administration.

Graybeal, B. 2006b. *Structural Behavior of Ultra-High Performance Concrete Prestressed I-Girders*. Report No. FHWA-HRT-06-115. Washington, DC: Federal Highway Administration.

Graybeal, B. 2009a. *Structural Behavior of a Prototype Ultra-High Performance Concrete Pi-Girder*. Report No. FHWA-HRT-10-027. Washington, DC: Federal Highway Administration.

Graybeal, B. 2009b. *Structural Behavior of a 2nd Generation Ultra-High Performance Concrete Pi-Girder*. Report No. FHWA-HRT-10-026. Washington, DC: Federal Highway Administration.

Graybeal, B. 2014. *TechNote: Design and Construction of Field-Cast UHPC Connections*. Report No. FHWA-HRT-14-084. Washington, DC: Federal Highway Administration.

Graybeal, B. 2015a. "Splice Length of Prestressing Strands in Field-Cast UHPC Connections." *Materials and Structures* 48, no. 6: 1831–1839.

Graybeal, B. 2015b. "Tensile Mechanical Response of Ultra-High-Performance Concrete." *ASTM Advances in Civil Engineering Materials* 4, no. 2: 62–74. doi: 10.1520/ACEM20140029.

Graybeal, B. 2019. *Design and Construction of Field-Cast UHPC Connections*. Report No. FHWA-HRT-19-011. Washington, DC: Federal Highway Administration.

Graybeal, B., and F. Baby. 2013. "Development of Direct Tension Test Method for Ultra-High-Performance Fiber-Reinforced Concrete." *ACI Materials Journal* 110, no. 2: 177–186.

Graybeal, B., E. Brühwiler, B.-S. Kim, F. Toutlemonde, Y. Voo, and A. Zaghi. 2020. "International Perspective on UHPC in Bridge Engineering." *ASCE Journal of Bridge Engineering* 25, no. 11. doi: 10.1061/(ASCE)BE.1943-5592.0001630.

Haber, Z., I. De la Varga, B. Graybeal, B. Nakashoji, and R. El-Helou. 2018. *Properties and Behavior of UHPC-Class Materials*. Report No. FHWA-HRT-18-036. Washington, DC: Federal Highway Administration.

Hanson, N., and P. Kaar. 1959. "Flexural Bond Tests of Pretensioned Prestressed Beams." *ACI Journal* 55, no. 7: 783–802.

John, E., E. Ruiz, R. Floyd, and W. Hale. 2011. "Transfer and Development Lengths and Prestress Losses in Ultra-High-Performance Concrete Beams." *Transportation Research Record* 2251, no. 1: 76–81.

Lubbers, A. 2003. "Bond Performance Between Ultra-High Performance Concrete and Prestressing Strands." Master's Thesis. Ohio University.

McCarter, W., T. Chrisp, G. Starrs, P. Basheer, S. Nanukuttan, S. Srinivasan, and B. Magee. 2015. "A Durability Performance-Index for Concrete: Developments in a Novel Test Method." *International Journal of Structural Engineering* 6, no. 1: 2–22.

MnDOT. 2018. *LRFD Bridge Design Manual.* Oakdale, MN: Minnesota Department of Transportation.

Mohebbi, A., R. G. El-Helou, and B. Graybeal. 2019. "End Zone Design and Behavior of Prestressed UHPC Girders," in *Proceedings of 2019 International Accelerated Bridge Construction Conference*. Miami, Florida: Florida International University.

Mohebbi, A., and B. Graybeal. 2022. "Prestress Loss Model for Ultra-High Performance Concrete." *Engineering Structures* 252: 113645. doi: 10.1016/j.engstruct.2021.113645.

Mohebbi, A., B. Graybeal, and Z. Haber. 2022. "Time-Dependent Properties of Ultrahigh-Performance Concrete: Compressive Creep and Shrinkage." *Journal of Materials in Civil Engineering* 34, no. 6. doi: 10.1061/(ASCE)MT.1943-5533.0004219.

Muzenski, S., Z. Haber, and B. Graybeal. 2022. "Interface Shear of Ultra-High Performance Concrete." *ACI Structural Journal* 119, no. 1: 267–280. doi: 10.14359/51733008.

Muzenski, S., Z. Haber, and B. Graybeal. 2023. "Monolithic and Non-Monolithic Interface Shear Performance of Ultra-High Performance Concrete." *Engineering Structures* 281: 115667. doi: 10.1016/j.engstruct.2023.115667.

Nordtest. 1999. *Concrete, Mortar and Cement-based Repair Materials: Chloride Migration Coefficient from Non-Steady-State Migration Experiments (NT BUILD 492)* (1999-11). Espoo, Finland: Nordtest.

PCI. 2014. *PCI Bridge Design Manual*, 3rd ed., 2nd release. Chicago, IL: Precast/Prestressed Concrete Institute.

PCI Concrete Materials Technology Committee. 2022. *Guidelines for the Use of Ultra High Performance Concrete (UHPC) in Precast and Prestressed Concrete*. TR-9-22. Chicago, IL: Precast/Prestressed Concrete Institute.

Popovics, S. 1973. "A Numerical Approach to the Complete Stress–Strain Curve of Concrete." *Cement and Concrete Research* 3, no. 5: 583–599.

Qiu, M., X. Shao, K. Wille, B. Yan, and J. Wu. 2020. "Experimental Investigation on Flexural Behavior of Reinforced Ultra High Performance Concrete Low-Profile T-Beams." *International Journal of Concrete Structures and Materials* 14, no. 1.

Rajabipour, F., G. Sant, and J. Weiss. 2007. "Development of Electrical Conductivity-Based Sensors for Health Monitoring of Concrete Materials Development." Presented at the *TRB Annual Conference*. Washington, DC: Transportation Research Board, vol. 16, p. 1–16.

Russell, H., and B. Graybeal. 2013. *Ultra-High Performance Concrete: A State-of-the Art Report for the Bridge Community*. Report No. FHWA-HRT-13-060. Washington, DC: Federal Highway Administration.

Snyder, K. A. 2001. "The Relationship Between the Formation Factor and the Diffusion Coefficient of Porous Materials Saturated with Concentrated Electrolytes: Theoretical and Experimental Considerations." *Concrete Science and Engineering* 3, no. 12: 216-224.

Spragg, R., B. Graybeal, N. Saladi, L. Montanari, and I. De la Varga. 2022. *Electrical Resistivity Testing to Rapidly Assess the Durability of UHPC-Class Materials*. Report No. FHWA-HRT-21-095. Washington, DC: Federal Highway Administration. doi: 10.20949/1521681.

Spragg, R., C. Qiao, T. Barrett, and J. Weiss. 2016. "Assessing a Concrete's Resistance to Chloride Ion Ingress Using the Formation Factor," in *Corrosion of Steel in Concrete Structures*, ed. A. Poursaee. London: Woodhead Publishing, p. 211–238.

Swiss Institute of Architects and Engineers. 2016. *Ultra-High Performance Fibre Reinforced Cement-Based Composites (UHPFRC)–Materials Design and Construction.* Technical Leaflet SIA 2052. Zurich, Switzerland: SIA.

Thorenfeldt, E., A., Tomaszewicz, and J. Jensen. 1987. "Mechanical Properties of High-strength Concrete and Application in Design," in *Proceedings of the Symposium Utilization of High-Strength Concrete, Tapir, Trondheim*, p. 149–159.

Vecchio, F., and M. Collins. 1986. "Modified Compression-Field Theory for Reinforced Concrete Elements Subjected to Shear." *ACI Journal* 83, no. 2: 219–231.

Yoo, D., N. Banthia, and Y. Yoon. 2017. "Experimental and Numerical Study on Flexural Behavior of Ultra-High-Performance Fiber-Reinforced Concrete Beams with Low Reinforcement Ratios." *Canadian Journal of Civil Engineering* 44, no. 1: 18-28.

Yoo, D., and Y. Yoon. 2015. "Structural Performance of Ultra-High-Performance Concrete Beams with Different Steel Fibers." *Engineering Structures* 102: 409–423.